이학박사학위논문

Effects of tropical cyclones and biological interactions on red tide dynamics by the ichthyotoxic dinoflagellate *Cochlodinium polykrikoides* in the Korean coastal waters

한국연안에서 태풍과 생물학적 상호작용이 코클로디니움 적조에 미치는 영향에 대한 연구

2016년 2월

서울대학교 대학원

지구환경과학부 해양학전공

임 안 숙

Effects of tropical cyclones and biological interactions on red tide dynamics by the ichthyotoxic dinoflagellate *Cochlodinium polykrikoides* in the Korean coastal waters

한국연안에서 태풍과 생물학적 상호작용이
코클로디니움 적조에 미치는 영향에 대한 연구

지도교수 정 해 진

이 논문을 이학박사 학위논문으로 제출함
2016년 2월

서울대학교 대학원
지구환경과학부 해양학전공
임 안 숙

임안숙의 박사학위논문을 인준함
2015년 12월

위 원 장 김종성 (인)

부 위 원 장 정 해 진 (인)

위 원 허 창 희 (인)

위 원 이 은 주 (인)

위 원 이 원 호 (인)

Abstract

Effects of tropical cyclones and biological interactions on red tide dynamics by the ichthyotoxic dinoflagellate *Cochlodinium polykrikoides* in the Korean coastal waters

Lim, An Suk

School of Earth and Environmental Sciences

The Graduate School

Seoul National University

Red tides are discoloration of the sea surface due to microalgal blooms. The mixotrophic dinoflagellate *Cochlodinium polykrikoides* often forms red tide patches in the coastal waters of many countries and has sometimes caused large-scaled mortality of fish in both cages and natural environments. This dinoflagellate has caused losses of USD $1-60 million to Korean aquaculture industry every year. The mechanism of the outbreak, persistence, and decline of *Cochlodinium* red tides have not been fully understood yet, although, ecophysiological characteristics of *C. polykrikoides* have been well documented.

Here, I explored effects of some critical physical and biological factors such as tropical cyclones, competing diatoms, and novel mixotrophic dinoflagellate grazers on the red tide dynamics of *C. polykrikoides.*

Korea usually experiences several tropical cyclones (typhoons) in *C. polykrikoides* red tide period every year. Tropical cyclones are generally accompanied by strong winds and heavy rains and thus can

change some critical factors affecting red tide dynamics. Strong winds often generate intensive turbulence which can inhibit growth of red tide organisms. Several studies reported that after the passage of tropical cyclones, the dominant red tide species in the water column were switched from flagellates to diatoms. Thus, tropical cyclones are likely to physically and biologically affect on the red tide dynamics of *C. polykrikoides*. However, effects of tropical cyclones on *Cochlodinium* red tides have not been well documented yet. Therefore, I explored the effects of tropical cyclones on the outbreak, persistence, and decline of *Cochlodinium* red tides by analyzing the daily maximum wind speed and daily maximum *Cochlodinium* cell abundance during the 14 tropical cyclone cases in South Sea of Korea in 2012–2014. I found that *Cochlodinium* red tides disappeared when daily maximum wind speeds exceeded 14 m s^{-1}, but were not markedly affected when daily maximum wind speeds were less than 5 m s^{-1}. Thus, this study suggests that daily maximum wind speeds of tropical cyclones may differentially affect the outbreak and persistence of *Cochlodinium* red tides.

I explored the effects of competing diatoms on dynamics of *Cochlodinium* and found that some competing diatoms reduced the growth and swimming speed of *Cochlodinium* through both physical contact and chemical stress when the concentration of the diatoms exceeds certain levels. This evidence suggests that the outbreak of *Cochlodinium* red tides can be prevented or delayed when the concentration of diatoms is high.

No effective mixotrophic dinoflagellate grazer on *C. polykrikoides* has been found yet, whereas several ciliates and heterotrophic protistan grazers have been reported. During *Cochlodinium* red tides in the coastal waters of eastern Korea, in

2014, I isolated a *Alexandrium* cell and established a clonal culture. This *Alexandrium* was revealed to be a mixotrophic dinoflagellate that exclusively feeds on *C. polykrikoides*. Based on the results from morphological and genetic analyses, the *Alexandrium* strain was revealed to be a new species, to be named as *Alexandrium pohangense* n. sp.

To explore the roles of *Alexandrium pohangense* in marine ecosystems, I measured the growth and ingestion rates of *A. pohangense* as a function of the concentration of only prey *C. polykrikoides* in the laboratory. The maximum ingestion rate of *A. pohangense* on *C. polykrikoides* was 7 cells predator^{-1} d^{-1}, and the maximum mixotrophic growth rate reached 0.5 d^{-1}, while the autotrophic growth rate was 0.1^{-1}. Furthermore, by combining the results from the feeding experiments and abundance data obtained in field, I estimated grazing impact of *A. pohangense* on populations of *C. polykrikoides* in the natural environments. The grazing coefficients attributable to *A. pohangense* on co-occurring *C. polykrikoides* were up to 1.57 d^{-1}. Thus, up to 79 % of the *C. polykrikoides* populations could be removed by *A. pohangense* population in a day.

Conclusively, through field observation, diverse feeding experiments in the laboratory, and morphological and molecular analyses, I found that tropical cyclones, competing diatoms, and a new mixotrophic dinoflagellate *A. pohangense* can significantly affect the red tide dynamics by *C. polykrikoides*.

Keywords: *Alexandrium, Cochlodinium polykrikoides,* Ecology, Grazing, Taxonomy, Typhoons, Harmful algal bloom,

Student Number: 2011-30921

Table of Contents

List of Tables

List of Figures

Chapter 1. Introduction

Red tide are discoloration of the sea surface water due to algal blooms. Red tides are known to occur almost all the countries which have their sea. Red tides often cause disturbance of marine ecosystems, large scale mortality of fish and shellfish in both natural environments and aquaculture cages, and even illness of human. Because of such damage, red tide events are critical issues to the government, scientists, and the public of many countries. The annual economic loss due to red tides is estimated tens of billions of dollars in the world. In Korea, losses of several thousand to million US dollar in the commercial fish farms every year have been reported. To minimize the damage caused by red tides, better understanding red tide dynamics is needed.

The red-tide causative species are approximately 300 species (Smayda, 1997). All red tide species increase their populations by binary division. Once a population of a certain red-tide species is inoculated in a certain area, to form red tides, its population density should increase more rapidly than co-occurring other species. The red tide formation can be affected by growth related factors (i.e., lights, temperature, nutrients, etc.), and mortality related factors (grazing impact). In addition, physical forces such as currents, internal waves, circulations, fronts, upwelling and down-welling, strong winds can affect red tide formation. Thus, overall equation for a change of cell abundance of a red tide species is as follows:

$$dC/dt = C\ (k - g \pm aBI)$$

where k = specific growth rate, g = mortality, aBI = effects of biological interactions with other species. According to this equation, a species having a greater growth rate and a less mortality rate than co-occurring species has an opportunity to become a red-tide causative species. Moreover, the species conducts diverse biological interactions with other species. There are two groups of biological interactions; direct biological interactions such as predator-prey relationships and inhibition by physical contact or chemical effects; indirect biological interactions such as space competition by growing faster than others under given conditions. Some biological interactions cause an increase in one species (+aBI), but a decrease in other species (-aBI). Thus, biological interactions between two species may play an important role in their competition. There have been many studies on these topics. However, many critical factors affecting dynamics of red tides species should be explored. The mixotrophic dinoflagellate *C. polykrikoides* is one of the red tide species to be fully studied because it has caused great loss in many countries. *Cochlodinium polykrikoides* often forms red tide patches in the coastal waters of Korea and has caused losses of USD $1-60 million in Korean aquaculture industry every year since 1995 (Park et al., 2013a).

To minimize this huge damage caused by *C. polykrikoides* red tides, scientists, officials, and aquaculture industry in many countries have spent a great deal of time and money on predicting the outbreak of the red tides and controlling them. Due to these intensive

efforts, the eco-physiology of this dinoflagellate (i.e., effects of temperature, light, salinity, and nutrients on the growth of *C. polykrikoides*) has been relatively well documented (Kim et al., 2001; Gobler et al., 2012) (Fig. 1.1). However, effects of some critical physical factors (i.e., tropical cyclones, turbulence, mixing on *C. polykrikoides*) have not been well studied. In addition, some critical biological interactions between *Cochlodinium* and co-occurring species (i.e., effects of physical contact on growth and swimming behavior) are not fully understood yet. Due to this limitation, it is very difficult to predict the outbreak, persistence, and decline of *Cochlodinium* red tides.

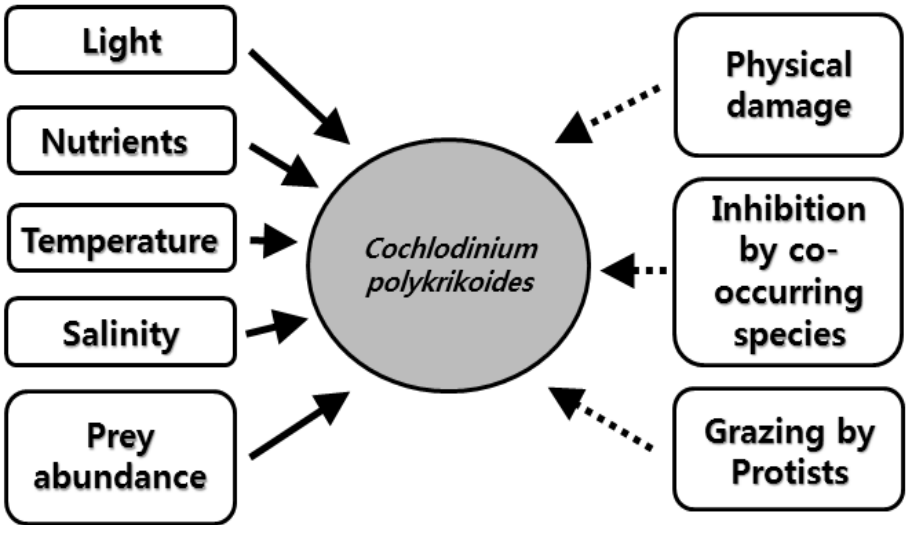

Fig. 1.1. Growth and mortality factors affecting the formation of *Cochlodinidum polykrikoides* red tides. Black arrows indicate that related studies are well documented, while dashed arrows indicate insufficient data on each subject.

The ranges of temperatures and salinities for the optimal growth of *C. polykrikoides* are known to be 25-30 ℃ and 25-40, obtained from experiments the laboratory and fields (Kudela and Gobler, 2012). Furthermore, the range of half-saturation values (i.e., the value meeting the half of the maximum growth rate) of the light is 29-45 μE $m^{-2}s^{-1}$ (Kim et al., 2004; Yamatogi et al., 2005; Oh et al., 2006). Under these conditions, the reported highest maximum growth rate of *C. polykrikoides* is 0.61 d^{-1} (Yamatogi et al., 2005), which is much lower than competing diatoms and small flagellates (i.g., 2.77 d^{-1} for the diatom *Thalassiosira pseudonana* and 1.32 d^{-1} for the raphidophyte *Heterosigma akashiwo*) (Passche, 1973; Tomas, 1978). Thus, it is likely to be difficult for *C. polykrikoides* to form red tides when the environmental conditions favorable for growth of most phytoplankton species are given.

How can *C. polykrikoides* outgrow over competing red tide species and form a red tide patch? The chain-forming dinoflagellate *C. polykrikoides* is one of the fastest swimming red-tide species and is able to conduct vertical migration through the water column. *C. polykrikoides* descends to the nutrient-rich deep water at night, but ascends to well lit surface water day time. The maximum swimming speed of *C. polykrikoides* is ~1,400 μm s^{-1} and thus theoretically it can reach 50 m during the day (10-hour travel). Thus, when the nutrients are limited in surface water, *C. polykrikoides* may uptake nutrients from the nutrient-rich deep water. Moreover, *C. polykrikodes* is known to be mixotrophic (Jeong et al., 2004b). Jeong et al. (2010a) proposed a mixotrophic ability as a possible mechanism

of the outbreak and/or the persistence of red tides in oceanic waters whose surface nutrient concentrations are too low for red tide flagellates to grow and also thermocline is too deep to reach eutrophic deep waters. Therefore, *C. polykrikoides* may able to form red tides oceanic waters by feeding on diverse prey including bacteria and small algae (Jeong et al., 2004b, 2005b).

There have been much fewer studies on mortality of *C. polykrikoides* due to predation, compared to those on its growth rates. Among the many potential protistan predators, only a naked ciliate *Strombidinopsis jeokjo* (Choreotrichida) was revealed to have a significant grazing impact on populations of *C. polykrikoides* (Jeong et al., 2008). Therefore, it is worthwhile to explore more predators on *C. polykrikoides.*

Biological interactions between *C. polykrikoides* and other phytoplankton are not well known. Most studies on these interactions have focussed on allellopathic effects (i.e., chemical effects) of *C. polykrikoides*. However, other red tide species may affect *C. polykrikoides.*

In chapter 2, I investigated the effects of tropical cyclones (typhoons) on *Cohlodinium polykrikoides* red tides in South Sea of Korea in 2012-2014. There have been a debate on effects of tropical cyclones on *C. polykrikoides* red tides; in some years, *C. polykrikoides* red tides were weaken or disappeared, but reinforced in other years. I guessed that C*. polykrikoides* red tides may be affected by the speed of wind produced by tropical cyclones and thus

explored this topic. In this study, I analyzed the daily maximum wind speed and the daily maximum abundance of *C. polykrikoides* in the red tide periods and found that *C. polykrikoides* red tides were differentially affected by wind speeds. The results of this study will provide a basis on understanding roles of tropical cyclones on dynamics of *C. polykrikoides* red tides.

In chapter 3, I explored the biological interactions between competitive diatoms and *C. polykrikoides*. Diatoms and phototrophic dinoflagellates are two major phytoplankton groups. They severally compete each other to form a red tide. Diatoms grow much faster than dinoflagellates having similar sizes (Banse, 1982). Thus, diatoms outgrow over dinoflagellates when the conditions favorable for photosynthesis are given. However, dinoflagellates can outgrow over diatoms by conducting vertical migration or mixotrophy. Furthermore, some toxic or harmful dinoflagellates are known to kill or lower growth of diatoms using chemicals (Fistarol et al., 2004). I guessed that fats swimming *C. polykrikoides* having thin cell membrane may be inhibited by dense diatoms. Thus, I investigated the possible physical and chemical effects of 3 common diatoms *Skeletonema costatum*, *Thalassiosira decipiense*, and *Chaetoceros danicus* on the growth rate and swimming speed of *C. polykrikoides*. The results of this study provide a basis on understanding roles of competing diatoms on dynamics of *C. polykrikoides* red tides.

In chapter 4, I reported a new dinoflagellate species, *Alexandrium pohangense.* I isolated a dinoflagellate from an estuary in East Sea at the decline stage of *C. polykrikodies*. Thus, I guessed

that this dinoflagellate may be a mixotrophic dinoflagellate which is able to feed on *C. polykrikodies*. After analyzing its morphological and genetical characterizations, I realized that it is a new species in the genus *Alexandrium*. Therefore, based on the morphological and phylogenetic criteria, I established a new *Alexandrium* species in this study. Many *Alexandrium* species are known to be toxic and thus many marine scientists are interested in *Alexandrium* species. The discovery of this new *Alexandrium* species may open some new topics in marine biology and fisheries.

In chapter 5, I explored the mixotrophic ability of *Alexandrium pohangense* and roles of this dinoflagellate in dynamics of *C. polykrikoides* red tides. Interestingly, this dinoflagellate fed on only *C. polykrikoides* among diverse phytoplankton prey species provided. In addition, the maximum growth rate of *A. pohangense* with added *C. polykrikoides* (i.e., mixotrophic growth) was higher than that without added prey (i.e., autotrphic growth). Thus, I*A. pohangense* may play important roles in the dynamics of *C. polykrikoides* red tides. The results of this study provide a basis on understanding roles of a new *Alexandrium* species on dynamics of *C. polykrikoides* red tides.

In chapter 6, I provided overall conclusions based on the results of field observation and experiments in the lab in this study.

This study clearly showed that tropical cyclones (in Chapter 2), competing diatoms (in Chapter 3), and a new *Alexandrium* species (may be another competing species; in Chapter 4 and 5) affect red tide dynamics of *C. polykrikoides* (Fig. 1.2). Therefore, we must

consider these effects in understanding *C. polykrikoides* red tides, establishing prediction models, and developing methods of controlling these red tides.

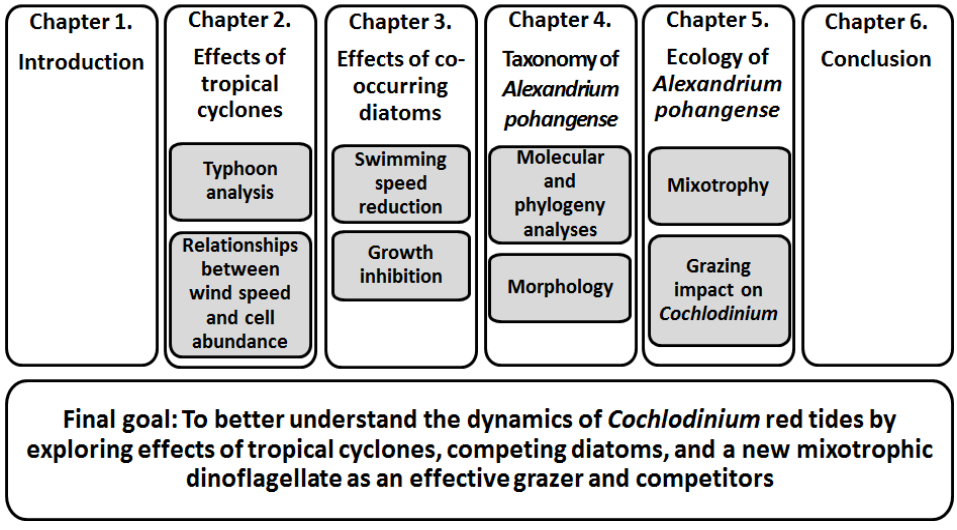

Fig. 1.2. Thesis Outline

Chapter 2. Effects of tropical cyclones on the dynamics of *Cochlodinium* red tides in the south sea of Korea

2.1. Introduction

Cochlodinium polykrikoides is an unarmored mixotrophic dinoflagellate and one of the noxious red tide forming organisms (Jeong et al., 2004b; Gobler et al., 2008; Mulholland et al., 2009). The occurrence of the dinoflagellate and its bloom events have expanded worldwide after first being identified in the coastal waters of Puerto Rico (Margalef, 1961; Kudela and Gobler, 2012). With increase of the red tide events, *Cochlodinium* caused large scale mortality of finfish in both cages and natural environments and resulted the huge economic loss in many countries including Korea (USD $ 60 million), China (USD $97 million), Japan (USD $ 0.1 million), and Canada (CAN $ 2 million) (Whyte et al. 2001; Fukuyo et al., 2002; Yan et al.,, 2002; Gárate-Lizárraga et al., 2004; Vargas-Montero et al., 2006; Anton et al., 2008; Azanza et al., 2008; Hamzehei et al., 2013; Park et al., 2013a). *C. polykrikoides* has been known to kill early stage of fish at the concentrations > 1,000 cells ml^{-1} (Rountos et al., 2014). Thus, the cell density of *C. polykrikoides* is critical to kill fish in cages. Some physical forces such as strong winds and turbulence can dissipate cells in red tide patches or kill cells. A tropical cyclone (so called, typhoons in north Pacific, hurricane in America, cyclone in Indian Ocean, willy-willy in Austria) usually produces strong winds

(Emanuel, 2003). Thus, a tropical cyclone may affect the cell density of *C. polykrikoides* and in turn survival of fish in cages. It is worthwhile to explore effects of tropic cyclones on the cell density of *C. polykrikoides*.

A tropical cyclone is generated at tropical region and brings strong winds and heavy rain from tropical region to high latitudes area (Emanuel, 2003). These tropical cyclones often cause great loss in economy of many countries and sometimes human death. A tropical cyclone influences on the marine ecosystem such as upwelling and vertical mixing (Prince, 1981; Lin et al., 2003; Zheng and Tang 2007), terrestrial runoff (Zheng and Tang, 2007; Chen et al., 2009), and sediment resuspension (Fogel et al., 1999). Thus, the occurrence of tropical cyclone can effect on the phytoplankton dynamics. Some studies showed diatoms often dominated phytoplankton assemblages after tropical cyclone passages in various regions (Chen et al., 2009). There are also some reports that red tide patches disappear after tropical cyclone passed (Lee et al., 2001; Lim et al., 2002; Lee, 2008). Therefore, it is worthwhile to explore the effects of tropical cyclone on the *Cochlodinium* red tide dynamics. However, these studies did not explore either relationship between the daily wind speed and cell abundance or critical wind speeds preventing outbreaks and recovery of red tide events or reducing red-tide cell abundances down to the level at which fish in aquaculture cages are not killed. Thus, to explore these relationship and critical wind speed, the daily variations in the abundances of *C. polykrikoides* and wind speeds in 3 study areas of South Sea of Korea in the periods of *C. polykrikoides* red tides and the passage of

14 tropical cyclones in 2012-2014 were analyzed. Our results provide a basis for understanding relationships between the daily wind speed of tropical cyclones and the abundance of *C. polykrikoides* and an insight on effects of reduced *C. polykrikoides* abundances on fate of fish in aquaculture cages and eventually economic loss due to its red tides.

2.2. Materials and methods

2.2.1. The Study area

Korea is one of the countries that have both *Cochlodinium polykrikoides* red tides and several tropical cyclones every year. *C. polykrikoides* have usually caused huge red tides in coastal and offshore waters of South Sea of Korea. Goheung (GO), Yeosu (YE), and Tongyoung (TO), located in South Sea of Korea, are the places where *C. polykrikoides* red tides have most frequently occurred (Fig. 2.1). Moreover, most aquaculture farms in Korea are located in these areas (MIFAFF, 2008). In addition, 1-7 tropical cyclones have passed these areas every year (http://typ.kma.go.kr). Thus, these 3 areas are the ideal places for investigating relationships between tropical cyclones and *C. polykrikoides* red tides.

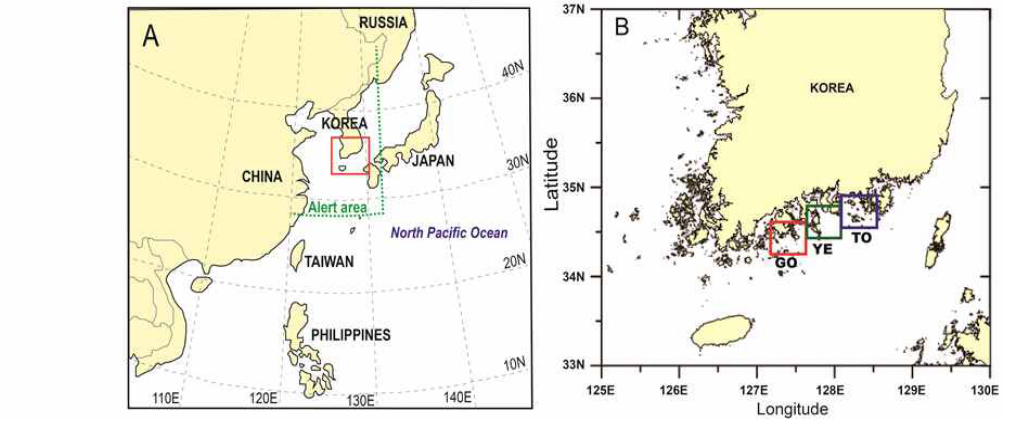

Fig. 2.1. Map of the study area (A). (B) enlarged from red box from (A). Three study areas, Goheung (GO), Yeosu (YE), and Tongyoung (TO), are shown in (B).

2.2.2. The tropical cyclone and wind speed

To investigate effects of tropical cyclones on *Cochlodinium polykrikoides* red tides, the tropical cyclones directly passing the study areas or nearby (i.e. < 800 km away from the tropical cyclone core) in *C. polykrikoides* red tide periods in 2012-2014 were analyzed (Table 2.1). The meteorological data related to the tropical cyclones (i.e., the created and dissipated dates and path of each tropical cyclone) were obtained from the Korea National Typhoon Center (KNTC, http://typ.kma.go.kr). To minimize damages due to tropical cyclones, KNTC has announced different levels of warning based on the location of the tropical cyclone. For example, when the tropical cyclone core is located in the latitude higher than 28 °N and also in the longitude smaller than 132 °E in which Korea has generally experiences strong winds and/or heavy rains by the tropical cyclone, KNTC announces so-called "the tropical cyclone alert stage". Thus, the north-western area of 28 °N and 132 °E is defined as the tropical cyclone alert area (Fig. 2.1). In this study, the passage period of a tropical cyclone in Korea was defined as the date when the tropical cyclone was positioned in this tropical cyclone alert area. In addition, the Korea Ocean Observing and Forecasting System (http://sms.khoa.go.kr) reports the wind speed in certain area every hour. This hourly wind speed is the value of averaging all wind speeds measured every minute. The daily maximum wind speed, the highest value among the hourly reported wind speed in a day, was used in this study. The period between created and dissipated dates of each tropical cyclone and that when the tropical cyclone reached the tropical cyclone alert area were provided as horizontal bars in the

figures.

2.2.3. The daily abundance of *Cochlodinium polykrikoides*

The Korea National Fisheries Research and Development Institute (NFRDI) has red tide monitoring system. Once the red tide patch was detected, the water samples were taken daily from the red tide patch and near the area and the causative species and its cell density were published as a daily red tide new latter. The density of *C. polykrikoides* are archived by the NFRDI (http://portal.nfrdi.re.kr/redtideInfo). Water samples were collected with a 2 L Hydro-Bios water sampler at 0.3-0.5 m in depth. Plankton samples for counting were poured into 1 L polyethylene bottles and fixed with acidic Lugol's solution (0.3 %). The samples were settled down for a week and concentrated by approximately 1/5 by evacuating the supernatant of the sample. After thorough mixing, 1-ml of sample was transferred into Sedgwick-Rafter counting chambers (SRCs) and *Cochlodinium* cells in SRCs were counted under an inverted microscope (Lee et al., 2013).

2.3. Results

2.3.1. The tropical cyclone and wind speed

The beginning and ending dates of *Cochlodinium polykrikoides* red tides were July 27 and October 25 in 2012, July 17 and September 4 in 2013, and July 24 and October 15 in 2014. Among the tropical cyclones occurred between 0–50 °N and 0–180 °E in these red tide periods, 5, 2, and 7 tropical cyclones in 2012, 2013, and 2014, respectively passed the alert areas (Fig. 2.2). Of these tropical cyclones, the tropical cyclones Tembin, Bolaven, and Sanba in 2012 and Nakri in 2014 generated strong winds whose maximum speeds exceeded 14 m s^{-1} in the study areas (Table 2.1). The daily maximum wind speed in one of Goheung (GO), Yeosu (YE), and Tongyoung (TO) was usually similar to another, but considerably different from the other one. For example, during passage of tropical cyclone Tembin, the maximum wind speeds in GO, YE, and TO were 23.3, 21.5, and 14.9 m s^{-1}, respectively, while during passage of tropical cyclone Sanba, the maximum wind speed in GO, YE, and TO were 18.1, 23.4, and 19.1 m s^{-1}, respectively. The centers (i.e., tropical cyclone eyes) of these 4 tropical cyclones were positioned within 200 km away from the study areas (Table 2.1). During the other tropical cyclones, the maximum wind speeds were ~3–13 m s^{-1} in the study areas. These tropical cyclones were positioned at ~200–800 km away from the study areas.

Table 2.1. The analyzed tropical cyclones and the maximum wind speed (m s^{-1}) in each study area.

Year	Tropical cyclone	Period in the alert area	Goheung	Yeosu	Tongyoung
2012	Damrey	Aug. 1-3	9.2	8.7	7.1
2012	Tembin	Aug. 28-31	23.3	21.5	14.9
2012	Bolaven	Aug. 26-29	23.3	21.5	14.9
2012	Sanba	Sep. 16-18	18.1	23.4	19.1
2012	Jelawat	Sep. 29 - Oct. 1	6.8	6.3	4.5
2013	Kong-rey	Aug. 29-31	7.5	6.3	5.5
2013	Toraji	Sep. 2-4	6.0	5.8	4.5
2014	Matmo	Jul. 24-25	11.9	5.5	5.4
2014	Halong	Aug. 8-10	7.4	8.7	8.0
2014	Nakri	Aug. 1-3	14.6	18.3	7.7
2014	Fengshen	Sep. 7	3.7	58.	2.5
2014	Phanfone	Oct. 5	4.6	4.5	3.4
2014	Vongfong	Oct. 12-14	5.5	10.6	8.4

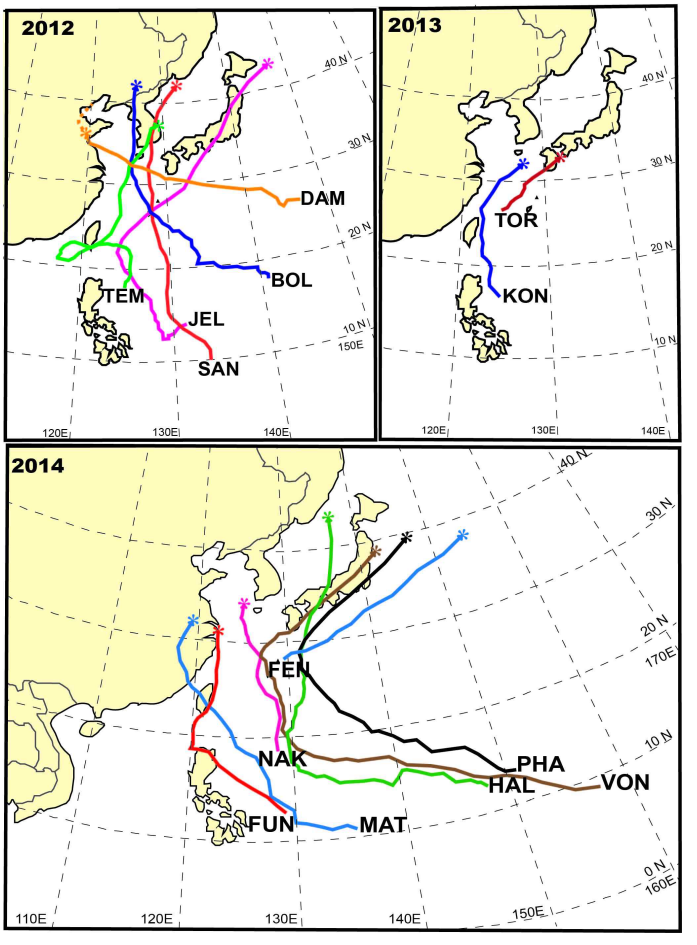

Fig. 2.2. Tropical cyclone paths of each study year. The star at the end of the each line indicates the location where the tropical cyclone dissipated. Damery (DAM), Tembin (TEM), Bolaven (BOL), Sanba (SAN), Jelawat (JEL) in 2012, Kong-Rey (KON), Toraji (TOR) in 2013, and Matmo (MAT), Halong (HAL), Nakri (NAK), Fengshen (FEN), Fung-Wong (Fun), Phanfone (PHA), and Vongfong (VON) in 2014 passed the alert area (28-90 °N latitude and 0-132 °E longitude).

2.3.2. The daily abundance of *Cochlodinium polykrikoides*

In 2012, the *C. polykrikoides* blooms occurred between July 27 and October 25. During the red tide period, the density of *C. polykrikoides* in each study area was changed in similar pattern (Fig. 2.3). In Goheung (GO) area, after the *C. polykrikoides* blooms occurred, the density of *C. polykrikoides* was maintained between 200 and 1,200 cells ml^{-1} for two weeks but suddenly increased. However, the abundance of *C. polykrikoides* decreased slowly and the red tide patches were disappeared on August 28. *C. polykrikoides* bloom patches appeared again on October 5 but dissipated in two weeks. In Yeosu (YO) area, the density of *C. polykrikoides* fluctuated for a month and then the red tide patches disappeared for 5 weeks. However, the abundance of *C. polykrikoides* suddenly increased and reached about 8,000 cells ml^{-1}. After highest density reached, the density decreased and then red tide event was terminated. In Tongyoung (TO) area, the abundance of *C. polykrikoides* was maintained below 2,000 cells ml^{-1} for a month and then the patches dissipated until October 5. However, the density of *C. polykrikoides* rapidly increased and reached highest density (18,000 cells ml^{-1}) after one week later and then the red tide event was terminated (Fig. 2.3).

In 2013, the *C. polykrikoides* blooms occurred between July 17 and September 4 (Fig. 2.4). During the red tide period, the change of the *C. polykrikoides* cell density in Goheung (GO) and Yeosu (YE) areas showed similar patterns. After *C. polykrikoides* blooms occurred on July 17, the density of *C. polykrikoides* cells reached about 8,000 cells ml^{-1} in Goheung and 14,000 cells ml^{-1} in Yeosu in early August.

The abundance of *C. polykrikoides* cells declined after August 16 and the red tide patches disappeared in early September. However, unlike Goheung and Yeosu areas, red tide patches in Tongyoung (TO) area maintained in high density (~10,000 cells ml^{-1}) from the beginning of the red tide period and reached at 38,000 cells ml^{-1} on August 8. Once the abundance of *C. polykrikoides* reached the highest density of the period, it declined and dissipated as time went by.

In 2014, the *C. polykrikoides* blooms occurred between July 24 and October 15 (Fig. 2.5). On July 28 in 2014 between the passages of the tropical cyclone Matmo and Halong-Nakri, *C. polykrikoides* red tide patches were found in TO (Fig. 2-5). However, red tide patches had not been found until August 28 in GO and August 12 in YE (Fig. 2.5). In TO, the DMAC increased up to 15,000 cells ml^{-1} with a big fluctuation after the passage of these two tropical cyclones, but decreased down to < 100 cells ml^{-1} with a fluctuation between September 7 and October 14 when 4 tropical cyclones Fengshen, Fung-Wong, Phanfone, and Vongfong passed the study areas (Fig. 2.5; Table 2.1). In GO, the MAC increased up to 9,100 cells ml^{-1} form August 29 to September 15 with a depression when the tropical cyclone Fengshen, but decreased with a small peak after the passage of the tropical cyclone Fung-Wong (Fig. 2.5). In YE, the DMAC increased up to 5,200 cells ml^{-1} form August 13 to September 11 with a fluctuation, but decreased after the passage of the tropical cyclone Fengshen and red tide patches were not found during the passage of the tropical cyclone Fung-Wong (Fig. 2.5). However, a large peak of the DMAC was found just before the tropical cyclone Phanfone passed the alert areas.

2.3.3. Relationships between tropical cyclone and wind speed and cell abundance

The DMAC in each study area in one day became very low as much as the red tide was not detectable after the passage of tropical cyclones Tembin, Bolaven, and Sanba in 2012 and Nakri in 2014 whose maximum speeds exceeded 14 m s^{-1} (Fig. 2.3 and 2.5). However, after the passage of tropical cyclone Damrey in 2012 and Halong and Fung-Wong in 2014 whose maximum speeds were 5-14 m s^{-1}, the MAC considerably reduced in the 3 study areas, but red tide events recovered within a week (Fig. 2.3 and Fig. 2.5). In 2013, *C. polykrikoides* red tides persisted for approximately 40 day from July 17 to August 25. In this red tide period, there was neither tropical cyclone nor strong wind whose maximum speeds exceeded 5 m s^{-1} (Fig. 2.4). *C. polykrikoides* red tides were terminated just after the passage of tropical cyclone Toraji in 2013 and Vongfong in 2014 (Fig. 2.4 and Fig. 2.5).

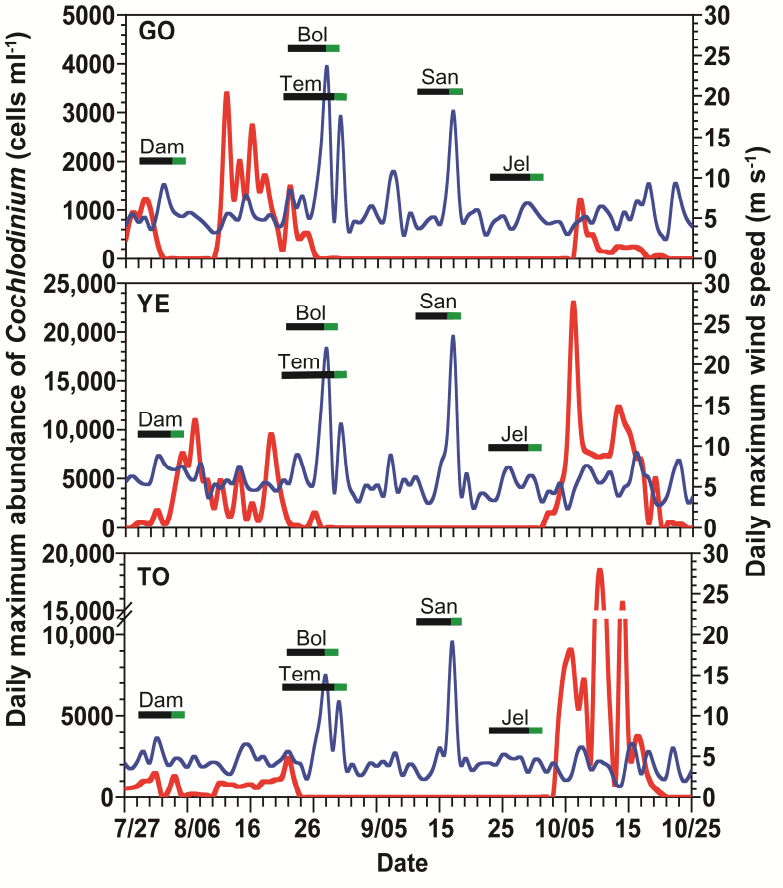

Fig. 2.3. Change of the daily maximum abundance of *Cochlodinium* cells and daily maximum wind speed in each study area in 2012. The black horizontal bar indicates the period between the created and dissipated date of each tropical cyclone and green bar indicates the period when the tropical cyclone was located in alert area (28-90 °N latitude and 0-132 °E longitude). Damery (DAM), Tembin (TEM), Bolaven (BOL), Sanba (SAN), and Jelawat (JEL) passed the alert area.

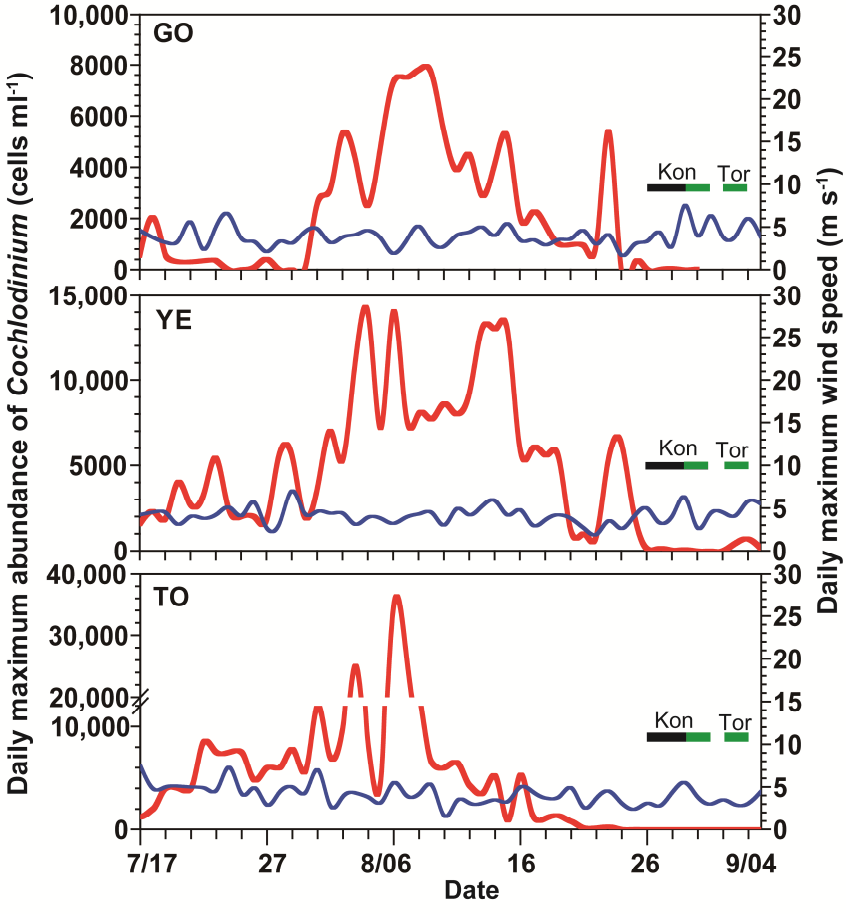

Fig. 2.4. Change of the daily maximum abundance of *Cochlodinium* cells and daily maximum wind speed in each study area in 2013. The black horizontal bar indicates the period between the created and dissipated date of each tropical cyclone and green bar indicates the period when the tropical cyclone was located in alert area (28-90 °N latitude and 0-132 °E longitude). Kong-Rey (KON) and Toraji (TOR) passed the alert area.

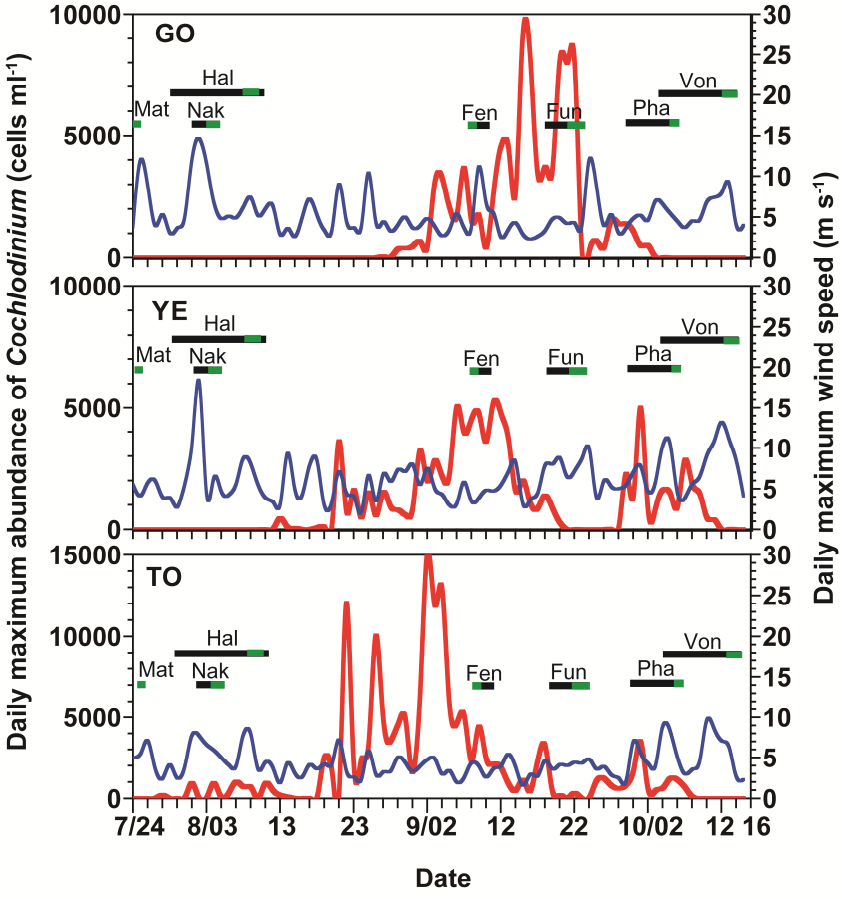

Fig. 2.5. Change of the daily maximum abundance of *Cochlodinium* cells and daily maximum wind speed in each study area in 2014. The black horizontal bar indicates the period between the created and dissipated date of each tropical cyclone and green bar indicates the period when the tropical cyclone was located in alert area (28-90 °N latitude and 0-132 °E longitude). Matmo (MAT), Halong (HAL), Nakri (NAK), Fengshen (FEN), Fung-Wong (Fun), Phanfone (PHA), and Vongfong (VON) passed alert area.

2.4. Discussion

2.4.1. Relationship between the wind speeds generated by tropical cyclones and the abundance of *Cochlodinium polykrikoides*

The daily maximum abundance of *Cochlodinium polykrikoides* (MAC) in each study area in 2013 and 2014 showed a bell shaped trend which is usually observed in other countries or other red tide events (Lee et al., 2001; Kang et al., 2009). However, the tropical cyclones giving maximum wind speeds > 14 m s^{-1} in 2012 are likely to alter this pattern. In addition, winds whose maximum wind speeds 5-14 m s^{-1} even make a big fluctuation in MAC. The change of MAC by tropical cyclones was also observed in other years (Lee et al., 2001; Lim et al., 2002). The MAC fluctuated in 1995 when the maximum wind speed induced by typhoon Ryan was 10 m s^{-1}. However, when the maximum wind speeds were 21.8 m s^{-1} (typhoon Oliwa) in 1997 and 23.3 m s^{-1} (typhoon Yanni) in 1998, the red tide events were terminated (Lee et al., 2001). Thus, this study suggests that tropical cyclones markedly affect *C. polykrikoides* red tides, but the degree of the effects of tropical cyclones depends on the maximum wind speeds. The maximum wind speed may play important role in maintenance of *C. polykrikoides* red tide.

The highest maximum abundances of *C. polykrikoides* was observed when no typhoon affected on the study areas and the maximum speeds of wind in non-typhoon period were mostly lower

than 5 m s^{-1}. However, when the maximum wind speeds were 5-14 m s^{-1}, the maximum abundance of *C. polykrikoides* decreased. Based on the laboratory experiments, the growth of the red tide dinoflagellate *Lingulodinium polyedrum* (previously *Gonyaulax polyedra*) is known to be inhibited at the wind speeds > 7.7 m s^{-1} (Thomas et al., 1995). Therefore, these two dinoflagellate species may be affected similarly by strong winds. Therefore, these speeded winds may dissipate *C. polykrikoides* cells, but not completely kill all cells. Moreover, there was no co-relationship between the maximum wind speed and DMAC. This evidence suggests that moderate winds affect the DMAC, but mild winds may not affect it. However, after the passage of Typhoon Bolaven, Tembin, Sanba, and Nakri whose maximum wind speeds were > 14 m s^{-1}, red tides did not recovered within two weeks. The strong wind generates the turbulence in the water column and turbulence could mechanically damage the cells such as cell disorientation, breakage of flagella, and even growth inhibition (White, 1976; Thomas and Gibson, 1990a, b). Thus, strong wind may destroy red tide patches and prevent to recover the red tide patch in weeks.

C. polykrikoides blooms are strongly ichthyotoxic and can kill many other organisms (Gárate-Lizárraga et al., 2004; Gobler et al., 2008; Tang and Gobler, 2009). Several studies reported that high percentage of the multiple fish species were killed or moribund when they were exposed to > 1,000 cells ml^{-1} of *C. polykrikoides* cells (Tang and Gobler, 2009; Rountos et al., 2014). Thus, the abundance of *C. polykrikoides* cells in the patches is an important factor that determines the fish mortality. In the study areas, when tropical

cyclone Damrey passed study areas in 2012, the maximum abundance of *C. polykrikoides* (DMAC) temporally decreased from 340 to 0 cells ml^{-1} in Goheung area and from 1,050 to 404 cells ml^{-1} in Tongyoung area and the maximum wind speed were 9.2 m s^{-1} in Goheung and 7.1 m s^{-1} in Tongyoung, respectively. In addition, when tropical cyclone Halong and Nakri whose the maximum wind speed 8.0 and 7.7 m s^{-1} passed Tongyoung area, the MAC decreased from 712 to 6 and 920 to 0 cells ml^{-1}. Thus, reduced cell abundance when the wind speed is greater than 7 m s^{-1} may effect on the mortality of fish in cages subsequently.

The mild winds below 5 m s^{-1} may have no effects on *C. polykrikoides* cells in the water column and result the increase of the abundance in the patches. Moreover, if the patches with high abundance of *C. polykrikoides* flow into the fish cages, the most fishes in the cages may be dead (Fig. 2.6). However, moderate winds (5–14 m s^{-1}) may temporally decrease *C. polykrikoides* abundance in the water column and it may reduce the mortality of the fishes in the cages (Fig. 2.6). Moreover, the maximum wind speeds of greater than 14 m s^{-1} may result the strong turbulence in the water column and inhibit the growth of *C. polykrikoides*. Such reduction of *C. polykrikoides* abundance in the water column may make most fishes in cages survive (Fig. 2.6). Therefore, to prevent economic losses in aquaculture during the red tide, the wind speed should be considered to predict the red tide of *C. polykrikoides*.

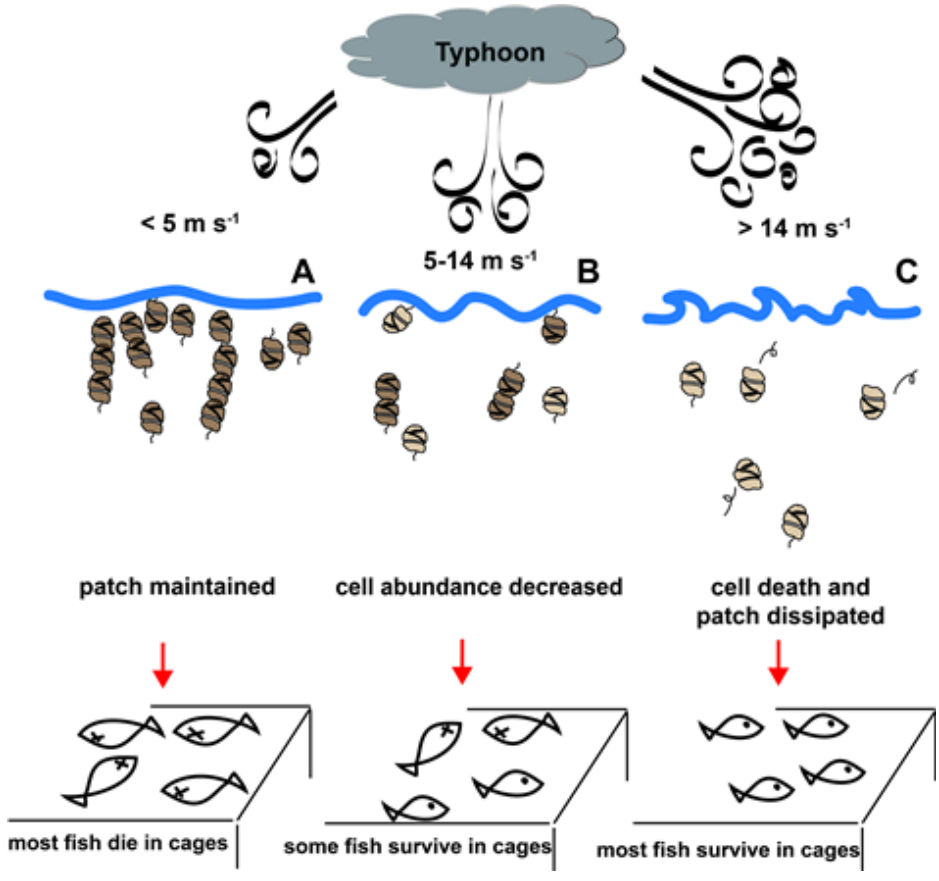

Fig. 2.6. Diagram of ecological implication of wind driven by typhoon. Mild wind (<5 m s^{-1}) has no effect on red tide patch and most fish in cages die because of maintained patch. Moderate wind (5-14 m s^{-1}) make patch disperse temporally, so some fish in cages can survive. Strong wind (>14 m s^{-1}) cause cell death and patch dissipation, so most fish in cages can survive.

Chapter 3. Effects of competing diatom species on the development of *Cochlodinium polykrikoides* red tide in the southern coastal waters of Korea.

3.1. Introduction

Dinoflagellates and diatoms are major components in planktonic communities (Allen, 1949; Chan, 1978; Ross and Sharples, 2007; Godhe et al., 2008). They often predominate the plankton assemblages and have caused red tides (Oviatt et al., 1989; Kremp et al., 2008; Jeong et al., 2010a, b). Some diatoms sometime caused red tides that kill fish, but most diatoms are not harmful to marine organisms. In particular, dinoflagellates have caused notorious red tides or harmful algal blooms (Hallegraeff, 1993; Anderson, 1997; Kudela and Gobler, 2012; Lee et al., 2013; Park et al., 2013a). Toxins produced by some dinoflagellates are very harmful to marine organisms (Geraci et al., 1989; Van Dolah, 2000; Pierce et al., 2003; Landsberg et al., 2009; Kudela and Gobler, 2012). In general, the growth rate of a dinoflagellate species is lower than that of a diatom species having a size similar to the dinoflagellate (Banse, 1982). The production of toxins, bioluminescence, feeding enzymes may cause lower growth rates of dinoflagellates. However, dinoflagellates sometimes outcompete diatoms by feeding and/or allelopathy (Fistarol et al., 2004; Kremp et al., 2008; Yoo et al., 2009; Tang and Gobler, 2010). To the contrary, diatoms may have negative effects on the growth

inhibition of dinoflagellates by allelochemicals (Elbrächter, 1977; Nagaseo et al., 2006a; Wang et al., 2013).

The distribution of *Cochlodinium polykrikoides* is often reverse to that of diatoms (Jeong et al., 2000; Cho 2010). Furthermore, *C. polykrikoides* patches are often replaced by diatoms at the decline stage of its red tides or the passage of typhoon (Lim et al., 2007, 2008, 2009; Chung et al., 2012). Therefore, diatoms may inhibit the growth of *C. polykrikoides* by some means. There are several studies that chemicals from diatoms may inhibit growth of dinoflagellates (Nagaseo et al., 2006a; Yamasaki et al., 2010; Wang et al. 2013). For instance, *Skeletonema costatum* inhibited the growth rate of *Gyrodinium instriatum* and caused morphological modification when the cultures incubated together for 15 days (Nagaseo et al., 2006a). *S. costatum* showed also inhibitory effects on *Prorocentrum dentatum* and *Prorocentrum triestinum* as *Prorocentrum* species had longer lag period time to reach the exponential growth stage than control cultures (Yamasaki et al., 2010). However, the most studies about the interactions between dinoflagelltes and diatoms are focused on the allelochemical effects.

To explore possible inhibitory effects by diatoms on *C. polykrikoides*, I measured the swimming speed of *C. polykrikoides* as a function of the concentration of each of the diatoms *Skeletonema costatum*, *Chaetoceros danicus*, and *Thalassiosira decipiens*. In addition, I monitored the abundance of *C. polykrikoides* for 10 days after this dinoflagellate was mixed with *S. costatum* and *C. danicus*. The results provide a basis for understanding the interactions

between *C. polykrikoides* and common diatoms and red tide dynamics of *C. polykrikoides*.

3.2. Materials and methods

3.2.1. Collection and culture of experimental organisms

Cochlodinium polykrikoides was isolated from plankton samples collected from the Tongyoung, Korea, in Aug 2002, when the water temperature and salinity were 21.1 °C and 32.1, respectively. The samples were screened gently through a 154-μm Nitex mesh and placed in 6-well tissue culture plates. A monoclonal culture of *C. polykrikoides* was established by two serial single cell isolations. As the concentration of *C. polykrikoides* increased, the cells were subsequently transferred to 32-, 270-, and 500-ml polycarbonate (PC) bottles in enriched f/2 seawater media (Guillard and Ryther, 1962). The bottles were placed at 20 °C under an illumination of 100 μE m^{-2} s^{-1} of cool white fluorescent light on a 14:10 h light-dark cycle.

Chaetoceros danicus (KMMCC 1364), *Skeletonema costatum* (KMMCC 660), *Thalassiosira decipiense* (KMMCC 698) were obtained from Korea Marine Microalgae Culture Center (KMMCC) in Korea. These *C. danicus* and *S. costatum* strains were isolated from coastal water off Jindong, Korea on December 2006 and February 1999, respectively. *T. decipiens* was isolated from coastal water off Hadong, Korea on October 1999 when the water temperature was 22 °C. The cultures were maintained in enriched f/2 sea water media under an illumination of 100 μE m^{-2} s^{-1} of cool white fluorescent light on a 14:10 h light-dark cycle at 20 °C.

3.2.2. Effects of diatoms on the swimming speed of *Cochlodinium polykrikoides*

To explore the effects of the diatom concentration and filtrates on the swimming speed of *C. polykrikoides*, we measured the swimming speeds of *C. polykrikoides* at 8 different concentrations of *S. costatum* (Expt 1) and at 6 different concentrations of *C. danicus* (Expt 3) and *T. decipiens* (Expt 5) (i.e., physical contact + chemical effect) and corresponding filtrates (Expt 2, 4, and 6) (i.e., chemical effect only) (Table 3.1).

Dense cultures of *C. polykrikoides*, *C. danicus*, *S. costatum*, and *T. decipiens* maintained in f/2 media were transferred to 270 ml polycarbonate (PC) bottles. Cells in three 1-ml aliquots from each bottle were enumerated to determine the concentration of each species.

In experiment 1, 3, and 5, the initial concentrations of *C. polykrikoides* and each target diatom were established using an autopipette to deliver predetermined volumes of known cell concentrations to the 6-well plates (Table 3.1). In experiments 2, 4, and 6, the water of a bottle containing diatoms of a target concentration was filtered through a 0.7-μm GF/F filter (i.e., filtrate) and then added to each experimental well. A predetermined volume of *C. polykrikoides* was added to the well. In this process, dilution effects were considered. A well containing *Cochlodinium* only without diatom cells in each experiment were set as a control well.

After 24 h incubation, wells were placed on the dissecting microscope with using a video analyzing system (Samsung, SV-C660, Seoul, Korea) and using a CCD camera (Hitachi, KP-D20BU, Tokyo, Japan). I measured swimming speeds of *C. polykrikoides* cells in each well. The video camera focused on an individual field viewed as a single circle in a cell culture flask under a dissecting microscope at 20 °C. Swimming of *C. polykrikoides* cells in each well was then recorded at a magnification of 40×. I analyzed the mean and maximum swimming velocities for all swimming cells viewed during the first 10 min. The average swimming speed (n = 10) for each diatom concentration or filtrate was calculated on the basis of the linear displacement of cells in 1 sec, during single-frame playback.

3.2.3. Effects of diatom concentrations on the growth rate of *Cochlodinium polykrikoides*

Experiment 7 and 8 were designed to investigate whether *C. danicus* and *S. costatum* affect growth of *C. polykrikoides* (Table 3.1).

The initial concentrations of *C. polykrikoides* and each target diatom were established using an autopipette to deliver predetermined volumes of known cell concentrations to the bottles. Triplicate 80-ml PC experiment bottles (containing mixtures of *Cochlodinium* and diatom species), triplicate control bottles (containing diatom species only), and triplicate control bottles (containing *Cochlodinium* only)

were set up for each *Cochlodinium*-diatom combination. To make the water conditions similar, the filtrates of a *Cochlodinium* culture was filtered through a 0.7-μm GF/F filter and then added into the diatom control bottles in the same amount as the volume of the *Cochlodinium* culture added into the experimental bottles for each *Cochlodinium*-diatom combination. Nutrients (nitrate, phosphate, and silicate) were added as much as the final concentrations of these reached the same amount of concentration of F/2 medium. The bottles were then filled to capacity with freshly-filtered seawater and capped. To determine the actual *Cochlodinium* and diatom concentrations, a 5-ml aliquot was removed from each bottle and fixed with 5% Lugol's solution, and all or >200 each species cells in three 1-ml SRCs were enumerated. Each bottle were filled again to capacity with F/2 medium, capped, and placed in the chamber. Total 5-ml aliquot was subsampled every other day for 10 days. The dilution of the cultures associated with refilling the bottles was considered in calculating the growth rates.

The specific growth rates of *Cochlodinium polykrikoides* and each diatom species were calculated as follows:

$$\mu = \frac{\mathrm{Ln}\,(C_t/C_0)}{t}$$

where C_0 is the initial concentration of each species and C_t is the final concentration after time t. The time period was 10 d.

Table 3.1. Experimental design. The numbers in the dinoflagellate and diatom columns are the initial densities (cells ml^{-1}) of algal species. Values shown in parentheses in the each column are the initial densities in the control bottles.

Dinoflagellate			Diatom	
Expt.	Species	Density	Species or filtrate	Density
1	*Cochlodinium polykrikoides*	400	*Skeletonema costatum*	0, 500, 5000, 25000, 50000, 100000, 200000, 500000
2	*Cochlodinium polykrikoides*	400	Filtrate of *S. costatum*	Filtrates from a culture with a cell concentration of 0, 500, 5000, 25000, 50000, 100000, 200000, or 500000
3	*Cochlodinium polykrikoides*	400	*Chaetoceros danicus*	0, 1000, 5000, 10000, 25000, 50000
4	*Cochlodinium polykrikoides*	400	Filtrate of *C. danicus*	Filtrates from a culture with a cell concentration of 0, 1000, 5000, 10000, 25000, or 50000
5	*Cochlodinium polykrikoides*	400	*Thalassiosira decipiens*	0, 1000, 5000, 10000, 25000, 50000
6	*Cochlodinium polykrikoides*	400	Filtrate of *T. decipiens*	Filtrates from a culture with a cell concentration of 0, 1000, 5000, 10000, 25000, or 50000
7	*Cochlodinium polykrikoides*	107 (118)	*S. costatum*	86 (116)
8	*Cochlodinium polykrikoides*	44 (25)	*C. danicus*	77 (85)

3.2.4. Statistical analyses

An ANOVA test was used to determine whether the swimming speeds of *Cochlodinium polykrikoides* varied significantly at different diatom or filtrate concentrations (Zar, 1984). In addition, a t-test was used to determine whether the swimming speed of *C. polykrikoides* at one diatom concentration or filtrate was different from that of the control (without added diatoms or filtrate). Statistical significance was defined as $p < 0.05$.

3.3. Results

3.3.1. Effects of diatom concentrations on the swimming speed of *Cochlodinium polykrikoides*

When the swimming behavior and speed of *C. polykrikoides* were observed under light microscopy, the diatoms *Skeletonema costatum, Chaetoceros danicus*, and *Thalassiosira decipiens* trapped *C. polykrikoides* cells and eventually lower swimming speed of the dinoflagellate (Fig. 3.1). In addition, dead *C. polykrikoides* cells were found after 24 h incubation with the diatoms (Fig. 3.1).

Fig. 3.1. Effects of diatoms on *Cochlodinium polykrikoides*. Intact *C. polykrikoides* cell in control at T = 0h (A). *C. polykrikoides* cells in controls after 24h without diatom cells (B). *C. polykrikoides* cells with diatom *Chaetoceros danicus* at T = 0h (C) and inflated and decomposed *C. polykrikoides* cells after 24h incubation with *C. danicus* (D). Scale bars = 20 μm.

The swimming speeds of *C. polykrikoides* at 8 different concentrations of *S. costatum* after 24 h incubation were significantly different from one another ($p < 0.005$, 2-tailed ANOVA) (Fig. 3.2A). The swimming speed (mean ± SE, n = 10) of *C. polykrikoides* in the control bottles (1,395 ± 75 μm) was significantly greater than that at the *Skeletonema* concentrations of 5,000-500,000 cells ml^{-1} ($p < 0.01$, 1-tailed t test), but was not greater than that at the *Skeletonema* concentration of 500 cells ml^{-1} ($p > 0.1$). When the filtrates from the cultures of *S. costatum* were added, the swimming speed (mean ± SE, n = 10) of *C. polykrikoides* in the control bottles (1,395 ± 75 μm) was significantly greater than that in the filtrates from the cultures originally containing the *Skeletonema* concentrations of 250,000-500,000 cells ml^{-1} ($p < 0.01$, 1-tailed t test), but it was not greater than that with the *Skeletonema* concentration of 500-100,000 cells ml^{-1} ($p > 0.1$) (Fig. 3.2B).

The swimming speeds of *C. polykrikoides* at 6 different concentrations of *Chaetoceros danicus* after 24 h incubation were significantly different from one another ($p<0.005$, 2-tailed ANOVA) (Fig. 3.3A). The swimming speed (mean ± SE, n = 10) of *C. polykrikoides* in the control bottles (978 ± 76 μm) was significantly greater than that at the *Chaetoceros* concentrations of 25,000-50,000 cells ml^{-1} ($p<0.01$, 1-tailed t test), but was not greater than that at the *Chaetoceros* concentration of 1,000-10,000 cells ml^{-1} ($p>0.1$). When the filtrates from the cultures of *C. danicus* were added, the swimming speed (mean ± SE, n=10) of *C. polykrikoides* in the control bottles (978 ± 76 μm) was significantly greater than that in the filtrates from the cultures originally containing the *Chaetoceros*

concentration of 50,000 cells ml^{-1} ($p<0.005$, 1-tailed t test), but it was not greater than that with the *Chaetoceros* concentration of 1,000-25,000 cells ml^{-1} ($p>0.05$) (Fig. 3.3B).

The swimming speeds of *C. polykrikoides* at 6 different concentrations of *Thalassiosira decipiens* after 24 h incubation were significantly different from one another ($p<0.005$, 2-tailed ANOVA) (Fig. 3.4A). The swimming speed (mean ± SE, n=10) of *C. polykrikoides* in the control bottles (1,250 ± 29 μm) was significantly greater than that at the *Thalassiosira* concentrations of 1,000-50,000 cells ml^{-1} ($p<0.01$, 1-tailed t test). When the filtrates from the cultures of *T. decipiens* were added, the swimming speed (mean ± SE, n=10) of *C. polykrikoides* in the control bottles (1,250 ± 29 μm) was significantly greater than that in the filtrates from the cultures originally containing the *Thalassiosira* concentration of 1,000-50,000 cells ml^{-1} ($p<0.005$ for the concentrations of 5,000-50,000 cells ml^{-1} and $p<0.01$ for the concentration of 1,000 cells ml^{-1}, 1-tailed t test) (Fig. 3.4B).

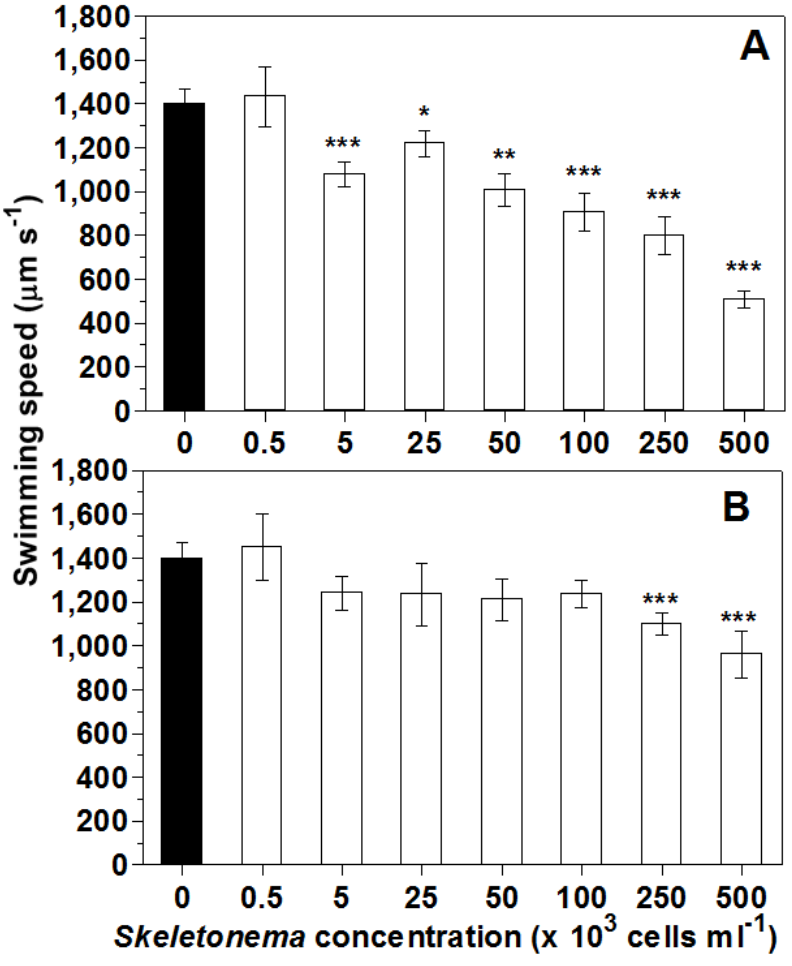

Fig. 3.2. Swimming speed (μm s^{-1}) of *Cochlodinium polykrikoides* at 8 different cell concentrations of *Skeletonema costatum* (A) or filtrates from a culture with a corresponding cell concentration (B) (see M&M for details). Symbols represent treatment means ± 1SE. *:$p<0.05$. **:$p<0.01$. ***:$p<0.005$.

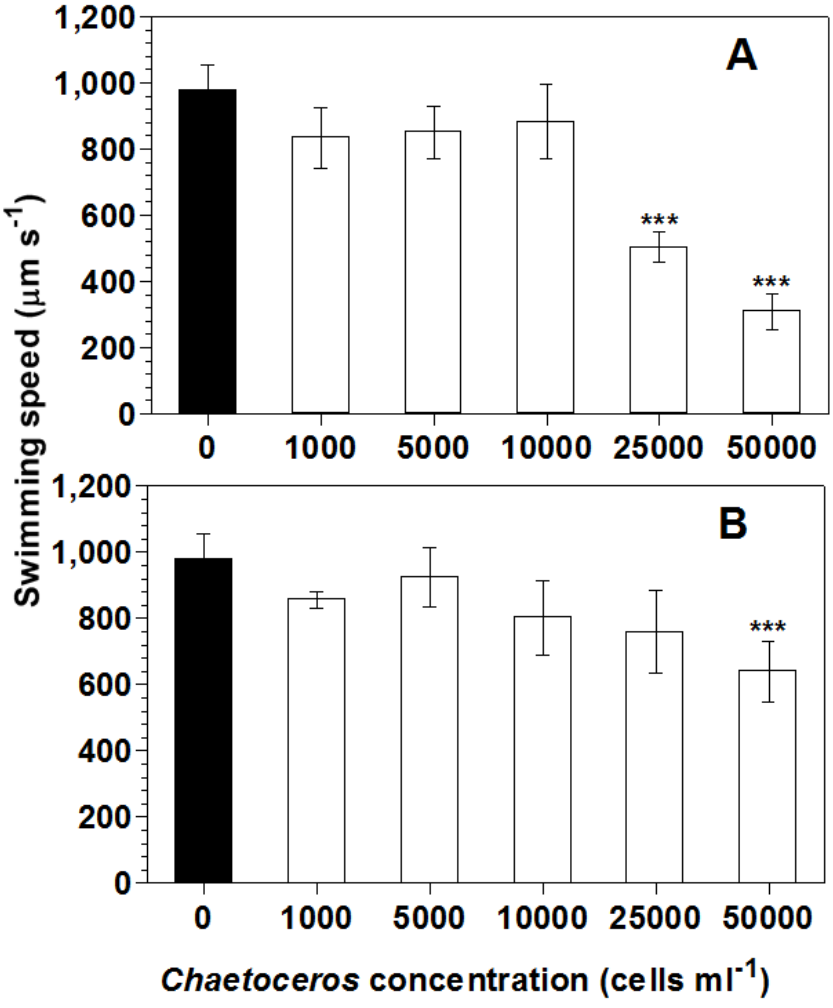

Fig. 3.3. Swimming speed (μm s^{-1}) of *Cochlodinium polykrikoides* at 6 different cell concentrations of *Chaetoceros danicus* (A) or filtrates from a culture with a corresponding cell concentration (B). Symbols represent treatment means ± 1SE. **:$p<0.01$. ***:$p<0.005$.

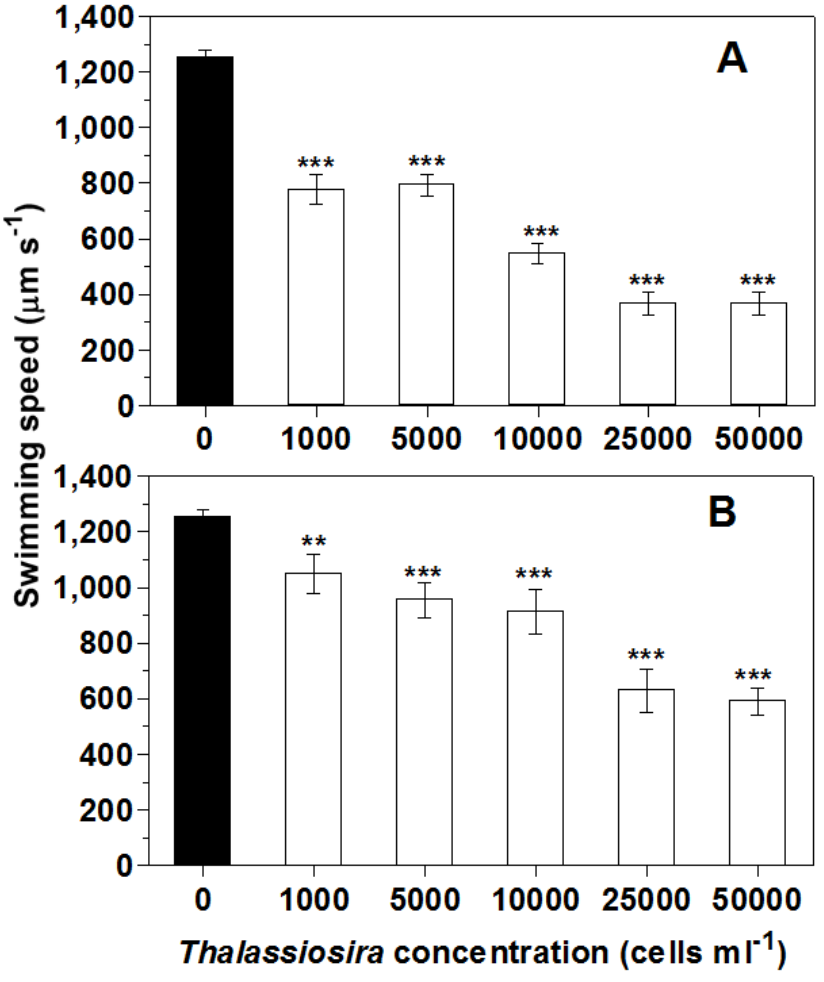

Fig. 3.4. Swimming speed (μm s^{-1}) of *Cochlodinium polykrikoides* at 6 different cell concentrations of *Thalassiosira decipiens* (A) or filtrates from a culture with a corresponding cell concentration (B). Symbols represent treatment means ± 1SE. **:$p<0.01$. ***:$p<0.005$

3.3.2. Effects of diatom concentrations on the growth rate of *Cochlodinium polykrikoides*

The abundances of *C. polykrikoides* incubated with *Skeletonema costatum* at 1:1 in cell abundance changed in the similar manner with those without *S. costatum* (i.e., in control bottle) for the first 4 elapsed days (Fig. 3.5A). In this period, the abundance of *S. costatum* in the experimental bottles increased from 44 to 132,995 cells ml^{-1}, while that in the control bottles increased from 118 to 49,811 cells ml^{-1} (Fig. 3.5B). However, the concentration of *C. polykrikoides* incubated with *S. costatum* at Day 4-10 decreased from 110 to 15 cells ml^{-1}, while that without *S. costatum* increased 133 to 144 cells ml^{-1} (Fig. 3.5A). In this period, the concentration of *S. costatum* in the experimental bottles increased from 132,995 to 407,514 cells ml^{-1}, while that in the control bottles increased from 49,811 to 644,931 cells ml^{-1}. Thus, *S. costatum* caused negative growth of *C. polykrikoides* at the *S. costatum* concentrations > 132,995 cells ml^{-1} (Fig. 3.5B).

The abundances of *C. polykrikoides* incubated with *Chaetoceros danicus* at 1:1 in cell abundance changed in the similar manner with those without *C. danicus* (i.e., in control bottle) for the first 4 elapsed days (Fig. 3.6A). In this period, the cell concentration of *C. danicus* in the experimental bottles increased from 84 to 1,134 cells ml^{-1}, while that in the control bottles increased from 81 to 1,493 cells ml^{-1} (Fig. 3.6B). However, the concentration of *C. polykrikoides* incubated with *C. danicus* at Day 4-8 decreased from 71 to 63 cells ml^{-1}, while that without *C. danicus* increased 35 to 71 cells ml^{-1} (Fig. 3.6A). In this period, the concentration of *C. danicus* in the experimental bottles

increased from 1,134 to 15,667 cells ml^{-1}, while that in the control bottles increased from 1,493 to 15,398 cells ml^{-1} (Fig. 3.6B). Furthermore, the abundance of *C. polykrikoides* incubated with *C. danicus* at Day 8-10 decreased from 63 to 40 cells ml^{-1}, while that without *C. danicus* increased 71 to 77 cells ml^{-1} (Fig. 3.6A). In this period, the concentration of *C. danicus* in the experimental bottles increased from 15,667 to 21,213 cells ml^{-1}, while that in the control bottles increased from 15,398 to 23,656 cells ml^{-1} (Fig. 3.6B). Thus, *C. danicus* did not affect growth of *C. polykrikoides* at the diatom concentration of 1,134 cells ml^{-1}. However, *C. danicus* caused negative growth of *C. polykrikoides* at the diatom concentrations of 5,781 - 21,210 cells ml^{-1}.

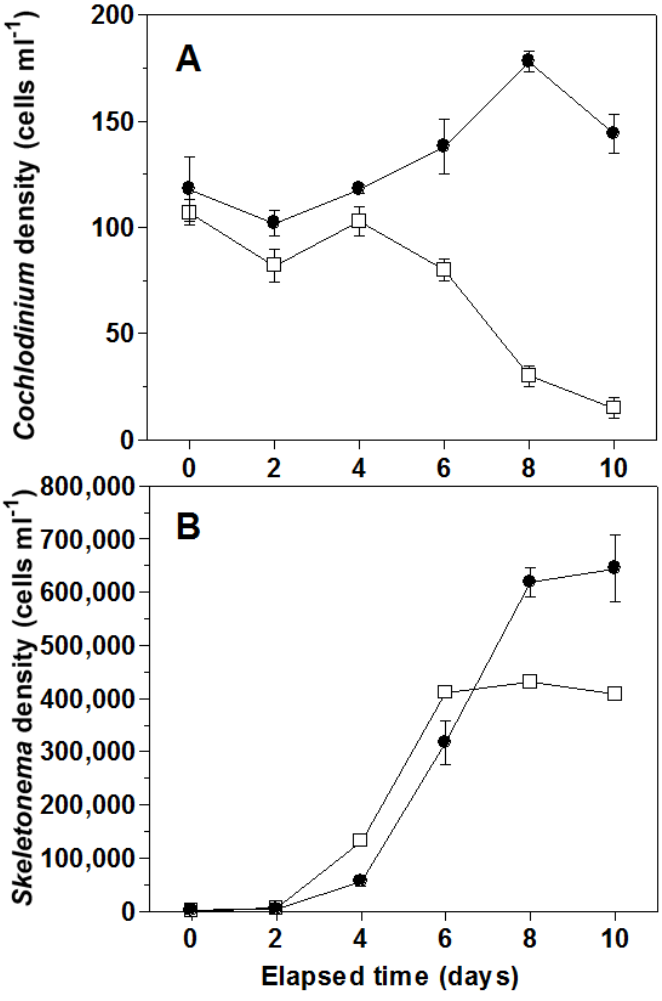

Fig. 3.5. The concentrations (cells ml^{-1}) of *Cochlodinium polykrikoides* (A) and *Skeletonema costatum* (B) as a function of elapsed incubation time. Symbols represent treatment means ± 1SE. Open squares: Concentrations in the experimental bottles (i.e., mixture of *C. polykrikoides* and *S. costatum*). Close circles: Concentrations in the control bottles (i.e., *C. polykrikoides* or *S. costatum* only).

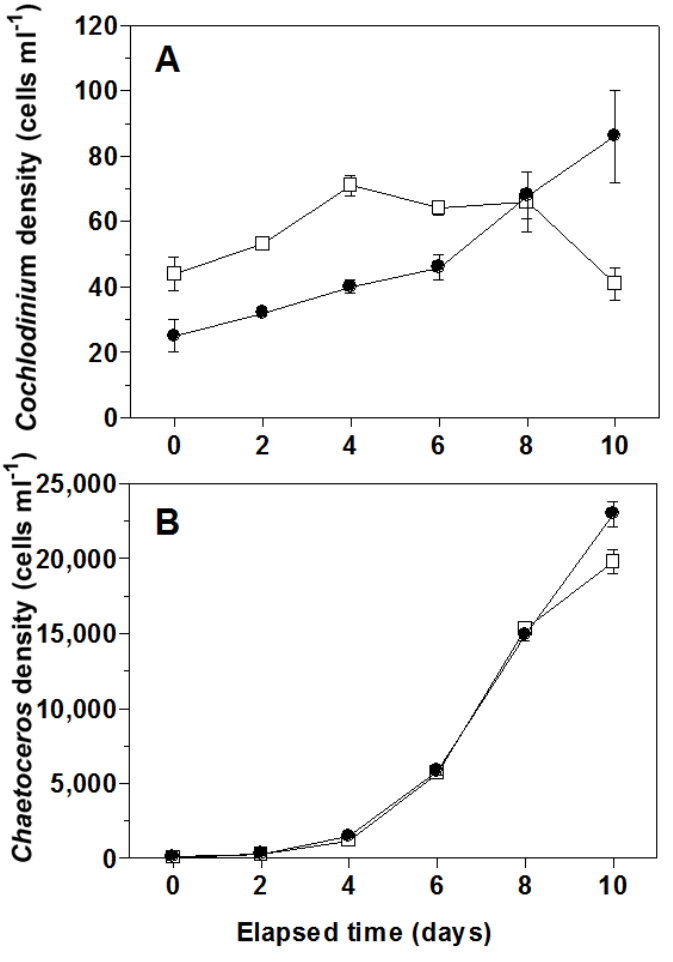

Fig. 3.6. The concentrations (cells ml^{-1}) of *Cochlodinium polykrikoides* (A) and *Chaetoceros danicus* (B) as a function of elapsed incubation time. Symbols represent treatment means ± 1SE. Open squares: Concentrations in the experimental bottles (i.e., mixture of *C. polykrikoides* and *C. danicus*). Close circles: Concentrations in the control bottles (i.e., *C. polykrikoides* or *C. danicus* only).

3.4. Discussion

3.4.1. Effects of diatom concentrations on the swimming speed of *Cochlodinium polykrikoides*

Skeletonema costatum, Chaetoceros danicus, and *Thalassiosira decipiens*, all 3 common diatoms tested in the present study lower swimming speed of *C. polykrikoides* cells when the concentrations of *S. costatum, C. danicus*, and *T. decipiens* exceed 5,000, 1,000, and 1,000 cells ml^{-1}. However, the filtrates of *S. costatum, C. danicus*, and *T. decipiens* lower swimming speed of *C. polykrikoides* cells when the concentrations of *S. costatum, C. danicus*, and *T. decipiens* exceed 25,000, 25,000, and 1,000 cells ml^{-1}. Thus, *S. costatum* lower the swimming speed of *C. polykrikoides* by both physical contact and chemical cue at the *S. costatum* concentrations of 250,000-500,000 cells ml^{-1}, but mainly by physical contact at the concentrations of 5,000-100,000 cells ml^{-1}. In the case of *C. danicus*, this diatom lower the swimming speed of *C. polykrikoides* by both physical contact and chemical cue at the *C. danicus* concentration of 50,000 cells ml^{-1}, but mainly by physical contact at the concentration of 25,000 cells ml^{-1}. *T. decipiens* lower the swimming speed of *C. polykrikoides* by both physical contact and chemical cue at the *T. decipiens* concentrations of 1,000-50,000 cells ml^{-1}. That is, the swimming speed of *C. polykrikoides* is affected by relatively low abundance of *T. decipiens*. The concentrations of *S. costatum* > 5,000 cells ml^{-1}, *C. danicus* > 1,000 cells ml^{-1}, and *T. decipiens* > 1,000 cells ml^{-1} are not unusual in natural environments (Jeong et al., 2013). Many diatoms produce some secondary metabolites such as polyunsaturated aldehydes

(PUAs) and polyunsaturated fatty acids (PUFAs)(Leflaive and Ten-Hage, 2009). These PUAs and PUFAs are considered to be a allelopatic chemicals to the competitiors. *Skeletonema costatum* are known to produce PUA (Wichard et al., 2005). Thus, the other two diatom species examined in this study may produce the PUAs and/or PUFAs, and may resulted the growth inhibition of *C. polykrikoides* at the high concentrations.

C. polykrikoides migrates between the surface and 20 m depth (Park et al., 2001; Kim et al., 2010). It can receive light for photosynthesis in the surface water, and nutrients in deep waters. The maximum growth rate of *C. polykrikoides* (0.54 d^{-1}) is lower than that of co-occurring competing dinoflagellates such as *Akashiwo sanguinea* (1.19 d^{-1}), *Prorocentrum minimum* (1.36 d^{-1}), and *Gymnodinium instriatum* (0.63 d^{-1}) (Matsubara et al., 2007; Yamatogi et al., 2005; Nagaseo et al., 2006b; Kondo et al., 1990). However, this fasts wimming ability may enable *C. polykrikoides* to defeat the relatively slow swimming dinoflagellates, in particular when the thermocline is located in deep waters and the concentration of nutrients in the surface waters is low. However, the reduction of swimming speed due to diatoms may give a disadvantage to *C. polykrikoides* (Fig. 3.7).

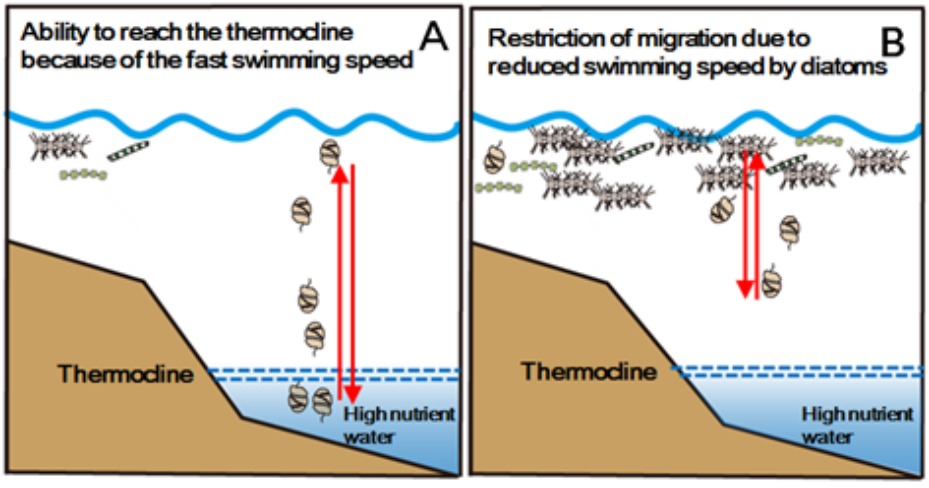

Fig. 3.7. Diagram of the ability of *Cochlodinium polykrikoides* to reach deep water where nutrient concentration is high and the location of thermocline when diatom concentrations are low (A) and high (B). Cells of *C. polykrikoides* pass the thermocline and reach deep water by active vertical migration when diatom concentrations are low (A), while the swimming speed and depth to which *C. polykrikoides* can swim are reduced when diatom concentrations are high (B).

3.4.2. Effects of diatom concentrations on the growth rate of *Cochlodinium polykrikoides*

The growth of *C. polykrikoides* was inhibited when *C. polykrikoides* was incubated with *Skeletonema costatum* or *Chaetoceros danicus*. After 4 elapsed days, when the abundance of *S. costatum* was reached approximately 50,000 cells ml^{-1}, the abundance of *C. polykrikoides* was start to decrease in experimental bottles. The abundance of *C. polykrikoides* in the experimental bottle was dropped down to 15 cells ml^{-1} at the end of the experiment, while that in the control bottles was increased to 144 cells ml^{-1} at the same periods. The abundance of *C. polykrikoides* incubated with *C. danicus* was also start to decrease at 4 elapsed days when the abundance of *C. danicus* was reached 1,188 cells ml^{-1} in the experimental bottles. The abundance of the *C. polykrikoides* in the experimental bottle was dropped down to 41 cells ml^{-1} at the end of the experiment, while that in the control bottles was increased to 86 cells ml^{-1} at the same periods. Thus, the fast growth of diatoms may inhibit the growth of *C. polykrikoides* when they coexist in the natural environment.

The rainfall plays an important role in influx of nutrients into the coastal waters (e.g. Kim et al., 2013). When the concentrations of nutrients in the water are high enough, diatoms grow faster than other flagellate (Banse, 1982). The maximum growth rates of *Thalassiosira pseudonana* is 2.77 d^{-1} while, the maximum growth of *C. polykrikoides* is 0.61 d^{-1} (Passche, 1973; Yamatogi et al., 2005). Thus, if the growth of diatoms is stimulated by high concentrations of nutrients by rainfall, the high abundance of diatom may prevent

the outbreak of the red tide of *C. polykrikoides* (Fig. 3.8).

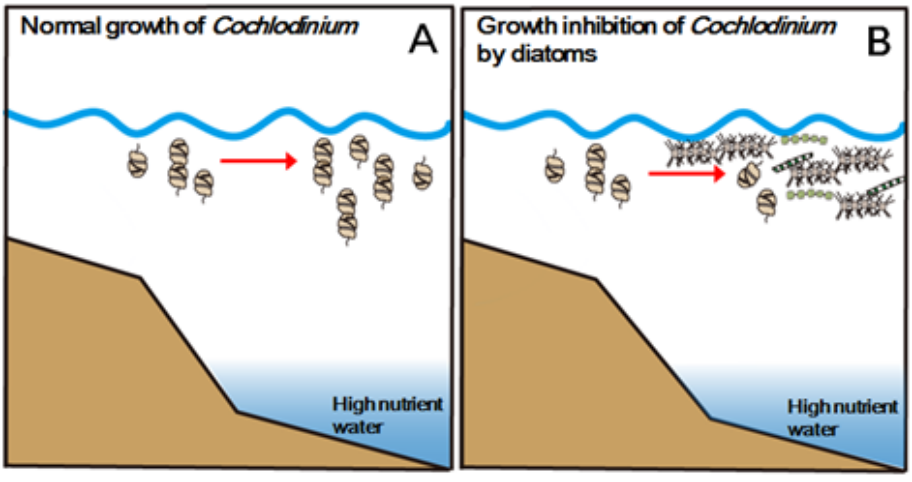

Fig. 3.8. Diagram of the growth of *Cochlodinium polykrikoides* when diatom concentrations are low (A) and high (B). The concentration of *C. polykrikoides* is maintained or increases when diatom concentrations are low (A), while concentration of *C. polykrikoides* decreases when diatom concentrations are high (B).

Prior to this study, most studies on interactions between *C. polykrikoides* and co-occurring species showed that *C. polykrikoides* had harmful effects on co-occurring species through allelochemicals or cell contact (Table 3.2); when co-occurring phytoplankton species were incubated with *C. polykrikoides*, they lost flagella and motility or experienced other cell morphological modification (Tang and Gobler, 2010). Furthermore, *C. polykrikoides* may inhibit the growth of *Akashiwo sanguinea* by cell contact (Yamasaki et al., 2007). However, the results of this study provide clear evidence that diatoms inhibit the swimming speeds, the growth rate, and the eventual depths that *C. polykrikoides* is able to reach.

Table 3.2. The interactions between *Cochlodinium polykrikoides* (Cp) and co-occurring phytoplankton species. DN, dinoflagellate; RA, raphidophyte; DA, diatom; GI, growth inhibition; MM, morphological modification.

Phytoplankton		Conditions	Effects	Ref.
DN	*Akashiwo sanguinea*	i) whole cell addition	GI, MM	(1)
		ii) 5 μm mesh barrier	GI, MM	(1)
DN	*Gyrodinium instriatum*	i) whole cell addition	GI, MM	(1)
		ii) 5 μm mesh barrier	GI, MM	(1)
DN	*Gymnodinium aureolum*	whole cell addition	GI, MM	(1)
DN	*Heterocapsa rotundata*	whole cell addition	GI, MM	(1)
DN	*Scrippsiella* cf. *trochoidea*	whole cell addition	GI, MM	(1)
RA	*Chattonella marina*	i) whole cell addition	GI, MM	(1)
		ii) 5 μm mesh barrier	GI, MM	(1)
RA	*Rhodomonas salina*	whole cell addition	GI, MM	(1)
DA	*Thalassiosira weissflogii*	whole cell addition	GI, MM	(1)
DN	*Akashiwo sanguinea*	i) whole cell addition	GI, MM	(2)
		ii) filtrates from Cp	no effect	(2)
		iii) non-contact condition	no effect	(2)

(1) Gobler et al. (2010), (2) Yamasaki et al., (2007)

Chapter 4. Taxonomy of *Alexandrium pohangense* n. sp., a new mixotrophic predator of *Cochlodinium polykrikoides*

4.1. Introduction

Cochlodinium polykrikoides is a bloom forming dinoflagellate in the coastal waters of many countries and causes massive fish mortality and economic loss in many countries (Gobler et al., 2008; Jeong et al., 2008; Mulholland et al., 2009; Park et al., 2013a; Lim et al., 2014a, 2015b). Moreover, some studies suggested that populations of grazers may have considerable grazing impact on populations of bloom forming species (Jeong et al., 2004a, 2005d; Yoo et al., 2013). Thus, the predators of *C. polykrikoides* may be important factors to understand the population dynamics of *C. polykrikoides*. Several heterotrophic protists and ciliate are known to feed on *C. polykrikoides* (Jeong et al., 1999b, 2006, 2007, 2008; Cho, 2006; Lim et al., 2014b). However, mixotrophic predators of *C. polykrikoides* have not been revealed yet. Mixotrophic ability of the dinoflagellate is also considered as an important factor to form a harmful algal bloom (e.g., Jeong et al., 2010a). Furthermore, some mixotrophic dinoflagellates have a greater growth rate when they feed on the prey compared to phototrophic mode (Lee et al., 2014a). Thus, to better understand the population dynamics of *C. polykrikoides*, the mixotrophic predators should be explored.

Recently, I newly isolated and established a clonal culture of *Alexandrium* sp. from waters off Pohang, Korea, in 2014 when a huge *Cochlodinium* red tide was occurred. The genus *Alexandrium* is one of the most studied dinoflagellates (Franks and Anderson, 1992; Hallegraeff, 1993; Scholin et al., 1994; Anderson et al., 2012). The genus *Alexandrium* was first described by Halim (1960). More than thirty species have been reported and new *Alexandrium* species have been continuously established (MacKenzie et al., 2004; Anderson et al., 2012; John et al., 2014; Murray et al., 2014). Some *Alexandrium* species are known to be responsible for paralytic shellfish poisoning (PSP) (Hallegraeff, 1993; Anderson et al., 2012). PSP has caused loss of wild and cultured shellfish, negative impact on tourism and recreation activities, and even human illness from consumption of contaminated shellfish or fish by *Alexandrium*. Due to their harmful effects, the scientists in many countries have paid attention on *Alexandrium*. Thus, an accurate identification is very important to prevent the potential risk by *Alexandrium* species.

Alexandrium species are identified based on the some morphological differences such as the size and shape of cells, the size and shape of the first apical (1′) and sixth precingular (6′′) plates, thecal ornamentation, the presence or absence of ventral pore and sulcal lists, the shape of the pore plate (Po), the connection between the Po and 1′ plate, the size and shape of sulcal plates, and the ability to form chains (Balech, 1995). However, due to ambiguity of some morphological features, the molecular and phylogenetic studies for identification of *Alexandrium* species have consistently used and some of morphological features have supported monophyletic clades

based on the ribosomal DNA regions (Scholin et al., 1994; John et al., 2003; Leaw et al., 2005; Lilly et al., 2007; Orr et al., 2011; John et al., 2014; Kremp et al., 2014).

To identify the *Alexandrium* species which is able to feed on *Cochlodinium polykrikoides*, the morphology of the strain analyzed using light microscopy, scanning electron microscopy (SEM) and the phylogenetic affinities using DNA sequences of the small subunit (SSU), internal transcribed spacers (ITS) 1 and 2, 5.8S, and the large subunit (LSU) rDNA examined. On the basis of morphological and phylogenetic criteria, I proposed that this is a new species of the genus *Alexandrium.*

4.2. Materials and methods

4.2.1. Collection and culture of *Alexandrium pohangense* n. sp.

Alexandrium pohangense was isolated from plankton samples collected from waters off Pohang, Korea, in September 2014, when the water temperature and salinity were 23.3 °C and 31.1, respectively (Fig. 4.1). Samples were sieved gently through a 154-μm Nitex mesh sieve and transferred to 6-well tissue culture plates. A clonal culture of *A. pohangense* strain was established by two serial single cell isolations. As the concentration of *A. pohangense* increased, the cells were subsequently transferred to 32-, 270-, and 500-ml polycarbonate (PC) bottles. The bottles were captaining fresh f/2 seawater media and *A. pohangense* capped, and placed on a shelf at 20 °C under an illumination of 50 μE m^{-2} $s^{-1}$of cool white fluorescent light on a 14:10 h light-dark cycle. When cultures became dense, they were transferred to new 500-ml PC bottles containing fresh f/2 seawater media approximately every 2-3 weeks. These cultures were used for genetic and morphological analyses. Only cultures in the exponential growth phase were used.

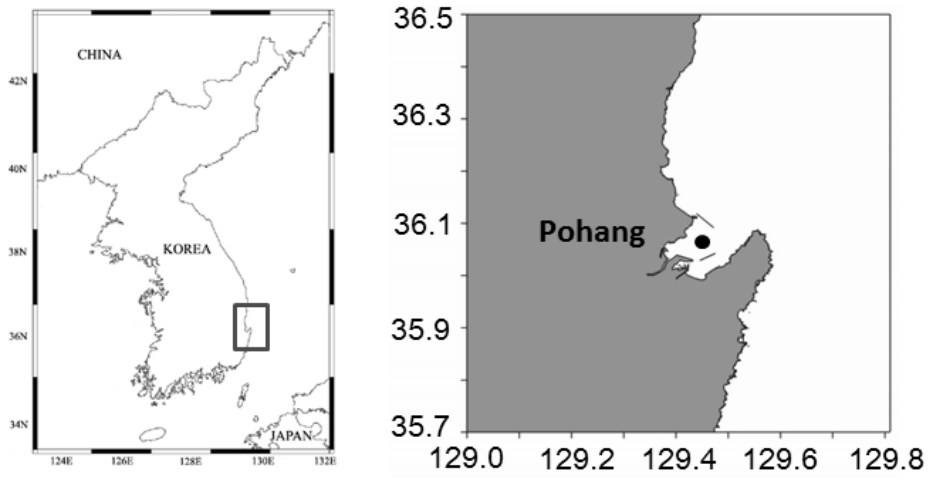

Fig. 4.1. The sampling site where *Alexandrium pohangense* n. sp. was isolated.

4.2.2. Morphology of *Alexandrium pohangense* n. sp.

The morphology of live vegetative flagellated cells and cells of *A. pohangense* preserved in 4% (v/v) glutaraldehyde were examined using a compound microscope (Zeiss-Axiovert 200M; Carl Zeiss Ltd, Göttingen, Germany). I measured the cell length and cell width of live cells using an image analysis system. Thecal plates were visualized by staining with Calcofluor white stain (Sigma, USA) and examination using epi-fluorescence illumination. For the analysis by SEM, a 10 ml aliquot of a dense culture (~500 cells ml^{-1}) was fixed with paraformaldehyde (final concentration = 2 %, w/v) for 10min. The fixed cells were collected on a PC membrane filter (pore size = 5 μm) without additional pressure and desalted by rinsing with distilled waters. PC membrane filters were carefully dehydrated in an ethanol series (50, 60, 70, 80, 90, and 100 %) and finally dried using

a critical point dryer (BAL-TEC, CPD 300, Balzers, Liechtenstein, Germany). The dried filters mounted on a tub and coated with gold-palladium. Cells were viewed with SEM (JSM-840A, SEM JEOL Ltd., Tokyo, Japan). More than 100 cells were observed under the SEM for the determination of the morphological features.

4.2.3. DNA extraction, PCR amplification, sequencing, and data analysis

The genomic DNA of *A. pohangense* was extracted using the AccuPrep Genomic DNA Extraction Kit (Bioneer, Daejeon, Korea). DNA yield was quantified with a spectrophotometer. The amplification reaction mixtures contained 1 x PCR buffer with 1.5 mM $MgCl_2$, 0.2 mM dNTPs, 0.5 mM each primer, 5 U of Taq DNA polymerase (Bioneer, Deajeon, Korea), and 200 ng template DNA. The primers that were used to amplify from the SSU to LSU region of rDNA listed in Table 4-1. The DNA was amplified in a Mastercycler ep gradient (Eppendorf, Hamburg, Germany) using the following cycling conditions: 3min at 95 ℃ followed by 40 x 45s at 95 ℃, 1 min at the selected temperature (AT), and 1 min at 72 ℃ with a final extension of 5 min at 72 ℃. The AT was adjusted depending on the primers used according to the manufacturer's instructions. PCR products were purified using AccuPrep DNA Purification Kit (Bioneer, Deajeon, Korea). Sequencing was performed with a ABIPRISM 3700 DNA Analyzer (Applied Biosystems, FosterCity, CA).

Table 4.1. Oligonucleotide primers used in this study to amplify and sequence th small subunit (SSU), internal transcribed spacer(ITS)1, 5.8S, ITS2, and large subunit (LSU) regions of rDNA of *Alexandrium pohangense*

Primer name	Sequence (5'-3')	Reference
Forward primers		
EUKA	CTGGTTGATCCTGCCAG	Medlin et al. 1988
EUK 1209F	GGGCATCACAGACCTG	Giovannoni et al. 1988
ITSF2	TACGTCCCTGCCCTTTGTAC	Litaker et al. 2003
D1R	ACCCGCTGAATTTAAGCATA	Scholin et al. 1994
Reverse Primers		
EUKB	TGATCCTTCTGCAGGTTCACCTAC	Medlin et al. 1988
ITSR2	TCCCTGTTCATTCGCCATTAC	Litaker et al. 2003
LSU B	ACGAACGATTTGCACGTCAG	Litaker et al. 2003
28-1483R	GCTACTACCACCAAGATCTGC	Daugbjerg et al. 2000

4.2.4. Sequence availability and phylogenetic analysis

Phylogenetic analyses of the SSU, ITS1-5.8S-ITS2, and LSU rDNA regions of *A. pohangense* were conducted using MEGA v.4 (Tamura et al., 2007) including sequences from closely related taxa obtained from GenBank. The Maximum likelihood (ML) analysis of the two regions was conducted using RAxML 7.0.3 program (Stamatakis, 2006) with default GTR+G+I model in the program. Tree likelihoods were estimated using a heuristic search with 100 random addition sequence replicates, and TBR branch swapping. Bayesian inference was performed using MrBayes v.3.1 (Huelsenbeck and Ronquist, 2001; Ronquist and Huelsenbeck, 2003) with the default GTR + G + I model to determine the best available model for the data of each region. For all sequence regions, posterior probabilities were estimated using four independent Markov Chain Monte Carlo (MCMC) chains, performed described by Kang et al. (2010).

4.3. Results

4.3.1. Molecular characterization of *Alexandrium pohangense* n. sp.

The small subunit (SSU), the large subunit (LSU), internal transcribed spacer regions (ITS1 and ITS2), and 5.8S of the ribosomal rDNA of *Alexandrium pohangense* were compared with other *Alexandrium* species. The SSU and LSU rDNA sequences of *A. pohangense* were 4-7% and 14-17%, respectively, different from those of *Alexandrium minutum, Alexandrium ostenfeldii, Alexandrium tamutum, Alexandrium margalefii,* and *Alexandrium pseudogonyaulax,* the closest species. In addition, 5.8s rDNA sequences of *A. pohangense* were also 12% different from those of *A. minutum, A. ostenfeldii, A. tamutum,* and *Alexandrium peruvianum*, while ITS1 and ITS2 regions of *A. pohangense* were found no significant similarity with those of other *Alexandrium* species (Table 4.2).

In the phylogenetic tree based on LSU rDNA sequences, *A. pohangense* was positioned at the basal of the clade of *A. margalefii* strains (Fig. 4.2). Moreover, in the phylogenetic tree based on SSU rDNA sequences, *A. pohangense* formed a clade with *Alexandrium leei*, and *A. margalefii* strain was positioned at the basal of this clade (Fig. 4.3).

Table 4.2. Comparison of the sequences of the small subunit (SSU), 5.8S, and large subunit (LSU) rDNA of the strain of *Alexandrium pohangense* with some genetically close species. The numbers indicate base pair differences. The numbers in parenthesis are dissimilarity (%), including gaps. There was no significant similarity in ITS1 and ITS2 regions between *A. pohangense* with other *Alexandrium* species.

A. SSU of *A. pohangense*

Species	*A. minutum*	*A. lusitanicum*	*A. ostenfeldii*	*A. tamutum*	*A. margalefii*	*A. pseudogonyaulax*
Accession No.	JF906998, AJ535380	JF906999	AJ535383, JF521637	AJ535379	U27498	AB088302
A. pohangense	79–80 (4)	79 (4)	77–82 (4)	82 (4)	94 (5)	127 (7)

B. 5.8S of *A. pohangense*

Species	*A. ostenfeldii*	*A. peruvianum*	*A. tamutum*	*A. minutum*	*A. lusitanicum*
Accession No.	AB538439, JX878431, JX865532	JX841261, JX841266	AM236857	KF018285	EU707539
A. pohangense	19 (12)	19 (12)	19 (12)	19 (12)	19 (12)

C. LSU of *A. pohangense*

Species	*A. tamutum*	*A. insuetum*	*A. pseudogonyaulax*	*A. ostenfeldii*	*A. margalefii*	*A. minutum*	*A. andersoni*
Accession No.	EU707459	JF521630	AY154958	JF521636, JF521637	JQ616827	JF906998	JF521621
A. pohangense	176 (14)	190 (14)	195 (15)	198–199 (15)	199 (15)	197 (15)	218 (17)

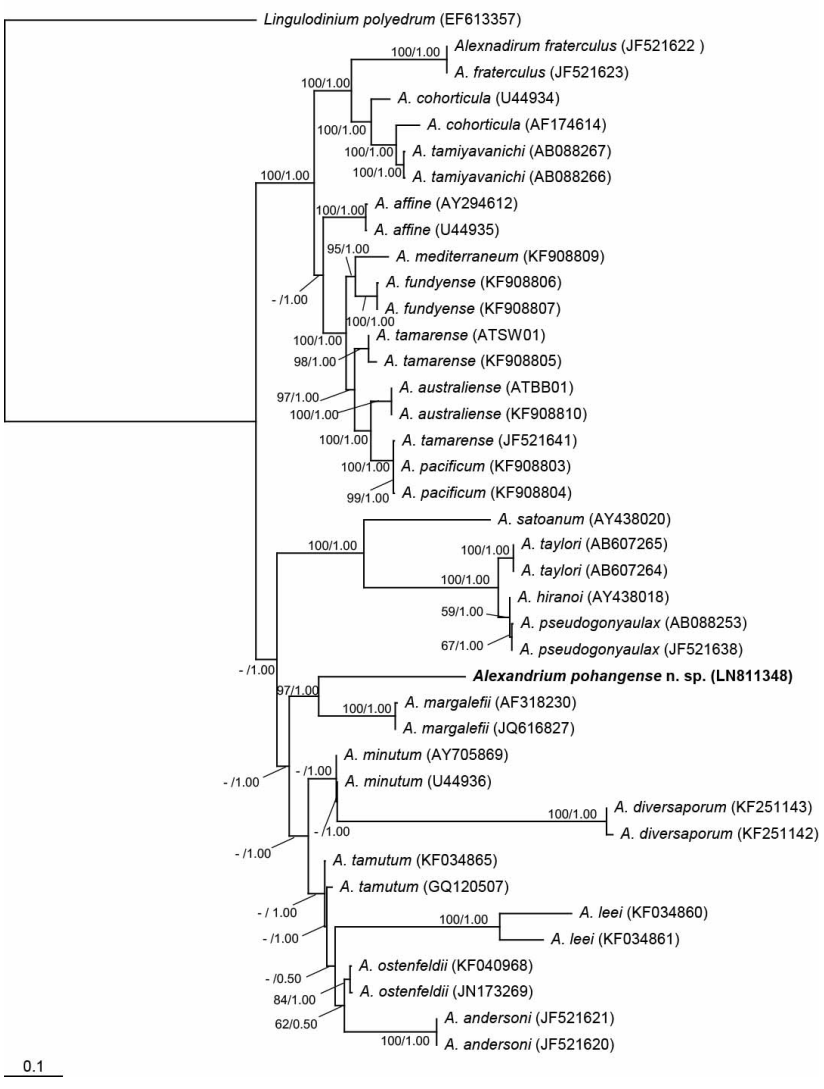

Fig. 4.2. Maximum likelihood (ML) tree based on 769 bp aligned positions of LSU ribosomal DNA region with *Lingulodnium polyedrum* as outgroup taxa. The branch lengths are proportional to the amount of character changes. The numbers above the branches indicate the Bayesian posterior probability (left) and ML bootstrap values (right). Posterior probabilities ≥0.5 are shown.

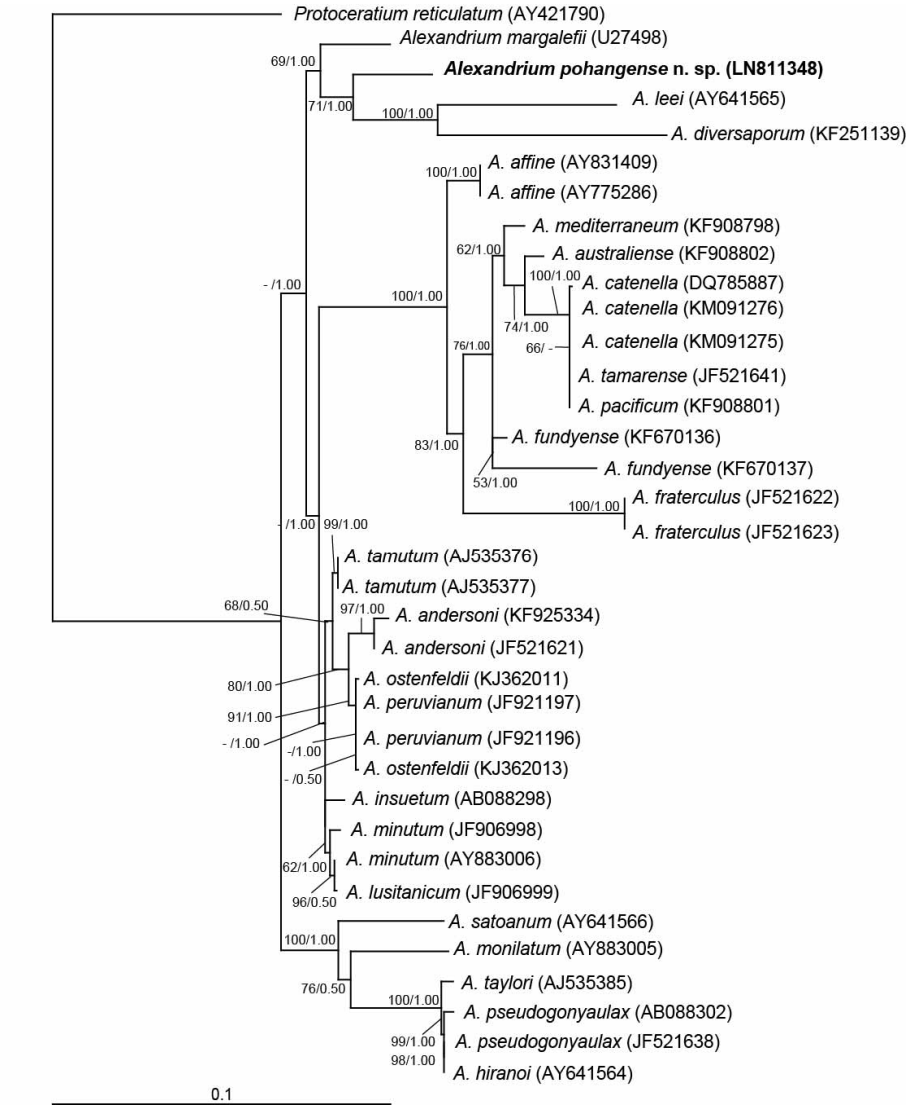

Fig. 4.3. Maximum likelihood (ML) tree based on 1,601 bp aligned positions of SSU ribosomal DNA region with *Protoceratium reticulatum* as outgroup taxa. The branch lengths are proportional to the amount of character changes. The numbers above the branches indicate the Bayesian posterior probability (left) and ML bootstrap values (right). Posterior probabilities ≥0.5 are shown

4.3.2. Morphology of *Alexandrium pohangense* n. sp.

Cells of *A. pohangense* were single, with chains of 2 cells observed very rarely. Cells of *A. pohangense* were spherical in shape, with a markedly impressed cingulum (Fig. 4.4). Comma shaped the apical pore located on epitheca, and the sulcus is deeply caved at the middle of the cell. Cells contained chloroplasts and the nucleus was located in the hypotheca (Fig. 4.4). The range of cell length and width of live cells (n = 25) as measured using light microscopy were 24–42 μm and 23 – 40 μm, respectively (Table 4.3). The ratio of cell length to cell width of live cells was almost 1 (range = 0.7–1.5, n = 25) (Table 4.3).

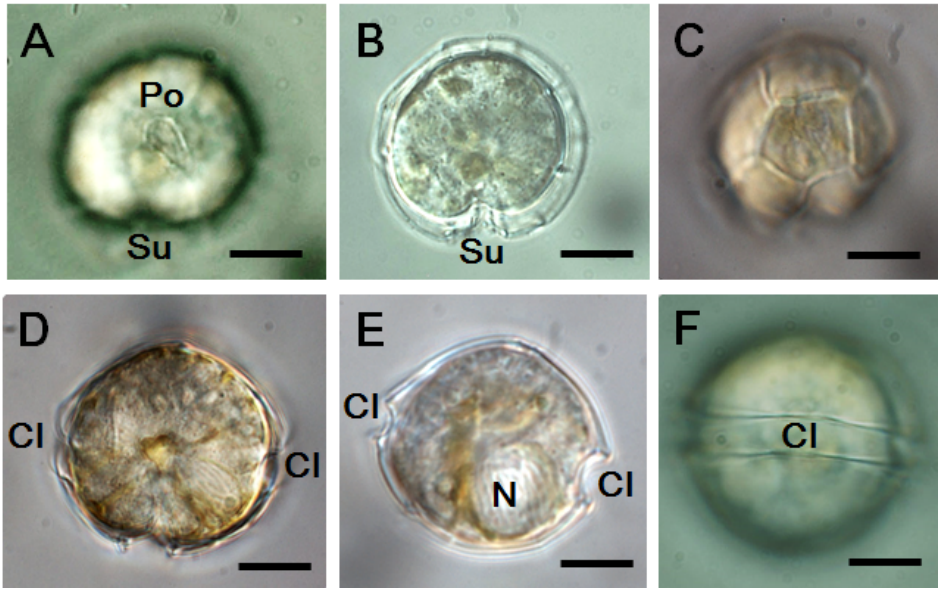

Fig. 4.4. Light micrographs of *Alexandrium pohangense* n. sp. (A, B) Apical view showing the apical pore (Po) located on the epitheca and sulcus (Su) in the middle of the cell. (C) Antapical view showing the plates pattern. (D) Oblique ventral view of *A. pohangense* showing the cingulum (CI). (E) Ventral view showing the nucleus (N) located in the hypotheca (F) Dosal view of A. pohagense with markedly impressed cingulum. Scale bars = 10 μm.

Morphological analysis using light microscopy with calcoflour white staining and SEM showed that *A. pohangense* had plates with a Kofoidian plate formula of Po, 4′, 6′′, 6c, 8s, 5′′′, and 2′′′′, which conformed to the genus *Alexandrium* (Figs. 4.5 and 4.6). *A. pohangense* had four apical plates. The wide quadrangular 1′ plate was vented and touched the 2′ plate and disconnected to the Po (Figs. 4.5). *A. pohangense* had a small ventral pore (average = 0.73 μm and 0.69 μm in LM and SEM, n = 20) on the 4′ plate (Table 4.3, Figs. 4.5). The large elongated 2′ plate was contacted the Po, 1′, 3′, 4′, 1′′, 2′′, and 3′′ plates (Fig. 4.6). The wide 3′ plate was hexagonal (Fig. 4.6). The 4′ plate, which had a ventral pore, was hexagonal and contacted the Po, 1′, 2′, 3′, 5′′, and 6′′ plates (Fig. 4.6). The first precingular plate (1′′) of *A. pohangense* was hexagonal and contacted 1′, 2′, 2′′, and cingular plate (Fig. 4.6). The second precingular (2′′) and forth precingular (4′′) plates were hexanonal, while third precingular (3′′) and fifth precingular (5′′) plates were pentagonal, respectively (Figs. 4.6). The sixth precingular (6′′) plate was pentagonal and the ratio of plate length to plate width of live cells was 0.88 (range = 0.7–1.2, n = 23) (Table 4.3, Fig. 4.6). The cingulum was consisted of six plates (Figs. 4.5, 4.6).

The shape of apical pore (Po) plate of *A. pohangense* was comma shaped and surrounded by marginal pores (Fig. 4.6). The marginal pores were only positioned dorsal part of comma pore. *A. pohangense* lacked an anterior attachment pore (aap) in the apical pore complex.

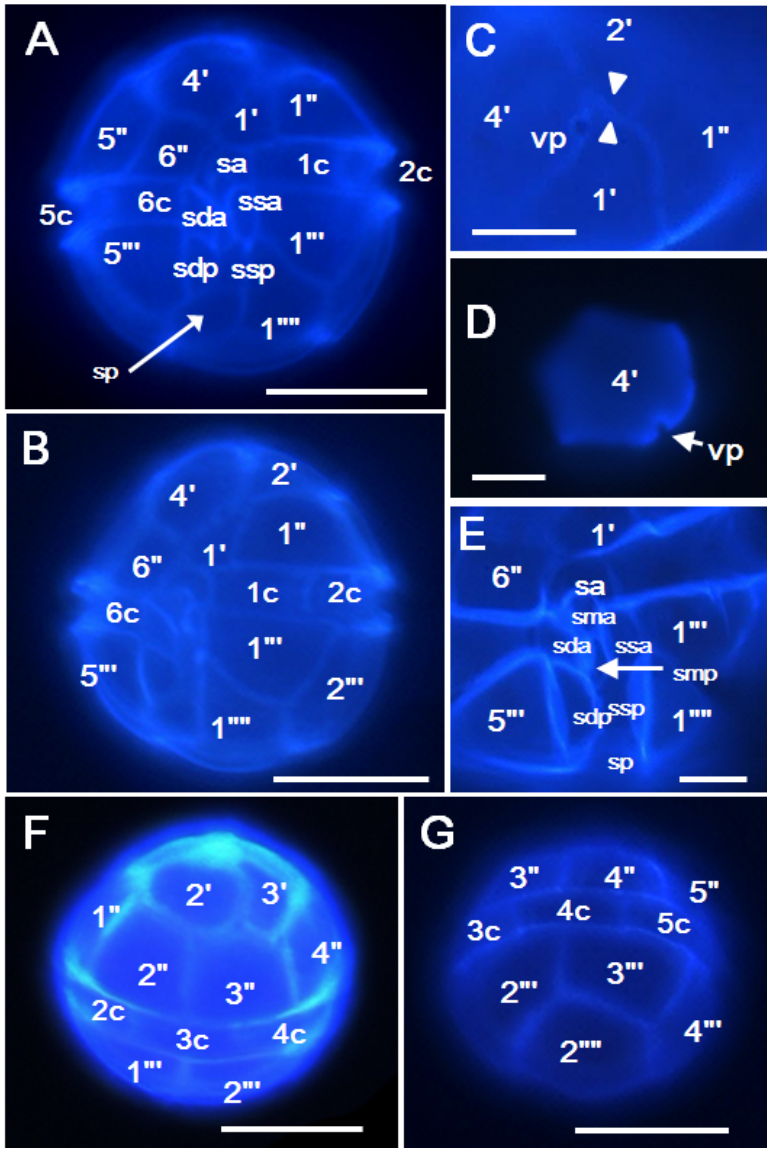

Fig. 4.5. Micrograph of calcofluor white stained *A. pohangense* showing the plate tabulation and pattern. (A, B) Ventral view. (C) Apical view showing the 1′ plate touching the 2′ plate and the ventral pore (vp) located on the 4′ plate. (D) The vp on the 4′ plate. (E) Sulcal plates. (F, G) Dorsal view. Scale bars = 20 μm for (A, B, F, G) and 5 μm for (C–E).

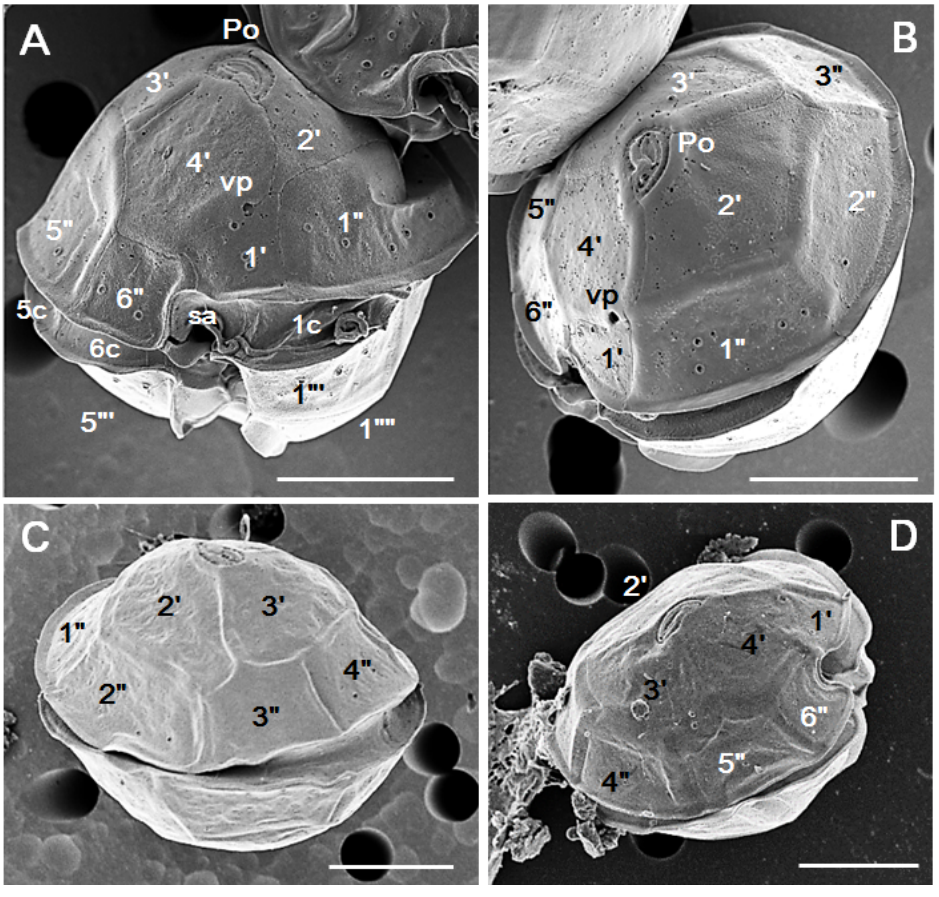

Fig. 4.6. Scanning electron microscopy images of *Alexandrium pohangense* n. sp. (A) Ventral view showing the cingular plates C1, C5, C6, and the anterior (sa) sulcal plates. (B) Apical view showing the 1′ plate whose left upper side is bent, protruding and touching the 2′ plate, but disconnected from the apical pore (Po). The ventral pore (vp) is located on the 4′ plate. (C, D) Lateral view showing the epithecal plate tabulation and pattern. Scale bars = 10 μm.

There were five postcingular plates: 1‴, 3‴, and 5‴ were quadrangular, but 2‴ and 4‴ plates were pentagonal (Fig. 4-7). *A. pohangense* had two antapical plates in hyposome. The first antapical plate (1⁗) was quadrangular and contacted 1‴, 2‴, 2⁗, and sulcal plates (Figs. 4-7). The second antapical plate (2⁗) was wide pentagonal and the ratio of plate length to plate width of live cells was 0.94 (range = 0.8-1.1, n = 19) (Fig. 4.7, Table 4.3). Moreover, the ratio of plate width to cell width of live cells was 0.52 and ratio of plate length to cell width of live cells was 0.47 (range = 0.4-0.7, n = 7) (Table 4.3).

The sulcal plates of *A. pohangense* consisted of eight plates: anterior sulcal plate (sa), posterior sulcal plate (sp), right anterior (sda), right posterior (sdp), left anterior (ssa), left posterior (ssp), and two small plates between lateral plates (the median anterior: sma, the median posterior: smp) (Fig. 4.8). The length of ssa plate was 7.09 μm (n = 7) in LM (Table 4.3). The ratio of sp plate was 1.13 (range = 0.7-1.6, n = 10) (Table 4.3). Moreover, two pairs of lateral plates (sda, ssa, sdp, and ssp) had list at the marginal of each plate (Fig. 4.8).

Cell surface was smooth, but two different sizes of pores were scattered (Figs. 4.8). The bigger pores were scattered randomly, but the several smaller pores were clustered together (Fig. 4.8).

Table 4.3. Comparison of the morphological characteristics of *Alexandrium pohangense* n. sp. and morphologically similar *Alexandrium* species. In all species depicted, the 1′ plate is disconnected from the apical pore complex and the thecal plates are smooth. Specimens were observed using light microscopy (LM) and scanning electron microscopy (SEM). The numbers in the parenthesis are the mean value. [a]Data were not directly mentioned but inferred from images provided in the respective references included in this study. α: the angle between the cingulum and the bottom margin side of 1′ plate, β: the angle between antero-posterioral axis of the cell and the point of the margin of apical pore plate, sa: anterior sulcal plate, ssa: left anterior sulcal plate, sp: posterior sulcal plate, pap: posterior attachment pore. The numbers in parenthesis are average values. NA: Not available.

Species	*A. pohangense*	*A. taylori*	*A. margalefii*	*A. hiranoi*	*A. pseudogonyaulax*	*A. camurascutulum*
Length (L, μm), live (LM)	24-42 (30)	31-44	28-39	18-75 (40)	32-40 (35)	26-28
Width (W, μm), live (LM)	23-40 (30)	32-46	28-35	18-75 (37)	28-42 (37)	21-24
Ratio of L relative to W	1	~1	~1	~1	~1	~1
Presence of ventral pore (vp)	yes	yes	yes	yes	yes	yes
Diameter of vp (μm) (LM)	0.73	NA	0.62[a]	1.81[a]	1.48[a]	NA
Diameter of vp (μm) (SEM)	0.69	0.88[a]	NA	NA	NA	0.68[a]

Table 4.3. continued

Species	*A. pohangense*	*A. taylori*	*A. margalefii*	*A. hiranoi*	*A. pseudogonyaulax*	*A. camurascutulum*
Plate on which vp is located	4′	4′	1′	1′	1′	4′
Plates connected to vp	1′, 4′	1′, 2′, 4′	1′, 4′, 1′′	1′, 4′	1′, 4′	1′, 4′
Ratio of length relative to width of the 2′′′′ plate (LM)	0.8–1.1 (0.9)	1.2[a]	1.3[a]	1.9[a]	1.2[a]	NA
Ratio of the 2′′′′ plate area relative to the total hypothecal area (LM)	0.21–0.34 (0.27)	0.16[a]	0.11[a]	0.16[a]	0.12[a]	NA
Shape of 1′ plate	quadrangular	pentagonal	quadrangular	pentagonal	pentagonal	pentagonal
Ratio of length relative to width of the 1′ plate (LM)	0.6–1.2 (0.9)	0.7[a]	1.5[a]	0.7[a]	0.8[a]	0.5–0.7[a]
Shape of 6′′ plate	pentagonal	pentagonal	pentagonal	pentagonal	pentagonal	hooked pentagonal
Ratio of length relative to width of the 6′′ plate (LM)	0.7–1.2 (0.9)	1.2[a]	1.4[a]	1.2[a]	1.4[a]	0.6[a]

Table 4.3. continued

Species	*A. pohangense*	*A. taylori*	*A. margalefii*	*A. hiranoi*	*A. pseudogonyaulax*	*A. camurascutulum*
Angle of α (°)	0	80[a]	0[a]	85[a]	0[a]	55–70[a]
Angle of β (°)	45–58	20[a]	30[a]	0[a]	0[a]	0[a]
Plates contacted to sa	6′′, 1′	6′′, 1′, 1′′	6′′, 1′	6′′, 1′	6′′, 1′	6′′, 1′, 1′′
Length of the ssa (μm) (LM)	7.09	6.66[a]	4.84[a]	7.06[a]	12.48[a]	NA
Ratio of length relative to width of the sp plate (LM)	0.7–1.6 (1.1)	2.1[a]	1.4[a]	1.4[a]	1.2[a]	NA
The number of the types of pores on the cell surface (SEM)	2	1	NA	1	1	2
Presence of pap	no	no	no	no	no	yes
Reference	(1)	(2), (3)	(2), (3), (4), (5)	(1), (6)	(3), (4), (7)	(8)

(1) This work, (2) Balech (1994), (3) Giacobbe and Yang (1999) (4) MacKenzie et al. (2004), (5) Selina and Morozova (2005), (6) Kita and Fukuyo (1988), (7) Gu et al. (2013), (8) MacKenzie and Todd (2002)

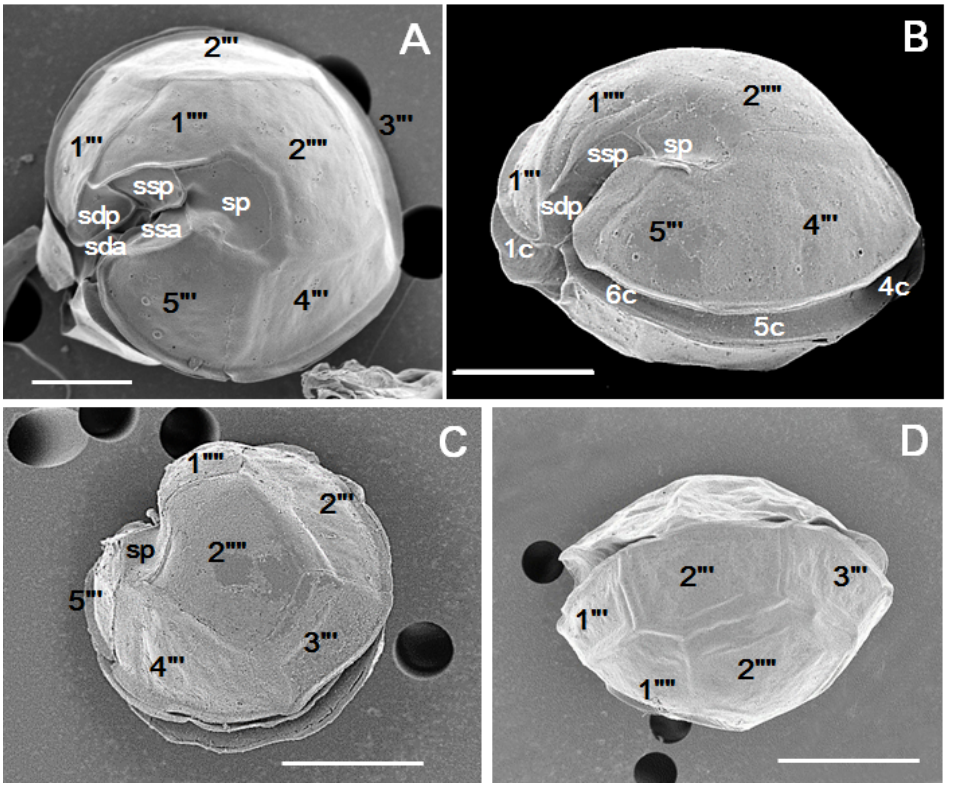

Fig. 4.7. Scanning electron microscopy images of *Alexandrium pohangense* n. sp. (A–D) Antapical view showing the hypothecal plate tabulation (postcingular plates, antapical plates) and sulcal plates. Scale bars = 10 μm.

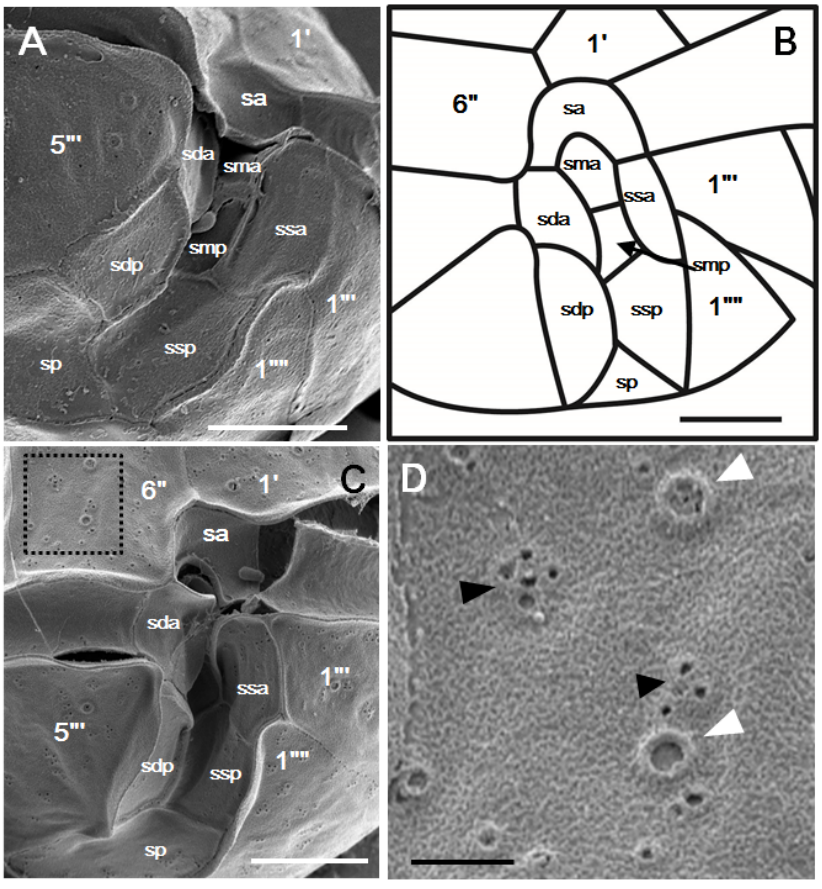

Fig. 4.8. Scanning electron microscopy images and drawings of *Alexandrium pohangense* n. sp. (A–C) Ventral view showing the sulcal plates. sa, anterior plate; sda, right anterior plate; sdp, right posterior plate; ssa, left anterior; ssp, left posterior; sma, median anterior plate; smp, median posterior plate; sp, posterior plate. (D) Enlarged view from Fig. 6C showing the smooth cell surface and two different types of pores. White arrowheads indicate single large pores and black arrowheads indicate clustered small pores. Scale bars = 5 μm for (A–C) and 1 μm for (D).

4.4. Discussion

4.4.1. Molecular characterization of *Alexandrium pohangense* n. sp.

The rDNA (SSU, ITS1, 5.8S, ITS2, and LSU) sequences of the strains of *Alexandrium pohangense* were considerably different from those of the strains of other *Alexandrium* species (Table 4.2). The sequences for the 5.8S of *A. pohangense* are 19 bp different from those of *Alexandrium minutum, Alexandrium lusitanicum, Alexandrium ostenfeldii, Alexandrium tamutum*, and *Alexandrium peruvianum*; moreover, its LSU sequences are 176-218 bp different from those of other *Alexandrium* species (Table 4.2). Several studies reported that the ribosomal sequence differences within *Alexandrium* speceies are few (John et al., 2003; John et al., 2014). The interspecies nucleotide differences in the LSU rDNA region of some *Alexandrium* species are only 3-36 bp (John et al., 2014). Therefore, the big base pair difference of *A. pohangense* from other *Alexandrium* species supported that *A. pohangense* is a genetically distinct new species.

In the phylogenetic trees based on LSU and SSU rDNA, *A. pohangense* was clustered with *Alexandrium margalefii* in both trees. However, *A. pohangense* was located in the basal of the *A. margalefii* in LSU tree, while *A. magalefii* was located in the basal of the cluster in the SSU tree. Because there were no much information

of the *A. magalefii* and there was only one strain of *A. pohangense*, it may be the reason of differences in location of *A. pohangense* in the both trees.

4.4.2. Morphology of *Alexandrium pohangense* n. sp.

Based measurement of established culture of *Alexandrium pohangense*, *A. pohangense* has a Kofoidian plate formula of Po, 4′, 6′′, 6c, 8s, 5′′′, and 2′′′′, which confirms its assignment to the genus *Alexandrium* (Fig. 4.9). The first apical (1′) plate is disconnected from the apical pore complex and *A. pohangense* has a smooth thecal surface like *A. taylori*, *A. margalefii*, *Alexandrium hiranoi*, *Alexandrium pseudogonyaulax*, and *Alexandrium camurascutulum*. In addition, overall cell sizes and the ratio of cell width and length of *A. pohangense* are similar to those of these five *Alexandrium* species (Table 4.3). However, the ventral pore of *A. pohangense* is considerably smaller (average: 0.73 and 0.69 μm, measured using LM and SEM, respectively) than those of *A. hiranoi* and *A. pseudogonyaulax* (1.48–1.81 μm in LM) (Table 4.3). In addition, *A. pohangense* has a ventral pore on the margin of the 4′ plate, unlike *A. margalefii* or *A. pseudogonyaulax*, which have a larger ventral pore on the 1′ plate. Moreover, *A. pohangense* has a wide quadrangular 1′ plate, which is bent and touches the 2′ plate, unlike *A. margalefii*, which has a wide rectangular 1′ plate not touching the 2′ plate, or *A. pseudogonyaulax*, which has a narrower elongated 1′ plate touching the 2′ plate. Furthermore, the 6′′ plate of

A. pohangense is a simple pentagonal shape, while that of *A. camurascutulum* has deeply concaved left margin, which gives a hooked appearance. The ratio of 6′′ plate length and width of *A. pohangense* (0.9) is markedly smaller than that of *A. taylori*, *A. margalefii*, *A. hiranoi*, and *A. pseudogonyaulax* (1.2–1.4), but greater than that of *A. camurascutulum* (0.6). Moreover, the shape of the 2′′′′ plate of *A. pohangense* (i.e., regular pentagonal with a ratio of plate length to plate width of 0.9) is clearly different from that of *A. taylori*, *A. margalefii*, *A. hiranoi*, and *A. pseudogonyaulax* (i.e., elongated pentagonal, ratio of plate length to plate width 1.2–1.9), and the area of the 2′′′′ plate relative to the total area of the hypotheca of *A. pohangense* (0.27, n = 10) is greater than that of *A. taylori*, *A. margalefii*, *A. hiranoi*, and *A. pseudogonyaulax* (0.11–0.16). Even though, the 2′′′′ plate of *A. camurascutulum* is shaded and partially covered by the other cell (MacKenzie and Todd, 2002; Fig. 4.9), the size of 2′′′′ plate is similar with that of 5′′′ plate, which is a medium-size in the hypotheca. The area of the 2′′′′ plate relative to the total area of the hypotheca of *A. camurascutulum* is smaller than that of *A. pohangense*.

The apical pore plate (Po) of *A. hophangense* is twisted toward to the left side of epitheca while, those of *A. hiranoi*, *A. psudogonyaulax*, and *A. camurascutulum* are straightly toward to the anterior sulcal plate (sa) (Fig. 4.10). The angle between vertical axis of cell and the point of the margin of Po (α) of *A. hophangense* (45–58°) is clearly greater than *A. taylori* and *A. margalefii*, but

smaller than *A. hiranoi*, *A. psudogonyaulax*, and *A. camurascutulum* (Table 4.3). While 1'' plate of *A. pohangense* straightly contacts to 1' plate, the right margins of 1'' plates of *A. hiranoi*, *A. pseudogonyaulax*, and *A. camurascutulum* are deeply curved toward 1' (Fig. 4-9). Thus, the angle between the cingulum and the bottom margin side of 1' plate (β) of *A. pohangense* is horizontal, while those of *A. taylori*, *A. hiranoi*, and *A. camurascutulum* are between 55-85° (Fig. 4.10).

The anterior sulcal plate (sa) of *A. pohangense* contacts to 1' and 6'' plates like *A. marglefii*, *A. pseudogonyaulax*, and *A. hiranoi*, while those of *A. taylori* and *A. camurascutukum* contacts to 1', 1'', and 6'' plates. The length of the left anterior sulcal plate (ssa) of *A. pohangense* (7.09) is considerably longer than *A. margalefii*, but shorter than *A. pseudogonyaulax* (12.48). Furthermore, *A. pohangense* has two different types of thecal pores (i.e., large and small pores), whereas *A. taylori*, *A. margalefii*, *A. hiranoi*, *A. pseudogonyaulax* have only small thecal pores. *A. pohangense* does not have posterior attachment pore (pap) on the posterior plate (sp) like *A. taylori*, *A. margalefii*, *A. hiranoi*, *A. pseudogonyaulax*, while *A. camurascutulum* has a pap on the sp. On the basis of morphological and phylogenetic criteria, we propose that *Alexandrium pohangense* is a new species of the genus *Alexandrium.*

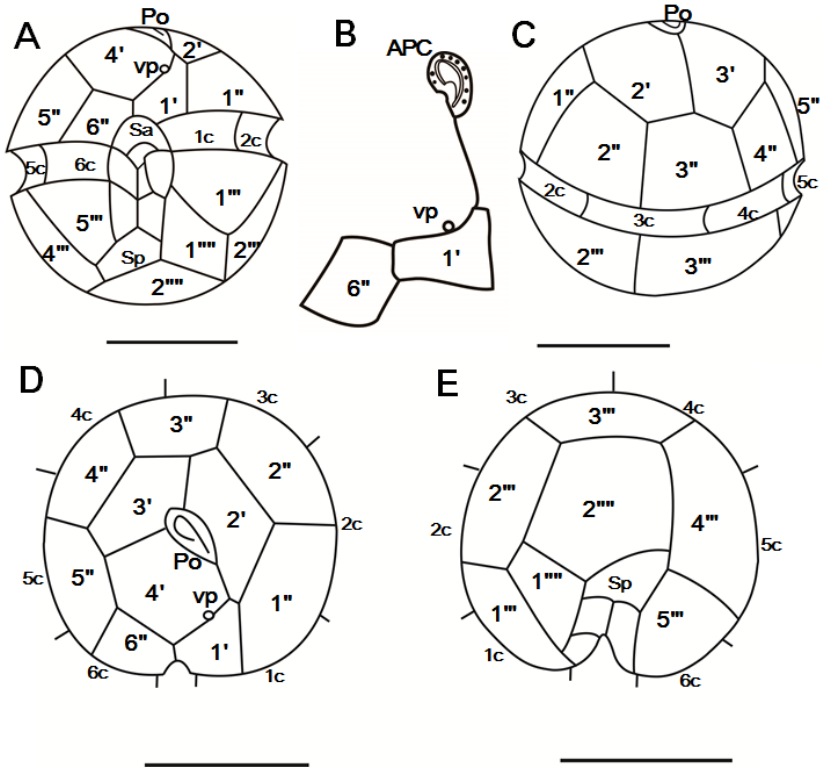

Fig. 4.9. Schematic diagram of *Alexandrium pohangense* n. sp. (A) Ventral view. (B) Relative positions of the apical pore complex (APC), first apical (1′) and sixth precingular (6′′) plates, and ventral pore (vp). (C) Dorsal view. (D) Apical view showing the epithecal plate tabulation and pattern. (E) Antapical view showing the hypothecal plate tabulation and pattern. Scale bars = 20 μm for (A, C–E), no scale bar for (B).

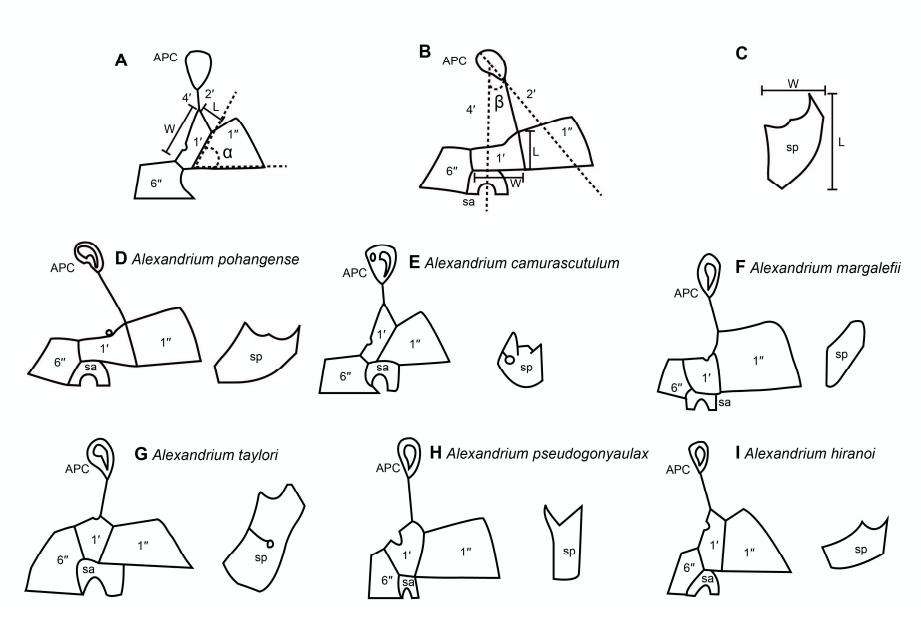

Fig. 4.10. A diagrammatic comparison in relative positions of the apical pore complex (APC), first apical (1′) and sixth precingular (6′′) plates, and anterior plate (sa) of the *Alexandrium* species morphologically similar to *Alexandrium pohangense* n. sp. (A) The angle between the cingulum and the bottom margin side of 1′ plate (α) and ratio of length (L) relative to width (W). (B) The angles between antero-posterioral axis of the cell and the point of the margin of apical pore plate (β) and ratio of L relative to W of the 1′ plate. (C) Ratio between L and W of the posterior sulcal plates (sp). (D) *A. pohangense*. (E) *A. camurascutulum.* (F) *A. margalefii.* (G) *A. taylori*. (H) *A. pseudogoniaulax*. (I) *A. hiranoi. A. margalefii* and *A. pseudogoniaulax* are redrawn from MacKenzie et al. (2004). *A. hiranoi, A. taylori,* and *A. camurascutulum* are redrawn from Kita and Fukuyo (1988), Balech (1994), and MacKenzie and Todd (2002).

Alexandrium pohangense n. sp. A. S. Lim, H. J. Jeong

Diagnosis. Phototrophic. The ranges of live cell length and width are 24-42 μm and 23-40 μm, respectively. The ratio of live cell length to width is 0.7-1.5. The comma shaped apical pore plate, surrounded by marginal pores, turns toward to left side of the epitheca and the angle between antero-posterioral axis of the cell and the point of the margin of apical pore plate is 45-58°. The number of the marginal pores on the apical pore plate is 8-17. Cells lack an anterior attachment pore in the apical pore complex. It has a wide rectangular 1′ plate whose left upper side is slightly bent and protruding and meeting the 2′ plate as a point, but being disconnected from the Po. The 1′ plate lies on the sa plate and meets the 1′′ plate as a straight vertical line. The angle etween the cingulum and the bottom margin side of 1′ plate is almost zero. It has a small ventral pore of ca. 0.7 μm on the 4′ plate. It has a relatively large regular pentagonal 2′′′′ plate whose area occupies ca. 21-34 % of total area of the hypotheca. It does not have posterior attachment pore (pap) on the posterior sulcal plate. The cell surface is smooth, but two different types of pores, single large pores of ca. 0.34 μm in diameter and 2-5 clustered small pores of ca. 0.12 μm, are widely distributed.

Etymology. The specific epithet "*pohangense*" is derived from Pohang City, Korea, which encloses Youngil Bay, from which this dinoflagellate was isolated.

Deposition of type material. A hapantotype slide as USNM slide 222987 of cells fixed with 2% paraformaldehyde has been deposited in the Protist Type Specimen Slide Collection, US Natural History Museum, Smithsonian Institution, Washington, DC, USA.

Gene sequence. The rDNA gene sequence – GenBank Accession No. LN811348

Chapter 5. Grazing impacts by *Alexandrium pohangense* n. sp. on *Cochlodinium polykrikoides*

5.1. Introduction

In the last two decades, many phototrophic dinoflagellates have been revealed to be mixotrophic (Bockstahler and Coats, 1993; Jacobson and Anderson, 1996; Stoecker, 1999; Li et al., 2000; Skovgaard et al., 2000; Jeong et al., 2010a, 2012; Park et al., 2006; Berge et al., 2008; Burkholder et al., 2008). They are able to feed on diverse prey items such as bacteria, algae, heterotrophic protists, and metazoans (e.g., Jeong et al., 2010a). Moreover, these mixotrophic dinoflagellates play diverse roles in food webs and the cycling of materials (Jeong et al., 1999a, 2010a; Glibert et al., 2009; Hansen, 2011; Sanders, 2011; Seong and Jeong, 2011). Mixotrophic ability of the dinoflagellate is also considered as an important factor to form a harmful algal bloom (e.g., Jeong et al., 2010a). Furthermore, some mixotrophic dinoflagellates have a greater growth rate when they feed on the prey compared to phototrophic mode (Lee et al., 2014a). Thus, the mixotrophic grazing effects on a certain population dynamics should be considered to better understand the population dynamics.

Alexandrium species are known to form a harmful algal bloom and cause massive fish death and even human illness

(Hallegraeff, 1993; Cembella et al., 2002; Anderson et al., 2012). Some *Alexandrium* species produce toxins such as saxitoxins, goniodomins, spirolides (Anderson et al., 2012). Moreover, some unknown lytic compounds produced by *Alexandrium* species are possibly involved the mixotrophy of some *Alexandrium* species (Blossom et al., 2012). Gribble et al. (2005) reported that most *A. ostenfeldii* cells found in the field contained food vacuole. However, among ~30 *Alexandrium* species, only 5 species, *Alexandrium minutum*, *Alexandrium tamarense*, *Alexandrium catenella*, *Alexandrium ostenfeldii*, and *Alexandrium pseudogonyaulax*, have up to now been revealed mixotrophic (Nygaard and Tobiesen, 1993; Jacobson and Anderson, 1996; Jeong et al., 2005a, b; Yoo et al., 2009; Blossom et al., 2012). Therefore, to understand ecological roles and bloom dynamics of the new species, it is worthwhile to investigate the mixotrophic ability of *Alexandrium* species.

Recently, I newly described *Alexandrium pohangense* which is able to feed on *Cochlodinium polykrikoides* from waters off Pohang, Korea. In the present study using the established monoclonal cultures, I investigated the ability of *A. pohangense* to feed on heterotrophic and autotrophic bacteria and a diverse algal species, and used high-resolution video microscopy to observe their feeding behavior and determine the mechanism of prey ingestion. To compare the feeding ability of *A. pohangense* and other *Alexandrium* species, I compared the type of prey that *A. pohangense* and other *Alexandrium* species were able to feed on. I also measured the growth and

ingestion rates for *A. pohangense* feeding on *Cochlodinium polykrikoides* as a function of prey concentration and compared them with other predators of *C. polykrikoides*. The results of the present study provide a basis for understanding the interactions between *A. pohangense* and their prey species and their feeding mechanism and ecological roles in marine food webs.

5.2. Material and methods

5.2.1. Preparation of experimental organisms

Phytoplankton species were grown at 20 °C in enriched f/2 seawater media (Guillard and Ryther, 1962) under a continuous illumination of 100 μE m^{-2} s^{-1} provided by cool white fluorescent lights (Table 5.1). The mean equivalent spherical diameter (ESD) was measured using an electronic particle counter (Coulter Multisizer II, Coulter Corporation, Miami, Florida, USA). The carbon content of phytoplankton was estimated from the cell volume according to Strathmann (1967).

5.2.2. Prey species

Experiment 1 was designed to investigate whether or not *Alexandrium pohangense* was able to feed on potential prey when unialgal diet of diverse microalgal species was provided (Table 5.1). The initial concentrations of each algal species provided were similar in terms of carbon biomass.

A dense culture of *A. pohangense* growing photosynthetically in f/2 media at 20 °C and under a 14:10 h light-dark cycle at 100 μE m^{-2} s^{-1} was transferred to one 2-L PC bottle containing F/2 medium. The culture was maintained in F/2 media for 2 d under the same conditions described above. Three 1-ml aliquots were then removed from the bottle and *A. pohangense* densities were determined using a compound light microscope.

For observing the ingestion of eukaryotic algal prey under a light microscope microscope, the initial concentrations of *A. pohangense* and each target algal species were established as described above (Table 5.1). Triplicate 42-ml PC experimental bottles and triplicate predator control bottles were set up for each target algal species. The bottles were filled to capacity with freshly filtered seawater, capped, and then placed on a shelf and incubated at 20 °C under a 14:10 h light-dark cycle of cool white fluorescent light at 100 μE $m^{-2}s^{-1}$. After 6, 12, 24, and 48 h of incubation, a 5-ml aliquot was removed from each bottle and transferred to a 20-ml bottle. Two 0.1-ml aliquots were placed on slides with cover-glasses. The protoplasms of > 200 *A. pohangense* cells were carefully examined using a light microscope microscope at a magnification of ×100 - 400 to determine whether *A. pohangense* was able to feed on the target algal prey species. *A. pohangense* cells containing the ingested cells of each target algal species were photographed using digital cameras on these microscopes at a magnification of ×400 - 1,000. To test whether the filtrates of *A. pohangense* culture affect the behavior of prey species, the initial concentration of *A. pohangense* culture was filtrated through 5 μm pore (Millipore co.) and added to target algal species. The protoplasms of >200 *A. pohangense* cells were also examined in the same manners.

5.2.3. Feeding mechanism

Expt 2 was designed to investigate the feeding mechanisms of *A. pohangense* when provided a unialgal diet of the dinoflagellates *Cochlodinium polykrikoides*. The initial concentrations of the predator and prey were the same as in Expt 1.

The initial concentrations of *A. pohangense* and the target algal species were established using an autopipette to deliver a predetermined volume of culture with a known cell density to the experimental bottles. One 42-ml PC bottle (mixtures of *A. pohangense* and algal prey) was set up for each target algal species. The bottle was filled to capacity with freshly filtered seawater, capped, and then mixed well. After 6, 24, and 48 h of incubation on the shelf, a 1-ml aliquot was removed from the bottle and then 200 μl were transferred onto a slide with a cover-glass. For each target prey species, the feeding behavior of > 60 *A. pohangense* cells was monitored using a light microscope and/or an epifluorescence microscope at a magnification of ×100 - 630. All of the feeding processes were observed, from the time a prey cell was captured to the time that it was engulfed by the predator. A series of photographs showing the process for a *A. pohangense* cell feeding on *C. polykrikoides* were taken using a video analyzing system (Sony DXC-C33; Sony Co., Tokyo, Japan) mounted on a light microscope at a magnification of ×100 - 630.

5.2.4. Effect of prey concentration

Expt 3 was designed to investigate the ingestion rates of *Alexandrium pohangense* on the mixotrophic dinoflagellate *C. polykrikoides* as a function of prey concentration. A dense culture of *A. pohangense* maintained in an f/2 medium and growing photosynthetically was transferred to a 1-l PC bottle. Three 1-ml aliquots from the bottle were examined using a compound microscope to determine the cell concentrations of *A. pohangense*. Triplicate 42-ml PC experimental bottles (containing mixtures of predators and prey), triplicated prey control bottles (containing prey only), and triplicate predator control bottles (containing predators only) were established. To ensure similar water conditions, we filtered the water of a predator culture through a 0.7-μm GF/F filter, and then added this to the prey control bottles in the same amount as the volume of the predator culture added into the experimental bottles for each predator-prey combination. We added 5 ml of f/2 medium to all of the bottles, which were then filled to capacity with freshly filtered seawater and capped. To determine the actual predator and algal prey concentrations at the start of the experiment and after 2 d, a 5-ml aliquot was removed from each bottle and fixed with 5% Lugol's solution; all or >200 predator and prey cells in triplicate 1-ml Sedgwick-Rafter chambers were then enumerated. The bottles were refilled to capacity with filtered seawater, capped, and placed on the shelf because *C. polykrikoides* has negative growth on the rotating wheel.

The dilution of the cultures associated with refilling the bottles was considered when calculating the growth and ingestion rates.

The specific growth rate of *A. pohangense* was calculated as follows:

$$\mu = \frac{\ln (C_t / C_0)}{t} \quad (1)$$

where C_0 is the initial concentration of *A. pohangense* and C_t is the final concentration after time t. The time period was 2 d. I calculated the mean prey concentrations by using the equation of Frost (1972). I calculated the ingestion and clearance rates by using the equations of Frost (1972) and Heinbokel (1978).

Data for *A. pohangense* growth rate were fitted to the following equation:

$$\mu = \frac{\mu_{max} (x - x')}{K_{GR} + (x - x')} \quad (2)$$

where m_{max} = the maximum growth rate (d^{-1}), x = prey concentration(cells ml^{-1} or ng C ml^{-1}), x′ = threshold prey concentration (i.e. the prey concentration where $\mu = 0$), and K_{GR} = the prey concentration sustaining 1/2 m_{max}. Data were iteratively fitted to the model by using DeltaGraph® (SPSS Inc., Chicago, IL, USA).

Ingestion rate data were fitted to a Michaelis-Menten equation:

$$IR = \frac{I_{max}(x)}{K_{IR} + (x)} \quad (3)$$

where I_{max} = the maximum ingestion rate (cells predator^{-1} d^{-1} or ng C predator^{-1} d^{-1}), x = prey concentration (cells ml^{-1} or ng C ml^{-1}), and K_{IR} = the prey concentration sustaining 1/2 $I_{max.}$

5.2.5. Grazing impact of *Alexandrium pohangense* on *Cochlodinium polykrikoides*

By combining field data on the concentration of the *Alexandrium* spp. and *Cochlodinium polykrikodies* with the ingestion rates of the *A. pohangense* on *C. polykrikodies* obtained in the present study, I estimated the grazing coefficients attributable to *A. pohangense* and the co-occurring *C. polykrikoides*. Data on the abundances of *Alexandrium* spp. and the co-occurring *C. polykrikoides* used in this estimate were obtained by counting the water samples taken from the waters off Pohang, Korea when *C. polykrikoides* red tide patches were observed in 2014. The morphological features of *A. pohangense* under the light microscope were hard to distinguish from another *Alexandrium* species, the abundance of *Alexandrium* spp. was used for the calculation.

The grazing coefficients (g, d^{-1}) were calculated as:

$$g = CR \times PC \times 24 \quad (4)$$

where CR (ml predator^{-1} h^{-1}) is the clearance rate of *A. pohangense* on a *C. polykrikoides* at a prey concentration and PC is a *Alexandrium* spp. concentration (cells ml^{-1}). The CR values were calculated as:

$$CR = IR/ x \quad (5)$$

where IR (cells eaten predator^{-1} h^{-1}) is the ingestion rate of *A. pohangense* on *C. polykrikoides* and x (cells ml^{-1}) is the *C. polykrikoides* concentration. Since the laboratory experiments were performed at 20 °C, theses CR values were corrected using Q_{10} = 2.8 (Hansen et al., 1997).

5.3. Results

5.3.1. The kind of prey and feeding mechanism

Among the algal prey offered, *Alexandrium pohangense* fed only on *Cochlodinium polykrikoides* (Table 5.1). However, *A. pohangense* did not feed on *Gymnodinium aureolum* or *Scrippsiella trochoidea*, whose mean equivalent spherical diameters were similar to *C. polykrikoides*. In addition, cryptophyte *Teleaulax* sp., *Rhodomonas salina*, *Storeatula major*, and a naked ciliate *Mesodinium rubrum* were lysed within 30 min after 300 cell ml^{-1} of *A. pohangense* cells were mixed into the prey cells (Fig. 5.1).

Chain formed *C. polykrikodies* cells were split into single or two cells when *A. pohangense* cells were incubated together and immobilized (Fig. 5.2). *A. pohangense* cells approached the immobilized *C. polykrikoides* cells and engulfed them through the sulcus. The time (mean ± standard error, n = 6) for a prey cell to be completely fed on by *A. pohangense* cell after *A. pohangense* started sucking the prey cell through the sulcus was 118 ± 17 s (Fig. 5.2).

Table 5.1. Taxa, size, and concentration of prey species offered to *Alexandrium pohangense.* Mean equivalent spherical diameter (ESD, μm). Y: Feeding by *A. pohangense*, L: the prey cells were lysed by *A. pohangense*, N: not ingested by *A. pohangense*, I: the prey cells were immobilized by *A. pohangense.*

Prey species	ESD (μm)	Initial prey concentration (cell ml^{-1})	Feeding (effect)
Diatom			
Skeletonema costatum	5.9	150,000	N
Prymnesiophytes			
Isochrysis galbana	4.8	150,000	N (I)
Cryptophytes			
Teleaulax sp.	5.6	100,000	N (L)
Storeatula major	6.0	50,000	N (L)
Rhodomonas salina	8.8	50,000	N (L)
Rhaphidophytes			
Heterosigma akashiwo	11.5	30,000	N (I)
Mixotrophic dinoflagellates			
Heterocapsa rotundata	5.8	100,000	N (I)
Amphidinium carterae	9.7	30,000	N (I)
Prorocentrum minimum	12.1	20,000	N (I)
Hetereocapsa triquetra	15.0	30,000	N (I)
Gymnodinium aureolum	19.5	3,000	N (I)
Scrippsiella trochoidea	22.8	15,000	N (I)
Cochlodinium polykrikoides	25.9	2,000	Y (I)
Prorocentrum micans	26.6	3,000	N (I)
Akashiwo sanguinea	30.8	1,000	N (I)
Gymnodinium catenatum	33.9	3,000	N (I)
Naked ciliate			
Mesodinium rubrum	22	2,000	N (L)

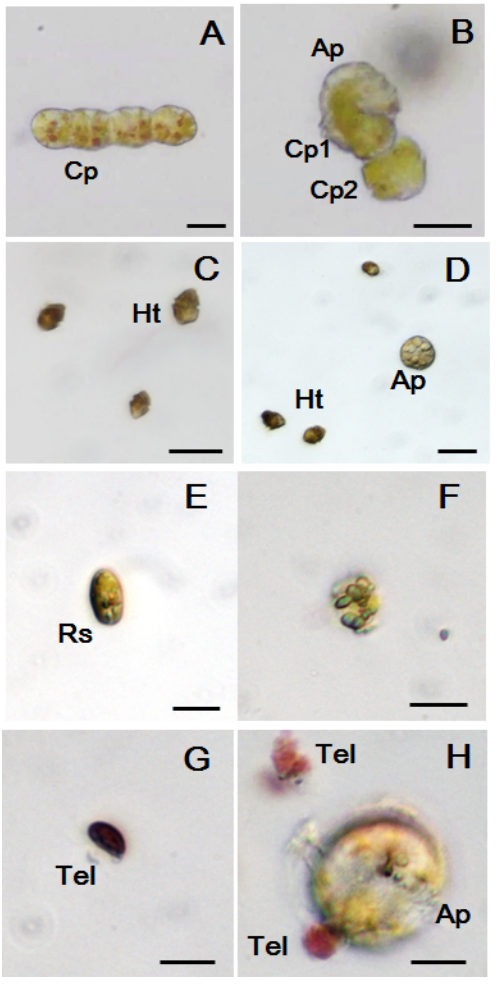

Fig. 5.1. *Alexandrium pohangense* (Ap) has different effects on the dinoflagellate *Cochlodinium polykrikoides* cells (Cp; A, B), *Heterocapsa triquetra* (Ht; C, D) and cryptophytes, *Rhodomonas salina* (Rs; E, F) and *Teleaulax* sp. (Tel; G, H). Ap divides chain-formed Cp cells into two cells of the chain, while Ht moves normally. Normal Rs and Tel cells (E, G) are lysed when they were incubated with Ap cells. Scale bars = 20 μm for (A-D) and 10 μm for (E-H).

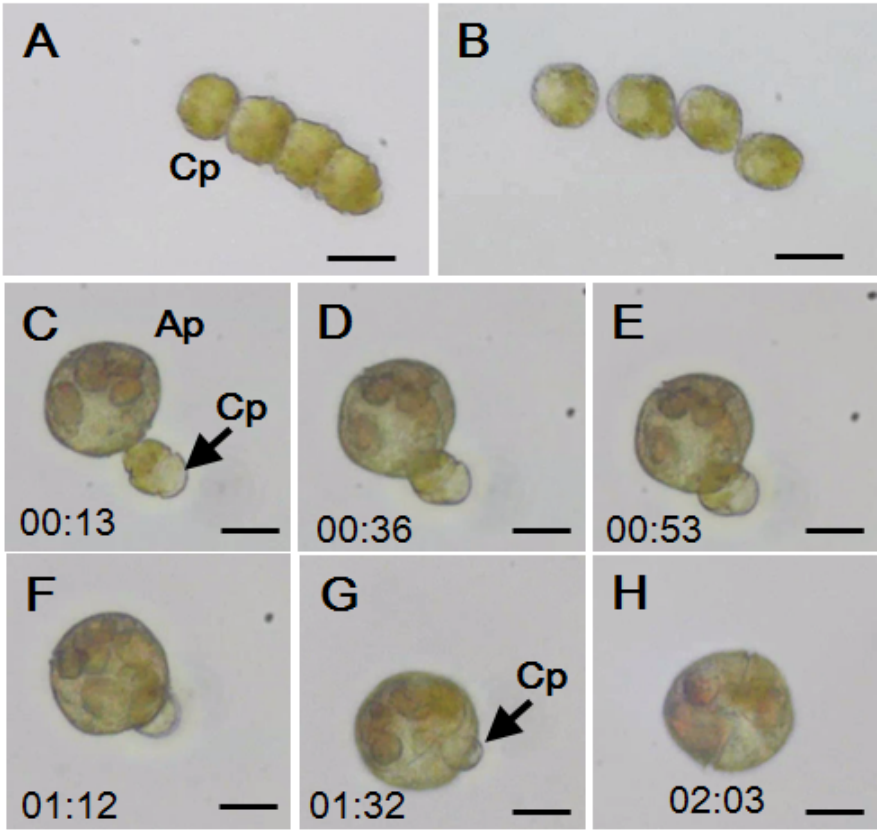

Fig. 5.2. Feeding process of *Alexandrium pohangense* (Ap) on *Cochlodinium polykrikoides* (Cp). When *A. pohangense* culture was added into *C. polykrikoides* culture, the chain formed *C. polykrikoides* cells (A) was splitted into one or two cells (B). *A. pohangense* contacts a *C. polykrikoides* (Cp) cell (C) and engulfs through the sulcus (D-G). Leaving *A. pohangense* cell after engulfing the whole Cp cell (H). Scale bars = 10 μm.

5.3.2. Growth and ingestion rates of *A. pohangense* on *C. polykrikoides*

A. pohangense grew well on *C. polykrikoides*. With increasing mean prey concentration, the specific growth rates of *A. pohangense* increased rapidly before saturating at a *C. polykrikoides* concentration of 138 ng C ml^{-1} (197 cells ml^{-1}) (Fig. 5.3A). When the data were fitted to Eq. (2), the maximum specific growth rate of *A. pohangense* on *C. polykrikoides* at 20 °C under a 14:10 h light-dark cycle of 100 μE m^{-2} s^{-1} was 0.487 d^{-1}. However, the autotrophic growth rate of *A. pohangense* at the same with mixotrophic condition was 0.091 d^{-1}. The K_{GR} (i.e. the prey concentration sustaining 1/2 μ_{max}) was 11.3 ng C ml^{-1} (16 cells ml^{-1}).

With increasing mean prey concentration, the ingestion rates of *A. pohangense* increased rapidly at a *C. polykrikoides* concentration of 99 ng C ml^{-1} (141 cells ml^{-1}), but slowly at the higher prey concentrations (Fig. 5-3B). When the data were fitted to Eq. (3), the maximum ingestion rate of *A. pohangense* on *C. polykrikoides* was 4.99 ng C $predator^{-1}$ d^{-1} (7.1 cells $predator^{-1}$ d^{-1}) and K_{IR} (the prey concentration sustaining 1/2 I_{max}) was 30.0 ng C $predator^{-1}$ d^{-1} (42.8 cells $predator^{-1}$ d^{-1}). The maximum clearance rate of *A. pohnagense* on *C. polykrikoides* was 3.23 μl $predator^{-1}$ h^{-1}.

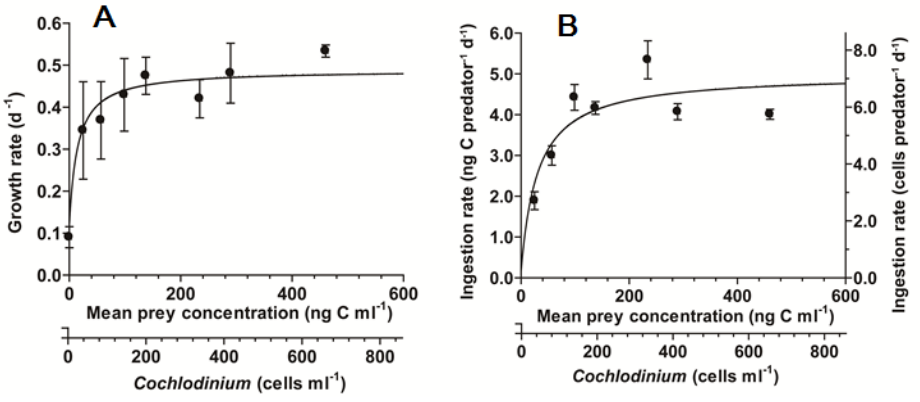

Fig. 5.3. Specific growth rates (A) and ingestion rates (B) of *Alexandrium pohangense* on *Cochlodinium polykrikoides* as a function of the mean prey concentration (x, ng C ml^{-1}). Symbols represent treatment means ± 1SE. The curve was fitted by a Michaelis-Menten equation [Eq.(2) for A, Eq. (3) for B] using all treatments in the experiment. Growth rate (GR, d^{-1}) = 0.487 [(x+2.6792) / (11.34 + (x-2.679))], r^2 = 0.564 and ingestion rate (IR, ng C predator^{-1} d^{-1}) = 4.99 [x / (30.0+x)], r^2=0.665

5.3.3. Grazing impact of *A. pohangense* on *C. polykrikoides*

The grazing coefficients attributable to *A. pohangense* on co-occurring *C. polykrikoides* in the water samples taken in the waters inside Yongil Bay, Pohang city, Korea in 2014, when the abundances of *A. pohangense* and *C. polykrikoides* were 1 - 13 cells ml^{-1} and 3 - 259 cells ml^{-1}, respectively, were 0.089 - 1.567 d^{-1} (Fig. 5.4).

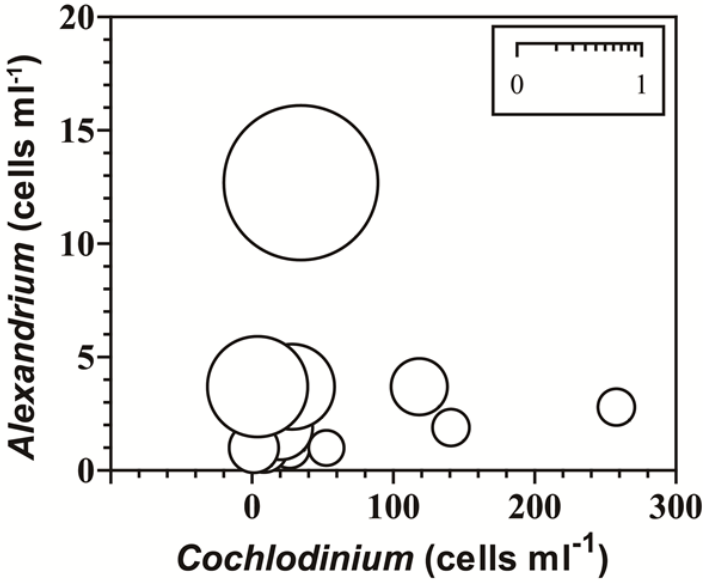

Fig. 5.4. Calculated grazing coefficients (g, d^{-1}) attributable to *Alexandrium pohangense* on natural populations of *Cochlodinium polykrikoides* (see text for calculation). n= 13.

5.4. Discussion

5.4.1. Prey species and feeding mechanism

Alexandrium pohangense fed only on *Cochlodinium polykrikoides* among offered as prey. Other dinoflagellate prey species, prymnesiophyte *Isochrysis galbana*, and raphidophyte *Heterosigma akashiwo* were immobilized by *A. pohangense*, but not ingested. Some studies suggested that predator and prey have specific recognition relationships such as chemosensory mechanism (Hansen and Calado, 1999; Wootton et al., 2007; Roberts et al., 2011; Sieg et al., 2011). Other *Alexandrium* species such as *A. minutum*, *A. tamarense*, *A. catenella*, *A. ostenfeldii*, and *A. pseudogonyaulax* are able to feed on some cryptophyte, dinoflagellate, ciliate and even diatom (Table 5.2, Nygaard and Tobiensen, 1993; Jacobson and Anderson, 1996; Jeong et al., 2005a, b; Yoo et al., 2009; Blossom et al., 2012). For example, while *A. tamarense* is able to feed on various prey including *Amphidinium carterae*, *Prorocentrum minimum*, and *Heterosigma akashiwo*, *A. pohangense* is able to feed only on *C. polykrikoides*. Thus, it is possible that *A. pohangense* has a specific relationship with *C. polykrikoides*. It is worthwhile to explore the recognition process between *A. pohangense* and *C. polykrikoides*.

The mixotrophic dinoflagellate *A. pohangense* fed on the prey cells by engulfing through the sulcus like other *Alexandrium* species. A tow filament to anchor the prey cell was not observed during the feeding process. However, *A. pohangense* cells immobilize *C. polykrikoides* cells and split into 1 or 2 cells. *A. pohangense* cells

approach the immobilized *C. polykrikoides* cells and engulf them through the sulcus. Moreover, filtrates from *A. pohangense* culture also immobilize or lyse the prey cells. Thus, it is possible that the *A. pohangense* immobilize and/or lyse the target prey cells by toxic substrates. It also suggests that toxic substrates secreted by *A. pohangense* may allow *A. pohangense* to feed on *C. polykrikodies* without a tow filament and/or trichocyst, even though *C. polykrikodies* is one of the fastest swimming dinoflagellates (~1,400 μm s^{-1}, Jeong et al., 1999a). Some *Alexandrium* speceis are known to lyse other protists using lytic compounds. The immobilization effects by substrates of harmful dinoflagellates may be species dependent and not dependent on paralytic shellfish poisoning toxic compound (Tillmann and John, 2002; Adolf et al., 2006). Moreover, putative *sxtA* gene for saxitoxins is not amplified from genomic DNA of *A. pohangense* and *A. pohangense* is not toxic to brain shrimp *Artemia salina* (Lim et al., 2015a). Thus, it is possible that the lytic substrates of *A. pohangense* are not exact toxins like saxitoxins. Ma et al. (2011) reported that lytic compounds of *A. tamarense* showed high affinity towards brassicasterol and thus suggested that lytic compounds may involve sterol components of cell membranes. Interestingly, *Rhodomonas salina* and *Storeatula major* which were lysed by *A. pohangense* have a brassicasterol as a major sterol (> 90 % of cell) (Adolf et al., 2006; Ma et al., 2011). It is worthwhile to analysis the sterol compounds of *A. pohangense* and prey species and explore the relationship between them and immobilizing and/or lytic activity.

Table 5.2. Comparison of the prey species of 6 *Alexandrium* species whose mixotrophic abilities have been reported. ESD, equivalent spherical diameter (μm). Ap: *A. pohangense,* Am: *A. minutum*, At: *A. tamarense*, Ac: *A. catenella*, Ao: *A. ostenfeldii,* Aps: *A. pseudogonyaulax.* Y: feeding on the prey species, N: not able to feed on the species.

Prey species	ESD	Ap	Am	At	Ac	Ao	Aps
Diatom							
Skeletonema costatum	5.9	N		Y	Y		
Prymnesiophytes							
Isochrysis galbana	4.8	N		Y			
Cryptophytes							
Teleaulax acuta			N		N		Y
Teleaulax sp.	5.6	N		Y			
Storeatula major	6.0	N					
Rhodomonas salina	8.8	N		Y			
Rhaphidophytes							
Heterosigma akashiwo	11.5	N		Y			
Mixotrophic dinoflagellates							
Heterocapsa rotundata	5.8	N	N		N		Y
Amphidinium carterae	9.7	N		Y			
Prorocentrum minimum	12.1	N		Y			
Hetereocapsa triquetra	15.0	N		N			Y
Gymnodinium aureolum	19.5	N		N			
Scrippsiella trochoidea	22.8	N					N
Cochlodinium polykrikoides	25.9	Y		N			
Prorocentrum micans	26.6	N		N			
Gymnodinium catenatum	33.9	N		N			
Dinophysis sp.						Y	
Naked ciliate							
Mesodinium rubrum	22.0	N					Y
Unidentified ciliate						Y	
Reference		(1)	(4)	(3, 4)	(3, 4)	(5)	(4)

(1) this study, (2) Jeong et al. (2005a), (3) Yoo et al. (2009), (4) Blossom et al. (2012), (5) Jacobson and Anderson (1996)

5.4.2. Contribution of mixotrophy to *Alexandrium pohangense*

The maximum growth rate (i.e., mixotrophic growth) of *Alexandrium pohangense* on the optimal prey obtained under a 14:10 h light-dark cycle of 100 μE $m^{-2}s^{-1}$ (4.9 d^{-1}) is higher than other *Alexandrium* species so far (Table 5.3). Under the similar light condition, the growth rates of *A. pseudogonyaulax* on *Heterocapsa rotundata* and *Teleaulax acuta* are 0.32 and 0.28, respectively (Blossom et al., 2012). *A. pohangense* and *A. pseudogonyaulax* do not share the prey item. Thus, they may have different biological niche. Furthermore, the ratio of mixotrophic to autotrophic growth rate of *A. pohangense* (4.9) is the greatest among the other engulfment feeding mixotrophic dinoflagellate (0.8 – 3.7), except for *Karlodinium armiger* (10.8) (Table 5.3). The mixotrophic growth rate of *A. pohangense* (0.49) is almost five times greater than its autotrophic growth rate (0.10). Thus, prey consumption of *A. pohangense* considerably contributes to the growth of *A. pohangense* when the prey is abundant in the natural environments. It is also possible that production of toxic metabolites of *A. pohangense* may be the reason for the low phototrophic growth rate. Producing toxin probably require high energy cost and thus toxin producing dinoflagellates may have lower growth rates than other group of phytoplankton such as diatom (Lim et al., 2014a). Therefore, it is worthwhile to explore production of toxic metabolites of *A. pohangense*.

Table 5.3. Optimal prey, maximum mixotrophic growth rate (MMGR), and autotrophic growth rate (AGR) of each mixotrophic engulfment feeding dinoflagellate predator species.

Predator	ESD	Optimal prey	ESD	T	LI	MMGR	AGR	RMAG	Ref.
Alexandrium pohangense	32.0	*Cochlodinium polykrikoides*	25.8	20	100	0.49	0.10	4.9	(1)
Ansanella granifera	10.5	*Pyramimonas* sp.	5.6	20	20	1.43	0.39	3.7	(2)
Prorocentrum donghaiense	13.2	*Teleaulax* sp.	5.6	20	20	0.51	0.38	1.4	(3)
Heterocapsa triquetra	15.0	*Teleaulax* sp.	5.6	20	20	0.28	0.18	1.5	(3)
Alexandrium minutum	16.7	*Teleaulax acuta*		15	17	0.11	0.13	0.8	(4)
Karlodinium armiger[a]	16.7	*Rhodomonas baltica*	10.7	15	180	0.65	0.06	10.8	(5)
Cochlodinium polykrikoides	25.8	*Teleaulax* sp.	5.6	20	50	0.32	0.17	2.0	(6)
Prorocentrum micans	26.6	*Teleaulax* sp.	5.6	20	20	0.20	0.11	1.9	(3)
Amylax triacantha	30.0	*Mesodinium rubrum*	22.0	15	20	0.68	-0.08		(7)
Gonyaulax polygramma	32.5	*Teleaulax* sp.	5.6	20	50	0.28	0.19	1.5	(8)
Alexandrium pseudogonyaulax	35.4	*Heterocapsa rotundata*	5.8	15	120	0.32	0.22	1.5	(4)
Lingulodinium polyedrum	36.6	*Scrippsiella trochoidea*	25.1	20	50	0.30	0.18	1.7	(3)
Fragilidium subglobosum	45.0	*Ceratium tripos*	59.5	15	45	0.50	0.16	3.1	(9, 10)
Fragilidium cf. *mexicanum*	54.5	*Lingulodinium polyedrum*	37.9	22	20	0.36	-0.05		(10, 11)

(1) this study, (2) Lee et al. (2014b), (3) Jeong et al. (2005a), (4) Blossom et al. (2012), (5) Berge et al. (2008), (6) Jeong et al. (2004b), (7) Park et al. (2013b), (8) Jeong et al. (2005c), (9) Hansen and Nielsen (1997), (10) Jeong et al., (2010a), (11) Jeong et al. (1999a)

5.4.3. Implications for *Cochlodinium polykrikoides* red tides

Cochlodinium polykrikoides is a bloom forming dinoflagellate in the coastal waters of many countries and causes massive fish mortality and economic loss in many countries (Gobler et al., 2008; Mulholland et al., 2009; Park et al., 2013a; Lim et al., 2014a, 2015b). Moreover, some studies suggested that populations of grazers may have considerable grazing impact on populations of bloom forming species (Jeong et al., 2004a, 2005d; Yoo et al., 2013). Thus, the predators of *C. polykrikoides* may be important factors to understand the population dynamics of *C. polykrikoides*. The grazing coefficients (g) attributable to *Alexandrium pohangense* on co-occurring *C. polykrikoides* obtained in the present study were up to 1.567 d^{-1} (i.e., up to 79 % of the *C. polykrikoides* populations were removed by a *A. pohangense* population in a day). Since *A. pohangense* has a lytic activity to some algal species, its ingestion rate (~7 cells $predator^{-1}$ d^{-1}) and grazing coefficients could be overestimated. However, they are still considerably high enough to effect on the population of *C. polykrikoides*. Therefore, *A. pohangense* may have a considerable grazing impact on populations of co-occurring *C. polykrikodies* to control when *C. polykrikodies* formed a bloom.

Alexandrium pohangense is a first reported mixotrophic dinoflagellate grazer on *C. polykrikoides*. Prior to this study, only several heterotrophic protists and ciliate are known to feed on *C. polykrikoides* (Table 5.4, Jeong et al., 1999b, 2006, 2007, 2008; Cho, 2006; Lim et al., 2014b). The maximum growth and ingestion rates of *A. pohangense* are greater than those of heterotrophic dinoflagellate *Pfiesteria piscicida*, but lower than ciliate *Strombidinopsis* spp.

Moreover, the maximum growth and ingestion rates of *Luciella masanensis* and *Stoeckeria changwonensis* are not considerable. Thus, it is possible that *A. pohangense* plays an important role as a predator when *C. polykrikoides* forms a bloom but there are no co-occurring *Strombidinopsis* species.

Table 5.4. Predators of *Cochlodinium polykrikoides* and comparisons of the maximum growth rates (MRG, d^{-1}) and maximum ingestion rates (MIR, ng C $predator^{-1}$ d^{-1}) of the predators. MTD: mixotrophic dinoflagellate, HTD: heterotrophic dinoflagellate, CIL: ciliate, NA: not available.

Predator	Trophic mode	MRG	MIR	Reference
Alexandrium pohangense	MTD	0.49	4.99	This study
Pfiesteria piscicida	HTD	0.16	0.03	Jeong et al., 2006
Luciella masanensis	HTD	NA	NA	Jeong et al., 2007
Stoeckeria changwonensis	HTD	NA	NA	Lim et al., 2014b
Protoperidinium sp.	HTD	NA	NA	Cho, 2006
Strombidinopsis jeokjo	CIL	1.782	127	Jeong et al., 2008
Strombidinopsis sp.	CIL	1.378	353	Jeong et al., 1999b

Chapter 6. Overall conclusion

In this thesis, I found that tropical cyclones (typhoons in Northwest Pacific), co-occurring diatoms, and a new dinoflagellate *Alexandrium pohangense* n. sp. clearly affect on the abundance of *Cochlodinium polykrikoides* (Fig. 6.1). However, the degrees of the impact are dependent on daily maximum wind speed generated by tropical cyclones, abundance of diatoms, and abundance of *A. pohangense*. Therefore, in models of predicting the outbreak, persistence, and decline of *C. polykrikoides*, these new critical factors should be taken into consideration.

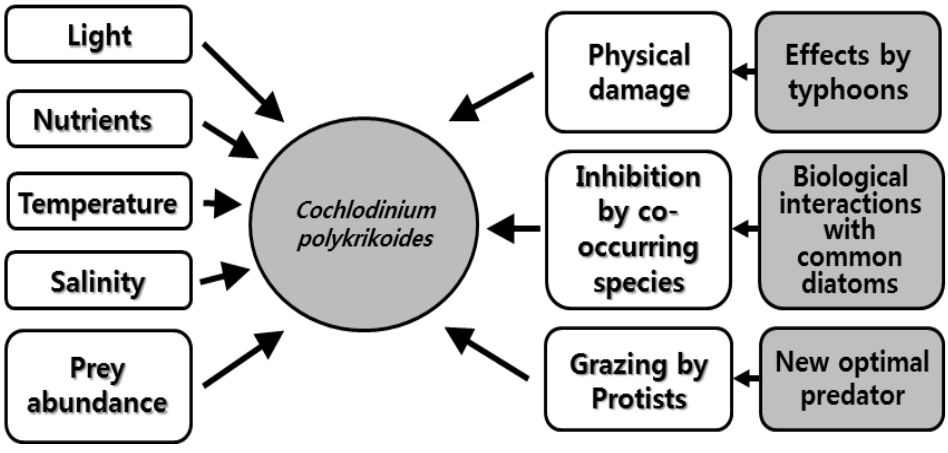

Fig. 6.1. Various factors affecting the dynamics of *Cochlodinium polykrikodes* red tides. The grey boxes indicate the factors explored by present study.

The tropical cyclones differentially affected *Cochlodinium polykrikodes* red tides in 2012–2014. The daily maximum wind speed generated by tropical cyclones was critical. Prior to my study, there were several studies on the effects of tropical cyclones on the *C. polykrikoides* red tides. However, they have not investigated relationships between the daily maximum wind speed and the daily maximum cell abundance. For example, *C. polykrikodes* red tides disappeared when the daily maximum wind speed driven by tropical cyclone was more than 14 m s^{-1}, but the abundance of *C. polykrikoides* is lowered when the daily maximum wind speed was 5–14 m s^{-1}. In general, the strong wind speed driven by tropical cyclones generates turbulence in the water column and such turbulence causing physical damage on the organism may directly reduce the abundance of *C. polykrikodes*.

The cell abundance of *C. polykrikoides* in its red tide patches advected into aquaculture cages are one of the critical factors affecting survival of fish in cages; if the abundance of *C. polykrikoides* in the aquaculture cages is < 1,000 cells ml^{-1}, fish mortality and in tern economic loss is likely to be greatly reduced. Thus, strong winds generated by tropical cyclones may contribute in preventing fish in aquaculture cages from being killed due to *C. polykrikoides* red tide patches. Approximately 28 million fish from aquaculture in the South Sea of Korea were reported to be killed in the *Cochlodinium* red tide period in 2013 when only two tropical cyclones passed the aquaculture areas, causing a loss of USD $ 24 billion, while only 5 million fish from aquaculture in Korea were killed in 2012 when five tropical cyclones passed the aquaculture areas (NFRDI, 2014; Park et al., 2013a), causing a loss of USD $ 4

billion. The results of the study on tropical cyclones effects could be applied to *Cochlodinium* red tides in the coastal waters of the other countries such as Japan, China, Philippines, Taiwan, the Middle East, the west coasts of North and Mid America, the eastern coast of the USA, and the western coasts of India and Australia, which experience both *Cochlodinium* red tides and tropical cyclones (equivalent to typhoons, hurricanes, and willy-willies) (Fig. 6.2). In these areas, *Cochlodinium* red tide has caused massive fish death and economic loss (Fudge, 1977; Hallegraeff, 1992; Whyte et al., 2001; Fukuyo et al., 2002; Yan et al., 2002; Gárate-Lizárraga et al., 2004; Lara et al., 2004; Vershinin et al., 2005; Imai et al., 2006; Vargas-Montero et al., 2006; Anton et al., 2008; Azanza et al., 2008; Curtiss et al., 2008; Gómez-Villarreal et al., 2008; Tomas and Smayda, 2008; Verity, 2010; Philps et al., 2011; D'Silva et al., 2012; Ke et al., 2012; Kudela and Goble, 2012; Munir et al., 2012; Hamzehei et al., 2013; Park et al., 2013a; Maciel-Baltazar et al., 2013). Therefore, there is a high possibility that tropical cyclones in these waters (called as typhoons, hurricanes, tropical cyclones, or willy-willies) affect the outbreak, persistence, and decline of *Cochlodinium* red tides and thus it is worthwhile to explore this topics in these waters.

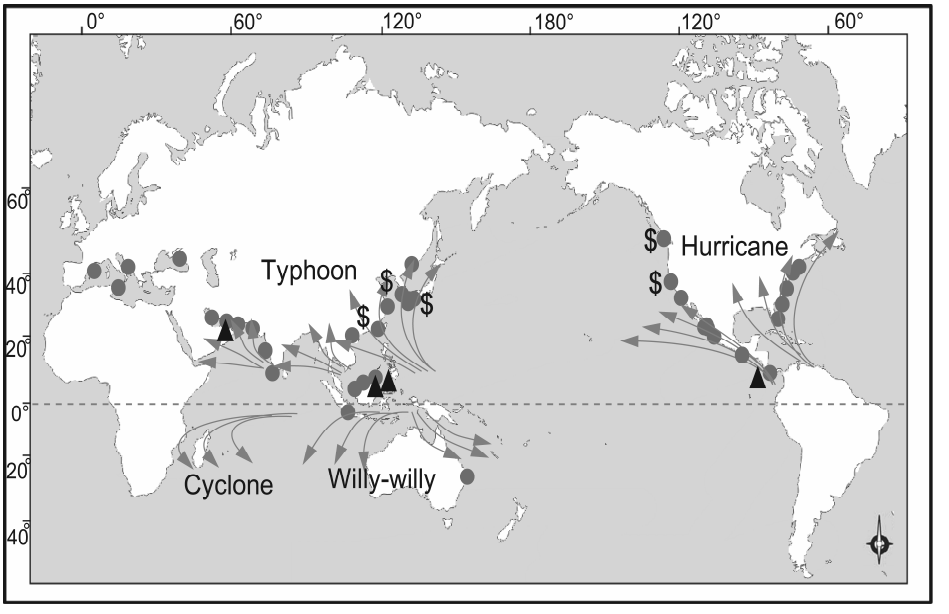

Fig. 6.2. Global distribution map of *Cochlodinium* red tides. Arrows indicate the general paths of tropical cyclones. Circles indicate the occurrence of *Cochlodinium* red tides. Dollar marks indicate the regions where economic loss occurred and solid triangles indicate massive fish death caused by the red tides.

The results of this study clearly show that fast-growing diatoms cause negative effects on *C. polykrikoides* with both physical contact and chemical stress; high abundance of *Skeletonema costatum*, *Chaetoceros danicus*, and *Thalassiosira decipiens* can reduce swimming speed of *C. polykrikoides*, which may inhibit vertical migration of *C. polykrikoides.* If *C. polykrikoides* does not reach nutrient-rich deep waters, it may not grow well. Moreover, *S. costatum* and *C. danicus* cause negative growth rates of *C. polykrikoides,* and thus they may directly lower the abundance of *C. polykrikoides* in the water column. Thus, if diatoms is abundant due to some reasons in the Korean coastal waters, the outbreak of

Cochlodinium red tides could be delayed or prevented by reducing swimming speed and the growth rate of *C. polykrikoides*. Diatoms usually grow faster than the other phytoplankton groups when the conditions favorable for photosynthesis are given. Nutrient concentrations in coastal waters are usually elevated after heavy rains. This condition may cause high abundances of diatoms and in turn low abundances of *C. polykrikoides*.

I established the 34th *Alexandrium* species, *Alexandrium pohangense* n. sp. Scientists and people in aquaculture industry are interested in *Alexandrium* species because several *Alexandrium* species are toxic and known to be responsible for paralytic shellfish poisoning (PSP). The productions of Pacific cupped oyster and Japanese carpet shell are approximately 4.27 million tons and 3.09 million tons, respectively, in 2007 in the world (KMI, 2009). The production of shellfish in aquaculture industry has gradually increased. The morphological characteristics in the genus *Alexandrium* are very complicated, and thus it is difficult to identify *Alexandrium* cells in the species level. In this study, I suggeste new useful criteria for identifying a species in the *Alexandrium* genus such as the angles between the cingulum and the bottom margin side of 1′ plate (α) and antero-posterioral axis of the cell and the point of the margin of apical pore plate (β).

I found that *Alexandrium pohangense* n. sp. is a mixotrophic dinoflagellate. Interestingly, this dinoflagellate is a specialist feeding on fast swimming *C. polykrikoides* cells. Furthermore, based on calculated grazing coefficients, it is suggested that *A. pohangense* sometimes has considerably grazing impacts on populations of *C.*

polykrikoides. Prior to this study, there have been no mixotrophic predator which is able to feed on *C. polykrikoides*. An *A. pohangense* cell is able to ingest maximum 7 *C. polykrikoides* cells a day and divide twice in three days (i.e., mixotrophic maximum growth rate = 0.5 d^{-1}). Moreover, *A. pohangense* lysed all cryptophyte species which are the nutritious prey to *C. polykrikoides*. Thus, *A. pohangense* may affect *C. polykrikoides* populations by feeding *C. polykrikodes* and lysing cryptophytes which are nutritional prey for *C. polykrikoides*. Jeong et al. (2004b) suggested that the presence of co-occurring cryptophytes may be partially responsible for the outbreak of *C. polykrikoides* in the offshore waters because the maximum mixotrophic growth rate of *C. polykrikoides* with added crptophyte *Teleaulax* sp. (0.324 d^{-1}) is almost twice the rate without prey (0.166 d^{-1}). Therefore, by eliminating the potential prey of *C. polykrikoides*, *A. pohangense* may lower the growth of *C. polykrikoides* and in turn delay or prevent the outbreak of *C. polykrikoides* red tides. Thus, *A. pohangense* should be taken into consideration in models for dynamics of *C. polykrikoides* red tides.

This study tested 3 hypotheses that tropical cyclones, competing diatoms, and a new mixotrophic species *A. pohangense* affect dynamics of *C. polykrikoides* red tides. These newly identified factors clearly give critical effects on dynamics of *C. polykrikoides* red tides directly or indirectly (Fig. 6.3). Tropical cyclones generate turbulence and it could directly damage the *Cochlodinium* cells or make the environment favorable for diatoms and small flagellates. Diatoms usually grow faster than dinoflagellates when surface nutrient concentrations are high and turbulence intensity is high (Banse, 1982; Thomas and Gibson, 1990a). Under these circumstances,

dense diatoms may reduce the *Cochlodinium* population by inhibition of swimming speed and growth rate of *Cochlodinium*. Moreover, the new predator, *A. pohagense,* also may reduce the *Cochlodinium* population by removing the potential prey of *Cochlodinium* and by directly removing *Cochlodinium* cells by feeding. I hope that the results of this study contribute in understanding harmful *C. polykrikoides* red tides, establishing prediction models, and developing methods of controlling the red tides.

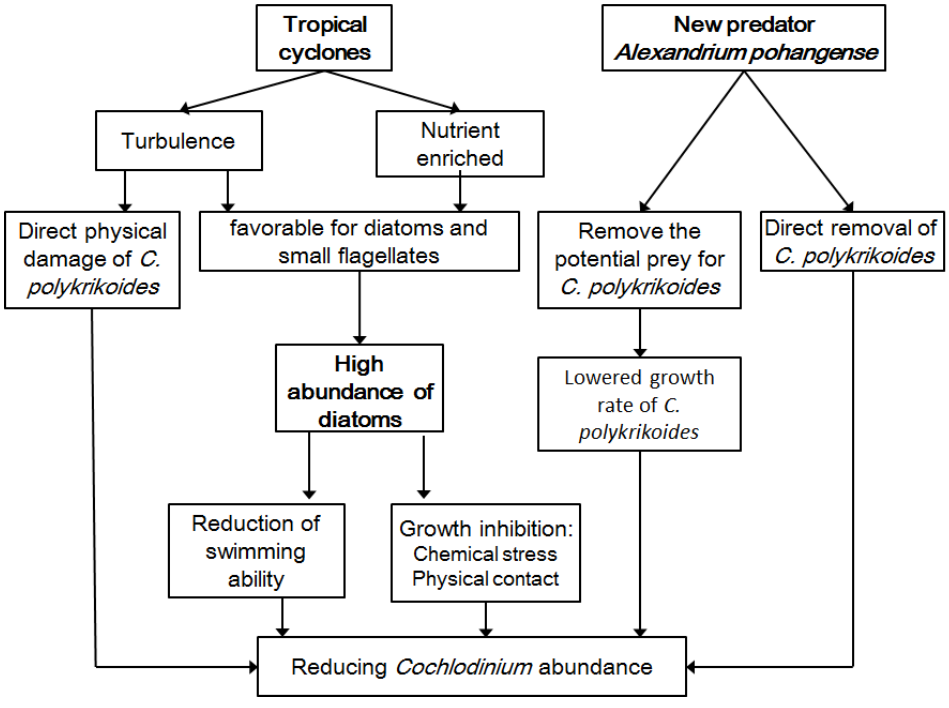

Fig. 6.3. Schematic diagram showing factors reducing the abundance of *Cochlodinium*.

Reference

Adolf, J.E., Bachvaroff, T.R., Krupatkina, D.N., Nonogaki, H., Brown, P.J.P., Lewitus, A.J., Harvey, H.R., Place, A.R., 2006. Species specificity and potential roles of *Karlodinium micrum* toxin, African J. Mar. Sci. 28, 415-419.

Allen, W.E., 1949. Data files, 1917-1949. Accession No. 81-19. Scripps Institution of Oceanography Archives, University of California, San Diego.

Anderson, D.M., 1997. Turning back the harmful red tide. Nature 388, 513-514.

Anderson, D.M., Alpermann, T.J., Cembella, A.D., Collos, Y., Masseret, E., Montresor, M., 2012. The globally distributed genus *Alexandrium*: multifaced roles in marine ecosystems and impacts on human health. Harmful Algae 14, 10-35.

Anton, A., Teoh, P.L., Mohd-Shaleh, S.R., Mohammad-Noor, N., 2008. First occurrence of *Cochlodinium* blooms in Sabah, Malaysia. Harmful Algae 7, 331-336.

Azanza, R.V., David, L.T., Borja, R.T., Baula, I.U., Fukuyo, Y., 2008. An extensive *Cochlodinium* bloom along the western coast of Palawan, Philippines. Harmful Algae 7, 324-330.

Balech, E., 1994. Three new species of the genus *Alexandrium* (dinoflagellate). Trans. Am. Microsc. Soc. 113, 216-220.

Balech, E., 1995. The genus *Alexandrium* Halim (Dinoflagellata). Sherkin Island Marine Station Publication, Sherkin Island, Co. Cork, Ireland.

Banse, K., 1982. Cell volumes, maximal growth rates of unicellular algae and ciliates and the role of ciliates in the marine pelagial.

Limnol. Oceanogr. 27, 1057-1071.

Berge, T., Hansen, P.J., Moestrup, Ø., 2008. Prey size spectrum and bioenergetics of the mixotrophic dinoflagellate *Karlodinium armiger*. Aquat. Microb. Ecol. 50, 289-299.

Blossom, H.E., Daugbjerg, N., Hansen, P.J., 2012. Toxic mucus traps: A novel mechanisms that mediates prey uptake in the mixotrophic dinoflagellate *Alexandrium pseudogonyaulax*. Harmful Algae 17, 40-53.

Bockstahler, K.R., Coats, D.W., 1993. Spatial and temporal aspects of mixotrophy in Chesapeake Bay dinoflagellates. J. Eukaryot. Microbiol. 40, 49-60.

Burkholder, J.M., Glibert, P.M., Skelton, H.M., 2008. Mixotrophy, a major mode of nutrition for harmful algal species in eutrophic waters. Harmful Algae 8, 77-93.

Cembella, A.D., Quilliam, M.A., Lewis, N.I., Bauder, A.G., Dell'Aversano, C., Thomas, K., Jellett, J., Cusack, R.R., 2002. The toxigenic marine dinoflagellate *Alexandrium tamarense* as the probable cause of mortality of caged salmon in Nova Scotia. Harmful Algae 1, 313-325.

Chan, A.T., 1978. Comparative physiological study of marine diatoms and dinoflagellates in relation to irradiance and cell size. I. Growth under continuous light. J. Phycol. 14, 396-402.

Chen, Y.L., Chen, H., Jan, S., Tuo, S., 2009. Phytoplankton productivity enhancement and assemblage change in the upstream Kuroshio after typhoons. Mar. Ecol. Prog. Ser. 385, 111-126.

Cho, E. 2006. Report on *Protoperidinium* sp. fed on *Cochlodinium*

polykrikodies (Gymnodiniales, Dinophyceae). Kor. J. Environ. Sci. 15, 385-386.

Cho, E., 2010. A comparative study on outbreak and non-outbreak of *Cochlodinium polykrikoides* Margalef in South Sea of Korea in 2007-2009. J. Kor. Soc. Mar. Environ. Safety 16, 31-41. (in Korean)

Chung, C., Gong, G., Hung, C., 2012. Effect of typhoon Morakot on microphytoplankton population dynamics in the subtropical Northwest Pacific. Mar. Ecol. Prog. Ser. 448, 39-49.

Curtiss, C.C., Langlois, G.W., Busse, L.B., Mazzillo, F., Silver, M. W., 2008. The emergence of *Cochlodinium* along the California Coast (USA). Harmful Algae 7, 337-346.

Daugbjerg, N., Hansen, G., Larsen, J., Moestrup, Ø., 2000. Phylogeny of some of the major genera of dinoflagellates based on ultrastructure and partial LSU rDNA sequence data, including the erection of three new genera of unarmoured dinoflagellates. Phycologia 39, 302-317.

D'Silva, M.S., Anil, A.C., Naik, R.K., D'Costa P.M., 2012. Algal blooms: a perspective from the coasts of India. Nat. Hazards 63, 1225-1253.

Elbrächter, M., 1977. On population dynamics in multi-species cultures of diatoms and dinoflagellates. Helgoländer wiss. Meeresunters 30, 192-200.

Emanuel, K., 2003. Tropical cyclones. Annu. Rev. Earth Planet. Sci. 31, 75-104.

Fistarol, G.O., Legrand, C., Selander, E., Hummert, C., Stolte, W., Granéli, E., 2004. Allelopathy in *Alexandrium* spp.: effect on a natural plankton community and on algal monocultures. Aquat. Microb. Ecol. 35, 45-56.

Fogel, M.L., Aguilar, C., Cuhel, R., Hollander, D.J., Willey, J.D., Paerl, H.W., 1999. Biological and isotopic changes in coastal waters induced by Hurricane Gordon. Limnol. Oceanogr. 44, 1359-1369.

Franks, P.J.S, Anderson, D.M., 1992. Alongshore transport of a toxic phytoplankton bloom in buoyancy current: *Alexandrium tamarense* in the Gulf of Maine. Mar. Bol. 112, 153-164.

Frost, B.W., 1972. Effects of size and concentration of food particles on the feeding behavior of the marine planktonic copepod *Calanus pacificus*. Limnol. Oceanogr. 17, 805-815.

Fudge, H., 1977. The "Red Tides" of Malta. Mar. Biol. 39, 381-386.

Fukuyo, Y., Imai, I., Kodama, M., Tamai, K., 2002. Red tide and other harmful algal blooms in Japan. In: Tayler, F.R.J., Trainer, V.L. (Eds.), Harmful algal blooms in the PICES region of the North Pacific. PICES Sci. Rep. No. 23, pp. 152.

Gárate-Lizárraga, I., López-Cortes, D.J., Bustillo-Guzmán, J.J., Hemández-Sandoval, F., 2004. Blooms of *Cochlodinium polykrikoides* (Gymnodiniaceae) in the Gulf of California, Mexico. Rev. Biol. Trop. 52(S1), 51-58.

Geraci, J.R., Anderson, D.M., Timperi, R.J., St. Aubin D.J., Early, G.A., Prescott, J.H., Mayo, C.A., 1989. Humpback whales (*Megaptera novaeangliae*) fatally poisoned by dinoflagellate toxin. Can. J. Fish. Aquat. Sci. 46, 1895-1898.

Giacobbe, M.G., Yang, X., 1999. The life history of *Alexandrium taylori* (Dinophyceae). J. Phycol. 35, 331-338.

Giovannoni, S.J., DeLong, E.F., Olsen, G.J., Pace, N.R., 1988. Phylogenetic group-specific oligodeoxynucleotide probes for identification of single microbial cells. J. Bacteriol. 170, 720-726.

Glibert, P.M., Burkholder, J.M., Kana, T.M., Alexander, J., Skelton,

H., Shilling, C., 2009. Grazing by *Karenia brevis* on *Synechococcus* enhances its growth rate and may help to sustain blooms. Aquat. Microb. Ecol. 55, 17-30.

Gobler, C.J., Berry, D.L., Anderson, O.R., Burson, A., Koch, F., Rodger, B.S., Moore, L.K., Goleski, J.A., Allam, B., Bowser, P., Tang, Y., Nuzzi, R., 2008. Characterization, dynamics, and ecological impacts of harmful *Cochlodinium polykrikoides* blooms on eastern Long Island, NY, USA. Harmful Algae 7, 293-307.

Gobler, C.J., Burson, A., Koch, F., Tang, Y., Mulholland, M.R., 2012. The role of nitrogenous nutrients in the occurrence of harmful algal blooms caused by *Cochlodinium polykrikoides* in New York estuaries (USA). Harmful Algae 17, 64-74.

Godhe, A., Asplund, M.E., Härnström, K., Saravanan, V., Tyagi, A., Karunasagar, I., 2008. Quantification of diatom and dinoflagellte biomasses in coastal marine seawater samples by Real-time PCR. Appl. Environ. Microbiol. 74, 7174-7182.

Gómez-Villarreal, M.C., Martínez-Gaxiola, M.D., Peña-Manjarrez, J.L., 2008. Algal blooms at Banderas Bay, Mexico (2000-2001), from SeaWiFS-sensor-data. Rev. Biol. Trop. 56, 1653-1664.

Gribble, K.E., Keafer, B.A., Quilliam, M.A., Cembella, A.D., Kulis, D.M., Manahan, A., Anderson, D.M., 2005. Distribution and toxicity of *Alexandrium ostenfeldii* (Dinophyceae) in the Gulf of Maine, USA. Deep-Sea Res. 52, 2745-2763.

Gu, H., Zeng, N., Liu, T., Yang, W., Müller, A., Krock, B., 2013. Morphology, toxicity, and phylogeny of *Alexandrium* (Dinophyceae) species along the coast of China. Harmful Algae 27, 68-81.

Guillard, R.R.L., Ryther, J.H., 1962. Studies of marine planktonic diatoms. I. *Cyclotella nana* Hustedt and *Detonula confervacea* (Cleve) Grun. Can. J. Microbiol. 8, 229-239.

Halim, Y., 1960. *Alexandrium minutum* n. gen. s. sp., dinoflagellate provocant "des eaus rouges". Vie. et Milieu 11, 102-105.

Hallegraeff, G.M., 1992. Harmful algal blooms in the Australian region. Mar. Pollut. Bull. 25, 185-190.

Hallegraeff, G.M., 1993. A review of harmful algal blooms and their apparent global increase. Phycologia 32, 79-99.

Hamzehei, S., Bidokhi, A.A., Mortazavi, M.S., Gheiby, A., 2013. Red tide monitoring in the Persian Gulf and Gulf of Oman using MODIS sensor data. Tech. J. Engin. App. Sci. 3, 1100-1107.

Hansen, P. J., 2011. The role of photosynthesis and food uptake for the growth of marine mixotrophic dinoflagellates. J. Eukaryot. Microbiol. 58, 203-214.

Hansen, P.J., Bjornsen, P.K., Hansen, B.W., 1997. Zooplankton grazing and growth: scaling within the 2-2,000 μm body size range. Limnol. Oceanogr. 42, 687-704.

Hansen, P.J., Nielsen, T.G., 1997. Mixotrophic feeding of *Fragilidium subglobosum* (Dinophyceae) on three species of *Ceratium*: effects of prey concentration, prey species and light intensity. Mar. Ecol. Prog. Ser. 147, 187-196.

Hansen, P.J., Calado, A. J., 1999. Phagotrophic mechanisms and prey selection in free-living dinoflagellates. J. Eukaryot. Microbiol. 46, 382-389.

Heinbokel, J.F., 1978. Studies on the functional role of tintinnids in the Southern California Bight. I. Grazing and growth rates in

laboratory cultures. Mar. Biol. 47, 177-189.

Huelsenbeck, J.P., Ronquist, F., 2001. MrBayes: Bayesian inference of phylogeny. Bioinformatics 17, 754-755.

Imai, I., Yamaguchi, M., Hori, Y., 2006. Eutrophication and occurrences of harmful algal blooms in the Seto Inland Sea, Japan. Plankton Benthos Res. 1, 71-84.

Jacobson, D.M., Anderson, D.M., 1996. Widespread phagocytosis of ciliates and other protists by marine mixotrphic and heterotrophic thecate dinoflagellates. J. Phycol. 32, 279-285.

Jeong, H.J., Shim, J.H., Kim, J.S., Park, J.Y., Lee, C.W., Lee, Y., 1999a. The feeding by the thecate mixotrophic dinoflagellate *Fragilidium* cf. *mexicanum* on red tide and toxic dinoflagellate. Mar. Ecol. Prog. Ser. 176, 263-277.

Jeong, H.J., Shim, J.H., Lee, C.W., Kim, J.S., Koh, S.M., 1999b. Growth and grazing rates of the marine planktonic ciliate *Strombidinopsis* sp. on red-tide and toxic dinoflagellates. J. Eukaryot. Microbiol.46, 69-76.

Jeong, H.J., Park, J.K., Choi, H.Y., Yang, J.S., Shim, J.H., Shin, Y.K., Yih, W.H., Kim, H.S., Cho, K.J., 2000. The outbreak of red tides in the coastal waters off Kohung, Chonnam, Korea. 2. The temporal and spatial waters variations in the phytoplanktonic community in 1997. J. Kor. Soc. Oceanogr. 5, 27-36. (written in Korean with English abstract)

Jeong, H.J., Yoo, Y.D., Kim, S.T., Kang, N.S., 2004a. Feeding by the heterotrophic dinoflagellate *Protoperidinium bipes* on the diatom *Skeletonema costatum*. Aquatic. Microb. Ecol. 36, 171-179.

Jeong, H.J., Yoo, Y.D., Kim, J.S., Kim, T.H., Kim, J.H., Kang, N.S., Yih, W., 2004b. Mixotrophy in the phototrophic harmful alga *Cochlodinium polykrikoides* (Dinophycean): prey species, the effects of prey concentration, and grazing impact. J. Eukaryot. Microbiol. 51, 563-569.

Jeong, H.J., Yoo, Y.D., Park, J.Y., Song, J.Y., Kim, S.T., Lee, S.H., Kim, K.Y., Yih, W.H., 2005a. Feeding by the phototrophic red-tide dinoflagellates: five species newly revealed and six species previously known to be mixotrophic. Aquat. Microb. Ecol. 40, 133-155.

Jeong, H.J., Park, J.Y., Nho, J.H., Park, M.O., Ha, J.H., Seong, K.A., Jeng, C., Seong, C.N., Lee, K.Y., Yih, W.H., 2005b. Feeding by red-tide dinoflagellates on the cyanobacterium *Synechococcus*. Aquat. Microb. Ecol. 41, 131-143.

Jeong, H.J., Yoo, Y.D., Seong, K.A., Kim, J.H., Park, J.Y., Kim, S.H., Lee, S.H., Ha, J.H., Yih, W.H., 2005c. Feeding by the mixotrophic dinoflagellate *Gonyaulax polygramma*: mechanisms, prey species, the effects of prey concentration, and grazing impact. Aquat. Microb. Ecol. 38, 249-257.

Jeong, H.J., Kim, J.S., Kim, J.H., Kim, S.T., Seong, K.A., Kim, T.H., Song, J.Y., Kim, S.K., 2005d. Feeding and grazing impact of the newly described heterotrophic dinoflagellate *Stoeckeria algicida* on the harmful alga *Heterosigma akashiwo*. Mar. Ecol. Prog. Ser. 295, 69-75.

Jeong, H.J., Ha, J.H., Park, J.Y., Kim, J.H., Kang, N.S., Kim, S., Kim, J.S., Yoo, Y.D., Yih, W., 2006. Distribution of the heterotrophic dinoflagellate *Pfiesteria piscicida* in Korean waters and its

consumption of mixotrophic dinoflagellates, raphidophytes and fish blood cells. Aquat. Microb. Ecol. 44, 263-278.

Jeong, H.J., Ha, J.H., Yoo, Y.D., Park, J.Y., Kim, J.H., Kang, N.S., Kim, T.H., Kim, H.S., Yih, W.H., 2007. Feeding by the *Pfiesteria*-like heterotrophic dinoflagellate *Luciella masanensis*. J. Eukaryot. Microbiol. 54, 231-241.

Jeong, H.J., Kim, J.S., Yoo, Y.D., Kim, S.T., Song, J.Y., Kim, T.H., Seong, K.A., Kang, N.S., Kim, M.S., Kim, J.H., Kim, S., Ryu, J., Lee, H.M., Yih, W.H., 2008. Control of the harmful alga *Cochlodinium polykrikoides* by the naked ciliate *Strombidinopsis jeokjo* in mesocosm enclosures. Harmful Algae 7, 368-377.

Jeong, H.J., Yoo, Y.D., Kim, J.S., Seong, K.A., Kang, N.S., Kim, T.H., 2010a. Growth, feeding and ecological roles of the mixotrophic and heterotrophic dinoflagellates in marine planktonic food webs. Ocean Sci. J. 45, 65-91.

Jeong, H.J., Yoo, Y.D., Kang, N.S., Rho, J.R., Seong, K.A., Park, J.W., Nam, G.S., Yih, W.H., 2010b. Ecology of *Gymnodinium aureolum*. I. Feeding in western Korean waters. Aquat. Microbial Ecol. 59, 239-255.

Jeong, H.J., Yoo, Y.D., Kang, N.S., Lim, A.S., Seong, K.A., Lee, S.Y., Lee, M.J., Lee, K.H., Kim, H.S., Shin, W., Nam, S.W., Yih, W., Lee, K., 2012. Heterotrophic feeding as a newly identified survival strategy of the dinoflagellate *Symbiodinium*. Proc. Nat. Acad. Sci. USA 109, 12604-12609.

Jeong, H.J., Yoo, Y.D., Lee, K.H., Kim, T.H., Seong, K.A., Kang, N.S., Lee, S.Y., Kim, J.S., Kim, S., Yih, W.H., 2013. Red tides

in Masan Bay, Korea in 2004-2005: I. Daily variations in the abundance of red tide organisms and environmental factors. Harmful Algae 30S, S75-S88.

John, U., Fensome, R.A., Medlin, L.K., 2003. The application of a molecular clock based on molecular sequences and the fossil record to explain biogeographic distributions within the *Alexandrium tamarense* "species complex" (Dinophyceae). Mol. Biol. Evol. 20, 1015-1027.

John, U., Litaker, R.W., Montresor, M., Murray, S., Brosnahan, M.L., Anderson, D.M., 2014. Formal revision of the *Alexandrium tamarense* species complex (Dinophyceae) taxonomy: The introduction of five species with emphasis on molecular-based (rDNA) classification. Protist 165, 779-804.

Kang, Y.S., Park, Y.T., Lim, W.A., Cho, E.S., Lee, C.K., Kang, Y.S., 2009. A comparative study on outbreak scale of *Cochlodinium polykrikoides* blooms. J. Kor. Soc. Oceanogr. 14, 229-239.

Kang, N.S., Jeong, H.J., Moestrup, Ø., Shin, W.G., Nam, S.W., Park, J.Y., de Salas, M.F., Kim, K.W., Noh, J.H., 2010. Description of a new planktonic mixotrophic dinoflagellate *Paragymnodinium shiwhaense* n. gen., n. sp. from the coastal waters off western Korea: morphology, pigments, and ribosomal DNA gene sequence. J. Eukaryot. Microbiol. 57, 121-144.

Ke, Z., Huang, L., Tan, Y., Song, X., 2012. A dinoflagellate *Cochlodinium geminatum* bloom in the Zhujiang (Pearl) River estuary in autumn 2009. Chin. J. Oceanol. Limn. 30, 371-378.

Kim, H., Lee, C., Lee, S., Kim, H., Park, C., 2001. Physico-chemical factors on the growth of *Cochlodinium polykrikoides* and nutrient utilization. J. Korean Fish. Soc. 34, 445-456.

Kim, D., Matsuyama, Y., Nagasoe, S., Yamaguchi, M., Yoon, Y., Oshima, Y., Imada, N., Honjo, T., 2004. Effects of temperature, salinity and irradiance on the growth of the harmful red tide dinoflagellate *Cochlodinium polykrikoides* Margalef (Dinophyceae). J. Plankton Res. 26, 61-66.

Kim, Y.S., Jeong, C.S., Seong, G.T., Han, I.S., Lee, Y.S., 2010. Diurnal vertical migration of *Cochlodinium polykrikoides* during the red tide in Korean coastal sea waters. J. Environ. Biol. 31, 687-693.

Kim, T.W., Lee, K., Lee, C.K., Jeong, H.D., Suh, Y.S., Lim, W.A., Kim, K.Y., Jeong, H.J., 2013. Interannual nutrient dynamics in Korean coastal waters. Harmful Algae 30S, S15-S27.

Kita, T., Fukuyo, Y., 1988. Description of the Gonyaulacoid dinoflagellate *Alexandrium hiranoi* sp. nov. inhabiting tidepools on Japanese Pacific coast. Bull. Plank. Soc. Japan 35, 1-7.

Kondo, K., Seike, Y., Date, Y., 1990. Red tides in the brackish lake Nakanoumi (II). Relationships between the occurrence of *Prorocentrum minimum* red tide and environmental conditions. Bull. Plankton Soc. Jpn, 37, 19-34.

Korea Maritime Institute (KMI). 2009. A basic study to advance Korea's fisheries industry. pp. 394.

Kremp, A., Tamminen, T., Spilling, K., 2008. Dinoflagellate bloom formation in natural assemblage with diatoms: nutrient competition and growth strategies in Baltic spring phytoplankton. Aquat. Microb. Ecol. 50, 181-196.

Kremp, A., Tahvanainen, P., Litaker, W., Krock, B., Suikkanen, S., Leaw, C.P., Tomas, C., 2014. Phylogenetic relationships, morphological variation, and toxin patterns in the *Alexandrium*

ostenfeldii (Dinophyceae) complex: implications for species boundaries and identities. J. Phycol. 50, 81-100.

Kudela, R.M., Gobler, C.J., 2012. Harmful dinoflagellate blooms caused by *Cochlodinium* sp.: global expansion and ecological strategies facilitating bloom formation. Harmful Algae 14, 71-86.

Landsberg, J.H., Flewelling, L.J., Naar, J., 2009. *Karenia brevis* red tides, brevetoxins in the food web, and impacts on natural resources: decadal advancements. Harmful Algae 8, 598-607.

Lara, M.D.C.C., Altamirano, R.C., Sierra-Beltrán, A.P., 2004. Presence of *Cochlodinium catenatum* (Gymnodiniales: Gymnodiniaceae) in red tides of Bahía de Banderas, Mexican Pacific. Rev. Biol. Trop. 52, 35-49.

Leaw, C.P., Lim, P.T., Ng, B.K., Cheah, M.Y., Ahmad, A., Usup, G., 2005. Phylogenetic analysis of *Alexandrium* species and *Pyrodinium bahamense* (Dinophyceae) based on theca morphology and nuclear ribosome gene sequence. J. Phycol. 44, 550-565.

Lee, D., 2008. *Cochlodinium polykrikoides* blooms and eco-physical conditions in the South Sea of Korea. Harmful Algae 7, 315-323.

Lee, Y.S., Park, Y.T., Kim, Y.S., Kim, K.Y., Park, J.S., Go, W.J., Jo, Y.J., Park, S.Y., 2001. Countermeasure and outbreak mechanism of *Cochlodinium polykrikoides* red tide. 1. Environmental characteristics on outbreak and disappearance of *Cochlodinium polykrikoides* bloom. The Sea 6, 259-264. (in Korean with English abstract)

Lee, C., Park, T., Park, Y., Lim, W., 2013. Monitoring and trends in harmful algal blooms and red tides in Korean coastal waters, with emphasis on *Cochlodinium polykrikoides*. Harmful Algae

30S, S3-S14.

Lee, K.H., Jeong, J.H., Jang, T.Y., Lim, A.S., Kang, N.S., Kim, J., Kim, K.W., Park, K., Lee, K., 2014a. Feeding by the newly described mixotrophic dinoflagellate *Gymnodinium smaydae*: Feeding mechanism, prey species, and effect of prey concentration. J. Exp. Mar. Biol. Ecol. 459, 114-125.

Lee, S.K., Jeong, H.J., Jang, S.H., Lee, K.H., Kang, N.S., Lee, M.J., Potvin, É., 2014b. Mixotrophy in the newly described dinoflagellate *Ansanella granifera*: feeding mechanism, prey species, and effect of prey concentration. Algae 29, 137-152.

Leflaive, J. and Ten-Hage, L., 2009. Chemical interactions in diatoms: role of polyunsaturated aldehydes and precursor. New Phytologist 184, 794-805.

Li, A., Stoecker, D.K., Coats, D.W., 2000. Mixotrophy in *Gyrodinium galatheanum* (dinophyceae): grazing responses to light intensity and inorganic nutrients. J. Phycol. 36, 33-45.

Lilly, E.L., Halanych, K.M., Anderson, D.M., 2007. Species boundaries and global biogeography of the *Alexandrium tamarense* complex (Dinophyceae). J. Phycol. 43, 1329-1338.

Lim, W.A., Jung, C.S., Lee, C.K., Cho, Y.C., Lee, S.G., Kim, H.G., Chung, I.K., 2002. The outbreak, maintenance and decline of the red tide dominated by *Cochlodinium polykrikoides* in the coastal waters off southern Korea from August to October, 2000. The Sea 7, 68-77. (in Korean with English abstract).

Lim, W.A., Lee, Y.S, Lee, S.G., Lee, J.Y., 2007. Distribution and community structure of phytoplankton in the southeast coastal waters during Summer 2006. J. Kor. Soc. Oceanogr. 12,

370-379. (written in Korean with English abstract)

Lim, W.A., Lee, Y.S., Lee, S.G., 2008. Characteristics of environmental factors related to outbreak and decline of *Cochlodinium polykrikoides* bloom in the southeast coastal waters of Korea, 2007. J. Kor. Soc. Oceanogr. 13, 325-332. (written in Korean with English abstract)

Lim, W.A., Lee, Y.S., Park, J.G., 2009. Characteristics of *Cochlodinium polykrikoides* bloom in southeast coastal waters of Korea, 2008. J. Kor. Soc. Oceanogr. 14, 155-162. (written in Korean with English abstract)

Lim, A.S., Jeong, H.J., Jang, T.Y., Jang, S.H., Franks, P.J.S., 2014a. Inhibition of growth rate and swimming speed of the harmful dinoflagellate *Cochlodinium polykrikoides* by diatoms: Implications for red tide formation. Harmful Algae 37, 53-61.

Lim, A.S., Jeong, H.J., Jang, T.Y., Yoo, Y.D., Kang, N.S., Yoon, E.Y., Kim, G.H., 2014b. Feeding by the newly described heterotrophic dinoflagellate *Stoeckeria changwonensis*: A comparison with other species in the family Pfiesteriaceae. Harmful Algae 34, 11-21.

Lim, A.S., Jeong, H.J., Kim, J.H., Lee, S.Y., 2015a. Description of the new phototrophic dinoflagellate *Alexandrium pohangense* sp. nov. from Korean coastal waters. Harmful Algae 46, 49-61.

Lim, A.S., Jeong, H.J., Jang, T.Y., Kang, N.S., Jang, S.H., Lee, M.J., 2015b. Differential effects of typhoons on ichthytoxic *Cochlodinium polykrikoides* red tides in the South sea of Korea during 2012-204. Harmful Algae 45, 26-32.

Lin, I., Liu, W.T., Wu, C., Wong, G.T.F., Hu, C., Chen, Z., Liang, W.,

Yang, Y., Liu, K., 2003. New evidence for enhanced ocean primary production triggered by tropical cyclone. Geophys. Res. Lett. 30, 1718, doi:10.1029/2003GL017141.

Litaker, R.W., Vandersea, M.W., Kibler, S.R., Reece, K.S., Stokes, N.A., Steidinger, K.A., Millie, D.F., Bendis, B.J., Pigg, R.J., Tester, P.A., 2003. Identification of *Pfiesteria piscicida* (Dinophyceae) and *Pfiesteria*-like organisms using internal transcribed spacer-specific PCR assays. J. Phycol. 39, 754-761.

Ma, H., Krock, B., Tillmann, U., Bickmeyer, U., Graeve, M., Cembella, A., 2011. Mode of action of membrane-disruptive lytic compounds from the marine dinoflagellate *Alexandrium tamarense*. Toxicon 58, 247-258.

Maciel-Baltazar, E., Hernández-Becerril, D.U., 2013. Species of athecate dinoflagellates (Dinophyta) from coasts of Chiapas, southern Mexican Pacific. Rev. Biol. Mar. oceanogr. 48, 245-259.

MacKenzie, L., Todd, K., 2002. *Alexandrium camutascutulum* sp. nov. (Dinophyceae): a new dinoflagellate species from New Zealand. Harmful Algae 1, 295-300.

MacKenzie, L., de Salas, M., Adamson, J., Beuzenberg, V., 2004. The dinoflagellate genus *Alexandrium* (Halim) in New Zealand coastal waters: comparative morphology, toxicity and molecular genetics. Harmful Algae 3, 71-92.

Margalef, R., 1961. Hidrografía y fitoplancton de un área marina de la costa meridional de Puerto Rico. Invest. Pesq. 18, 33-96.

Matsubara, T., Nagaseo, S., Yamasaki, Y., Shikata, T., Shimasaki, Y., Oshima, Y., Honjo, T., 2007. Effects of water temperature, salinity and irradiance on the growth of the dinoflagellate

Akashiwo sanguinea. J. Exp. Mar. Biol. Ecol. 342, 226-230.

Medlin, L., Elwood, H.J., Stickel, S., Sogin, M.L., 1988. The characterization of enzymatically amplified eukaryokic 16S-like rRNA-coding regions. Gene 71,491-499.

Ministry for Food, Agriculture, Forestry and Fisheries (MIFAFF), 2008. The Technique of Wintering Culture of the Sea Bream in Net-cage Culture System in the Southern Sea, Korea. Report of MIFAFF, Busan, Korea. pp. 262.

Mulhollannd, M., Morse, R.E., Boneillo, G.E., Bernhardt, P.W., Filippino, K.C., Procise, L.A., Blanco-Garcia, J.L., Marshall, H.G., Egerton, T.A., Hunley, W.S., Moore, K.A., Berry, D.L., Gobler, C.J., 2009. Understanding causes and impacts of the dinoflagellate, *Cochlodinium polykrikoides*, blooms in the Chesapeake Bay. Estuaries and Coasts 32, 734-747.

Munir, S., Naz, T., Burhan, Z., Siddiqui, P.J.A., Morton S.L., 2012. First report of the athecate, chain forming dinoflagellate *Cochlodinium fulvescens* (Gymnodiniales) from Pakistan. Pak. J. Bot. 44, 2129-2134.

Murray, S., Hoppenrath, M., Orr, R.J.S., Bolch, C., John, U., Diwan, R., Yauwenas, R., Harwood, T., de Salas, M., Neilan, B., Hallegraeff, G., 2014. *Alexandrium diversaporum* sp. nov., a new non-saxitoxin producing species: Phylogeny, morphology and *sxtA* genes. Harmful Algae 31, 54-65.

Nagasoe, S., Toda, S., Shimasaki, Y., Oshima, Y., Uchida, T., Honjo, T., 2006a. Growth inhibition of *Gyrodinium instriatum* (Dianophyceae) by *Skeletonema costatum* (Bacillariophyceae). African J. Marine Sci. 28, 325-329.

Nagasoe, S., Kim, D., Shimasaki, Y., Oshima, Y., Tamaguchi, M.,

Honjo, T., 2006b. Effects of water temperature, salinity and irradiance on the growth of the red tide dinoflagellate *Gyrodinium instriatum* Freudenthal et Lee. Harmful Algae 5, 20-25.

National Fisheries Research & Development Institute (NFRDI), 2014. Monitoring, management and mitigation of red tide. Annual report of NFRDI on red tide of Korea, Busan, Korea (written in Korean).

Nygaard, K., Tobiesen, A., 1993. Bacterivory in algae: A survival strategy during nutrient limitation. Limnol. Oceanogr. 38, 273-379.

Oh, S.J., Yoon, Y.H., Kim, D.-I., Shimasaki, Y., Oshima, Y., Honjo, T., 2006. Effects of light quantity and quality on he growth of the harmful dinoflagellate *Cochlodinium polykrikoides* Margalef (Dinophyceae). Algae 21, 311-316.

Orr, R.J.S., Stüken, A., Rundberget, T., Eikrem, W., Jakobson, K.S., 2011. Improved phylogenetic resolution of toxic and non-toxic *Alexandrium* strains using a concatenated rDNA approach. Harmful Algae 10, 676-688.

Oviatt, C., Lane, P., French III.F., Donaghay, P., 1989. Phytoplankton species and abundance in response to eutrophication in coastal marine mesocosms. J. Plankton Res. 11, 1223-1244.

Paasche, E. 1973. Silicon and the ecology ofmarine plankton diatoms. 1. *Thalassiosira pseuclonana* (Cyclotella nana) grown in a chemost at with silicate as limiting nutrient.Mar. Biol. 19, 117-126.

Park, J.G., Jeong, M.K., Lee, J.A., Cho, K., Kwon, O., 2001. Diurnal vertical migration of a harmful dinoflagellate, *Cochlodinium*

polykrikoides (Dinophyceae), during a red tide in coastal waters of Namhae Island, Korea. Phycologia 40, 292-297.

Park, M.G., Kim, S.J., Kim, H.S., Myung, G.O., Kang, Y.G., Yih, W.H., 2006. First successful culture of the marine dinoflagellate *Dinophysis acuminata*. Aquat. Microb. Ecol. 45, 101-106.

Park, T.G., Lim, W.A., Park, Y.T., Lee, C.K, Jeong, H.J., 2013a. Economic impact, management and mitigation of red tides in Korea. Harmful Algae 30S, S131-S143.

Park, J. Jeong, H.J., Yoo, Y.D., Yoon, E.Y., 2013b. Mixotrophic dinoflagellate red tides in Koean waters: distribution and ecophysiology. Harmful Algae 30S, S28-S40.

Park, M.G., Kim, M., Kang, M., 2013c. A dinoflagellate *Amylax triacantha* with plastids of the Cryptophyte origin: phylogeny, feeding mechanism, and growth and grazing responses. J. Eukaryot. Microbiol. 60, 363-376.

Philps, E.J., Badylak, S., Christman, M., Wolny, J., Brame, J., Garland, J., Hall, J., Hart, J., Landsberg, J., Lasi, L., Lockwood, J., Paperno, R., Scheidt, D., Staples, A., Steidinger, K., 2011. Scales of temporal and spatial variability in the distribution of harmful algae species in the Indian River Lagoon, Florida, USA. Harmful Algae 10, 277-290.

Pierce, R.H., Henry, M.S., Blum, P.C., Lyons, J., Cheng, Y.S., Yazzie, D., Zhou, Y., 2003. Brevetoxin concentrations in marine aerosol: human exposure levels during a *Karenia brevis* harmful algal bloom. Bull. Environ. Contam. Toxicol. 70, 161-165.

Prince, J.F., 1981. Upper ocean response to a hurricane. J. Phys. Oceanogr. 11, 153-175.

Roberts, E.C., Wootton, E.C., Davidson, K., Jeong, H.J., Lowe, C.D., Montagnes, D.J.S., 2011. Feeding in the dinoflagellate *Oxyrrhis marina*: linking behavior with mechanisms. J. Plankton Res. 33, 603-614.

Ronquist, F., Huelsenbeck, J.P., 2003. MRBAYES 3: Bayesian phylogenetic inference under mixed models. Bioinformatics 19, 1572-1574.

Ross, O.N., Sharples, J., 2007. Phytoplankton motility and the competition for nutrients in the thermocline. Mar. Ecol. Prog. Ser. 347, 21-38.

Rountos, K.J., Tang, Y., Cerrato, R.M., Gobler, C.J., Pikitch, E.K., 2014. Toxicity of the harmful dinoflagellate *Cochlodinium polykrikoides* to early life stages of three estuarine forage fish. Mar. Ecol. Prog. Ser. 505, 81-84.

Sanders, R.W., 2011. Alternative nutritional strategies in protists: symposium introduction and a review of freshwater protists that combine photosynthesis and heterotrophy. J. Eukaryot. Microbiol. 58, 181-184.

Scholin, C.A., Herzog, M., Sogin, M., Anderson, D.M., 1994. Identification of group and strain specific genetic makers for globally distributed *Alexandrium* (Dinophyceae) Ⅱ. Sequence analysis of a fragment of the LSU rRNA gene. J. Phycol. 30, 999-1011.

Selina, M.S., Morozova, T.V., 2005. First records of dinoflagellates *Alexandrium margalefi* Balech, 1994 and *A. tamutum* Montresor, Beran et John, 2004 in the seas of the Russian far east. Russ. J. Mar. Biol. 31, 187-191.

Seong, K.A., Jeong, H.J., 2011. Interactions between the pathogenic

bacterium *Vibrio parahaemolyticus* and red-tide dinoflagellates. Ocean Sci. J. 46, 105-115.

Sieg, R.D., Poulson-Ellestad, K.L., Kubanek, J., 2011. Chemical ecology of the marine plankton. Nat. Prod. Rep. 28, 388-399.

Skovgaard, A., Hansen, P.J., Stoecker, D.K., 2000. Physiology of the mixotrophic dinoflagellate *Fragilidium subglobosum*. 1. Effects of phagotrophy and irradiance on photosynthesis and carbon content. Mar. Ecol. Prog. Ser. 201, 129-136.

Smayda, T.J., 1997. Harmful algal blooms: their ecophysiology and general relevance to phytoplankton blooms in the sea. Limnol. Oceanogr. 42, 1137-1153.

Stamatakis, A., 2006. RaxML-VI-HPC: maximum likelihood-based phylogenetic analyses with thousands of taxa and mixed models. Bioinformatics 22, 2688-2690.

Stoecker, D.K., 1999. Mixotrophy among dinoflagellates. J. Eukaryot. Microbiol. 46, 397-401.

Strathmann, R.R., 1967. Estimating the organic carbon content of phytoplankton from cell volume or plasma volume. Limnol. Oceanogr. 12, 411-418.

Tamura, K., Dudley, J., Nei, M., Kumar, S., 2007. MEGA4: molecular evolutionary genetics analysis (MEGA) software v. 4.0. Mol. Biol. Evol. 24, 1596-1599.

Tang, Y., Gobler, C.J., 2009. Characterization of the toxicity of *Cochlodinium polykrikoides* isolates from Northeast US estuaries to finfish and shellfish. Harmful Algae 8, 454-462.

Tang, Y.Z., Gobler, C.J., 2010. Allelopathic effects of *Cochlodinium*

polykrikoides isolates and blooms from the estuaries of Long Island, New York, on co-occurring phytoplankton. Mar. Ecol. Prog. Ser. 406, 19-31.

Thomas, W.H., Gibson, C.H., 1990a. Effects of small-scale turbulence on microalgae. J. Applied Phycol. 2, 71-77.

Thomas, W.H., Gibson, C.H., 1990b. Quantified small-scale turbulence inhibits a red tide dinoflagellate, *Gonyaulax polyedra* Stein. Deep-Sea Res. 37, 1583-1593.

Thomas, W.H., Vernet, M., Gibson, C.H., 1995. Effects of small-scale turbulence on photosynthesis, pigmentation, cell division, and cell size in the marine dinoflagellate *Gonyaulax polyedra* (Dinophyceae). J. Phycol. 31, 50-59.

Tillmann, U., John, U., 2002. Toxic effects of *Alexandrium* spp. on heterotrophic dinoflagellates: an allelochemical defense mechanism independent of PSP-toxin content. Mar. Ecol. Prog. Ser. 230, 47-58.

Tomas, C.R., 1978. *Olisthodiscus luteus* (Chrysophyceae). I. Effects of salinity and temperature on growth, mortality and survival. J. Phycol. 14, 309-313.

Tomas, C.R., Smayda, T.J., 2008. Red tide blooms of *Cochlodinium polykrikoides* in a coastal cove. Harmful Algae 7, 308-317.

Van Dolah, F.M., 2000. Marine algal toxins: origins, health effects, and their increased occurrence. Environ. Health Perspect. 108(S1), 133-141.

Vargas-Montero, M., Freer, E., Jiménez-Montealegre, R., Guzmán, J.C., 2006. Occurrence and predominance of the fish killer *Cochlodinium polykrikoides* on the Pacific coast of Costa Rica. African J. Mar. Sci. 28, 215-217.

Verity, P.G., 2010. Expansion of potentially harmful algal taxa in a Georgia Estuary (USA). Harmful Algae 9, 144-152.

Vershinin, A.O., Moruchkov, A.A., Leighfield, T., Sukhanova, I.N., Pan'kov, S.L., Morton, S.L., Ramsdell, J.S., 2005. Potentially toxic algae in the coastal phytoplankton of the Northeast Black Sea in 2001-2002. Oceanology 45, 224-232.

Wang, J., Zhang, Y., Li, H., Cao, J., 2013. Competitive interaction between diatom *Skeletonema costatum* and dinoflagellate *Prorocentrum donghaiense* in laboratory culture. J. Plankton Res. 35, 367-378.

White, A.W., 1976. Growth inhibition caused by turbulence in the toxic marine dinoflagellate *Gonyaulax excavata*. J. Fish. Res. Bd. Can. 33, 2598-2602.

Whyte, J.N.C., Haigh, N., Ginther, N.G., Keddy, L.J., 2001. First record of blooms of *Cochlodinium* sp. (Gymnodiniales, Dinophyceae) causing mortality to aquacultured salmon on the west coast of Canada. Phycologia 40, 298-304.

Wichard, T., Poulet S.A., Halsband-lenk, C., Albaina, A., Harris, R., Lie, D., Pohnert, G., 2005. Survey of the chemical defeence potential of diatoms: screening of fifty one species for α, β, ɣ, δ-unsaturated aldehydes. J. Chem. Ecol. 31, 949-958.

Wootton, E.C., Zubkov, M.V., Jones, D.H., Jones, R.H., Martel, C.M., Thornton, C.A., Roberts, E.C., 2007. Biochemical prey recognition by planktonic protozoa. Envion. Microbiol. 9, 216-222.

Yamasaki, Y., Nagaseo, S., Matsubara, T., Shikata. T., Shimasaki, Y., Oshima Y., Honjo, T., 2007. Growth inhibition and formation of morphologically abnormal cells of *Akashiwo sanguinea*

(Hirasaka) G. Hansen et Moestrup by cell contact with *Cochlodinium polykrikoides* Margalef. Mar. Biol. 152, 157-163.

Yamasaki, Y., Ohmichi, Y., Shikata, T., Hirose, M., Shimasaki, Y., Oshima Y., Honjo, T., 2010. Species-specific alleopathic effects of the diatom *Skeletonema costatum*. An Int. J. Mar. Sci., Thalassas 27, 21-32.

Yamatogi, T., Sakaguchi, M., Takagi, N., Iwataki, M., Matsuoka, K., 2005. Effects of temperature, salinity and light intensity on the growth of a harmful dinoflagellate *Cochlodinium polykrikoides* Margalef occurring in coastal waters of west Kyushu, Japan. Bull. Plankton Soc. Jp 52, 4-10.

Yan, T., Zhou, M., Zou, J., 2002. A national report on harmful algal blooms in China. In: Tayler, F.R.J., Trainer, V.L. (Eds.) Harmful algal blooms in the PICES region of the North Pacific. PICES Sci. Rep. No. 23, pp. 152.

Yoo, Y.D., Jeong, H.J., Kim, M.S., Kang, N.S., Song, J.Y., Shin, W., Kim, K.Y., Lee, K., 2009. Feeding by phototrophic red-tide dinoflagellates on the ubiquitous marine diatom *Skeletonema costatum*. J. Eukaryot. Microbiol. 56, 413-420.

Yoo, Y.D., Yoon, E.Y., Jeong, H.J., Lee. K.H., Hwang, Y.J., Seong, K.A., Kim, J.S., Park, J.Y., 2013. The newly described heterotrophic dinoflagellate *Gyrodinium moestrupii*, an effective protistan grazer of toxic dinoflagellates. J. Eukaryot. Microbiol. 60, 13-24.

Zar, J.H., 1984. Biostatistical analysis. Prentice Hall, Englewood Cliffs, New Jersey. pp. 97-235.

Zheng, M.G., Tang, D., 2007. Offshore and nearshore chlorophyll

increases induced by typhoon winds and subsequent terrestrial rainwater runoff. Mar. Ecol. Prog. Ser. 333, 61-74.

국문초록

적조란 미세조류의 대번성에 의해 해수 표면의 색이 변화하는 것을 말한다. 혼합영양성인 *Cochlodinium polykrikoides*는 종종 많은 나라의 연안에서 적조 패치를 형성하고 때때로 그로 인해 자연환경과 양식장 내에서 물고기 대량 폐사를 야기하기도 한다. 이 종에 의해 우리나라의 양식업에서는 매년 1-60만 달러에 해당하는 피해를 입고 있다. 이 종에 대한 생리학적 연구 즉, 성장에 있어서의 온도, 빛, 염분, 그리고 영양염류에 의한 성장 반응 연구는 많이 이루어졌음에도 불구하고, *Cochlodinium* 적조의 발생과 지속 그리고 감소의 메커니즘은 아직 완전히 이해되지 않은 상태이다.

Cochlodinium polykrikoides 적조 변동의 더 나은 이해를 위하여, 태풍, 경쟁적인 규조류, 그리고 새로운 혼합영양성 천적과 같은 지금까지 밝혀진 바 없는 물리학적, 생물학적 요인들에 의한 영향을 살펴보았다.

우리나라는 매년 *Cochlodinium* 적조 기간 동안 수개의 태풍을 경험한다. 태풍은 일반적으로 강한 바람과 많은 비를 동반하며, 이는 적조에 영향을 주는 중요한 환경적 생물학적 요인들을 변화시킨다. 강한 바람은 적조생물의 성장에 영향을 줄 수 있는 다양한 와류를 형성 시키고 식물플랑크톤 군집의 변화를 야기한다. 몇몇의 연구에 의하면 태풍이 지난 후 수층의 우점종이 편모류에서 규조류로 변화한 것으로 나타났다. 또한 *Cochlodinium*의 분포는 규조류의 분포와 서로 상반된 경향을 보인다. 그러나 *Cochlodinium* 적조에 대한 태풍의 영향에 대해서는 아직 잘 연구된 바가 없다. 태풍이 *Cochlodinium* 적조의 발생과 지속 그리고 쇠퇴에 미치는 영향을 알아보기 위해 2012년부터 2014년까지 우리나라 남해안에 영향을 주었던 14개의 태풍, 일일최대풍속과 일일 최대

Cochlodinium 밀도를 분석하였다. 그 결과 일일최대풍속이 14 m s^{-1} 이상의 바람이 불었을 때 *Cochlodinium* 적조발생이 억제되었으나, 5m s^{-1} 이하의 풍속은 큰 영향을 미치지 않는 것으로 나타났다. 따라서 태풍은 일일최대 풍속에 따라 *Cochlodinium*움 적조의 발생과 지속에 다른 영향을 주는 것으로 나타났다.

경쟁적인 규조류가 *Cochlodinium* 적조에 미치는 영향을 연구한 결과, 경쟁적인 규조류가 일정 밀도 이상을 초과하였을 때 물리적 접촉과 화학적 스트레스를 통해 *Cochlodinium*의 성장률과 수영속도를 낮추는 것으로 나타났다. 따라서 규조류의 밀도가 높을 때 *Cochlodinium* 적조의 발생이 예방되거나 지연될 수 있음을 알 수 있다.

현재까지 *Cochlodinium*에 대한 몇몇 섬모충과 종속영양성 원생생물 천적은 발견된 바 있으나, 효과적인 혼합영양성 와편모조류 천척은 발견되지 않았다. 2014년 코클로디니움 적조 기간 동안 우리나라 동해안의 연안에서 *Alexandrium* 속의 종을 발견하여 단종배양체를 확립하였다. 이 *Alexandrium* 종은 혼합영양성 종으로 코클로디니움 만을 선택적으로 섭식하는 것을 밝혔다. 또한 이 종의 형태학적 분자생물학적 특성을 분석하여 그 결과를 바탕으로 신종이라는 것을 밝혔으며, *Alexandrium pohangense*로 명명하였다.

해양생태계에서의 *Alexandrium pohangense*의 역할을 알아보기 위해, 실내실험을 통해 코클로디니움의 밀도에 따른 *A. pohangense*의 성장률과 섭식률을 측정하였다. 그 결과 *C. polykoides*에 대한 *A. pohangense*의 최대섭식률은 7 cells $predator^{-1}$ d^{-1}이였으며, 자가영양성 최대 성장률이 0.1 d^{-1}인데 비해 혼합영양성 최대 성장률은 0.5 d^{-1}에 달하였다. 또한 실내실험의 결과와 현장의 밀도 데이터를 혼합하여 자연상태에서의 *A. pohagense*의 코클로디니움 군집에 대한 포식압을 구하였다. *A. pohangense*와 동시에 출현하는 *C. polykrikoides*에 대한 포식압

은 1.57 d^{-1}에 달하였으며 이는 하루 동안 *A. pohangense* 군집에 의해 *C. polykrikoides* 군집이 최대 79 %까지 제거가 될 수 있음을 의미한다.

결과적으로 현장 관찰, 다양한 형태의 데이터의 분석, 실내에서의 다양한 섭식 실험과 형태학적 분자생물학적 분석을 통해 태풍, 경쟁적인 규조류, 그리고 새로운 혼합영양성 와편모류인 *A. pohangense*가 *Cochlodinium* 밀도에 큰 영향을 줄 수 있음을 밝혔으며, 이로 인해 *C. polykrikoides* 적조에 영향을 줄 수 있을 것으로 판단된다. 코클로디니움 적조의 발생과 지속, 소멸에 대한 예측 및 제어에 태풍과 경쟁적인 생물 종들의 상호작용이 고려되어야 할 것으로 판단된다.

주 요 어: 알렉산드리움, 코클로디니움, 태풍, 생태학, 포식, 분류학, 유해조류 번성
학 번: 2011-30921

이학박사학위논문

Effects of tropical cyclones and biological interactions on red tide dynamics by the ichthyotoxic dinoflagellate *Cochlodinium polykrikoides* in the Korean coastal waters

한국연안에서 태풍과 생물학적 상호작용이 코클로디니움 적조에 미치는 영향에 대한 연구

2016년 2월

서울대학교 대학원

지구환경과학부 해양학전공

임 안 숙

Effects of tropical cyclones and biological interactions on red tide dynamics by the ichthyotoxic dinoflagellate *Cochlodinium polykrikoides* in the Korean coastal waters

한국연안에서 태풍과 생물학적 상호작용이
코클로디니움 적조에 미치는 영향에 대한 연구

지도교수 정 해 진

이 논문을 이학박사 학위논문으로 제출함
2016년 2월

서울대학교 대학원
지구환경과학부 해양학전공
임 안 숙

임안숙의 박사학위논문을 인준함
2015년 12월

위 원 장 김종성 (인)

부 위 원 장 정 해 진 (인)

위 원 허 창 희 (인)

위 원 이 은 주 (인)

위 원 이 원 호 (인)

Abstract

Effects of tropical cyclones and biological interactions on red tide dynamics by the ichthyotoxic dinoflagellate *Cochlodinium polykrikoides* in the Korean coastal waters

Lim, An Suk

School of Earth and Environmental Sciences

The Graduate School

Seoul National University

Red tides are discoloration of the sea surface due to microalgal blooms. The mixotrophic dinoflagellate *Cochlodinium polykrikoides* often forms red tide patches in the coastal waters of many countries and has sometimes caused large-scaled mortality of fish in both cages and natural environments. This dinoflagellate has caused losses of USD $1-60 million to Korean aquaculture industry every year. The mechanism of the outbreak, persistence, and decline of *Cochlodinium* red tides have not been fully understood yet, although, ecophysiological characteristics of *C. polykrikoides* have been well documented.

Here, I explored effects of some critical physical and biological factors such as tropical cyclones, competing diatoms, and novel mixotrophic dinoflagellate grazers on the red tide dynamics of *C. polykrikoides.*

Korea usually experiences several tropical cyclones (typhoons) in *C. polykrikoides* red tide period every year. Tropical cyclones are generally accompanied by strong winds and heavy rains and thus can

change some critical factors affecting red tide dynamics. Strong winds often generate intensive turbulence which can inhibit growth of red tide organisms. Several studies reported that after the passage of tropical cyclones, the dominant red tide species in the water column were switched from flagellates to diatoms. Thus, tropical cyclones are likely to physically and biologically affect on the red tide dynamics of *C. polykrikoides*. However, effects of tropical cyclones on *Cochlodinium* red tides have not been well documented yet. Therefore, I explored the effects of tropical cyclones on the outbreak, persistence, and decline of *Cochlodinium* red tides by analyzing the daily maximum wind speed and daily maximum *Cochlodinium* cell abundance during the 14 tropical cyclone cases in South Sea of Korea in 2012–2014. I found that *Cochlodinium* red tides disappeared when daily maximum wind speeds exceeded 14 m s^{-1}, but were not markedly affected when daily maximum wind speeds were less than 5 m s^{-1}. Thus, this study suggests that daily maximum wind speeds of tropical cyclones may differentially affect the outbreak and persistence of *Cochlodinium* red tides.

I explored the effects of competing diatoms on dynamics of *Cochlodinium* and found that some competing diatoms reduced the growth and swimming speed of *Cochlodinium* through both physical contact and chemical stress when the concentration of the diatoms exceeds certain levels. This evidence suggests that the outbreak of *Cochlodinium* red tides can be prevented or delayed when the concentration of diatoms is high.

No effective mixotrophic dinoflagellate grazer on *C. polykrikoides* has been found yet, whereas several ciliates and heterotrophic protistan grazers have been reported. During *Cochlodinium* red tides in the coastal waters of eastern Korea, in

2014, I isolated a *Alexandrium* cell and established a clonal culture. This *Alexandrium* was revealed to be a mixotrophic dinoflagellate that exclusively feeds on *C. polykrikoides*. Based on the results from morphological and genetic analyses, the *Alexandrium* strain was revealed to be a new species, to be named as *Alexandrium pohangense* n. sp.

To explore the roles of *Alexandrium pohangense* in marine ecosystems, I measured the growth and ingestion rates of *A. pohangense* as a function of the concentration of only prey *C. polykrikoides* in the laboratory. The maximum ingestion rate of *A. pohangense* on *C. polykrikoides* was 7 cells predator^{-1} d^{-1}, and the maximum mixotrophic growth rate reached 0.5 d^{-1}, while the autotrophic growth rate was 0.1^{-1}. Furthermore, by combining the results from the feeding experiments and abundance data obtained in field, I estimated grazing impact of *A. pohangense* on populations of *C. polykrikoides* in the natural environments. The grazing coefficients attributable to *A. pohangense* on co-occurring *C. polykrikoides* were up to 1.57 d^{-1}. Thus, up to 79 % of the *C. polykrikoides* populations could be removed by *A. pohangense* population in a day.

Conclusively, through field observation, diverse feeding experiments in the laboratory, and morphological and molecular analyses, I found that tropical cyclones, competing diatoms, and a new mixotrophic dinoflagellate *A. pohangense* can significantly affect the red tide dynamics by *C. polykrikoides*.

Keywords: *Alexandrium, Cochlodinium polykrikoides,* Ecology, Grazing, Taxonomy, Typhoons, Harmful algal bloom,

Student Number: 2011-30921

Table of Contents

List of Tables

List of Figures

Chapter 1. Introduction

Red tide are discoloration of the sea surface water due to algal blooms. Red tides are known to occur almost all the countries which have their sea. Red tides often cause disturbance of marine ecosystems, large scale mortality of fish and shellfish in both natural environments and aquaculture cages, and even illness of human. Because of such damage, red tide events are critical issues to the government, scientists, and the public of many countries. The annual economic loss due to red tides is estimated tens of billions of dollars in the world. In Korea, losses of several thousand to million US dollar in the commercial fish farms every year have been reported. To minimize the damage caused by red tides, better understanding red tide dynamics is needed.

The red-tide causative species are approximately 300 species (Smayda, 1997). All red tide species increase their populations by binary division. Once a population of a certain red-tide species is inoculated in a certain area, to form red tides, its population density should increase more rapidly than co-occurring other species. The red tide formation can be affected by growth related factors (i.e., lights, temperature, nutrients, etc.), and mortality related factors (grazing impact). In addition, physical forces such as currents, internal waves, circulations, fronts, upwelling and down-welling, strong winds can affect red tide formation. Thus, overall equation for a change of cell abundance of a red tide species is as follows:

$$dC/dt = C\ (k - g \pm aBI)$$

where k = specific growth rate, g = mortality, aBI = effects of biological interactions with other species. According to this equation, a species having a greater growth rate and a less mortality rate than co-occurring species has an opportunity to become a red-tide causative species. Moreover, the species conducts diverse biological interactions with other species. There are two groups of biological interactions; direct biological interactions such as predator-prey relationships and inhibition by physical contact or chemical effects; indirect biological interactions such as space competition by growing faster than others under given conditions. Some biological interactions cause an increase in one species (+aBI), but a decrease in other species (-aBI). Thus, biological interactions between two species may play an important role in their competition. There have been many studies on these topics. However, many critical factors affecting dynamics of red tides species should be explored. The mixotrophic dinoflagellate *C. polykrikoides* is one of the red tide species to be fully studied because it has caused great loss in many countries. *Cochlodinium polykrikoides* often forms red tide patches in the coastal waters of Korea and has caused losses of USD $1-60 million in Korean aquaculture industry every year since 1995 (Park et al., 2013a).

To minimize this huge damage caused by *C. polykrikoides* red tides, scientists, officials, and aquaculture industry in many countries have spent a great deal of time and money on predicting the outbreak of the red tides and controlling them. Due to these intensive

efforts, the eco-physiology of this dinoflagellate (i.e., effects of temperature, light, salinity, and nutrients on the growth of *C. polykrikoides*) has been relatively well documented (Kim et al., 2001; Gobler et al., 2012) (Fig. 1.1). However, effects of some critical physical factors (i.e., tropical cyclones, turbulence, mixing on *C. polykrikoides*) have not been well studied. In addition, some critical biological interactions between *Cochlodinium* and co-occurring species (i.e., effects of physical contact on growth and swimming behavior) are not fully understood yet. Due to this limitation, it is very difficult to predict the outbreak, persistence, and decline of *Cochlodinium* red tides.

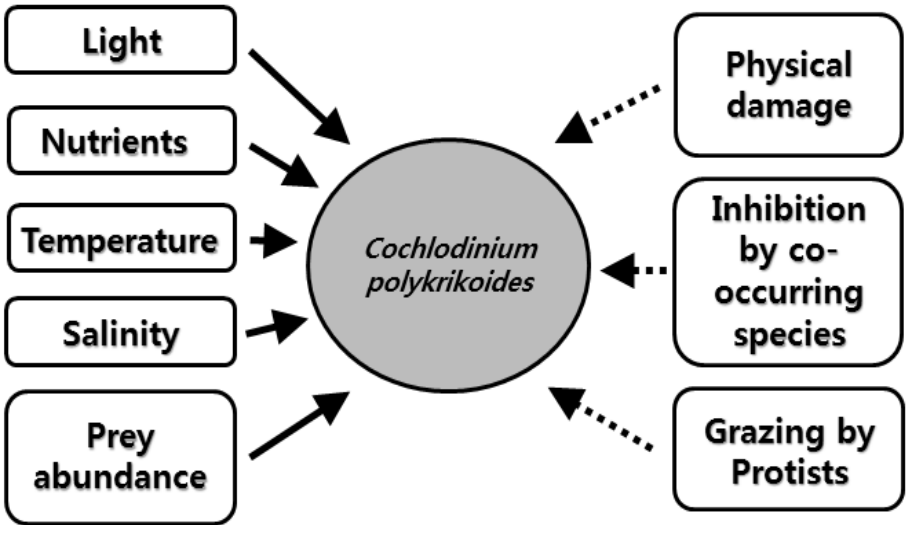

Fig. 1.1. Growth and mortality factors affecting the formation of *Cochlodinidum polykrikoides* red tides. Black arrows indicate that related studies are well documented, while dashed arrows indicate insufficient data on each subject.

The ranges of temperatures and salinities for the optimal growth of *C. polykrikoides* are known to be 25-30 ℃ and 25-40, obtained from experiments the laboratory and fields (Kudela and Gobler, 2012). Furthermore, the range of half-saturation values (i.e., the value meeting the half of the maximum growth rate) of the light is 29-45 μE $m^{-2}s^{-1}$ (Kim et al., 2004; Yamatogi et al., 2005; Oh et al., 2006). Under these conditions, the reported highest maximum growth rate of *C. polykrikoides* is 0.61 d^{-1} (Yamatogi et al., 2005), which is much lower than competing diatoms and small flagellates (i.g., 2.77 d^{-1} for the diatom *Thalassiosira pseudonana* and 1.32 d^{-1} for the raphidophyte *Heterosigma akashiwo*) (Passche, 1973; Tomas, 1978). Thus, it is likely to be difficult for *C. polykrikoides* to form red tides when the environmental conditions favorable for growth of most phytoplankton species are given.

How can *C. polykrikoides* outgrow over competing red tide species and form a red tide patch? The chain-forming dinoflagellate *C. polykrikoides* is one of the fastest swimming red-tide species and is able to conduct vertical migration through the water column. *C. polykrikoides* descends to the nutrient-rich deep water at night, but ascends to well lit surface water day time. The maximum swimming speed of *C. polykrikoides* is ~1,400 μm s^{-1} and thus theoretically it can reach 50 m during the day (10-hour travel). Thus, when the nutrients are limited in surface water, *C. polykrikoides* may uptake nutrients from the nutrient-rich deep water. Moreover, *C. polykrikodes* is known to be mixotrophic (Jeong et al., 2004b). Jeong et al. (2010a) proposed a mixotrophic ability as a possible mechanism

of the outbreak and/or the persistence of red tides in oceanic waters whose surface nutrient concentrations are too low for red tide flagellates to grow and also thermocline is too deep to reach eutrophic deep waters. Therefore, *C. polykrikoides* may able to form red tides oceanic waters by feeding on diverse prey including bacteria and small algae (Jeong et al., 2004b, 2005b).

There have been much fewer studies on mortality of *C. polykrikoides* due to predation, compared to those on its growth rates. Among the many potential protistan predators, only a naked ciliate *Strombidinopsis jeokjo* (Choreotrichida) was revealed to have a significant grazing impact on populations of *C. polykrikoides* (Jeong et al., 2008). Therefore, it is worthwhile to explore more predators on *C. polykrikoides.*

Biological interactions between *C. polykrikoides* and other phytoplankton are not well known. Most studies on these interactions have focussed on allellopathic effects (i.e., chemical effects) of *C. polykrikoides*. However, other red tide species may affect *C. polykrikoides.*

In chapter 2, I investigated the effects of tropical cyclones (typhoons) on *Cohlodinium polykrikoides* red tides in South Sea of Korea in 2012-2014. There have been a debate on effects of tropical cyclones on *C. polykrikoides* red tides; in some years, *C. polykrikoides* red tides were weaken or disappeared, but reinforced in other years. I guessed that C*. polykrikoides* red tides may be affected by the speed of wind produced by tropical cyclones and thus

explored this topic. In this study, I analyzed the daily maximum wind speed and the daily maximum abundance of *C. polykrikoides* in the red tide periods and found that *C. polykrikoides* red tides were differentially affected by wind speeds. The results of this study will provide a basis on understanding roles of tropical cyclones on dynamics of *C. polykrikoides* red tides.

In chapter 3, I explored the biological interactions between competitive diatoms and *C. polykrikoides*. Diatoms and phototrophic dinoflagellates are two major phytoplankton groups. They severally compete each other to form a red tide. Diatoms grow much faster than dinoflagellates having similar sizes (Banse, 1982). Thus, diatoms outgrow over dinoflagellates when the conditions favorable for photosynthesis are given. However, dinoflagellates can outgrow over diatoms by conducting vertical migration or mixotrophy. Furthermore, some toxic or harmful dinoflagellates are known to kill or lower growth of diatoms using chemicals (Fistarol et al., 2004). I guessed that fats swimming *C. polykrikoides* having thin cell membrane may be inhibited by dense diatoms. Thus, I investigated the possible physical and chemical effects of 3 common diatoms *Skeletonema costatum*, *Thalassiosira decipiense*, and *Chaetoceros danicus* on the growth rate and swimming speed of *C. polykrikoides*. The results of this study provide a basis on understanding roles of competing diatoms on dynamics of *C. polykrikoides* red tides.

In chapter 4, I reported a new dinoflagellate species, *Alexandrium pohangense.* I isolated a dinoflagellate from an estuary in East Sea at the decline stage of *C. polykrikodies*. Thus, I guessed

that this dinoflagellate may be a mixotrophic dinoflagellate which is able to feed on *C. polykrikodies*. After analyzing its morphological and genetical characterizations, I realized that it is a new species in the genus *Alexandrium*. Therefore, based on the morphological and phylogenetic criteria, I established a new *Alexandrium* species in this study. Many *Alexandrium* species are known to be toxic and thus many marine scientists are interested in *Alexandrium* species. The discovery of this new *Alexandrium* species may open some new topics in marine biology and fisheries.

In chapter 5, I explored the mixotrophic ability of *Alexandrium pohangense* and roles of this dinoflagellate in dynamics of *C. polykrikoides* red tides. Interestingly, this dinoflagellate fed on only *C. polykrikoides* among diverse phytoplankton prey species provided. In addition, the maximum growth rate of *A. pohangense* with added *C. polykrikoides* (i.e., mixotrophic growth) was higher than that without added prey (i.e., autotrphic growth). Thus, I*A. pohangense* may play important roles in the dynamics of *C. polykrikoides* red tides. The results of this study provide a basis on understanding roles of a new *Alexandrium* species on dynamics of *C. polykrikoides* red tides.

In chapter 6, I provided overall conclusions based on the results of field observation and experiments in the lab in this study.

This study clearly showed that tropical cyclones (in Chapter 2), competing diatoms (in Chapter 3), and a new *Alexandrium* species (may be another competing species; in Chapter 4 and 5) affect red tide dynamics of *C. polykrikoides* (Fig. 1.2). Therefore, we must

consider these effects in understanding *C. polykrikoides* red tides, establishing prediction models, and developing methods of controlling these red tides.

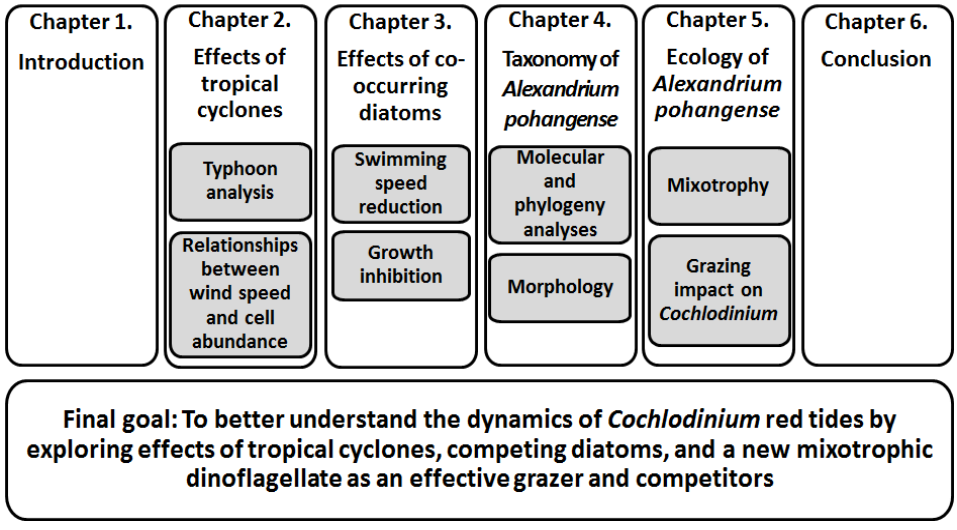

Fig. 1.2. Thesis Outline

Chapter 2. Effects of tropical cyclones on the dynamics of *Cochlodinium* red tides in the south sea of Korea

2.1. Introduction

Cochlodinium polykrikoides is an unarmored mixotrophic dinoflagellate and one of the noxious red tide forming organisms (Jeong et al., 2004b; Gobler et al., 2008; Mulholland et al., 2009). The occurrence of the dinoflagellate and its bloom events have expanded worldwide after first being identified in the coastal waters of Puerto Rico (Margalef, 1961; Kudela and Gobler, 2012). With increase of the red tide events, *Cochlodinium* caused large scale mortality of finfish in both cages and natural environments and resulted the huge economic loss in many countries including Korea (USD $ 60 million), China (USD $97 million), Japan (USD $ 0.1 million), and Canada (CAN $ 2 million) (Whyte et al. 2001; Fukuyo et al., 2002; Yan et al.,, 2002; Gárate-Lizárraga et al., 2004; Vargas-Montero et al., 2006; Anton et al., 2008; Azanza et al., 2008; Hamzehei et al., 2013; Park et al., 2013a). *C. polykrikoides* has been known to kill early stage of fish at the concentrations > 1,000 cells ml^{-1} (Rountos et al., 2014). Thus, the cell density of *C. polykrikoides* is critical to kill fish in cages. Some physical forces such as strong winds and turbulence can dissipate cells in red tide patches or kill cells. A tropical cyclone (so called, typhoons in north Pacific, hurricane in America, cyclone in Indian Ocean, willy-willy in Austria) usually produces strong winds

(Emanuel, 2003). Thus, a tropical cyclone may affect the cell density of *C. polykrikoides* and in turn survival of fish in cages. It is worthwhile to explore effects of tropic cyclones on the cell density of *C. polykrikoides*.

A tropical cyclone is generated at tropical region and brings strong winds and heavy rain from tropical region to high latitudes area (Emanuel, 2003). These tropical cyclones often cause great loss in economy of many countries and sometimes human death. A tropical cyclone influences on the marine ecosystem such as upwelling and vertical mixing (Prince, 1981; Lin et al., 2003; Zheng and Tang 2007), terrestrial runoff (Zheng and Tang, 2007; Chen et al., 2009), and sediment resuspension (Fogel et al., 1999). Thus, the occurrence of tropical cyclone can effect on the phytoplankton dynamics. Some studies showed diatoms often dominated phytoplankton assemblages after tropical cyclone passages in various regions (Chen et al., 2009). There are also some reports that red tide patches disappear after tropical cyclone passed (Lee et al., 2001; Lim et al., 2002; Lee, 2008). Therefore, it is worthwhile to explore the effects of tropical cyclone on the *Cochlodinium* red tide dynamics. However, these studies did not explore either relationship between the daily wind speed and cell abundance or critical wind speeds preventing outbreaks and recovery of red tide events or reducing red-tide cell abundances down to the level at which fish in aquaculture cages are not killed. Thus, to explore these relationship and critical wind speed, the daily variations in the abundances of *C. polykrikoides* and wind speeds in 3 study areas of South Sea of Korea in the periods of *C. polykrikoides* red tides and the passage of

14 tropical cyclones in 2012-2014 were analyzed. Our results provide a basis for understanding relationships between the daily wind speed of tropical cyclones and the abundance of *C. polykrikoides* and an insight on effects of reduced *C. polykrikoides* abundances on fate of fish in aquaculture cages and eventually economic loss due to its red tides.

2.2. Materials and methods

2.2.1. The Study area

Korea is one of the countries that have both *Cochlodinium polykrikoides* red tides and several tropical cyclones every year. *C. polykrikoides* have usually caused huge red tides in coastal and offshore waters of South Sea of Korea. Goheung (GO), Yeosu (YE), and Tongyoung (TO), located in South Sea of Korea, are the places where *C. polykrikoides* red tides have most frequently occurred (Fig. 2.1). Moreover, most aquaculture farms in Korea are located in these areas (MIFAFF, 2008). In addition, 1-7 tropical cyclones have passed these areas every year (http://typ.kma.go.kr). Thus, these 3 areas are the ideal places for investigating relationships between tropical cyclones and *C. polykrikoides* red tides.

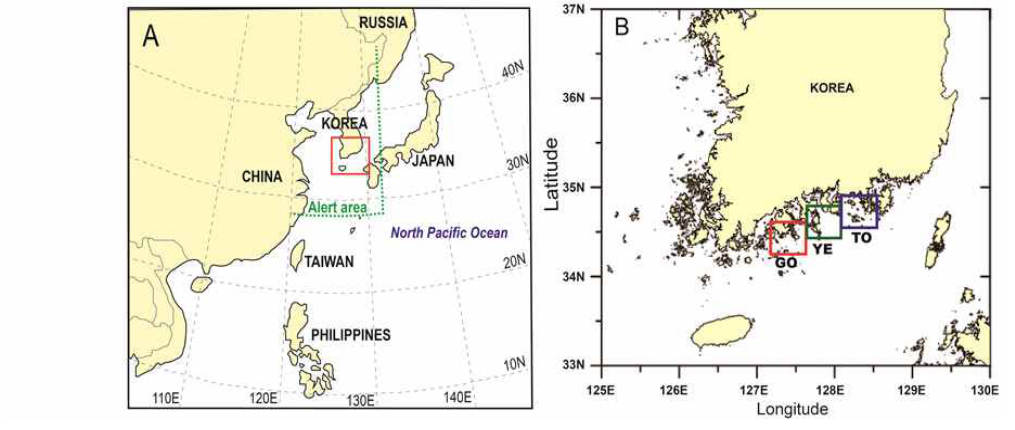

Fig. 2.1. Map of the study area (A). (B) enlarged from red box from (A). Three study areas, Goheung (GO), Yeosu (YE), and Tongyoung (TO), are shown in (B).

2.2.2. The tropical cyclone and wind speed

To investigate effects of tropical cyclones on *Cochlodinium polykrikoides* red tides, the tropical cyclones directly passing the study areas or nearby (i.e. < 800 km away from the tropical cyclone core) in *C. polykrikoides* red tide periods in 2012-2014 were analyzed (Table 2.1). The meteorological data related to the tropical cyclones (i.e., the created and dissipated dates and path of each tropical cyclone) were obtained from the Korea National Typhoon Center (KNTC, http://typ.kma.go.kr). To minimize damages due to tropical cyclones, KNTC has announced different levels of warning based on the location of the tropical cyclone. For example, when the tropical cyclone core is located in the latitude higher than 28 °N and also in the longitude smaller than 132 °E in which Korea has generally experiences strong winds and/or heavy rains by the tropical cyclone, KNTC announces so-called "the tropical cyclone alert stage". Thus, the north-western area of 28 °N and 132 °E is defined as the tropical cyclone alert area (Fig. 2.1). In this study, the passage period of a tropical cyclone in Korea was defined as the date when the tropical cyclone was positioned in this tropical cyclone alert area. In addition, the Korea Ocean Observing and Forecasting System (http://sms.khoa.go.kr) reports the wind speed in certain area every hour. This hourly wind speed is the value of averaging all wind speeds measured every minute. The daily maximum wind speed, the highest value among the hourly reported wind speed in a day, was used in this study. The period between created and dissipated dates of each tropical cyclone and that when the tropical cyclone reached the tropical cyclone alert area were provided as horizontal bars in the

figures.

2.2.3. The daily abundance of *Cochlodinium polykrikoides*

The Korea National Fisheries Research and Development Institute (NFRDI) has red tide monitoring system. Once the red tide patch was detected, the water samples were taken daily from the red tide patch and near the area and the causative species and its cell density were published as a daily red tide new latter. The density of *C. polykrikoides* are archived by the NFRDI (http://portal.nfrdi.re.kr/redtideInfo). Water samples were collected with a 2 L Hydro-Bios water sampler at 0.3-0.5 m in depth. Plankton samples for counting were poured into 1 L polyethylene bottles and fixed with acidic Lugol's solution (0.3 %). The samples were settled down for a week and concentrated by approximately 1/5 by evacuating the supernatant of the sample. After thorough mixing, 1-ml of sample was transferred into Sedgwick-Rafter counting chambers (SRCs) and *Cochlodinium* cells in SRCs were counted under an inverted microscope (Lee et al., 2013).

2.3. Results

2.3.1. The tropical cyclone and wind speed

The beginning and ending dates of *Cochlodinium polykrikoides* red tides were July 27 and October 25 in 2012, July 17 and September 4 in 2013, and July 24 and October 15 in 2014. Among the tropical cyclones occurred between 0–50 °N and 0–180 °E in these red tide periods, 5, 2, and 7 tropical cyclones in 2012, 2013, and 2014, respectively passed the alert areas (Fig. 2.2). Of these tropical cyclones, the tropical cyclones Tembin, Bolaven, and Sanba in 2012 and Nakri in 2014 generated strong winds whose maximum speeds exceeded 14 m s^{-1} in the study areas (Table 2.1). The daily maximum wind speed in one of Goheung (GO), Yeosu (YE), and Tongyoung (TO) was usually similar to another, but considerably different from the other one. For example, during passage of tropical cyclone Tembin, the maximum wind speeds in GO, YE, and TO were 23.3, 21.5, and 14.9 m s^{-1}, respectively, while during passage of tropical cyclone Sanba, the maximum wind speed in GO, YE, and TO were 18.1, 23.4, and 19.1 m s^{-1}, respectively. The centers (i.e., tropical cyclone eyes) of these 4 tropical cyclones were positioned within 200 km away from the study areas (Table 2.1). During the other tropical cyclones, the maximum wind speeds were ~3–13 m s^{-1} in the study areas. These tropical cyclones were positioned at ~200–800 km away from the study areas.

Table 2.1. The analyzed tropical cyclones and the maximum wind speed (m s^{-1}) in each study area.

Year	Tropical cyclone	Period in the alert area	Goheung	Yeosu	Tongyoung
2012	Damrey	Aug. 1-3	9.2	8.7	7.1
2012	Tembin	Aug. 28-31	23.3	21.5	14.9
2012	Bolaven	Aug. 26-29	23.3	21.5	14.9
2012	Sanba	Sep. 16-18	18.1	23.4	19.1
2012	Jelawat	Sep. 29 - Oct. 1	6.8	6.3	4.5
2013	Kong-rey	Aug. 29-31	7.5	6.3	5.5
2013	Toraji	Sep. 2-4	6.0	5.8	4.5
2014	Matmo	Jul. 24-25	11.9	5.5	5.4
2014	Halong	Aug. 8-10	7.4	8.7	8.0
2014	Nakri	Aug. 1-3	14.6	18.3	7.7
2014	Fengshen	Sep. 7	3.7	58.	2.5
2014	Phanfone	Oct. 5	4.6	4.5	3.4
2014	Vongfong	Oct. 12-14	5.5	10.6	8.4

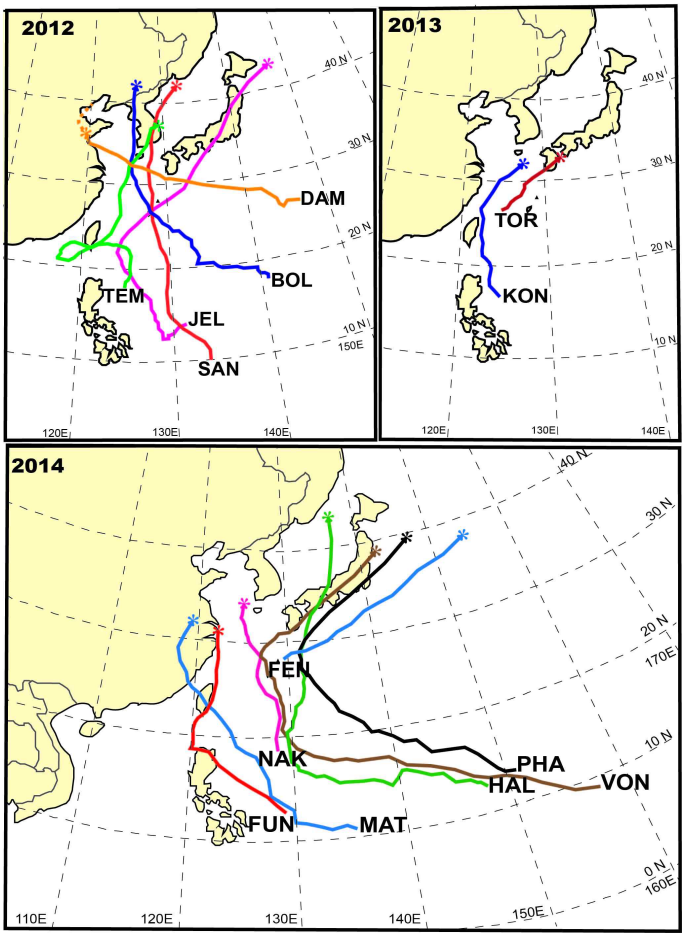

Fig. 2.2. Tropical cyclone paths of each study year. The star at the end of the each line indicates the location where the tropical cyclone dissipated. Damery (DAM), Tembin (TEM), Bolaven (BOL), Sanba (SAN), Jelawat (JEL) in 2012, Kong-Rey (KON), Toraji (TOR) in 2013, and Matmo (MAT), Halong (HAL), Nakri (NAK), Fengshen (FEN), Fung-Wong (Fun), Phanfone (PHA), and Vongfong (VON) in 2014 passed the alert area (28-90 °N latitude and 0-132 °E longitude).

2.3.2. The daily abundance of *Cochlodinium polykrikoides*

In 2012, the *C. polykrikoides* blooms occurred between July 27 and October 25. During the red tide period, the density of *C. polykrikoides* in each study area was changed in similar pattern (Fig. 2.3). In Goheung (GO) area, after the *C. polykrikoides* blooms occurred, the density of *C. polykrikoides* was maintained between 200 and 1,200 cells ml^{-1} for two weeks but suddenly increased. However, the abundance of *C. polykrikoides* decreased slowly and the red tide patches were disappeared on August 28. *C. polykrikoides* bloom patches appeared again on October 5 but dissipated in two weeks. In Yeosu (YO) area, the density of *C. polykrikoides* fluctuated for a month and then the red tide patches disappeared for 5 weeks. However, the abundance of *C. polykrikoides* suddenly increased and reached about 8,000 cells ml^{-1}. After highest density reached, the density decreased and then red tide event was terminated. In Tongyoung (TO) area, the abundance of *C. polykrikoides* was maintained below 2,000 cells ml^{-1} for a month and then the patches dissipated until October 5. However, the density of *C. polykrikoides* rapidly increased and reached highest density (18,000 cells ml^{-1}) after one week later and then the red tide event was terminated (Fig. 2.3).

In 2013, the *C. polykrikoides* blooms occurred between July 17 and September 4 (Fig. 2.4). During the red tide period, the change of the *C. polykrikoides* cell density in Goheung (GO) and Yeosu (YE) areas showed similar patterns. After *C. polykrikoides* blooms occurred on July 17, the density of *C. polykrikoides* cells reached about 8,000 cells ml^{-1} in Goheung and 14,000 cells ml^{-1} in Yeosu in early August.

The abundance of *C. polykrikoides* cells declined after August 16 and the red tide patches disappeared in early September. However, unlike Goheung and Yeosu areas, red tide patches in Tongyoung (TO) area maintained in high density (~10,000 cells ml^{-1}) from the beginning of the red tide period and reached at 38,000 cells ml^{-1} on August 8. Once the abundance of *C. polykrikoides* reached the highest density of the period, it declined and dissipated as time went by.

In 2014, the *C. polykrikoides* blooms occurred between July 24 and October 15 (Fig. 2.5). On July 28 in 2014 between the passages of the tropical cyclone Matmo and Halong-Nakri, *C. polykrikoides* red tide patches were found in TO (Fig. 2-5). However, red tide patches had not been found until August 28 in GO and August 12 in YE (Fig. 2.5). In TO, the DMAC increased up to 15,000 cells ml^{-1} with a big fluctuation after the passage of these two tropical cyclones, but decreased down to < 100 cells ml^{-1} with a fluctuation between September 7 and October 14 when 4 tropical cyclones Fengshen, Fung-Wong, Phanfone, and Vongfong passed the study areas (Fig. 2.5; Table 2.1). In GO, the MAC increased up to 9,100 cells ml^{-1} form August 29 to September 15 with a depression when the tropical cyclone Fengshen, but decreased with a small peak after the passage of the tropical cyclone Fung-Wong (Fig. 2.5). In YE, the DMAC increased up to 5,200 cells ml^{-1} form August 13 to September 11 with a fluctuation, but decreased after the passage of the tropical cyclone Fengshen and red tide patches were not found during the passage of the tropical cyclone Fung-Wong (Fig. 2.5). However, a large peak of the DMAC was found just before the tropical cyclone Phanfone passed the alert areas.

2.3.3. Relationships between tropical cyclone and wind speed and cell abundance

The DMAC in each study area in one day became very low as much as the red tide was not detectable after the passage of tropical cyclones Tembin, Bolaven, and Sanba in 2012 and Nakri in 2014 whose maximum speeds exceeded 14 m s^{-1} (Fig. 2.3 and 2.5). However, after the passage of tropical cyclone Damrey in 2012 and Halong and Fung-Wong in 2014 whose maximum speeds were 5-14 m s^{-1}, the MAC considerably reduced in the 3 study areas, but red tide events recovered within a week (Fig. 2.3 and Fig. 2.5). In 2013, *C. polykrikoides* red tides persisted for approximately 40 day from July 17 to August 25. In this red tide period, there was neither tropical cyclone nor strong wind whose maximum speeds exceeded 5 m s^{-1} (Fig. 2.4). *C. polykrikoides* red tides were terminated just after the passage of tropical cyclone Toraji in 2013 and Vongfong in 2014 (Fig. 2.4 and Fig. 2.5).

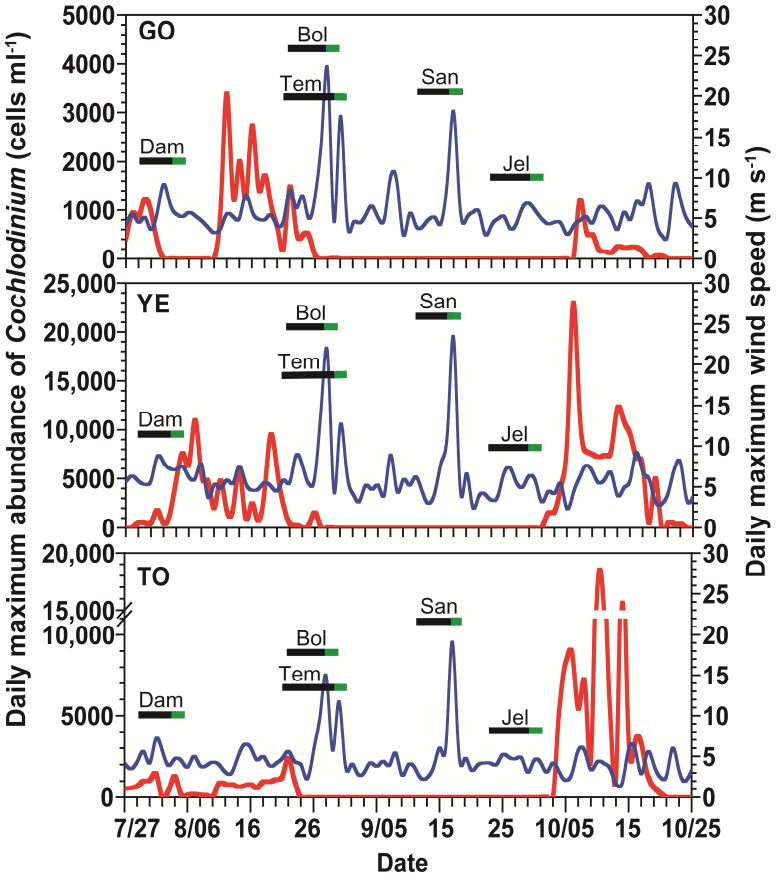

Fig. 2.3. Change of the daily maximum abundance of *Cochlodinium* cells and daily maximum wind speed in each study area in 2012. The black horizontal bar indicates the period between the created and dissipated date of each tropical cyclone and green bar indicates the period when the tropical cyclone was located in alert area (28-90 °N latitude and 0-132 °E longitude). Damery (DAM), Tembin (TEM), Bolaven (BOL), Sanba (SAN), and Jelawat (JEL) passed the alert area.

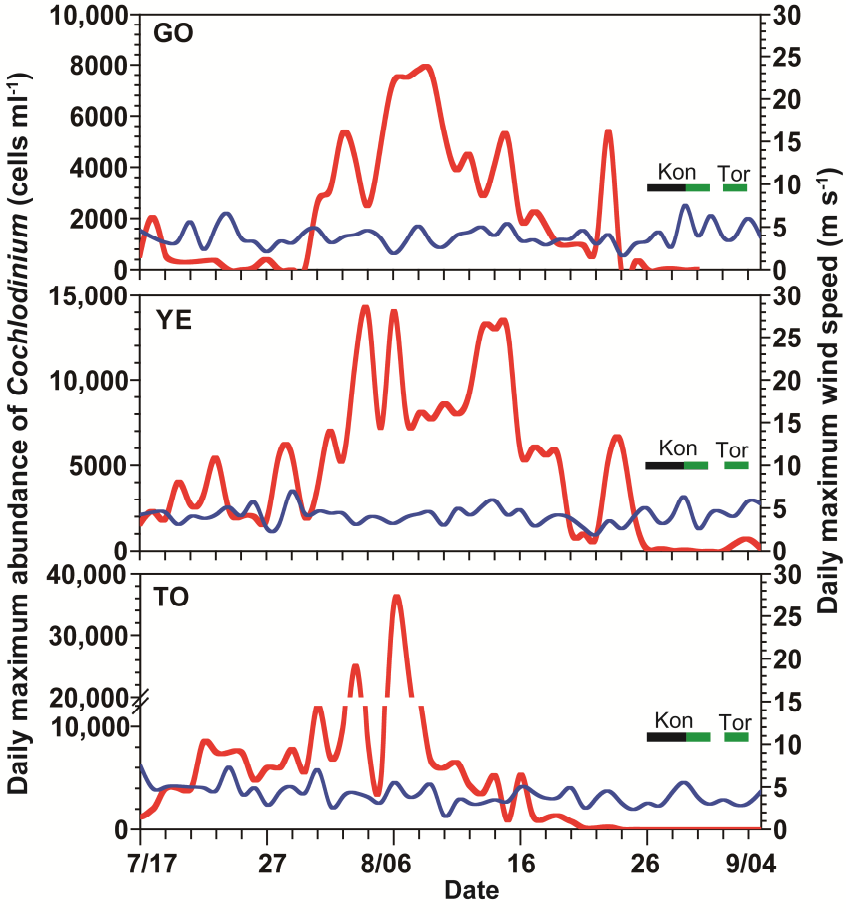

Fig. 2.4. Change of the daily maximum abundance of *Cochlodinium* cells and daily maximum wind speed in each study area in 2013. The black horizontal bar indicates the period between the created and dissipated date of each tropical cyclone and green bar indicates the period when the tropical cyclone was located in alert area (28-90 °N latitude and 0-132 °E longitude). Kong-Rey (KON) and Toraji (TOR) passed the alert area.

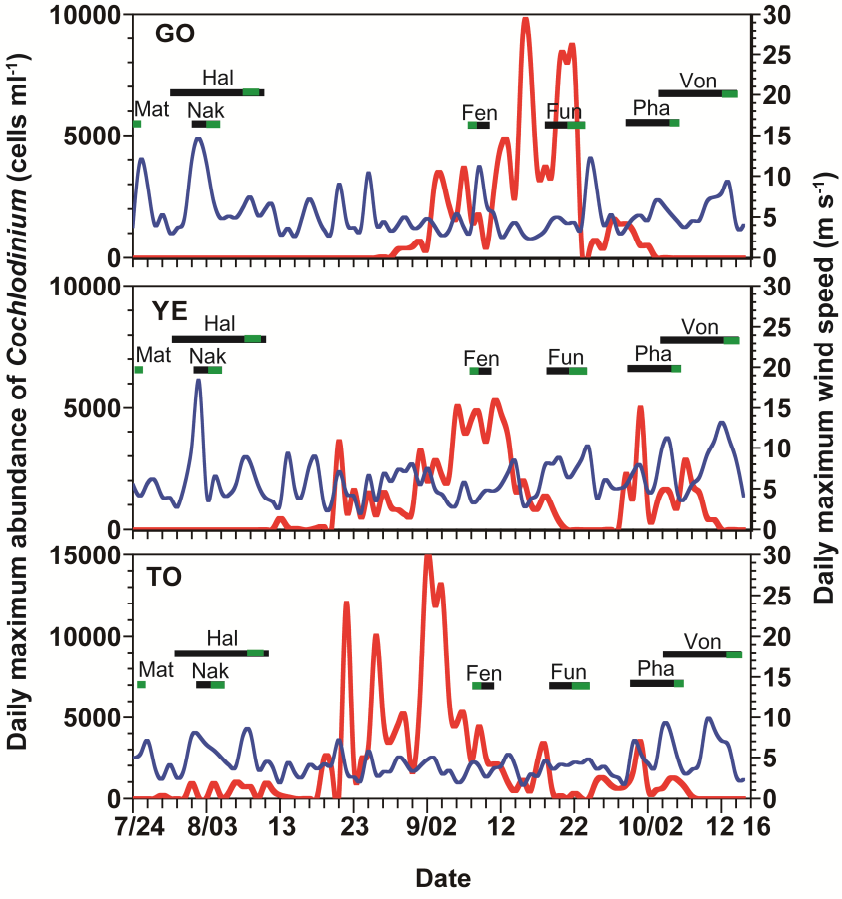

Fig. 2.5. Change of the daily maximum abundance of *Cochlodinium* cells and daily maximum wind speed in each study area in 2014. The black horizontal bar indicates the period between the created and dissipated date of each tropical cyclone and green bar indicates the period when the tropical cyclone was located in alert area (28-90 °N latitude and 0-132 °E longitude). Matmo (MAT), Halong (HAL), Nakri (NAK), Fengshen (FEN), Fung-Wong (Fun), Phanfone (PHA), and Vongfong (VON) passed alert area.

2.4. Discussion

2.4.1. Relationship between the wind speeds generated by tropical cyclones and the abundance of *Cochlodinium polykrikoides*

The daily maximum abundance of *Cochlodinium polykrikoides* (MAC) in each study area in 2013 and 2014 showed a bell shaped trend which is usually observed in other countries or other red tide events (Lee et al., 2001; Kang et al., 2009). However, the tropical cyclones giving maximum wind speeds > 14 m s^{-1} in 2012 are likely to alter this pattern. In addition, winds whose maximum wind speeds 5-14 m s^{-1} even make a big fluctuation in MAC. The change of MAC by tropical cyclones was also observed in other years (Lee et al., 2001; Lim et al., 2002). The MAC fluctuated in 1995 when the maximum wind speed induced by typhoon Ryan was 10 m s^{-1}. However, when the maximum wind speeds were 21.8 m s^{-1} (typhoon Oliwa) in 1997 and 23.3 m s^{-1} (typhoon Yanni) in 1998, the red tide events were terminated (Lee et al., 2001). Thus, this study suggests that tropical cyclones markedly affect *C. polykrikoides* red tides, but the degree of the effects of tropical cyclones depends on the maximum wind speeds. The maximum wind speed may play important role in maintenance of *C. polykrikoides* red tide.

The highest maximum abundances of *C. polykrikoides* was observed when no typhoon affected on the study areas and the maximum speeds of wind in non-typhoon period were mostly lower

than 5 m s^{-1}. However, when the maximum wind speeds were 5-14 m s^{-1}, the maximum abundance of *C. polykrikoides* decreased. Based on the laboratory experiments, the growth of the red tide dinoflagellate *Lingulodinium polyedrum* (previously *Gonyaulax polyedra*) is known to be inhibited at the wind speeds > 7.7 m s^{-1} (Thomas et al., 1995). Therefore, these two dinoflagellate species may be affected similarly by strong winds. Therefore, these speeded winds may dissipate *C. polykrikoides* cells, but not completely kill all cells. Moreover, there was no co-relationship between the maximum wind speed and DMAC. This evidence suggests that moderate winds affect the DMAC, but mild winds may not affect it. However, after the passage of Typhoon Bolaven, Tembin, Sanba, and Nakri whose maximum wind speeds were > 14 m s^{-1}, red tides did not recovered within two weeks. The strong wind generates the turbulence in the water column and turbulence could mechanically damage the cells such as cell disorientation, breakage of flagella, and even growth inhibition (White, 1976; Thomas and Gibson, 1990a, b). Thus, strong wind may destroy red tide patches and prevent to recover the red tide patch in weeks.

C. polykrikoides blooms are strongly ichthyotoxic and can kill many other organisms (Gárate-Lizárraga et al., 2004; Gobler et al., 2008; Tang and Gobler, 2009). Several studies reported that high percentage of the multiple fish species were killed or moribund when they were exposed to > 1,000 cells ml^{-1} of *C. polykrikoides* cells (Tang and Gobler, 2009; Rountos et al., 2014). Thus, the abundance of *C. polykrikoides* cells in the patches is an important factor that determines the fish mortality. In the study areas, when tropical

cyclone Damrey passed study areas in 2012, the maximum abundance of *C. polykrikoides* (DMAC) temporally decreased from 340 to 0 cells ml^{-1} in Goheung area and from 1,050 to 404 cells ml^{-1} in Tongyoung area and the maximum wind speed were 9.2 m s^{-1} in Goheung and 7.1 m s^{-1} in Tongyoung, respectively. In addition, when tropical cyclone Halong and Nakri whose the maximum wind speed 8.0 and 7.7 m s^{-1} passed Tongyoung area, the MAC decreased from 712 to 6 and 920 to 0 cells ml^{-1}. Thus, reduced cell abundance when the wind speed is greater than 7 m s^{-1} may effect on the mortality of fish in cages subsequently.

The mild winds below 5 m s^{-1} may have no effects on *C. polykrikoides* cells in the water column and result the increase of the abundance in the patches. Moreover, if the patches with high abundance of *C. polykrikoides* flow into the fish cages, the most fishes in the cages may be dead (Fig. 2.6). However, moderate winds (5–14 m s^{-1}) may temporally decrease *C. polykrikoides* abundance in the water column and it may reduce the mortality of the fishes in the cages (Fig. 2.6). Moreover, the maximum wind speeds of greater than 14 m s^{-1} may result the strong turbulence in the water column and inhibit the growth of *C. polykrikoides*. Such reduction of *C. polykrikoides* abundance in the water column may make most fishes in cages survive (Fig. 2.6). Therefore, to prevent economic losses in aquaculture during the red tide, the wind speed should be considered to predict the red tide of *C. polykrikoides*.

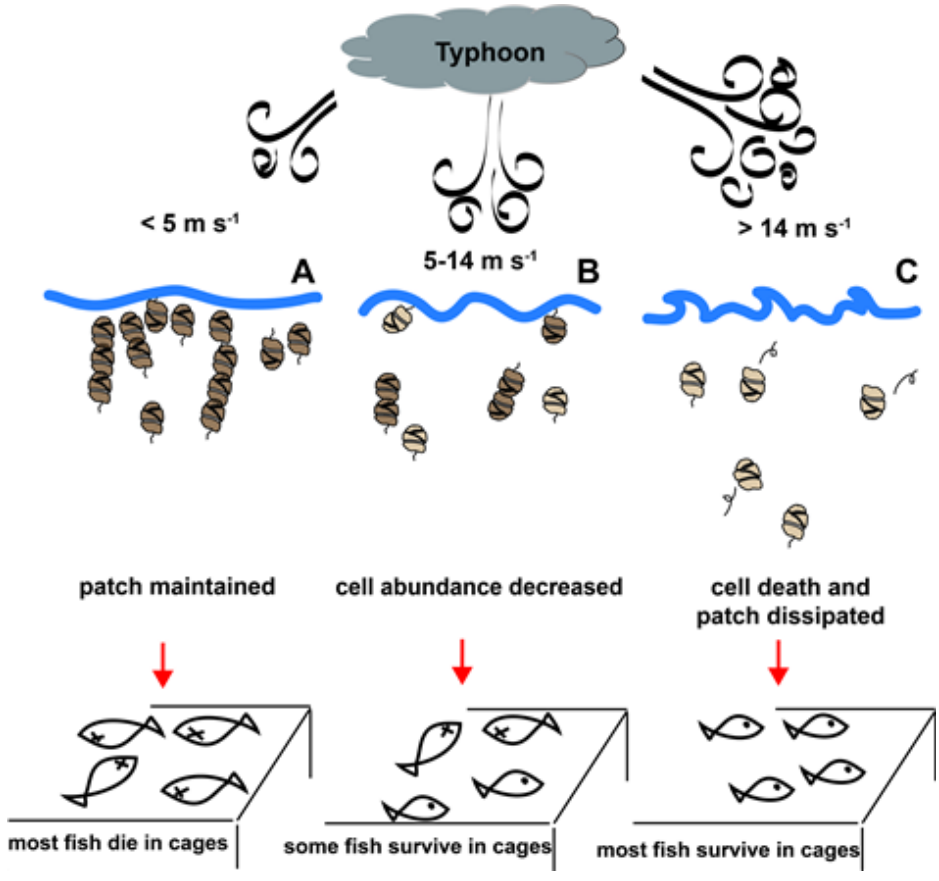

Fig. 2.6. Diagram of ecological implication of wind driven by typhoon. Mild wind (<5 m s^{-1}) has no effect on red tide patch and most fish in cages die because of maintained patch. Moderate wind (5-14 m s^{-1}) make patch disperse temporally, so some fish in cages can survive. Strong wind (>14 m s^{-1}) cause cell death and patch dissipation, so most fish in cages can survive.

Chapter 3. Effects of competing diatom species on the development of *Cochlodinium polykrikoides* red tide in the southern coastal waters of Korea.

3.1. Introduction

Dinoflagellates and diatoms are major components in planktonic communities (Allen, 1949; Chan, 1978; Ross and Sharples, 2007; Godhe et al., 2008). They often predominate the plankton assemblages and have caused red tides (Oviatt et al., 1989; Kremp et al., 2008; Jeong et al., 2010a, b). Some diatoms sometime caused red tides that kill fish, but most diatoms are not harmful to marine organisms. In particular, dinoflagellates have caused notorious red tides or harmful algal blooms (Hallegraeff, 1993; Anderson, 1997; Kudela and Gobler, 2012; Lee et al., 2013; Park et al., 2013a). Toxins produced by some dinoflagellates are very harmful to marine organisms (Geraci et al., 1989; Van Dolah, 2000; Pierce et al., 2003; Landsberg et al., 2009; Kudela and Gobler, 2012). In general, the growth rate of a dinoflagellate species is lower than that of a diatom species having a size similar to the dinoflagellate (Banse, 1982). The production of toxins, bioluminescence, feeding enzymes may cause lower growth rates of dinoflagellates. However, dinoflagellates sometimes outcompete diatoms by feeding and/or allelopathy (Fistarol et al., 2004; Kremp et al., 2008; Yoo et al., 2009; Tang and Gobler, 2010). To the contrary, diatoms may have negative effects on the growth

inhibition of dinoflagellates by allelochemicals (Elbrächter, 1977; Nagaseo et al., 2006a; Wang et al., 2013).

The distribution of *Cochlodinium polykrikoides* is often reverse to that of diatoms (Jeong et al., 2000; Cho 2010). Furthermore, *C. polykrikoides* patches are often replaced by diatoms at the decline stage of its red tides or the passage of typhoon (Lim et al., 2007, 2008, 2009; Chung et al., 2012). Therefore, diatoms may inhibit the growth of *C. polykrikoides* by some means. There are several studies that chemicals from diatoms may inhibit growth of dinoflagellates (Nagaseo et al., 2006a; Yamasaki et al., 2010; Wang et al. 2013). For instance, *Skeletonema costatum* inhibited the growth rate of *Gyrodinium instriatum* and caused morphological modification when the cultures incubated together for 15 days (Nagaseo et al., 2006a). *S. costatum* showed also inhibitory effects on *Prorocentrum dentatum* and *Prorocentrum triestinum* as *Prorocentrum* species had longer lag period time to reach the exponential growth stage than control cultures (Yamasaki et al., 2010). However, the most studies about the interactions between dinoflagelltes and diatoms are focused on the allelochemical effects.

To explore possible inhibitory effects by diatoms on *C. polykrikoides*, I measured the swimming speed of *C. polykrikoides* as a function of the concentration of each of the diatoms *Skeletonema costatum*, *Chaetoceros danicus*, and *Thalassiosira decipiens*. In addition, I monitored the abundance of *C. polykrikoides* for 10 days after this dinoflagellate was mixed with *S. costatum* and *C. danicus*. The results provide a basis for understanding the interactions

between *C. polykrikoides* and common diatoms and red tide dynamics of *C. polykrikoides*.

3.2. Materials and methods

3.2.1. Collection and culture of experimental organisms

Cochlodinium polykrikoides was isolated from plankton samples collected from the Tongyoung, Korea, in Aug 2002, when the water temperature and salinity were 21.1 °C and 32.1, respectively. The samples were screened gently through a 154-μm Nitex mesh and placed in 6-well tissue culture plates. A monoclonal culture of *C. polykrikoides* was established by two serial single cell isolations. As the concentration of *C. polykrikoides* increased, the cells were subsequently transferred to 32-, 270-, and 500-ml polycarbonate (PC) bottles in enriched f/2 seawater media (Guillard and Ryther, 1962). The bottles were placed at 20 °C under an illumination of 100 μE m^{-2} s^{-1} of cool white fluorescent light on a 14:10 h light-dark cycle.

Chaetoceros danicus (KMMCC 1364), *Skeletonema costatum* (KMMCC 660), *Thalassiosira decipiense* (KMMCC 698) were obtained from Korea Marine Microalgae Culture Center (KMMCC) in Korea. These *C. danicus* and *S. costatum* strains were isolated from coastal water off Jindong, Korea on December 2006 and February 1999, respectively. *T. decipiens* was isolated from coastal water off Hadong, Korea on October 1999 when the water temperature was 22 °C. The cultures were maintained in enriched f/2 sea water media under an illumination of 100 μE m^{-2} s^{-1} of cool white fluorescent light on a 14:10 h light-dark cycle at 20 °C.

3.2.2. Effects of diatoms on the swimming speed of *Cochlodinium polykrikoides*

To explore the effects of the diatom concentration and filtrates on the swimming speed of *C. polykrikoides*, we measured the swimming speeds of *C. polykrikoides* at 8 different concentrations of *S. costatum* (Expt 1) and at 6 different concentrations of *C. danicus* (Expt 3) and *T. decipiens* (Expt 5) (i.e., physical contact + chemical effect) and corresponding filtrates (Expt 2, 4, and 6) (i.e., chemical effect only) (Table 3.1).

Dense cultures of *C. polykrikoides*, *C. danicus*, *S. costatum*, and *T. decipiens* maintained in f/2 media were transferred to 270 ml polycarbonate (PC) bottles. Cells in three 1-ml aliquots from each bottle were enumerated to determine the concentration of each species.

In experiment 1, 3, and 5, the initial concentrations of *C. polykrikoides* and each target diatom were established using an autopipette to deliver predetermined volumes of known cell concentrations to the 6-well plates (Table 3.1). In experiments 2, 4, and 6, the water of a bottle containing diatoms of a target concentration was filtered through a 0.7-μm GF/F filter (i.e., filtrate) and then added to each experimental well. A predetermined volume of *C. polykrikoides* was added to the well. In this process, dilution effects were considered. A well containing *Cochlodinium* only without diatom cells in each experiment were set as a control well.

After 24 h incubation, wells were placed on the dissecting microscope with using a video analyzing system (Samsung, SV-C660, Seoul, Korea) and using a CCD camera (Hitachi, KP-D20BU, Tokyo, Japan). I measured swimming speeds of *C. polykrikoides* cells in each well. The video camera focused on an individual field viewed as a single circle in a cell culture flask under a dissecting microscope at 20 °C. Swimming of *C. polykrikoides* cells in each well was then recorded at a magnification of 40×. I analyzed the mean and maximum swimming velocities for all swimming cells viewed during the first 10 min. The average swimming speed (n = 10) for each diatom concentration or filtrate was calculated on the basis of the linear displacement of cells in 1 sec, during single-frame playback.

3.2.3. Effects of diatom concentrations on the growth rate of *Cochlodinium polykrikoides*

Experiment 7 and 8 were designed to investigate whether *C. danicus* and *S. costatum* affect growth of *C. polykrikoides* (Table 3.1).

The initial concentrations of *C. polykrikoides* and each target diatom were established using an autopipette to deliver predetermined volumes of known cell concentrations to the bottles. Triplicate 80-ml PC experiment bottles (containing mixtures of *Cochlodinium* and diatom species), triplicate control bottles (containing diatom species only), and triplicate control bottles (containing *Cochlodinium* only)

were set up for each *Cochlodinium*-diatom combination. To make the water conditions similar, the filtrates of a *Cochlodinium* culture was filtered through a 0.7-μm GF/F filter and then added into the diatom control bottles in the same amount as the volume of the *Cochlodinium* culture added into the experimental bottles for each *Cochlodinium*-diatom combination. Nutrients (nitrate, phosphate, and silicate) were added as much as the final concentrations of these reached the same amount of concentration of F/2 medium. The bottles were then filled to capacity with freshly-filtered seawater and capped. To determine the actual *Cochlodinium* and diatom concentrations, a 5-ml aliquot was removed from each bottle and fixed with 5% Lugol's solution, and all or >200 each species cells in three 1-ml SRCs were enumerated. Each bottle were filled again to capacity with F/2 medium, capped, and placed in the chamber. Total 5-ml aliquot was subsampled every other day for 10 days. The dilution of the cultures associated with refilling the bottles was considered in calculating the growth rates.

The specific growth rates of *Cochlodinium polykrikoides* and each diatom species were calculated as follows:

$$\mu = \frac{\mathrm{Ln}\,(C_t/C_0)}{t}$$

where C_0 is the initial concentration of each species and C_t is the final concentration after time t. The time period was 10 d.

Table 3.1. Experimental design. The numbers in the dinoflagellate and diatom columns are the initial densities (cells ml^{-1}) of algal species. Values shown in parentheses in the each column are the initial densities in the control bottles.

Dinoflagellate			Diatom	
Expt.	Species	Density	Species or filtrate	Density
1	*Cochlodinium polykrikoides*	400	*Skeletonema costatum*	0, 500, 5000, 25000, 50000, 100000, 200000, 500000
2	*Cochlodinium polykrikoides*	400	Filtrate of *S. costatum*	Filtrates from a culture with a cell concentration of 0, 500, 5000, 25000, 50000, 100000, 200000, or 500000
3	*Cochlodinium polykrikoides*	400	*Chaetoceros danicus*	0, 1000, 5000, 10000, 25000, 50000
4	*Cochlodinium polykrikoides*	400	Filtrate of *C. danicus*	Filtrates from a culture with a cell concentration of 0, 1000, 5000, 10000, 25000, or 50000
5	*Cochlodinium polykrikoides*	400	*Thalassiosira decipiens*	0, 1000, 5000, 10000, 25000, 50000
6	*Cochlodinium polykrikoides*	400	Filtrate of *T. decipiens*	Filtrates from a culture with a cell concentration of 0, 1000, 5000, 10000, 25000, or 50000
7	*Cochlodinium polykrikoides*	107 (118)	*S. costatum*	86 (116)
8	*Cochlodinium polykrikoides*	44 (25)	*C. danicus*	77 (85)

3.2.4. Statistical analyses

An ANOVA test was used to determine whether the swimming speeds of *Cochlodinium polykrikoides* varied significantly at different diatom or filtrate concentrations (Zar, 1984). In addition, a t-test was used to determine whether the swimming speed of *C. polykrikoides* at one diatom concentration or filtrate was different from that of the control (without added diatoms or filtrate). Statistical significance was defined as $p < 0.05$.

3.3. Results

3.3.1. Effects of diatom concentrations on the swimming speed of *Cochlodinium polykrikoides*

When the swimming behavior and speed of *C. polykrikoides* were observed under light microscopy, the diatoms *Skeletonema costatum, Chaetoceros danicus*, and *Thalassiosira decipiens* trapped *C. polykrikoides* cells and eventually lower swimming speed of the dinoflagellate (Fig. 3.1). In addition, dead *C. polykrikoides* cells were found after 24 h incubation with the diatoms (Fig. 3.1).

Fig. 3.1. Effects of diatoms on *Cochlodinium polykrikoides*. Intact *C. polykrikoides* cell in control at T = 0h (A). *C. polykrikoides* cells in controls after 24h without diatom cells (B). *C. polykrikoides* cells with diatom *Chaetoceros danicus* at T = 0h (C) and inflated and decomposed *C. polykrikoides* cells after 24h incubation with *C. danicus* (D). Scale bars = 20 μm.

The swimming speeds of *C. polykrikoides* at 8 different concentrations of *S. costatum* after 24 h incubation were significantly different from one another ($p < 0.005$, 2-tailed ANOVA) (Fig. 3.2A). The swimming speed (mean ± SE, n = 10) of *C. polykrikoides* in the control bottles (1,395 ± 75 μm) was significantly greater than that at the *Skeletonema* concentrations of 5,000-500,000 cells ml^{-1} ($p < 0.01$, 1-tailed t test), but was not greater than that at the *Skeletonema* concentration of 500 cells ml^{-1} ($p > 0.1$). When the filtrates from the cultures of *S. costatum* were added, the swimming speed (mean ± SE, n = 10) of *C. polykrikoides* in the control bottles (1,395 ± 75 μm) was significantly greater than that in the filtrates from the cultures originally containing the *Skeletonema* concentrations of 250,000-500,000 cells ml^{-1} ($p < 0.01$, 1-tailed t test), but it was not greater than that with the *Skeletonema* concentration of 500-100,000 cells ml^{-1} ($p > 0.1$) (Fig. 3.2B).

The swimming speeds of *C. polykrikoides* at 6 different concentrations of *Chaetoceros danicus* after 24 h incubation were significantly different from one another ($p<0.005$, 2-tailed ANOVA) (Fig. 3.3A). The swimming speed (mean ± SE, n = 10) of *C. polykrikoides* in the control bottles (978 ± 76 μm) was significantly greater than that at the *Chaetoceros* concentrations of 25,000-50,000 cells ml^{-1} ($p<0.01$, 1-tailed t test), but was not greater than that at the *Chaetoceros* concentration of 1,000-10,000 cells ml^{-1} ($p>0.1$). When the filtrates from the cultures of *C. danicus* were added, the swimming speed (mean ± SE, n=10) of *C. polykrikoides* in the control bottles (978 ± 76 μm) was significantly greater than that in the filtrates from the cultures originally containing the *Chaetoceros*

concentration of 50,000 cells ml^{-1} ($p<0.005$, 1-tailed t test), but it was not greater than that with the *Chaetoceros* concentration of 1,000-25,000 cells ml^{-1} ($p>0.05$) (Fig. 3.3B).

The swimming speeds of *C. polykrikoides* at 6 different concentrations of *Thalassiosira decipiens* after 24 h incubation were significantly different from one another ($p<0.005$, 2-tailed ANOVA) (Fig. 3.4A). The swimming speed (mean ± SE, n=10) of *C. polykrikoides* in the control bottles (1,250 ± 29 μm) was significantly greater than that at the *Thalassiosira* concentrations of 1,000-50,000 cells ml^{-1} ($p<0.01$, 1-tailed t test). When the filtrates from the cultures of *T. decipiens* were added, the swimming speed (mean ± SE, n=10) of *C. polykrikoides* in the control bottles (1,250 ± 29 μm) was significantly greater than that in the filtrates from the cultures originally containing the *Thalassiosira* concentration of 1,000-50,000 cells ml^{-1} ($p<0.005$ for the concentrations of 5,000-50,000 cells ml^{-1} and $p<0.01$ for the concentration of 1,000 cells ml^{-1}, 1-tailed t test) (Fig. 3.4B).

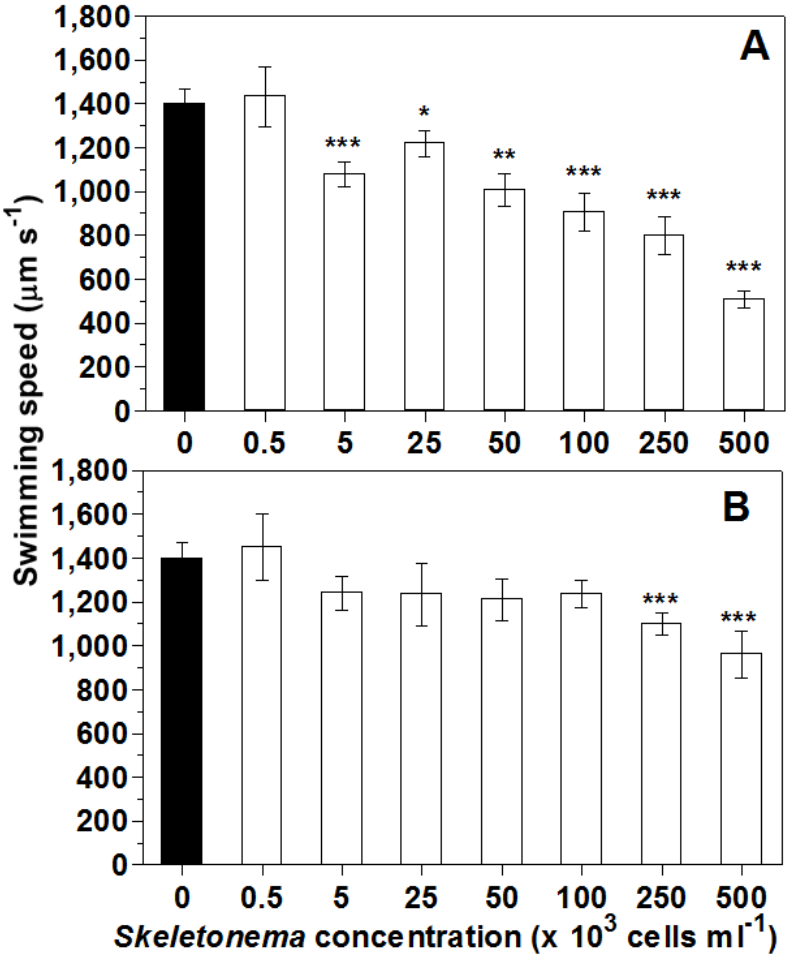

Fig. 3.2. Swimming speed (μm s^{-1}) of *Cochlodinium polykrikoides* at 8 different cell concentrations of *Skeletonema costatum* (A) or filtrates from a culture with a corresponding cell concentration (B) (see M&M for details). Symbols represent treatment means ± 1SE. *:$p<0.05$. **:$p<0.01$. ***:$p<0.005$.

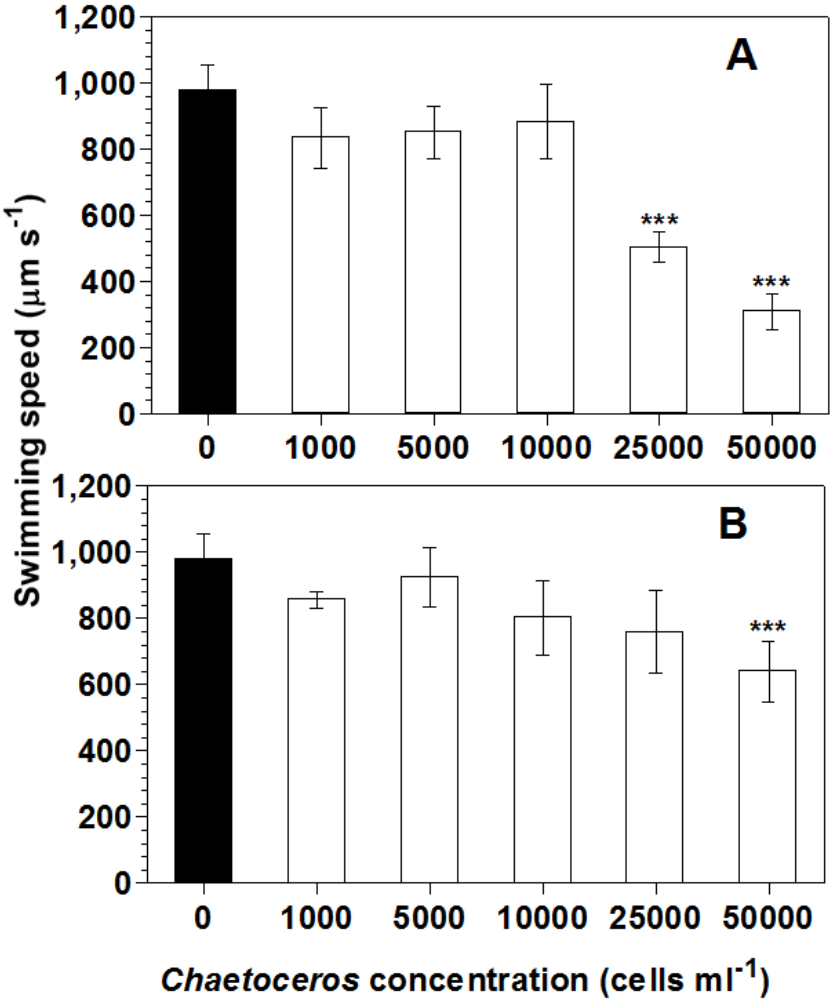

Fig. 3.3. Swimming speed (μm s^{-1}) of *Cochlodinium polykrikoides* at 6 different cell concentrations of *Chaetoceros danicus* (A) or filtrates from a culture with a corresponding cell concentration (B). Symbols represent treatment means ± 1SE. **:$p<0.01$. ***:$p<0.005$.

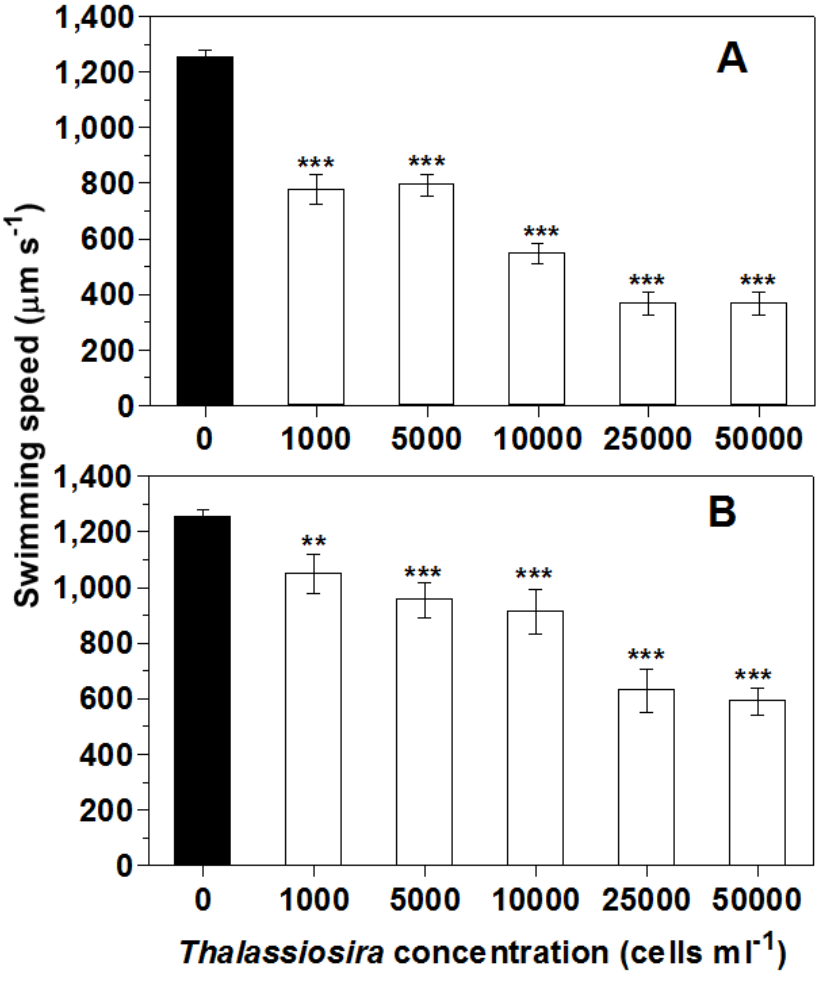

Fig. 3.4. Swimming speed (μm s^{-1}) of *Cochlodinium polykrikoides* at 6 different cell concentrations of *Thalassiosira decipiens* (A) or filtrates from a culture with a corresponding cell concentration (B). Symbols represent treatment means ± 1SE. **:$p<0.01$. ***:$p<0.005$

3.3.2. Effects of diatom concentrations on the growth rate of *Cochlodinium polykrikoides*

The abundances of *C. polykrikoides* incubated with *Skeletonema costatum* at 1:1 in cell abundance changed in the similar manner with those without *S. costatum* (i.e., in control bottle) for the first 4 elapsed days (Fig. 3.5A). In this period, the abundance of *S. costatum* in the experimental bottles increased from 44 to 132,995 cells ml^{-1}, while that in the control bottles increased from 118 to 49,811 cells ml^{-1} (Fig. 3.5B). However, the concentration of *C. polykrikoides* incubated with *S. costatum* at Day 4-10 decreased from 110 to 15 cells ml^{-1}, while that without *S. costatum* increased 133 to 144 cells ml^{-1} (Fig. 3.5A). In this period, the concentration of *S. costatum* in the experimental bottles increased from 132,995 to 407,514 cells ml^{-1}, while that in the control bottles increased from 49,811 to 644,931 cells ml^{-1}. Thus, *S. costatum* caused negative growth of *C. polykrikoides* at the *S. costatum* concentrations > 132,995 cells ml^{-1} (Fig. 3.5B).

The abundances of *C. polykrikoides* incubated with *Chaetoceros danicus* at 1:1 in cell abundance changed in the similar manner with those without *C. danicus* (i.e., in control bottle) for the first 4 elapsed days (Fig. 3.6A). In this period, the cell concentration of *C. danicus* in the experimental bottles increased from 84 to 1,134 cells ml^{-1}, while that in the control bottles increased from 81 to 1,493 cells ml^{-1} (Fig. 3.6B). However, the concentration of *C. polykrikoides* incubated with *C. danicus* at Day 4-8 decreased from 71 to 63 cells ml^{-1}, while that without *C. danicus* increased 35 to 71 cells ml^{-1} (Fig. 3.6A). In this period, the concentration of *C. danicus* in the experimental bottles

increased from 1,134 to 15,667 cells ml^{-1}, while that in the control bottles increased from 1,493 to 15,398 cells ml^{-1} (Fig. 3.6B). Furthermore, the abundance of *C. polykrikoides* incubated with *C. danicus* at Day 8-10 decreased from 63 to 40 cells ml^{-1}, while that without *C. danicus* increased 71 to 77 cells ml^{-1} (Fig. 3.6A). In this period, the concentration of *C. danicus* in the experimental bottles increased from 15,667 to 21,213 cells ml^{-1}, while that in the control bottles increased from 15,398 to 23,656 cells ml^{-1} (Fig. 3.6B). Thus, *C. danicus* did not affect growth of *C. polykrikoides* at the diatom concentration of 1,134 cells ml^{-1}. However, *C. danicus* caused negative growth of *C. polykrikoides* at the diatom concentrations of 5,781 - 21,210 cells ml^{-1}.

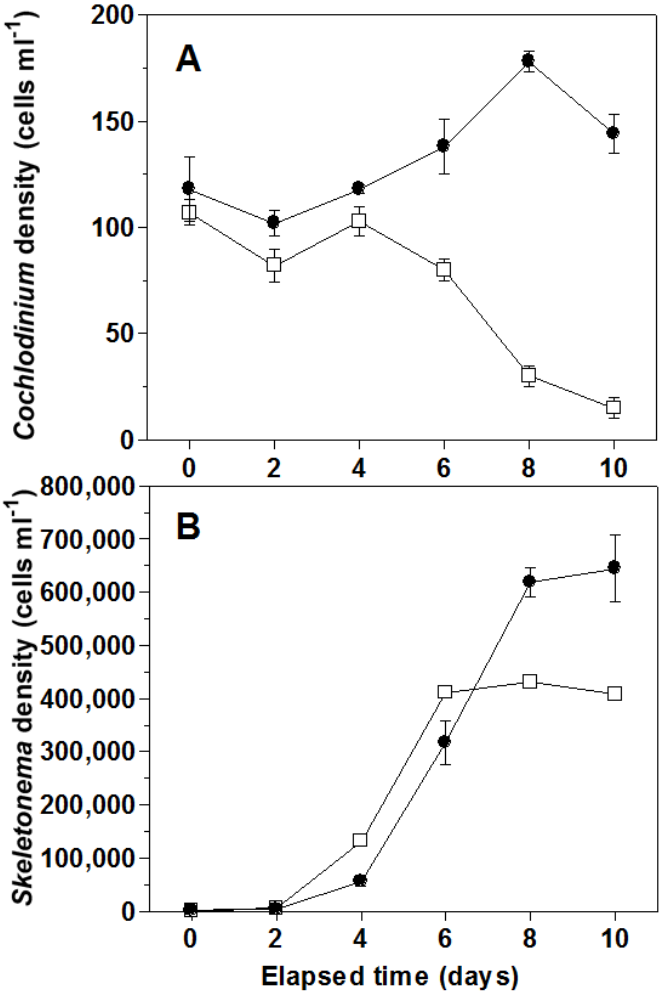

Fig. 3.5. The concentrations (cells ml^{-1}) of *Cochlodinium polykrikoides* (A) and *Skeletonema costatum* (B) as a function of elapsed incubation time. Symbols represent treatment means ± 1SE. Open squares: Concentrations in the experimental bottles (i.e., mixture of *C. polykrikoides* and *S. costatum*). Close circles: Concentrations in the control bottles (i.e., *C. polykrikoides* or *S. costatum* only).

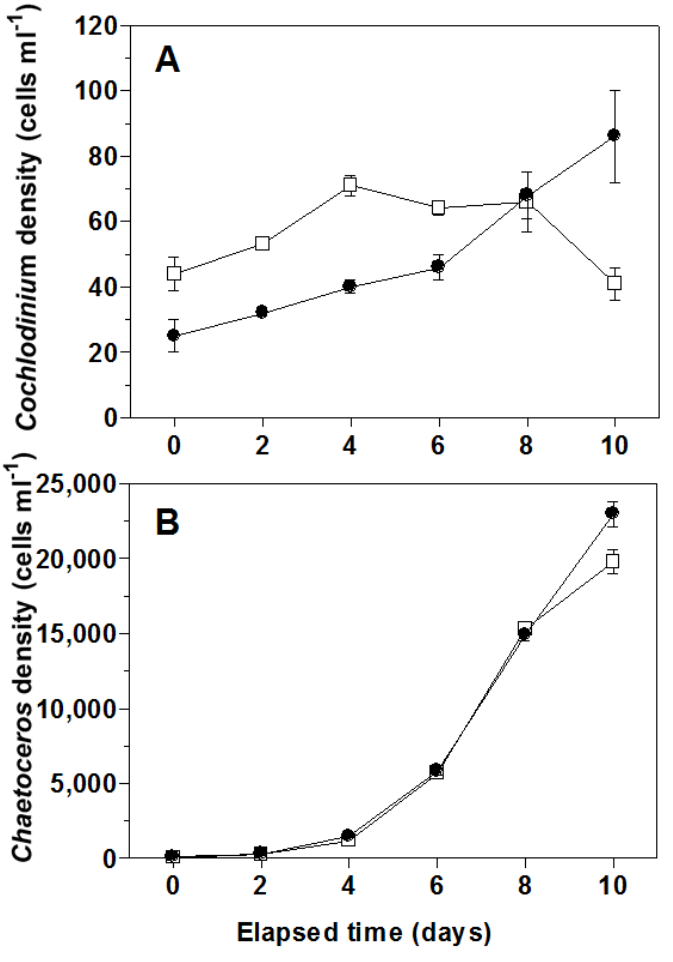

Fig. 3.6. The concentrations (cells ml^{-1}) of *Cochlodinium polykrikoides* (A) and *Chaetoceros danicus* (B) as a function of elapsed incubation time. Symbols represent treatment means ± 1SE. Open squares: Concentrations in the experimental bottles (i.e., mixture of *C. polykrikoides* and *C. danicus*). Close circles: Concentrations in the control bottles (i.e., *C. polykrikoides* or *C. danicus* only).

3.4. Discussion

3.4.1. Effects of diatom concentrations on the swimming speed of *Cochlodinium polykrikoides*

Skeletonema costatum, Chaetoceros danicus, and *Thalassiosira decipiens*, all 3 common diatoms tested in the present study lower swimming speed of *C. polykrikoides* cells when the concentrations of *S. costatum, C. danicus*, and *T. decipiens* exceed 5,000, 1,000, and 1,000 cells ml^{-1}. However, the filtrates of *S. costatum, C. danicus*, and *T. decipiens* lower swimming speed of *C. polykrikoides* cells when the concentrations of *S. costatum, C. danicus*, and *T. decipiens* exceed 25,000, 25,000, and 1,000 cells ml^{-1}. Thus, *S. costatum* lower the swimming speed of *C. polykrikoides* by both physical contact and chemical cue at the *S. costatum* concentrations of 250,000-500,000 cells ml^{-1}, but mainly by physical contact at the concentrations of 5,000-100,000 cells ml^{-1}. In the case of *C. danicus*, this diatom lower the swimming speed of *C. polykrikoides* by both physical contact and chemical cue at the *C. danicus* concentration of 50,000 cells ml^{-1}, but mainly by physical contact at the concentration of 25,000 cells ml^{-1}. *T. decipiens* lower the swimming speed of *C. polykrikoides* by both physical contact and chemical cue at the *T. decipiens* concentrations of 1,000-50,000 cells ml^{-1}. That is, the swimming speed of *C. polykrikoides* is affected by relatively low abundance of *T. decipiens*. The concentrations of *S. costatum* > 5,000 cells ml^{-1}, *C. danicus* > 1,000 cells ml^{-1}, and *T. decipiens* > 1,000 cells ml^{-1} are not unusual in natural environments (Jeong et al., 2013). Many diatoms produce some secondary metabolites such as polyunsaturated aldehydes

(PUAs) and polyunsaturated fatty acids (PUFAs)(Leflaive and Ten-Hage, 2009). These PUAs and PUFAs are considered to be a allelopatic chemicals to the competitiors. *Skeletonema costatum* are known to produce PUA (Wichard et al., 2005). Thus, the other two diatom species examined in this study may produce the PUAs and/or PUFAs, and may resulted the growth inhibition of *C. polykrikoides* at the high concentrations.

C. polykrikoides migrates between the surface and 20 m depth (Park et al., 2001; Kim et al., 2010). It can receive light for photosynthesis in the surface water, and nutrients in deep waters. The maximum growth rate of *C. polykrikoides* (0.54 d^{-1}) is lower than that of co-occurring competing dinoflagellates such as *Akashiwo sanguinea* (1.19 d^{-1}), *Prorocentrum minimum* (1.36 d^{-1}), and *Gymnodinium instriatum* (0.63 d^{-1}) (Matsubara et al., 2007; Yamatogi et al., 2005; Nagaseo et al., 2006b; Kondo et al., 1990). However, this fasts wimming ability may enable *C. polykrikoides* to defeat the relatively slow swimming dinoflagellates, in particular when the thermocline is located in deep waters and the concentration of nutrients in the surface waters is low. However, the reduction of swimming speed due to diatoms may give a disadvantage to *C. polykrikoides* (Fig. 3.7).

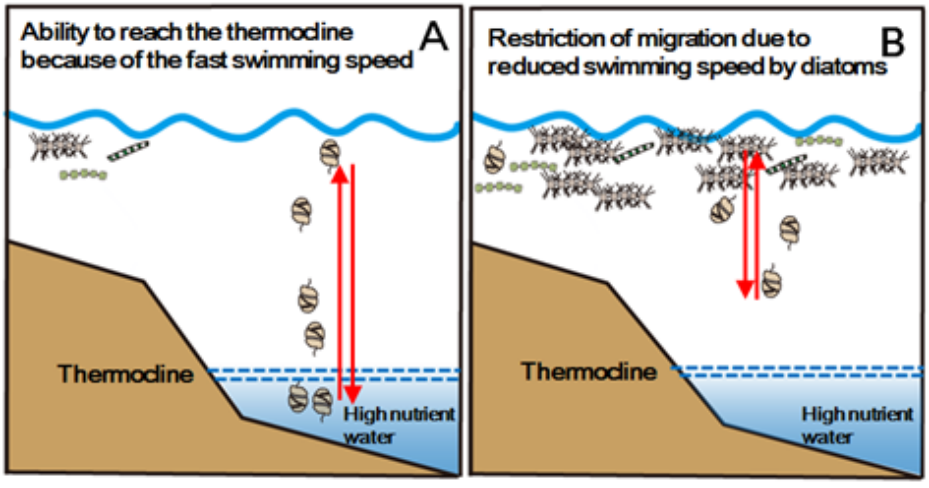

Fig. 3.7. Diagram of the ability of *Cochlodinium polykrikoides* to reach deep water where nutrient concentration is high and the location of thermocline when diatom concentrations are low (A) and high (B). Cells of *C. polykrikoides* pass the thermocline and reach deep water by active vertical migration when diatom concentrations are low (A), while the swimming speed and depth to which *C. polykrikoides* can swim are reduced when diatom concentrations are high (B).

3.4.2. Effects of diatom concentrations on the growth rate of *Cochlodinium polykrikoides*

The growth of *C. polykrikoides* was inhibited when *C. polykrikoides* was incubated with *Skeletonema costatum* or *Chaetoceros danicus*. After 4 elapsed days, when the abundance of *S. costatum* was reached approximately 50,000 cells ml^{-1}, the abundance of *C. polykrikoides* was start to decrease in experimental bottles. The abundance of *C. polykrikoides* in the experimental bottle was dropped down to 15 cells ml^{-1} at the end of the experiment, while that in the control bottles was increased to 144 cells ml^{-1} at the same periods. The abundance of *C. polykrikoides* incubated with *C. danicus* was also start to decrease at 4 elapsed days when the abundance of *C. danicus* was reached 1,188 cells ml^{-1} in the experimental bottles. The abundance of the *C. polykrikoides* in the experimental bottle was dropped down to 41 cells ml^{-1} at the end of the experiment, while that in the control bottles was increased to 86 cells ml^{-1} at the same periods. Thus, the fast growth of diatoms may inhibit the growth of *C. polykrikoides* when they coexist in the natural environment.

The rainfall plays an important role in influx of nutrients into the coastal waters (e.g. Kim et al., 2013). When the concentrations of nutrients in the water are high enough, diatoms grow faster than other flagellate (Banse, 1982). The maximum growth rates of *Thalassiosira pseudonana* is 2.77 d^{-1} while, the maximum growth of *C. polykrikoides* is 0.61 d^{-1} (Passche, 1973; Yamatogi et al., 2005). Thus, if the growth of diatoms is stimulated by high concentrations of nutrients by rainfall, the high abundance of diatom may prevent

the outbreak of the red tide of *C. polykrikoides* (Fig. 3.8).

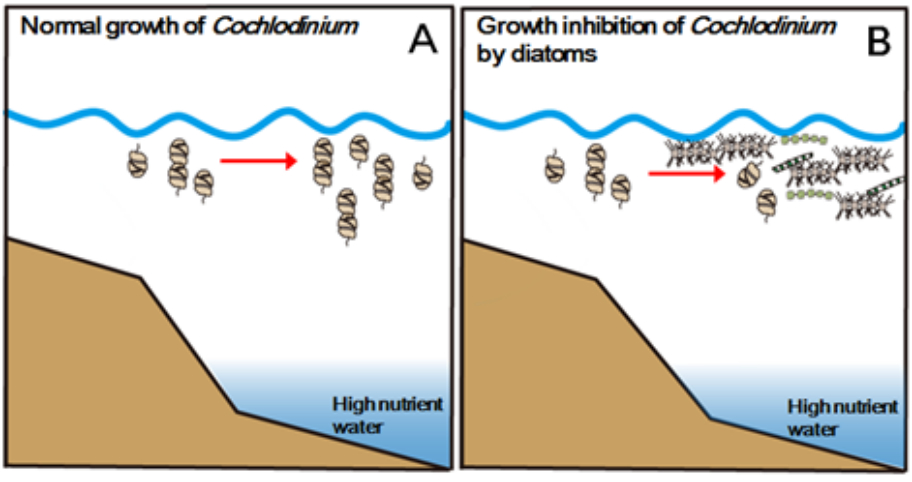

Fig. 3.8. Diagram of the growth of *Cochlodinium polykrikoides* when diatom concentrations are low (A) and high (B). The concentration of *C. polykrikoides* is maintained or increases when diatom concentrations are low (A), while concentration of *C. polykrikoides* decreases when diatom concentrations are high (B).

Prior to this study, most studies on interactions between *C. polykrikoides* and co-occurring species showed that *C. polykrikoides* had harmful effects on co-occurring species through allelochemicals or cell contact (Table 3.2); when co-occurring phytoplankton species were incubated with *C. polykrikoides*, they lost flagella and motility or experienced other cell morphological modification (Tang and Gobler, 2010). Furthermore, *C. polykrikoides* may inhibit the growth of *Akashiwo sanguinea* by cell contact (Yamasaki et al., 2007). However, the results of this study provide clear evidence that diatoms inhibit the swimming speeds, the growth rate, and the eventual depths that *C. polykrikoides* is able to reach.

Table 3.2. The interactions between *Cochlodinium polykrikoides* (Cp) and co-occurring phytoplankton species. DN, dinoflagellate; RA, raphidophyte; DA, diatom; GI, growth inhibition; MM, morphological modification.

Phytoplankton		Conditions	Effects	Ref.
DN	*Akashiwo sanguinea*	i) whole cell addition	GI, MM	(1)
		ii) 5 μm mesh barrier	GI, MM	(1)
DN	*Gyrodinium instriatum*	i) whole cell addition	GI, MM	(1)
		ii) 5 μm mesh barrier	GI, MM	(1)
DN	*Gymnodinium aureolum*	whole cell addition	GI, MM	(1)
DN	*Heterocapsa rotundata*	whole cell addition	GI, MM	(1)
DN	*Scrippsiella* cf. *trochoidea*	whole cell addition	GI, MM	(1)
RA	*Chattonella marina*	i) whole cell addition	GI, MM	(1)
		ii) 5 μm mesh barrier	GI, MM	(1)
RA	*Rhodomonas salina*	whole cell addition	GI, MM	(1)
DA	*Thalassiosira weissflogii*	whole cell addition	GI, MM	(1)
DN	*Akashiwo sanguinea*	i) whole cell addition	GI, MM	(2)
		ii) filtrates from Cp	no effect	(2)
		iii) non-contact condition	no effect	(2)

(1) Gobler et al. (2010), (2) Yamasaki et al., (2007)

Chapter 4. Taxonomy of *Alexandrium pohangense* n. sp., a new mixotrophic predator of *Cochlodinium polykrikoides*

4.1. Introduction

Cochlodinium polykrikoides is a bloom forming dinoflagellate in the coastal waters of many countries and causes massive fish mortality and economic loss in many countries (Gobler et al., 2008; Jeong et al., 2008; Mulholland et al., 2009; Park et al., 2013a; Lim et al., 2014a, 2015b). Moreover, some studies suggested that populations of grazers may have considerable grazing impact on populations of bloom forming species (Jeong et al., 2004a, 2005d; Yoo et al., 2013). Thus, the predators of *C. polykrikoides* may be important factors to understand the population dynamics of *C. polykrikoides*. Several heterotrophic protists and ciliate are known to feed on *C. polykrikoides* (Jeong et al., 1999b, 2006, 2007, 2008; Cho, 2006; Lim et al., 2014b). However, mixotrophic predators of *C. polykrikoides* have not been revealed yet. Mixotrophic ability of the dinoflagellate is also considered as an important factor to form a harmful algal bloom (e.g., Jeong et al., 2010a). Furthermore, some mixotrophic dinoflagellates have a greater growth rate when they feed on the prey compared to phototrophic mode (Lee et al., 2014a). Thus, to better understand the population dynamics of *C. polykrikoides*, the mixotrophic predators should be explored.

Recently, I newly isolated and established a clonal culture of *Alexandrium* sp. from waters off Pohang, Korea, in 2014 when a huge *Cochlodinium* red tide was occurred. The genus *Alexandrium* is one of the most studied dinoflagellates (Franks and Anderson, 1992; Hallegraeff, 1993; Scholin et al., 1994; Anderson et al., 2012). The genus *Alexandrium* was first described by Halim (1960). More than thirty species have been reported and new *Alexandrium* species have been continuously established (MacKenzie et al., 2004; Anderson et al., 2012; John et al., 2014; Murray et al., 2014). Some *Alexandrium* species are known to be responsible for paralytic shellfish poisoning (PSP) (Hallegraeff, 1993; Anderson et al., 2012). PSP has caused loss of wild and cultured shellfish, negative impact on tourism and recreation activities, and even human illness from consumption of contaminated shellfish or fish by *Alexandrium*. Due to their harmful effects, the scientists in many countries have paid attention on *Alexandrium*. Thus, an accurate identification is very important to prevent the potential risk by *Alexandrium* species.

Alexandrium species are identified based on the some morphological differences such as the size and shape of cells, the size and shape of the first apical (1′) and sixth precingular (6′′) plates, thecal ornamentation, the presence or absence of ventral pore and sulcal lists, the shape of the pore plate (Po), the connection between the Po and 1′ plate, the size and shape of sulcal plates, and the ability to form chains (Balech, 1995). However, due to ambiguity of some morphological features, the molecular and phylogenetic studies for identification of *Alexandrium* species have consistently used and some of morphological features have supported monophyletic clades

based on the ribosomal DNA regions (Scholin et al., 1994; John et al., 2003; Leaw et al., 2005; Lilly et al., 2007; Orr et al., 2011; John et al., 2014; Kremp et al., 2014).

To identify the *Alexandrium* species which is able to feed on *Cochlodinium polykrikoides*, the morphology of the strain analyzed using light microscopy, scanning electron microscopy (SEM) and the phylogenetic affinities using DNA sequences of the small subunit (SSU), internal transcribed spacers (ITS) 1 and 2, 5.8S, and the large subunit (LSU) rDNA examined. On the basis of morphological and phylogenetic criteria, I proposed that this is a new species of the genus *Alexandrium.*

4.2. Materials and methods

4.2.1. Collection and culture of *Alexandrium pohangense* n. sp.

Alexandrium pohangense was isolated from plankton samples collected from waters off Pohang, Korea, in September 2014, when the water temperature and salinity were 23.3 °C and 31.1, respectively (Fig. 4.1). Samples were sieved gently through a 154-μm Nitex mesh sieve and transferred to 6-well tissue culture plates. A clonal culture of *A. pohangense* strain was established by two serial single cell isolations. As the concentration of *A. pohangense* increased, the cells were subsequently transferred to 32-, 270-, and 500-ml polycarbonate (PC) bottles. The bottles were captaining fresh f/2 seawater media and *A. pohangense* capped, and placed on a shelf at 20 °C under an illumination of 50 μE m^{-2} $s^{-1}$of cool white fluorescent light on a 14:10 h light-dark cycle. When cultures became dense, they were transferred to new 500-ml PC bottles containing fresh f/2 seawater media approximately every 2-3 weeks. These cultures were used for genetic and morphological analyses. Only cultures in the exponential growth phase were used.

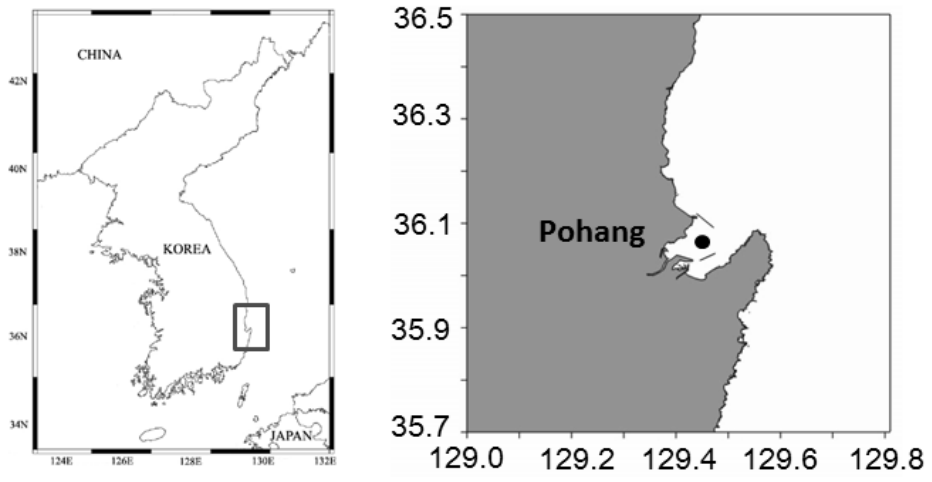

Fig. 4.1. The sampling site where *Alexandrium pohangense* n. sp. was isolated.

4.2.2. Morphology of *Alexandrium pohangense* n. sp.

The morphology of live vegetative flagellated cells and cells of *A. pohangense* preserved in 4% (v/v) glutaraldehyde were examined using a compound microscope (Zeiss-Axiovert 200M; Carl Zeiss Ltd, Göttingen, Germany). I measured the cell length and cell width of live cells using an image analysis system. Thecal plates were visualized by staining with Calcofluor white stain (Sigma, USA) and examination using epi-fluorescence illumination. For the analysis by SEM, a 10 ml aliquot of a dense culture (~500 cells ml^{-1}) was fixed with paraformaldehyde (final concentration = 2 %, w/v) for 10min. The fixed cells were collected on a PC membrane filter (pore size = 5 μm) without additional pressure and desalted by rinsing with distilled waters. PC membrane filters were carefully dehydrated in an ethanol series (50, 60, 70, 80, 90, and 100 %) and finally dried using

a critical point dryer (BAL-TEC, CPD 300, Balzers, Liechtenstein, Germany). The dried filters mounted on a tub and coated with gold-palladium. Cells were viewed with SEM (JSM-840A, SEM JEOL Ltd., Tokyo, Japan). More than 100 cells were observed under the SEM for the determination of the morphological features.

4.2.3. DNA extraction, PCR amplification, sequencing, and data analysis

The genomic DNA of *A. pohangense* was extracted using the AccuPrep Genomic DNA Extraction Kit (Bioneer, Daejeon, Korea). DNA yield was quantified with a spectrophotometer. The amplification reaction mixtures contained 1 x PCR buffer with 1.5 mM $MgCl_2$, 0.2 mM dNTPs, 0.5 mM each primer, 5 U of Taq DNA polymerase (Bioneer, Deajeon, Korea), and 200 ng template DNA. The primers that were used to amplify from the SSU to LSU region of rDNA listed in Table 4-1. The DNA was amplified in a Mastercycler ep gradient (Eppendorf, Hamburg, Germany) using the following cycling conditions: 3min at 95 ℃ followed by 40 x 45s at 95 ℃, 1 min at the selected temperature (AT), and 1 min at 72 ℃ with a final extension of 5 min at 72 ℃. The AT was adjusted depending on the primers used according to the manufacturer's instructions. PCR products were purified using AccuPrep DNA Purification Kit (Bioneer, Deajeon, Korea). Sequencing was performed with a ABIPRISM 3700 DNA Analyzer (Applied Biosystems, FosterCity, CA).

Table 4.1. Oligonucleotide primers used in this study to amplify and sequence th small subunit (SSU), internal transcribed spacer(ITS)1, 5.8S, ITS2, and large subunit (LSU) regions of rDNA of *Alexandrium pohangense*

Primer name	Sequence (5'-3')	Reference
Forward primers		
EUKA	CTGGTTGATCCTGCCAG	Medlin et al. 1988
EUK 1209F	GGGCATCACAGACCTG	Giovannoni et al. 1988
ITSF2	TACGTCCCTGCCCTTTGTAC	Litaker et al. 2003
D1R	ACCCGCTGAATTTAAGCATA	Scholin et al. 1994
Reverse Primers		
EUKB	TGATCCTTCTGCAGGTTCACCTAC	Medlin et al. 1988
ITSR2	TCCCTGTTCATTCGCCATTAC	Litaker et al. 2003
LSU B	ACGAACGATTTGCACGTCAG	Litaker et al. 2003
28-1483R	GCTACTACCACCAAGATCTGC	Daugbjerg et al. 2000

4.2.4. Sequence availability and phylogenetic analysis

Phylogenetic analyses of the SSU, ITS1-5.8S-ITS2, and LSU rDNA regions of *A. pohangense* were conducted using MEGA v.4 (Tamura et al., 2007) including sequences from closely related taxa obtained from GenBank. The Maximum likelihood (ML) analysis of the two regions was conducted using RAxML 7.0.3 program (Stamatakis, 2006) with default GTR+G+I model in the program. Tree likelihoods were estimated using a heuristic search with 100 random addition sequence replicates, and TBR branch swapping. Bayesian inference was performed using MrBayes v.3.1 (Huelsenbeck and Ronquist, 2001; Ronquist and Huelsenbeck, 2003) with the default GTR + G + I model to determine the best available model for the data of each region. For all sequence regions, posterior probabilities were estimated using four independent Markov Chain Monte Carlo (MCMC) chains, performed described by Kang et al. (2010).

4.3. Results

4.3.1. Molecular characterization of *Alexandrium pohangense* n. sp.

The small subunit (SSU), the large subunit (LSU), internal transcribed spacer regions (ITS1 and ITS2), and 5.8S of the ribosomal rDNA of *Alexandrium pohangense* were compared with other *Alexandrium* species. The SSU and LSU rDNA sequences of *A. pohangense* were 4-7% and 14-17%, respectively, different from those of *Alexandrium minutum, Alexandrium ostenfeldii, Alexandrium tamutum, Alexandrium margalefii,* and *Alexandrium pseudogonyaulax,* the closest species. In addition, 5.8s rDNA sequences of *A. pohangense* were also 12% different from those of *A. minutum, A. ostenfeldii, A. tamutum,* and *Alexandrium peruvianum*, while ITS1 and ITS2 regions of *A. pohangense* were found no significant similarity with those of other *Alexandrium* species (Table 4.2).

In the phylogenetic tree based on LSU rDNA sequences, *A. pohangense* was positioned at the basal of the clade of *A. margalefii* strains (Fig. 4.2). Moreover, in the phylogenetic tree based on SSU rDNA sequences, *A. pohangense* formed a clade with *Alexandrium leei*, and *A. margalefii* strain was positioned at the basal of this clade (Fig. 4.3).

Table 4.2. Comparison of the sequences of the small subunit (SSU), 5.8S, and large subunit (LSU) rDNA of the strain of *Alexandrium pohangense* with some genetically close species. The numbers indicate base pair differences. The numbers in parenthesis are dissimilarity (%), including gaps. There was no significant similarity in ITS1 and ITS2 regions between *A. pohangense* with other *Alexandrium* species.

A. SSU of *A. pohangense*

Species	*A. minutum*	*A. lusitanicum*	*A. ostenfeldii*	*A. tamutum*	*A. margalefii*	*A. pseudogonyaulax*
Accession No.	JF906998, AJ535380	JF906999	AJ535383, JF521637	AJ535379	U27498	AB088302
A. pohangense	79–80 (4)	79 (4)	77–82 (4)	82 (4)	94 (5)	127 (7)

B. 5.8S of *A. pohangense*

Species	*A. ostenfeldii*	*A. peruvianum*	*A. tamutum*	*A. minutum*	*A. lusitanicum*
Accession No.	AB538439, JX878431, JX865532	JX841261, JX841266	AM236857	KF018285	EU707539
A. pohangense	19 (12)	19 (12)	19 (12)	19 (12)	19 (12)

C. LSU of *A. pohangense*

Species	*A. tamutum*	*A. insuetum*	*A. pseudogonyaulax*	*A. ostenfeldii*	*A. margalefii*	*A. minutum*	*A. andersoni*
Accession No.	EU707459	JF521630	AY154958	JF521636, JF521637	JQ616827	JF906998	JF521621
A. pohangense	176 (14)	190 (14)	195 (15)	198–199 (15)	199 (15)	197 (15)	218 (17)

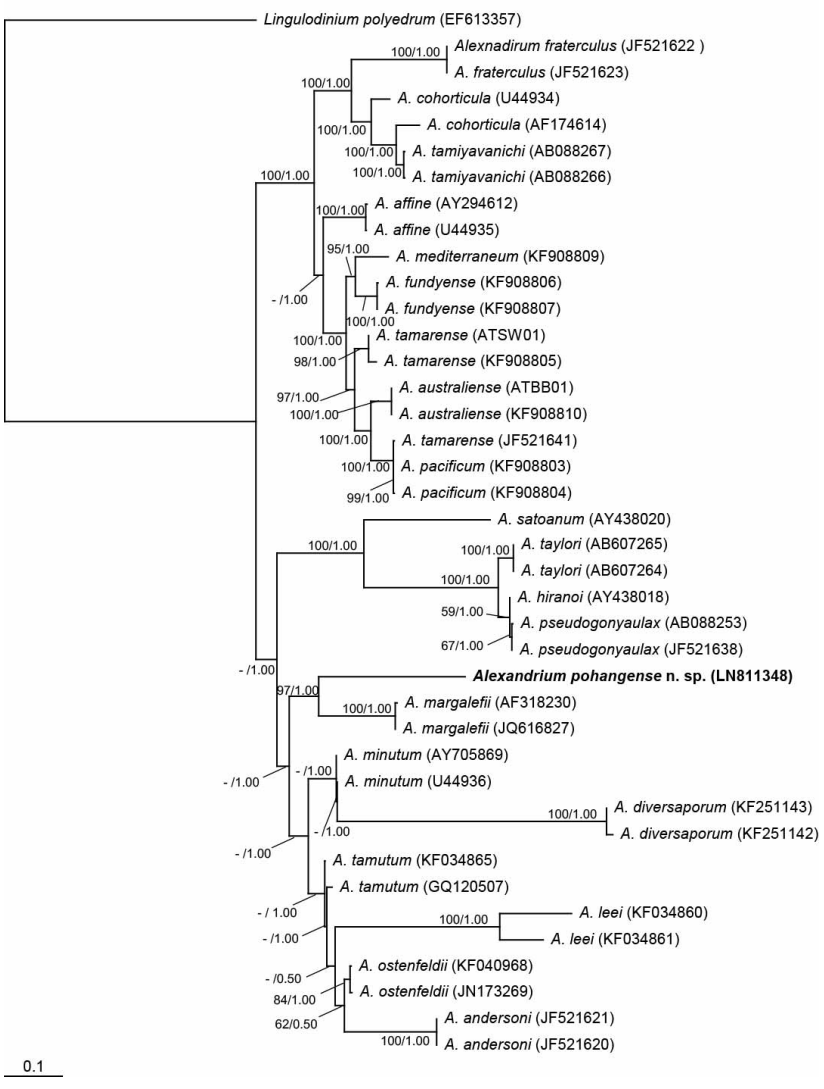

Fig. 4.2. Maximum likelihood (ML) tree based on 769 bp aligned positions of LSU ribosomal DNA region with *Lingulodnium polyedrum* as outgroup taxa. The branch lengths are proportional to the amount of character changes. The numbers above the branches indicate the Bayesian posterior probability (left) and ML bootstrap values (right). Posterior probabilities ≥0.5 are shown.

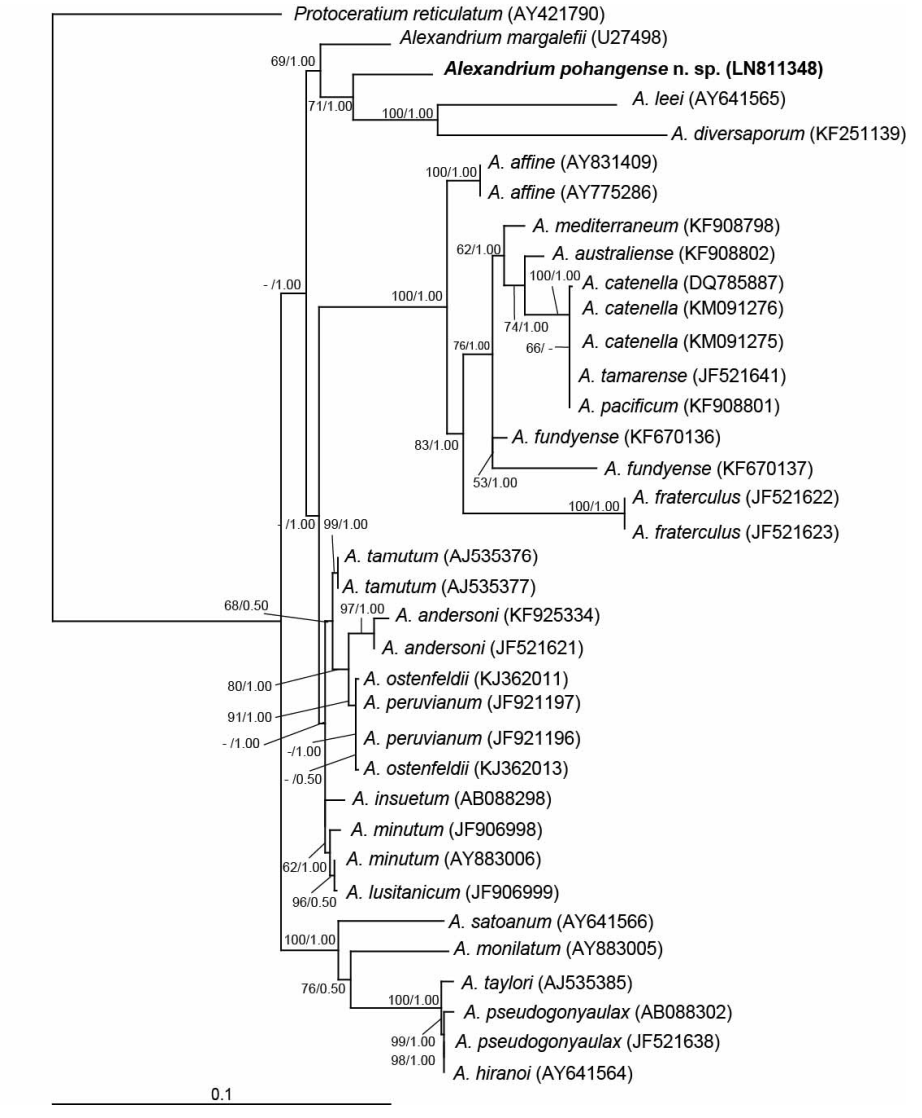

Fig. 4.3. Maximum likelihood (ML) tree based on 1,601 bp aligned positions of SSU ribosomal DNA region with *Protoceratium reticulatum* as outgroup taxa. The branch lengths are proportional to the amount of character changes. The numbers above the branches indicate the Bayesian posterior probability (left) and ML bootstrap values (right). Posterior probabilities ≥0.5 are shown

4.3.2. Morphology of *Alexandrium pohangense* n. sp.

Cells of *A. pohangense* were single, with chains of 2 cells observed very rarely. Cells of *A. pohangense* were spherical in shape, with a markedly impressed cingulum (Fig. 4.4). Comma shaped the apical pore located on epitheca, and the sulcus is deeply caved at the middle of the cell. Cells contained chloroplasts and the nucleus was located in the hypotheca (Fig. 4.4). The range of cell length and width of live cells (n = 25) as measured using light microscopy were 24–42 μm and 23 – 40 μm, respectively (Table 4.3). The ratio of cell length to cell width of live cells was almost 1 (range = 0.7–1.5, n = 25) (Table 4.3).

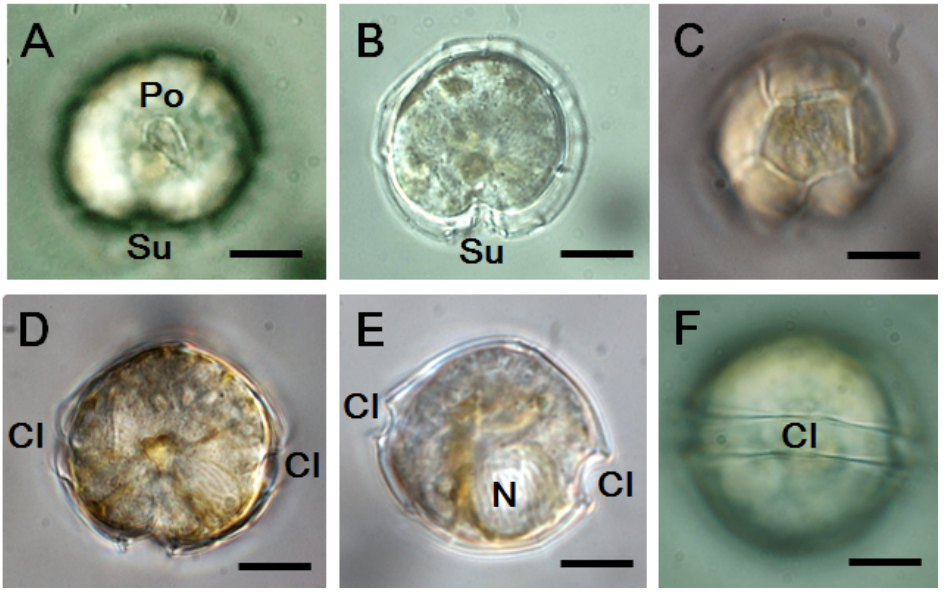

Fig. 4.4. Light micrographs of *Alexandrium pohangense* n. sp. (A, B) Apical view showing the apical pore (Po) located on the epitheca and sulcus (Su) in the middle of the cell. (C) Antapical view showing the plates pattern. (D) Oblique ventral view of *A. pohangense* showing the cingulum (CI). (E) Ventral view showing the nucleus (N) located in the hypotheca (F) Dosal view of A. pohagense with markedly impressed cingulum. Scale bars = 10 μm.

Morphological analysis using light microscopy with calcoflour white staining and SEM showed that *A. pohangense* had plates with a Kofoidian plate formula of Po, 4′, 6′′, 6c, 8s, 5′′′, and 2′′′′, which conformed to the genus *Alexandrium* (Figs. 4.5 and 4.6). *A. pohangense* had four apical plates. The wide quadrangular 1′ plate was vented and touched the 2′ plate and disconnected to the Po (Figs. 4.5). *A. pohangense* had a small ventral pore (average = 0.73 μm and 0.69 μm in LM and SEM, n = 20) on the 4′ plate (Table 4.3, Figs. 4.5). The large elongated 2′ plate was contacted the Po, 1′, 3′, 4′, 1′′, 2′′, and 3′′ plates (Fig. 4.6). The wide 3′ plate was hexagonal (Fig. 4.6). The 4′ plate, which had a ventral pore, was hexagonal and contacted the Po, 1′, 2′, 3′, 5′′, and 6′′ plates (Fig. 4.6). The first precingular plate (1′′) of *A. pohangense* was hexagonal and contacted 1′, 2′, 2′′, and cingular plate (Fig. 4.6). The second precingular (2′′) and forth precingular (4′′) plates were hexanonal, while third precingular (3′′) and fifth precingular (5′′) plates were pentagonal, respectively (Figs. 4.6). The sixth precingular (6′′) plate was pentagonal and the ratio of plate length to plate width of live cells was 0.88 (range = 0.7–1.2, n = 23) (Table 4.3, Fig. 4.6). The cingulum was consisted of six plates (Figs. 4.5, 4.6).

The shape of apical pore (Po) plate of *A. pohangense* was comma shaped and surrounded by marginal pores (Fig. 4.6). The marginal pores were only positioned dorsal part of comma pore. *A. pohangense* lacked an anterior attachment pore (aap) in the apical pore complex.

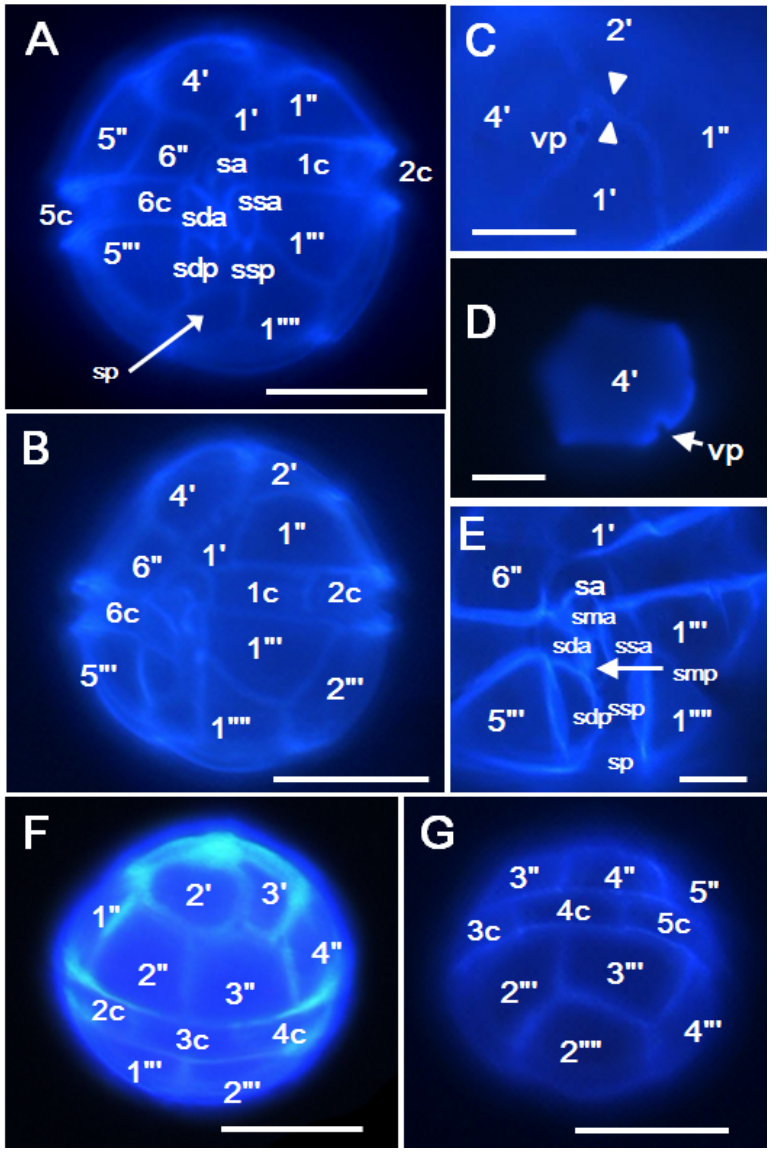

Fig. 4.5. Micrograph of calcofluor white stained *A. pohangense* showing the plate tabulation and pattern. (A, B) Ventral view. (C) Apical view showing the 1′ plate touching the 2′ plate and the ventral pore (vp) located on the 4′ plate. (D) The vp on the 4′ plate. (E) Sulcal plates. (F, G) Dorsal view. Scale bars = 20 μm for (A, B, F, G) and 5 μm for (C–E).

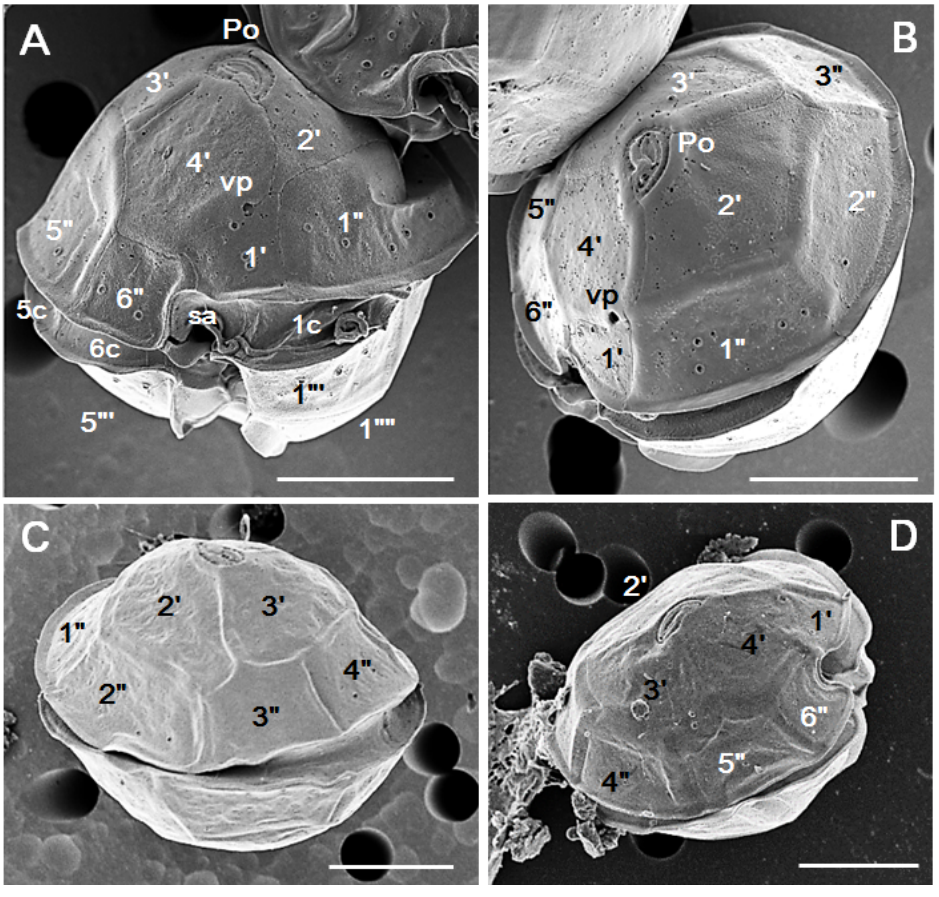

Fig. 4.6. Scanning electron microscopy images of *Alexandrium pohangense* n. sp. (A) Ventral view showing the cingular plates C1, C5, C6, and the anterior (sa) sulcal plates. (B) Apical view showing the 1′ plate whose left upper side is bent, protruding and touching the 2′ plate, but disconnected from the apical pore (Po). The ventral pore (vp) is located on the 4′ plate. (C, D) Lateral view showing the epithecal plate tabulation and pattern. Scale bars = 10 μm.

There were five postcingular plates: 1‴, 3‴, and 5‴ were quadrangular, but 2‴ and 4‴ plates were pentagonal (Fig. 4-7). *A. pohangense* had two antapical plates in hyposome. The first antapical plate (1⁗) was quadrangular and contacted 1‴, 2‴, 2⁗, and sulcal plates (Figs. 4-7). The second antapical plate (2⁗) was wide pentagonal and the ratio of plate length to plate width of live cells was 0.94 (range = 0.8-1.1, n = 19) (Fig. 4.7, Table 4.3). Moreover, the ratio of plate width to cell width of live cells was 0.52 and ratio of plate length to cell width of live cells was 0.47 (range = 0.4-0.7, n = 7) (Table 4.3).

The sulcal plates of *A. pohangense* consisted of eight plates: anterior sulcal plate (sa), posterior sulcal plate (sp), right anterior (sda), right posterior (sdp), left anterior (ssa), left posterior (ssp), and two small plates between lateral plates (the median anterior: sma, the median posterior: smp) (Fig. 4.8). The length of ssa plate was 7.09 μm (n = 7) in LM (Table 4.3). The ratio of sp plate was 1.13 (range = 0.7-1.6, n = 10) (Table 4.3). Moreover, two pairs of lateral plates (sda, ssa, sdp, and ssp) had list at the marginal of each plate (Fig. 4.8).

Cell surface was smooth, but two different sizes of pores were scattered (Figs. 4.8). The bigger pores were scattered randomly, but the several smaller pores were clustered together (Fig. 4.8).

Table 4.3. Comparison of the morphological characteristics of *Alexandrium pohangense* n. sp. and morphologically similar *Alexandrium* species. In all species depicted, the 1′ plate is disconnected from the apical pore complex and the thecal plates are smooth. Specimens were observed using light microscopy (LM) and scanning electron microscopy (SEM). The numbers in the parenthesis are the mean value. [a]Data were not directly mentioned but inferred from images provided in the respective references included in this study. α: the angle between the cingulum and the bottom margin side of 1′ plate, β: the angle between antero-posterioral axis of the cell and the point of the margin of apical pore plate, sa: anterior sulcal plate, ssa: left anterior sulcal plate, sp: posterior sulcal plate, pap: posterior attachment pore. The numbers in parenthesis are average values. NA: Not available.

Species	*A. pohangense*	*A. taylori*	*A. margalefii*	*A. hiranoi*	*A. pseudogonyaulax*	*A. camurascutulum*
Length (L, μm), live (LM)	24-42 (30)	31-44	28-39	18-75 (40)	32-40 (35)	26-28
Width (W, μm), live (LM)	23-40 (30)	32-46	28-35	18-75 (37)	28-42 (37)	21-24
Ratio of L relative to W	1	~1	~1	~1	~1	~1
Presence of ventral pore (vp)	yes	yes	yes	yes	yes	yes
Diameter of vp (μm) (LM)	0.73	NA	0.62[a]	1.81[a]	1.48[a]	NA
Diameter of vp (μm) (SEM)	0.69	0.88[a]	NA	NA	NA	0.68[a]

Table 4.3. continued

Species	*A. pohangense*	*A. taylori*	*A. margalefii*	*A. hiranoi*	*A. pseudogonyaulax*	*A. camurascutulum*
Plate on which vp is located	4′	4′	1′	1′	1′	4′
Plates connected to vp	1′, 4′	1′, 2′, 4′	1′, 4′, 1′′	1′, 4′	1′, 4′	1′, 4′
Ratio of length relative to width of the 2′′′′ plate (LM)	0.8–1.1 (0.9)	1.2[a]	1.3[a]	1.9[a]	1.2[a]	NA
Ratio of the 2′′′′ plate area relative to the total hypothecal area (LM)	0.21–0.34 (0.27)	0.16[a]	0.11[a]	0.16[a]	0.12[a]	NA
Shape of 1′ plate	quadrangular	pentagonal	quadrangular	pentagonal	pentagonal	pentagonal
Ratio of length relative to width of the 1′ plate (LM)	0.6–1.2 (0.9)	0.7[a]	1.5[a]	0.7[a]	0.8[a]	0.5–0.7[a]
Shape of 6′′ plate	pentagonal	pentagonal	pentagonal	pentagonal	pentagonal	hooked pentagonal
Ratio of length relative to width of the 6′′ plate (LM)	0.7–1.2 (0.9)	1.2[a]	1.4[a]	1.2[a]	1.4[a]	0.6[a]

Table 4.3. continued

Species	*A. pohangense*	*A. taylori*	*A. margalefii*	*A. hiranoi*	*A. pseudogonyaulax*	*A. camurascutulum*
Angle of α (°)	0	80[a]	0[a]	85[a]	0[a]	55–70[a]
Angle of β (°)	45–58	20[a]	30[a]	0[a]	0[a]	0[a]
Plates contacted to sa	6′′, 1′	6′′, 1′, 1′′	6′′, 1′	6′′, 1′	6′′, 1′	6′′, 1′, 1′′
Length of the ssa (μm) (LM)	7.09	6.66[a]	4.84[a]	7.06[a]	12.48[a]	NA
Ratio of length relative to width of the sp plate (LM)	0.7–1.6 (1.1)	2.1[a]	1.4[a]	1.4[a]	1.2[a]	NA
The number of the types of pores on the cell surface (SEM)	2	1	NA	1	1	2
Presence of pap	no	no	no	no	no	yes
Reference	(1)	(2), (3)	(2), (3), (4), (5)	(1), (6)	(3), (4), (7)	(8)

(1) This work, (2) Balech (1994), (3) Giacobbe and Yang (1999) (4) MacKenzie et al. (2004), (5) Selina and Morozova (2005), (6) Kita and Fukuyo (1988), (7) Gu et al. (2013), (8) MacKenzie and Todd (2002)

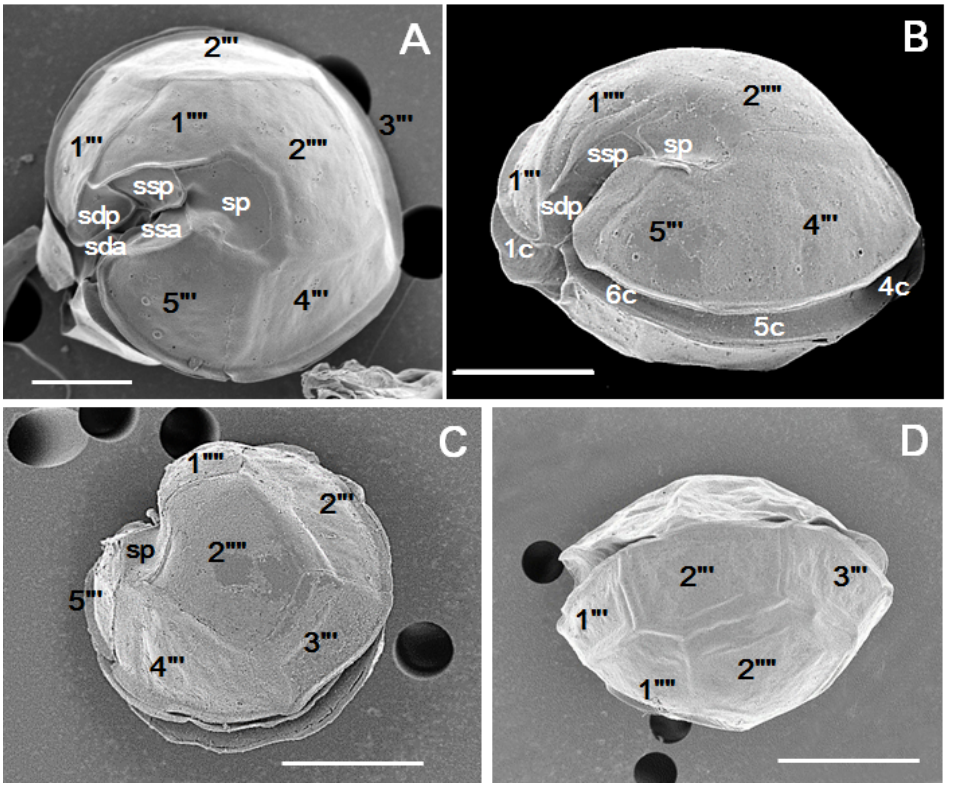

Fig. 4.7. Scanning electron microscopy images of *Alexandrium pohangense* n. sp. (A–D) Antapical view showing the hypothecal plate tabulation (postcingular plates, antapical plates) and sulcal plates. Scale bars = 10 μm.

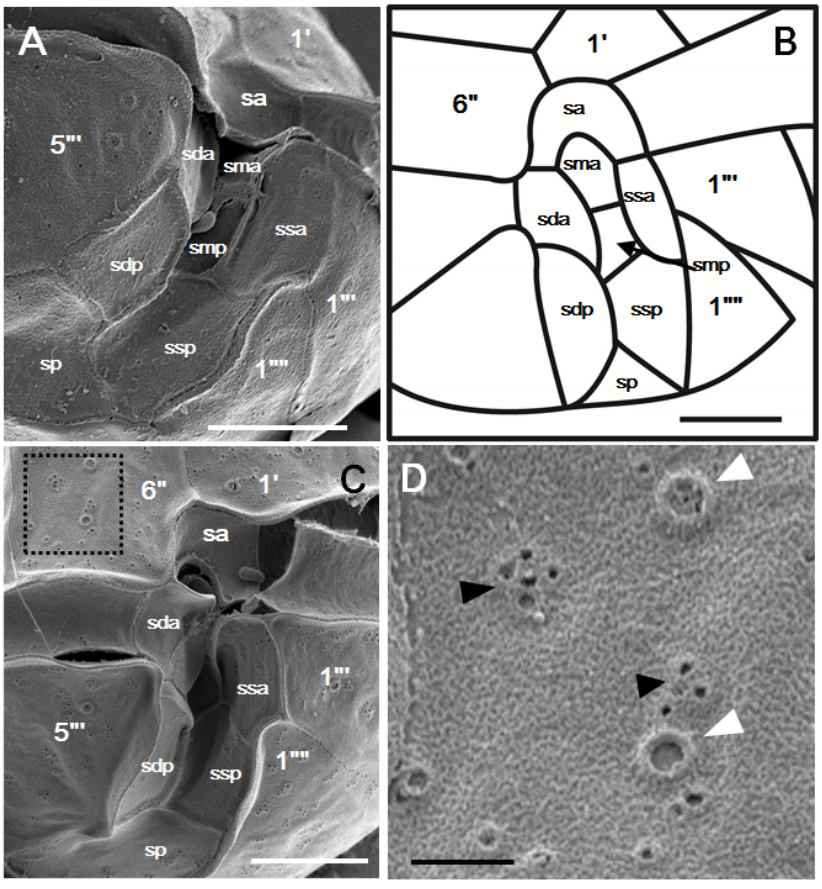

Fig. 4.8. Scanning electron microscopy images and drawings of *Alexandrium pohangense* n. sp. (A–C) Ventral view showing the sulcal plates. sa, anterior plate; sda, right anterior plate; sdp, right posterior plate; ssa, left anterior; ssp, left posterior; sma, median anterior plate; smp, median posterior plate; sp, posterior plate. (D) Enlarged view from Fig. 6C showing the smooth cell surface and two different types of pores. White arrowheads indicate single large pores and black arrowheads indicate clustered small pores. Scale bars = 5 μm for (A–C) and 1 μm for (D).

4.4. Discussion

4.4.1. Molecular characterization of *Alexandrium pohangense* n. sp.

The rDNA (SSU, ITS1, 5.8S, ITS2, and LSU) sequences of the strains of *Alexandrium pohangense* were considerably different from those of the strains of other *Alexandrium* species (Table 4.2). The sequences for the 5.8S of *A. pohangense* are 19 bp different from those of *Alexandrium minutum, Alexandrium lusitanicum, Alexandrium ostenfeldii, Alexandrium tamutum*, and *Alexandrium peruvianum*; moreover, its LSU sequences are 176-218 bp different from those of other *Alexandrium* species (Table 4.2). Several studies reported that the ribosomal sequence differences within *Alexandrium* speceies are few (John et al., 2003; John et al., 2014). The interspecies nucleotide differences in the LSU rDNA region of some *Alexandrium* species are only 3-36 bp (John et al., 2014). Therefore, the big base pair difference of *A. pohangense* from other *Alexandrium* species supported that *A. pohangense* is a genetically distinct new species.

In the phylogenetic trees based on LSU and SSU rDNA, *A. pohangense* was clustered with *Alexandrium margalefii* in both trees. However, *A. pohangense* was located in the basal of the *A. margalefii* in LSU tree, while *A. magalefii* was located in the basal of the cluster in the SSU tree. Because there were no much information

of the *A. magalefii* and there was only one strain of *A. pohangense*, it may be the reason of differences in location of *A. pohangense* in the both trees.

4.4.2. Morphology of *Alexandrium pohangense* n. sp.

Based measurement of established culture of *Alexandrium pohangense*, *A. pohangense* has a Kofoidian plate formula of Po, 4′, 6′′, 6c, 8s, 5′′′, and 2′′′′, which confirms its assignment to the genus *Alexandrium* (Fig. 4.9). The first apical (1′) plate is disconnected from the apical pore complex and *A. pohangense* has a smooth thecal surface like *A. taylori*, *A. margalefii*, *Alexandrium hiranoi*, *Alexandrium pseudogonyaulax*, and *Alexandrium camurascutulum*. In addition, overall cell sizes and the ratio of cell width and length of *A. pohangense* are similar to those of these five *Alexandrium* species (Table 4.3). However, the ventral pore of *A. pohangense* is considerably smaller (average: 0.73 and 0.69 μm, measured using LM and SEM, respectively) than those of *A. hiranoi* and *A. pseudogonyaulax* (1.48–1.81 μm in LM) (Table 4.3). In addition, *A. pohangense* has a ventral pore on the margin of the 4′ plate, unlike *A. margalefii* or *A. pseudogonyaulax*, which have a larger ventral pore on the 1′ plate. Moreover, *A. pohangense* has a wide quadrangular 1′ plate, which is bent and touches the 2′ plate, unlike *A. margalefii*, which has a wide rectangular 1′ plate not touching the 2′ plate, or *A. pseudogonyaulax*, which has a narrower elongated 1′ plate touching the 2′ plate. Furthermore, the 6′′ plate of

A. pohangense is a simple pentagonal shape, while that of *A. camurascutulum* has deeply concaved left margin, which gives a hooked appearance. The ratio of 6′′ plate length and width of *A. pohangense* (0.9) is markedly smaller than that of *A. taylori*, *A. margalefii*, *A. hiranoi*, and *A. pseudogonyaulax* (1.2–1.4), but greater than that of *A. camurascutulum* (0.6). Moreover, the shape of the 2′′′′ plate of *A. pohangense* (i.e., regular pentagonal with a ratio of plate length to plate width of 0.9) is clearly different from that of *A. taylori*, *A. margalefii*, *A. hiranoi*, and *A. pseudogonyaulax* (i.e., elongated pentagonal, ratio of plate length to plate width 1.2–1.9), and the area of the 2′′′′ plate relative to the total area of the hypotheca of *A. pohangense* (0.27, n = 10) is greater than that of *A. taylori*, *A. margalefii*, *A. hiranoi*, and *A. pseudogonyaulax* (0.11–0.16). Even though, the 2′′′′ plate of *A. camurascutulum* is shaded and partially covered by the other cell (MacKenzie and Todd, 2002; Fig. 4.9), the size of 2′′′′ plate is similar with that of 5′′′ plate, which is a medium-size in the hypotheca. The area of the 2′′′′ plate relative to the total area of the hypotheca of *A. camurascutulum* is smaller than that of *A. pohangense*.

The apical pore plate (Po) of *A. hophangense* is twisted toward to the left side of epitheca while, those of *A. hiranoi*, *A. psudogonyaulax*, and *A. camurascutulum* are straightly toward to the anterior sulcal plate (sa) (Fig. 4.10). The angle between vertical axis of cell and the point of the margin of Po (α) of *A. hophangense* (45–58°) is clearly greater than *A. taylori* and *A. margalefii*, but

smaller than *A. hiranoi*, *A. psudogonyaulax*, and *A. camurascutulum* (Table 4.3). While 1'' plate of *A. pohangense* straightly contacts to 1' plate, the right margins of 1'' plates of *A. hiranoi*, *A. pseudogonyaulax*, and *A. camurascutulum* are deeply curved toward 1' (Fig. 4-9). Thus, the angle between the cingulum and the bottom margin side of 1' plate (β) of *A. pohangense* is horizontal, while those of *A. taylori*, *A. hiranoi*, and *A. camurascutulum* are between 55-85° (Fig. 4.10).

The anterior sulcal plate (sa) of *A. pohangense* contacts to 1' and 6'' plates like *A. marglefii*, *A. pseudogonyaulax*, and *A. hiranoi*, while those of *A. taylori* and *A. camurascutukum* contacts to 1', 1'', and 6'' plates. The length of the left anterior sulcal plate (ssa) of *A. pohangense* (7.09) is considerably longer than *A. margalefii*, but shorter than *A. pseudogonyaulax* (12.48). Furthermore, *A. pohangense* has two different types of thecal pores (i.e., large and small pores), whereas *A. taylori*, *A. margalefii*, *A. hiranoi*, *A. pseudogonyaulax* have only small thecal pores. *A. pohangense* does not have posterior attachment pore (pap) on the posterior plate (sp) like *A. taylori*, *A. margalefii*, *A. hiranoi*, *A. pseudogonyaulax*, while *A. camurascutulum* has a pap on the sp. On the basis of morphological and phylogenetic criteria, we propose that *Alexandrium pohangense* is a new species of the genus *Alexandrium.*

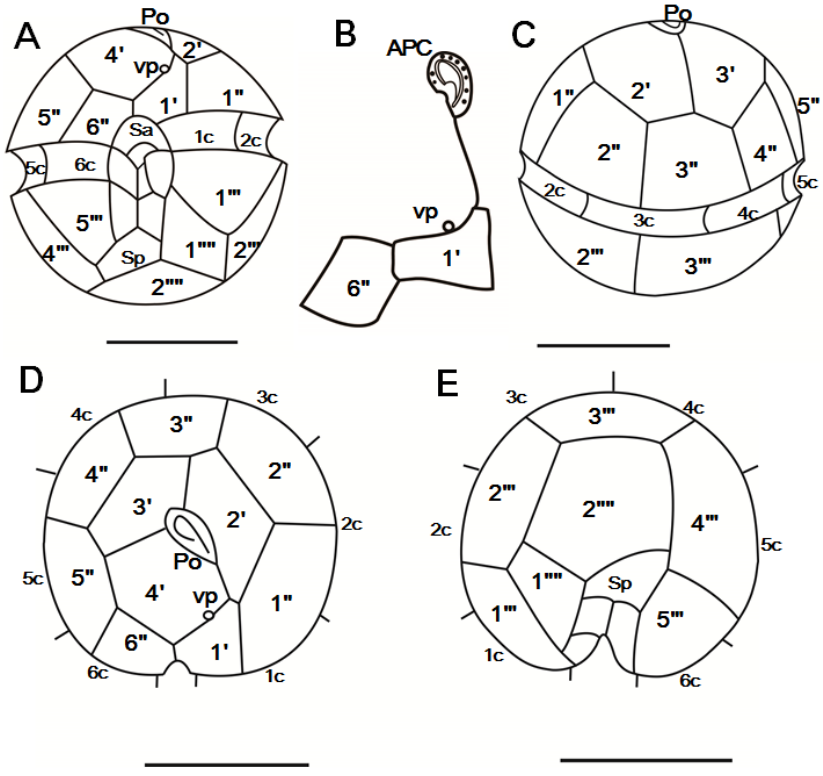

Fig. 4.9. Schematic diagram of *Alexandrium pohangense* n. sp. (A) Ventral view. (B) Relative positions of the apical pore complex (APC), first apical (1′) and sixth precingular (6′′) plates, and ventral pore (vp). (C) Dorsal view. (D) Apical view showing the epithecal plate tabulation and pattern. (E) Antapical view showing the hypothecal plate tabulation and pattern. Scale bars = 20 μm for (A, C–E), no scale bar for (B).

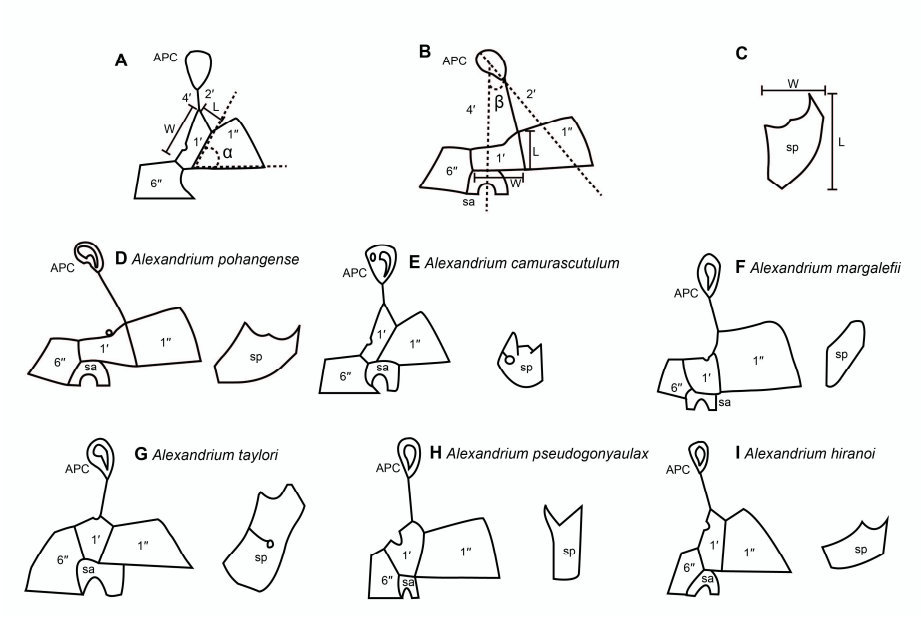

Fig. 4.10. A diagrammatic comparison in relative positions of the apical pore complex (APC), first apical (1′) and sixth precingular (6′′) plates, and anterior plate (sa) of the *Alexandrium* species morphologically similar to *Alexandrium pohangense* n. sp. (A) The angle between the cingulum and the bottom margin side of 1′ plate (α) and ratio of length (L) relative to width (W). (B) The angles between antero-posterioral axis of the cell and the point of the margin of apical pore plate (β) and ratio of L relative to W of the 1′ plate. (C) Ratio between L and W of the posterior sulcal plates (sp). (D) *A. pohangense*. (E) *A. camurascutulum.* (F) *A. margalefii.* (G) *A. taylori*. (H) *A. pseudogoniaulax*. (I) *A. hiranoi. A. margalefii* and *A. pseudogoniaulax* are redrawn from MacKenzie et al. (2004). *A. hiranoi, A. taylori,* and *A. camurascutulum* are redrawn from Kita and Fukuyo (1988), Balech (1994), and MacKenzie and Todd (2002).

Alexandrium pohangense n. sp. A. S. Lim, H. J. Jeong

Diagnosis. Phototrophic. The ranges of live cell length and width are 24-42 μm and 23-40 μm, respectively. The ratio of live cell length to width is 0.7-1.5. The comma shaped apical pore plate, surrounded by marginal pores, turns toward to left side of the epitheca and the angle between antero-posterioral axis of the cell and the point of the margin of apical pore plate is 45-58°. The number of the marginal pores on the apical pore plate is 8-17. Cells lack an anterior attachment pore in the apical pore complex. It has a wide rectangular 1′ plate whose left upper side is slightly bent and protruding and meeting the 2′ plate as a point, but being disconnected from the Po. The 1′ plate lies on the sa plate and meets the 1′′ plate as a straight vertical line. The angle etween the cingulum and the bottom margin side of 1′ plate is almost zero. It has a small ventral pore of ca. 0.7 μm on the 4′ plate. It has a relatively large regular pentagonal 2′′′′ plate whose area occupies ca. 21-34 % of total area of the hypotheca. It does not have posterior attachment pore (pap) on the posterior sulcal plate. The cell surface is smooth, but two different types of pores, single large pores of ca. 0.34 μm in diameter and 2-5 clustered small pores of ca. 0.12 μm, are widely distributed.

Etymology. The specific epithet "*pohangense*" is derived from Pohang City, Korea, which encloses Youngil Bay, from which this dinoflagellate was isolated.

Deposition of type material. A hapantotype slide as USNM slide 222987 of cells fixed with 2% paraformaldehyde has been deposited in the Protist Type Specimen Slide Collection, US Natural History Museum, Smithsonian Institution, Washington, DC, USA.

Gene sequence. The rDNA gene sequence – GenBank Accession No. LN811348

Chapter 5. Grazing impacts by *Alexandrium pohangense* n. sp. on *Cochlodinium polykrikoides*

5.1. Introduction

In the last two decades, many phototrophic dinoflagellates have been revealed to be mixotrophic (Bockstahler and Coats, 1993; Jacobson and Anderson, 1996; Stoecker, 1999; Li et al., 2000; Skovgaard et al., 2000; Jeong et al., 2010a, 2012; Park et al., 2006; Berge et al., 2008; Burkholder et al., 2008). They are able to feed on diverse prey items such as bacteria, algae, heterotrophic protists, and metazoans (e.g., Jeong et al., 2010a). Moreover, these mixotrophic dinoflagellates play diverse roles in food webs and the cycling of materials (Jeong et al., 1999a, 2010a; Glibert et al., 2009; Hansen, 2011; Sanders, 2011; Seong and Jeong, 2011). Mixotrophic ability of the dinoflagellate is also considered as an important factor to form a harmful algal bloom (e.g., Jeong et al., 2010a). Furthermore, some mixotrophic dinoflagellates have a greater growth rate when they feed on the prey compared to phototrophic mode (Lee et al., 2014a). Thus, the mixotrophic grazing effects on a certain population dynamics should be considered to better understand the population dynamics.

Alexandrium species are known to form a harmful algal bloom and cause massive fish death and even human illness

(Hallegraeff, 1993; Cembella et al., 2002; Anderson et al., 2012). Some *Alexandrium* species produce toxins such as saxitoxins, goniodomins, spirolides (Anderson et al., 2012). Moreover, some unknown lytic compounds produced by *Alexandrium* species are possibly involved the mixotrophy of some *Alexandrium* species (Blossom et al., 2012). Gribble et al. (2005) reported that most *A. ostenfeldii* cells found in the field contained food vacuole. However, among ~30 *Alexandrium* species, only 5 species, *Alexandrium minutum*, *Alexandrium tamarense*, *Alexandrium catenella*, *Alexandrium ostenfeldii*, and *Alexandrium pseudogonyaulax*, have up to now been revealed mixotrophic (Nygaard and Tobiesen, 1993; Jacobson and Anderson, 1996; Jeong et al., 2005a, b; Yoo et al., 2009; Blossom et al., 2012). Therefore, to understand ecological roles and bloom dynamics of the new species, it is worthwhile to investigate the mixotrophic ability of *Alexandrium* species.

Recently, I newly described *Alexandrium pohangense* which is able to feed on *Cochlodinium polykrikoides* from waters off Pohang, Korea. In the present study using the established monoclonal cultures, I investigated the ability of *A. pohangense* to feed on heterotrophic and autotrophic bacteria and a diverse algal species, and used high-resolution video microscopy to observe their feeding behavior and determine the mechanism of prey ingestion. To compare the feeding ability of *A. pohangense* and other *Alexandrium* species, I compared the type of prey that *A. pohangense* and other *Alexandrium* species were able to feed on. I also measured the growth and

ingestion rates for *A. pohangense* feeding on *Cochlodinium polykrikoides* as a function of prey concentration and compared them with other predators of *C. polykrikoides*. The results of the present study provide a basis for understanding the interactions between *A. pohangense* and their prey species and their feeding mechanism and ecological roles in marine food webs.

5.2. Material and methods

5.2.1. Preparation of experimental organisms

Phytoplankton species were grown at 20 °C in enriched f/2 seawater media (Guillard and Ryther, 1962) under a continuous illumination of 100 μE m^{-2} s^{-1} provided by cool white fluorescent lights (Table 5.1). The mean equivalent spherical diameter (ESD) was measured using an electronic particle counter (Coulter Multisizer II, Coulter Corporation, Miami, Florida, USA). The carbon content of phytoplankton was estimated from the cell volume according to Strathmann (1967).

5.2.2. Prey species

Experiment 1 was designed to investigate whether or not *Alexandrium pohangense* was able to feed on potential prey when unialgal diet of diverse microalgal species was provided (Table 5.1). The initial concentrations of each algal species provided were similar in terms of carbon biomass.

A dense culture of *A. pohangense* growing photosynthetically in f/2 media at 20 °C and under a 14:10 h light-dark cycle at 100 μE m^{-2} s^{-1} was transferred to one 2-L PC bottle containing F/2 medium. The culture was maintained in F/2 media for 2 d under the same conditions described above. Three 1-ml aliquots were then removed from the bottle and *A. pohangense* densities were determined using a compound light microscope.

For observing the ingestion of eukaryotic algal prey under a light microscope microscope, the initial concentrations of *A. pohangense* and each target algal species were established as described above (Table 5.1). Triplicate 42-ml PC experimental bottles and triplicate predator control bottles were set up for each target algal species. The bottles were filled to capacity with freshly filtered seawater, capped, and then placed on a shelf and incubated at 20 °C under a 14:10 h light-dark cycle of cool white fluorescent light at 100 μE $m^{-2}s^{-1}$. After 6, 12, 24, and 48 h of incubation, a 5-ml aliquot was removed from each bottle and transferred to a 20-ml bottle. Two 0.1-ml aliquots were placed on slides with cover-glasses. The protoplasms of > 200 *A. pohangense* cells were carefully examined using a light microscope microscope at a magnification of ×100 - 400 to determine whether *A. pohangense* was able to feed on the target algal prey species. *A. pohangense* cells containing the ingested cells of each target algal species were photographed using digital cameras on these microscopes at a magnification of ×400 - 1,000. To test whether the filtrates of *A. pohangense* culture affect the behavior of prey species, the initial concentration of *A. pohangense* culture was filtrated through 5 μm pore (Millipore co.) and added to target algal species. The protoplasms of >200 *A. pohangense* cells were also examined in the same manners.

5.2.3. Feeding mechanism

Expt 2 was designed to investigate the feeding mechanisms of *A. pohangense* when provided a unialgal diet of the dinoflagellates *Cochlodinium polykrikoides*. The initial concentrations of the predator and prey were the same as in Expt 1.

The initial concentrations of *A. pohangense* and the target algal species were established using an autopipette to deliver a predetermined volume of culture with a known cell density to the experimental bottles. One 42-ml PC bottle (mixtures of *A. pohangense* and algal prey) was set up for each target algal species. The bottle was filled to capacity with freshly filtered seawater, capped, and then mixed well. After 6, 24, and 48 h of incubation on the shelf, a 1-ml aliquot was removed from the bottle and then 200 μl were transferred onto a slide with a cover-glass. For each target prey species, the feeding behavior of > 60 *A. pohangense* cells was monitored using a light microscope and/or an epifluorescence microscope at a magnification of ×100 - 630. All of the feeding processes were observed, from the time a prey cell was captured to the time that it was engulfed by the predator. A series of photographs showing the process for a *A. pohangense* cell feeding on *C. polykrikoides* were taken using a video analyzing system (Sony DXC-C33; Sony Co., Tokyo, Japan) mounted on a light microscope at a magnification of ×100 - 630.

5.2.4. Effect of prey concentration

Expt 3 was designed to investigate the ingestion rates of *Alexandrium pohangense* on the mixotrophic dinoflagellate *C. polykrikoides* as a function of prey concentration. A dense culture of *A. pohangense* maintained in an f/2 medium and growing photosynthetically was transferred to a 1-l PC bottle. Three 1-ml aliquots from the bottle were examined using a compound microscope to determine the cell concentrations of *A. pohangense*. Triplicate 42-ml PC experimental bottles (containing mixtures of predators and prey), triplicated prey control bottles (containing prey only), and triplicate predator control bottles (containing predators only) were established. To ensure similar water conditions, we filtered the water of a predator culture through a 0.7-μm GF/F filter, and then added this to the prey control bottles in the same amount as the volume of the predator culture added into the experimental bottles for each predator-prey combination. We added 5 ml of f/2 medium to all of the bottles, which were then filled to capacity with freshly filtered seawater and capped. To determine the actual predator and algal prey concentrations at the start of the experiment and after 2 d, a 5-ml aliquot was removed from each bottle and fixed with 5% Lugol's solution; all or >200 predator and prey cells in triplicate 1-ml Sedgwick-Rafter chambers were then enumerated. The bottles were refilled to capacity with filtered seawater, capped, and placed on the shelf because *C. polykrikoides* has negative growth on the rotating wheel.

The dilution of the cultures associated with refilling the bottles was considered when calculating the growth and ingestion rates.

The specific growth rate of *A. pohangense* was calculated as follows:

$$\mu = \frac{\ln (C_t / C_0)}{t} \quad (1)$$

where C_0 is the initial concentration of *A. pohangense* and C_t is the final concentration after time t. The time period was 2 d. I calculated the mean prey concentrations by using the equation of Frost (1972). I calculated the ingestion and clearance rates by using the equations of Frost (1972) and Heinbokel (1978).

Data for *A. pohangense* growth rate were fitted to the following equation:

$$\mu = \frac{\mu_{max} (x - x')}{K_{GR} + (x - x')} \quad (2)$$

where m_{max} = the maximum growth rate (d^{-1}), x = prey concentration(cells ml^{-1} or ng C ml^{-1}), x′ = threshold prey concentration (i.e. the prey concentration where $\mu = 0$), and K_{GR} = the prey concentration sustaining 1/2 m_{max}. Data were iteratively fitted to the model by using DeltaGraph® (SPSS Inc., Chicago, IL, USA).

Ingestion rate data were fitted to a Michaelis-Menten equation:

$$IR = \frac{I_{max}(x)}{K_{IR} + (x)} \quad (3)$$

where I_{max} = the maximum ingestion rate (cells predator^{-1} d^{-1} or ng C predator^{-1} d^{-1}), x = prey concentration (cells ml^{-1} or ng C ml^{-1}), and K_{IR} = the prey concentration sustaining 1/2 $I_{max.}$

5.2.5. Grazing impact of *Alexandrium pohangense* on *Cochlodinium polykrikoides*

By combining field data on the concentration of the *Alexandrium* spp. and *Cochlodinium polykrikodies* with the ingestion rates of the *A. pohangense* on *C. polykrikodies* obtained in the present study, I estimated the grazing coefficients attributable to *A. pohangense* and the co-occurring *C. polykrikoides*. Data on the abundances of *Alexandrium* spp. and the co-occurring *C. polykrikoides* used in this estimate were obtained by counting the water samples taken from the waters off Pohang, Korea when *C. polykrikoides* red tide patches were observed in 2014. The morphological features of *A. pohangense* under the light microscope were hard to distinguish from another *Alexandrium* species, the abundance of *Alexandrium* spp. was used for the calculation.

The grazing coefficients (g, d^{-1}) were calculated as:

$$g = CR \times PC \times 24 \quad (4)$$

where CR (ml predator^{-1} h^{-1}) is the clearance rate of *A. pohangense* on a *C. polykrikoides* at a prey concentration and PC is a *Alexandrium* spp. concentration (cells ml^{-1}). The CR values were calculated as:

$$CR = IR/ x \quad (5)$$

where IR (cells eaten predator^{-1} h^{-1}) is the ingestion rate of *A. pohangense* on *C. polykrikoides* and x (cells ml^{-1}) is the *C. polykrikoides* concentration. Since the laboratory experiments were performed at 20 °C, theses CR values were corrected using Q_{10} = 2.8 (Hansen et al., 1997).

5.3. Results

5.3.1. The kind of prey and feeding mechanism

Among the algal prey offered, *Alexandrium pohangense* fed only on *Cochlodinium polykrikoides* (Table 5.1). However, *A. pohangense* did not feed on *Gymnodinium aureolum* or *Scrippsiella trochoidea*, whose mean equivalent spherical diameters were similar to *C. polykrikoides*. In addition, cryptophyte *Teleaulax* sp., *Rhodomonas salina*, *Storeatula major*, and a naked ciliate *Mesodinium rubrum* were lysed within 30 min after 300 cell ml^{-1} of *A. pohangense* cells were mixed into the prey cells (Fig. 5.1).

Chain formed *C. polykrikodies* cells were split into single or two cells when *A. pohangense* cells were incubated together and immobilized (Fig. 5.2). *A. pohangense* cells approached the immobilized *C. polykrikoides* cells and engulfed them through the sulcus. The time (mean ± standard error, n = 6) for a prey cell to be completely fed on by *A. pohangense* cell after *A. pohangense* started sucking the prey cell through the sulcus was 118 ± 17 s (Fig. 5.2).

Table 5.1. Taxa, size, and concentration of prey species offered to *Alexandrium pohangense.* Mean equivalent spherical diameter (ESD, μm). Y: Feeding by *A. pohangense*, L: the prey cells were lysed by *A. pohangense*, N: not ingested by *A. pohangense*, I: the prey cells were immobilized by *A. pohangense.*

Prey species	ESD (μm)	Initial prey concentration (cell ml^{-1})	Feeding (effect)
Diatom			
Skeletonema costatum	5.9	150,000	N
Prymnesiophytes			
Isochrysis galbana	4.8	150,000	N (I)
Cryptophytes			
Teleaulax sp.	5.6	100,000	N (L)
Storeatula major	6.0	50,000	N (L)
Rhodomonas salina	8.8	50,000	N (L)
Rhaphidophytes			
Heterosigma akashiwo	11.5	30,000	N (I)
Mixotrophic dinoflagellates			
Heterocapsa rotundata	5.8	100,000	N (I)
Amphidinium carterae	9.7	30,000	N (I)
Prorocentrum minimum	12.1	20,000	N (I)
Hetereocapsa triquetra	15.0	30,000	N (I)
Gymnodinium aureolum	19.5	3,000	N (I)
Scrippsiella trochoidea	22.8	15,000	N (I)
Cochlodinium polykrikoides	25.9	2,000	Y (I)
Prorocentrum micans	26.6	3,000	N (I)
Akashiwo sanguinea	30.8	1,000	N (I)
Gymnodinium catenatum	33.9	3,000	N (I)
Naked ciliate			
Mesodinium rubrum	22	2,000	N (L)

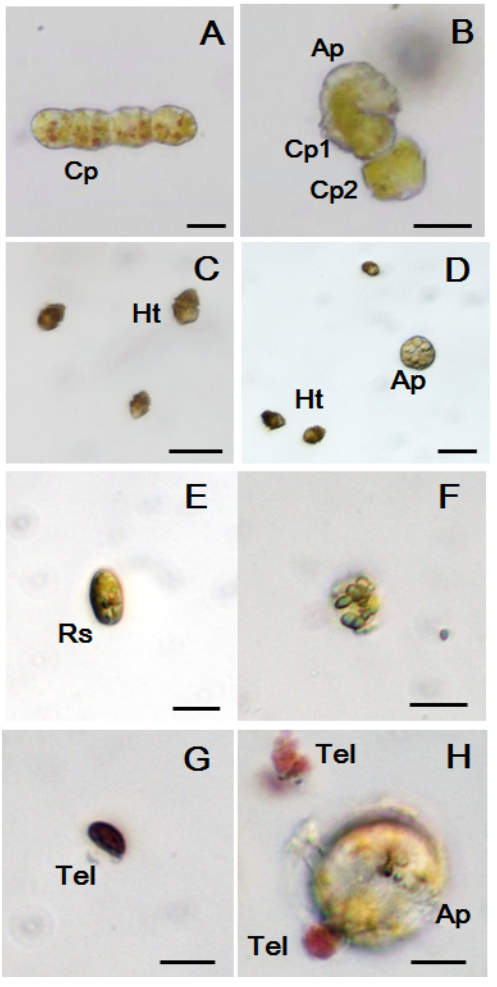

Fig. 5.1. *Alexandrium pohangense* (Ap) has different effects on the dinoflagellate *Cochlodinium polykrikoides* cells (Cp; A, B), *Heterocapsa triquetra* (Ht; C, D) and cryptophytes, *Rhodomonas salina* (Rs; E, F) and *Teleaulax* sp. (Tel; G, H). Ap divides chain-formed Cp cells into two cells of the chain, while Ht moves normally. Normal Rs and Tel cells (E, G) are lysed when they were incubated with Ap cells. Scale bars = 20 μm for (A-D) and 10 μm for (E-H).

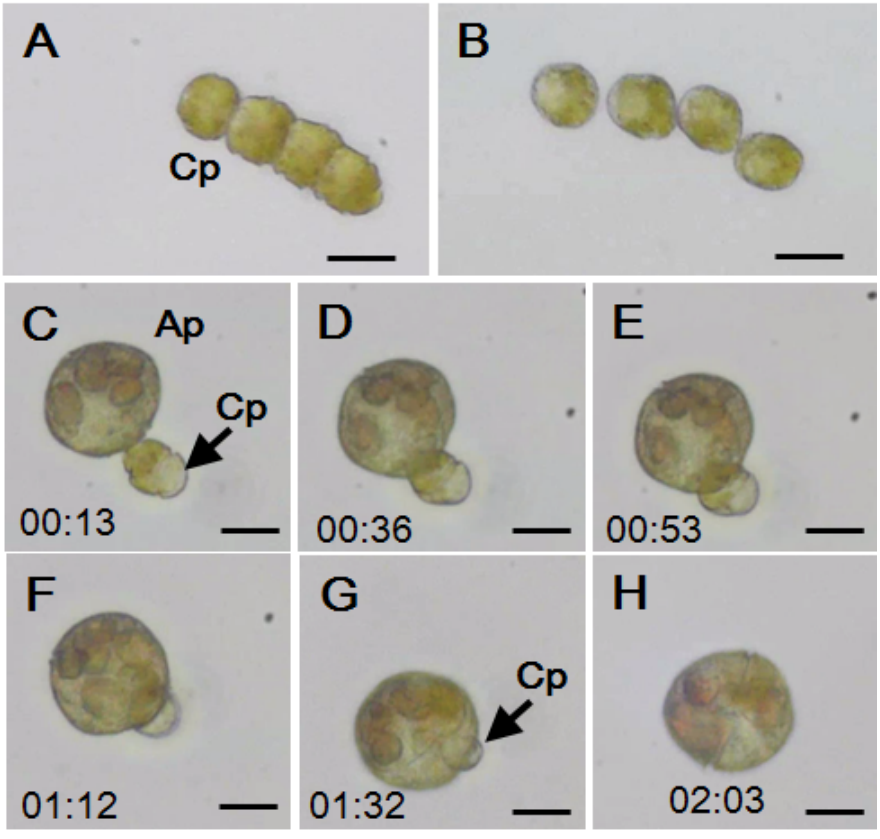

Fig. 5.2. Feeding process of *Alexandrium pohangense* (Ap) on *Cochlodinium polykrikoides* (Cp). When *A. pohangense* culture was added into *C. polykrikoides* culture, the chain formed *C. polykrikoides* cells (A) was splitted into one or two cells (B). *A. pohangense* contacts a *C. polykrikoides* (Cp) cell (C) and engulfs through the sulcus (D-G). Leaving *A. pohangense* cell after engulfing the whole Cp cell (H). Scale bars = 10 μm.

5.3.2. Growth and ingestion rates of *A. pohangense* on *C. polykrikoides*

A. pohangense grew well on *C. polykrikoides*. With increasing mean prey concentration, the specific growth rates of *A. pohangense* increased rapidly before saturating at a *C. polykrikoides* concentration of 138 ng C ml^{-1} (197 cells ml^{-1}) (Fig. 5.3A). When the data were fitted to Eq. (2), the maximum specific growth rate of *A. pohangense* on *C. polykrikoides* at 20 °C under a 14:10 h light-dark cycle of 100 μE m^{-2} s^{-1} was 0.487 d^{-1}. However, the autotrophic growth rate of *A. pohangense* at the same with mixotrophic condition was 0.091 d^{-1}. The K_{GR} (i.e. the prey concentration sustaining 1/2 μ_{max}) was 11.3 ng C ml^{-1} (16 cells ml^{-1}).

With increasing mean prey concentration, the ingestion rates of *A. pohangense* increased rapidly at a *C. polykrikoides* concentration of 99 ng C ml^{-1} (141 cells ml^{-1}), but slowly at the higher prey concentrations (Fig. 5-3B). When the data were fitted to Eq. (3), the maximum ingestion rate of *A. pohangense* on *C. polykrikoides* was 4.99 ng C $predator^{-1}$ d^{-1} (7.1 cells $predator^{-1}$ d^{-1}) and K_{IR} (the prey concentration sustaining 1/2 I_{max}) was 30.0 ng C $predator^{-1}$ d^{-1} (42.8 cells $predator^{-1}$ d^{-1}). The maximum clearance rate of *A. pohnagense* on *C. polykrikoides* was 3.23 μl $predator^{-1}$ h^{-1}.

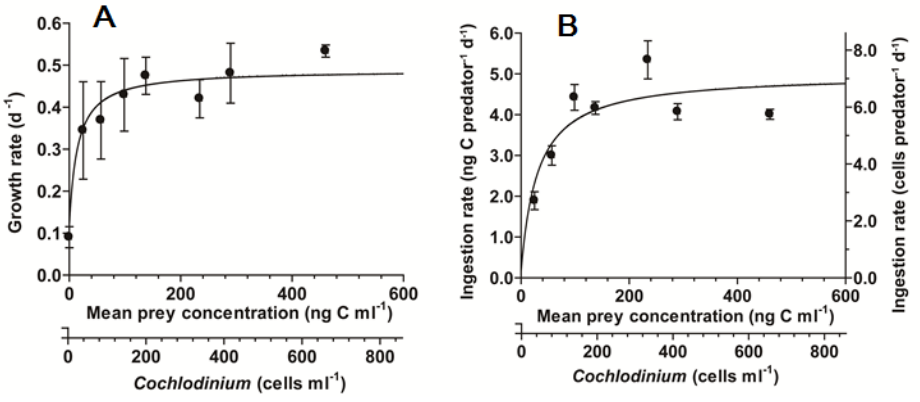

Fig. 5.3. Specific growth rates (A) and ingestion rates (B) of *Alexandrium pohangense* on *Cochlodinium polykrikoides* as a function of the mean prey concentration (x, ng C ml^{-1}). Symbols represent treatment means ± 1SE. The curve was fitted by a Michaelis-Menten equation [Eq.(2) for A, Eq. (3) for B] using all treatments in the experiment. Growth rate (GR, d^{-1}) = 0.487 [(x+2.6792) / (11.34 + (x-2.679))], r^2 = 0.564 and ingestion rate (IR, ng C predator^{-1} d^{-1}) = 4.99 [x / (30.0+x)], r^2=0.665

5.3.3. Grazing impact of *A. pohangense* on *C. polykrikoides*

The grazing coefficients attributable to *A. pohangense* on co-occurring *C. polykrikoides* in the water samples taken in the waters inside Yongil Bay, Pohang city, Korea in 2014, when the abundances of *A. pohangense* and *C. polykrikoides* were 1 - 13 cells ml^{-1} and 3 - 259 cells ml^{-1}, respectively, were 0.089 - 1.567 d^{-1} (Fig. 5.4).

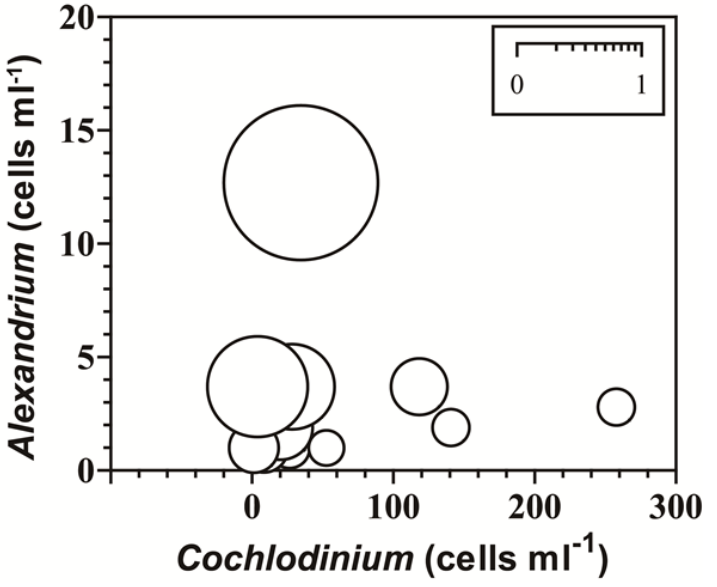

Fig. 5.4. Calculated grazing coefficients (g, d^{-1}) attributable to *Alexandrium pohangense* on natural populations of *Cochlodinium polykrikoides* (see text for calculation). n= 13.

5.4. Discussion

5.4.1. Prey species and feeding mechanism

Alexandrium pohangense fed only on *Cochlodinium polykrikoides* among offered as prey. Other dinoflagellate prey species, prymnesiophyte *Isochrysis galbana*, and raphidophyte *Heterosigma akashiwo* were immobilized by *A. pohangense*, but not ingested. Some studies suggested that predator and prey have specific recognition relationships such as chemosensory mechanism (Hansen and Calado, 1999; Wootton et al., 2007; Roberts et al., 2011; Sieg et al., 2011). Other *Alexandrium* species such as *A. minutum*, *A. tamarense*, *A. catenella*, *A. ostenfeldii*, and *A. pseudogonyaulax* are able to feed on some cryptophyte, dinoflagellate, ciliate and even diatom (Table 5.2, Nygaard and Tobiensen, 1993; Jacobson and Anderson, 1996; Jeong et al., 2005a, b; Yoo et al., 2009; Blossom et al., 2012). For example, while *A. tamarense* is able to feed on various prey including *Amphidinium carterae*, *Prorocentrum minimum*, and *Heterosigma akashiwo*, *A. pohangense* is able to feed only on *C. polykrikoides*. Thus, it is possible that *A. pohangense* has a specific relationship with *C. polykrikoides*. It is worthwhile to explore the recognition process between *A. pohangense* and *C. polykrikoides*.

The mixotrophic dinoflagellate *A. pohangense* fed on the prey cells by engulfing through the sulcus like other *Alexandrium* species. A tow filament to anchor the prey cell was not observed during the feeding process. However, *A. pohangense* cells immobilize *C. polykrikoides* cells and split into 1 or 2 cells. *A. pohangense* cells

approach the immobilized *C. polykrikoides* cells and engulf them through the sulcus. Moreover, filtrates from *A. pohangense* culture also immobilize or lyse the prey cells. Thus, it is possible that the *A. pohangense* immobilize and/or lyse the target prey cells by toxic substrates. It also suggests that toxic substrates secreted by *A. pohangense* may allow *A. pohangense* to feed on *C. polykrikodies* without a tow filament and/or trichocyst, even though *C. polykrikodies* is one of the fastest swimming dinoflagellates (~1,400 μm s^{-1}, Jeong et al., 1999a). Some *Alexandrium* speceis are known to lyse other protists using lytic compounds. The immobilization effects by substrates of harmful dinoflagellates may be species dependent and not dependent on paralytic shellfish poisoning toxic compound (Tillmann and John, 2002; Adolf et al., 2006). Moreover, putative *sxtA* gene for saxitoxins is not amplified from genomic DNA of *A. pohangense* and *A. pohangense* is not toxic to brain shrimp *Artemia salina* (Lim et al., 2015a). Thus, it is possible that the lytic substrates of *A. pohangense* are not exact toxins like saxitoxins. Ma et al. (2011) reported that lytic compounds of *A. tamarense* showed high affinity towards brassicasterol and thus suggested that lytic compounds may involve sterol components of cell membranes. Interestingly, *Rhodomonas salina* and *Storeatula major* which were lysed by *A. pohangense* have a brassicasterol as a major sterol (> 90 % of cell) (Adolf et al., 2006; Ma et al., 2011). It is worthwhile to analysis the sterol compounds of *A. pohangense* and prey species and explore the relationship between them and immobilizing and/or lytic activity.

Table 5.2. Comparison of the prey species of 6 *Alexandrium* species whose mixotrophic abilities have been reported. ESD, equivalent spherical diameter (μm). Ap: *A. pohangense,* Am: *A. minutum*, At: *A. tamarense*, Ac: *A. catenella*, Ao: *A. ostenfeldii,* Aps: *A. pseudogonyaulax.* Y: feeding on the prey species, N: not able to feed on the species.

Prey species	ESD	Ap	Am	At	Ac	Ao	Aps
Diatom							
Skeletonema costatum	5.9	N		Y	Y		
Prymnesiophytes							
Isochrysis galbana	4.8	N		Y			
Cryptophytes							
Teleaulax acuta			N		N		Y
Teleaulax sp.	5.6	N		Y			
Storeatula major	6.0	N					
Rhodomonas salina	8.8	N		Y			
Rhaphidophytes							
Heterosigma akashiwo	11.5	N		Y			
Mixotrophic dinoflagellates							
Heterocapsa rotundata	5.8	N	N		N		Y
Amphidinium carterae	9.7	N		Y			
Prorocentrum minimum	12.1	N		Y			
Hetereocapsa triquetra	15.0	N		N			Y
Gymnodinium aureolum	19.5	N		N			
Scrippsiella trochoidea	22.8	N					N
Cochlodinium polykrikoides	25.9	Y		N			
Prorocentrum micans	26.6	N		N			
Gymnodinium catenatum	33.9	N		N			
Dinophysis sp.						Y	
Naked ciliate							
Mesodinium rubrum	22.0	N					Y
Unidentified ciliate						Y	
Reference		(1)	(4)	(3, 4)	(3, 4)	(5)	(4)

(1) this study, (2) Jeong et al. (2005a), (3) Yoo et al. (2009), (4) Blossom et al. (2012), (5) Jacobson and Anderson (1996)

5.4.2. Contribution of mixotrophy to *Alexandrium pohangense*

The maximum growth rate (i.e., mixotrophic growth) of *Alexandrium pohangense* on the optimal prey obtained under a 14:10 h light-dark cycle of 100 μE $m^{-2}s^{-1}$ (4.9 d^{-1}) is higher than other *Alexandrium* species so far (Table 5.3). Under the similar light condition, the growth rates of *A. pseudogonyaulax* on *Heterocapsa rotundata* and *Teleaulax acuta* are 0.32 and 0.28, respectively (Blossom et al., 2012). *A. pohangense* and *A. pseudogonyaulax* do not share the prey item. Thus, they may have different biological niche. Furthermore, the ratio of mixotrophic to autotrophic growth rate of *A. pohangense* (4.9) is the greatest among the other engulfment feeding mixotrophic dinoflagellate (0.8 – 3.7), except for *Karlodinium armiger* (10.8) (Table 5.3). The mixotrophic growth rate of *A. pohangense* (0.49) is almost five times greater than its autotrophic growth rate (0.10). Thus, prey consumption of *A. pohangense* considerably contributes to the growth of *A. pohangense* when the prey is abundant in the natural environments. It is also possible that production of toxic metabolites of *A. pohangense* may be the reason for the low phototrophic growth rate. Producing toxin probably require high energy cost and thus toxin producing dinoflagellates may have lower growth rates than other group of phytoplankton such as diatom (Lim et al., 2014a). Therefore, it is worthwhile to explore production of toxic metabolites of *A. pohangense*.

Table 5.3. Optimal prey, maximum mixotrophic growth rate (MMGR), and autotrophic growth rate (AGR) of each mixotrophic engulfment feeding dinoflagellate predator species.

Predator	ESD	Optimal prey	ESD	T	LI	MMGR	AGR	RMAG	Ref.
Alexandrium pohangense	32.0	*Cochlodinium polykrikoides*	25.8	20	100	0.49	0.10	4.9	(1)
Ansanella granifera	10.5	*Pyramimonas* sp.	5.6	20	20	1.43	0.39	3.7	(2)
Prorocentrum donghaiense	13.2	*Teleaulax* sp.	5.6	20	20	0.51	0.38	1.4	(3)
Heterocapsa triquetra	15.0	*Teleaulax* sp.	5.6	20	20	0.28	0.18	1.5	(3)
Alexandrium minutum	16.7	*Teleaulax acuta*		15	17	0.11	0.13	0.8	(4)
Karlodinium armiger[a]	16.7	*Rhodomonas baltica*	10.7	15	180	0.65	0.06	10.8	(5)
Cochlodinium polykrikoides	25.8	*Teleaulax* sp.	5.6	20	50	0.32	0.17	2.0	(6)
Prorocentrum micans	26.6	*Teleaulax* sp.	5.6	20	20	0.20	0.11	1.9	(3)
Amylax triacantha	30.0	*Mesodinium rubrum*	22.0	15	20	0.68	-0.08		(7)
Gonyaulax polygramma	32.5	*Teleaulax* sp.	5.6	20	50	0.28	0.19	1.5	(8)
Alexandrium pseudogonyaulax	35.4	*Heterocapsa rotundata*	5.8	15	120	0.32	0.22	1.5	(4)
Lingulodinium polyedrum	36.6	*Scrippsiella trochoidea*	25.1	20	50	0.30	0.18	1.7	(3)
Fragilidium subglobosum	45.0	*Ceratium tripos*	59.5	15	45	0.50	0.16	3.1	(9, 10)
Fragilidium cf. *mexicanum*	54.5	*Lingulodinium polyedrum*	37.9	22	20	0.36	-0.05		(10, 11)

(1) this study, (2) Lee et al. (2014b), (3) Jeong et al. (2005a), (4) Blossom et al. (2012), (5) Berge et al. (2008), (6) Jeong et al. (2004b), (7) Park et al. (2013b), (8) Jeong et al. (2005c), (9) Hansen and Nielsen (1997), (10) Jeong et al., (2010a), (11) Jeong et al. (1999a)

5.4.3. Implications for *Cochlodinium polykrikoides* red tides

Cochlodinium polykrikoides is a bloom forming dinoflagellate in the coastal waters of many countries and causes massive fish mortality and economic loss in many countries (Gobler et al., 2008; Mulholland et al., 2009; Park et al., 2013a; Lim et al., 2014a, 2015b). Moreover, some studies suggested that populations of grazers may have considerable grazing impact on populations of bloom forming species (Jeong et al., 2004a, 2005d; Yoo et al., 2013). Thus, the predators of *C. polykrikoides* may be important factors to understand the population dynamics of *C. polykrikoides*. The grazing coefficients (g) attributable to *Alexandrium pohangense* on co-occurring *C. polykrikoides* obtained in the present study were up to 1.567 d^{-1} (i.e., up to 79 % of the *C. polykrikoides* populations were removed by a *A. pohangense* population in a day). Since *A. pohangense* has a lytic activity to some algal species, its ingestion rate (~7 cells $predator^{-1}$ d^{-1}) and grazing coefficients could be overestimated. However, they are still considerably high enough to effect on the population of *C. polykrikoides*. Therefore, *A. pohangense* may have a considerable grazing impact on populations of co-occurring *C. polykrikodies* to control when *C. polykrikodies* formed a bloom.

Alexandrium pohangense is a first reported mixotrophic dinoflagellate grazer on *C. polykrikoides*. Prior to this study, only several heterotrophic protists and ciliate are known to feed on *C. polykrikoides* (Table 5.4, Jeong et al., 1999b, 2006, 2007, 2008; Cho, 2006; Lim et al., 2014b). The maximum growth and ingestion rates of *A. pohangense* are greater than those of heterotrophic dinoflagellate *Pfiesteria piscicida*, but lower than ciliate *Strombidinopsis* spp.

Moreover, the maximum growth and ingestion rates of *Luciella masanensis* and *Stoeckeria changwonensis* are not considerable. Thus, it is possible that *A. pohangense* plays an important role as a predator when *C. polykrikoides* forms a bloom but there are no co-occurring *Strombidinopsis* species.

Table 5.4. Predators of *Cochlodinium polykrikoides* and comparisons of the maximum growth rates (MRG, d^{-1}) and maximum ingestion rates (MIR, ng C $predator^{-1}$ d^{-1}) of the predators. MTD: mixotrophic dinoflagellate, HTD: heterotrophic dinoflagellate, CIL: ciliate, NA: not available.

Predator	Trophic mode	MRG	MIR	Reference
Alexandrium pohangense	MTD	0.49	4.99	This study
Pfiesteria piscicida	HTD	0.16	0.03	Jeong et al., 2006
Luciella masanensis	HTD	NA	NA	Jeong et al., 2007
Stoeckeria changwonensis	HTD	NA	NA	Lim et al., 2014b
Protoperidinium sp.	HTD	NA	NA	Cho, 2006
Strombidinopsis jeokjo	CIL	1.782	127	Jeong et al., 2008
Strombidinopsis sp.	CIL	1.378	353	Jeong et al., 1999b

Chapter 6. Overall conclusion

In this thesis, I found that tropical cyclones (typhoons in Northwest Pacific), co-occurring diatoms, and a new dinoflagellate *Alexandrium pohangense* n. sp. clearly affect on the abundance of *Cochlodinium polykrikoides* (Fig. 6.1). However, the degrees of the impact are dependent on daily maximum wind speed generated by tropical cyclones, abundance of diatoms, and abundance of *A. pohangense*. Therefore, in models of predicting the outbreak, persistence, and decline of *C. polykrikoides*, these new critical factors should be taken into consideration.

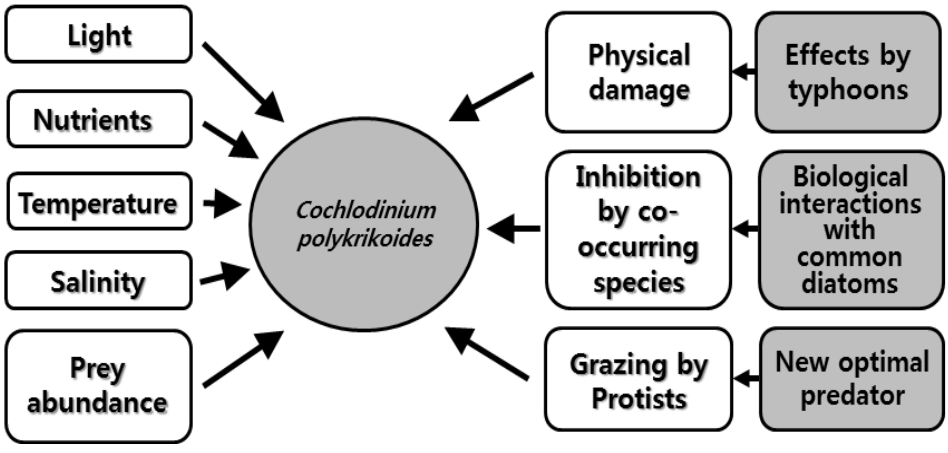

Fig. 6.1. Various factors affecting the dynamics of *Cochlodinium polykrikodes* red tides. The grey boxes indicate the factors explored by present study.

The tropical cyclones differentially affected *Cochlodinium polykrikodes* red tides in 2012–2014. The daily maximum wind speed generated by tropical cyclones was critical. Prior to my study, there were several studies on the effects of tropical cyclones on the *C. polykrikoides* red tides. However, they have not investigated relationships between the daily maximum wind speed and the daily maximum cell abundance. For example, *C. polykrikodes* red tides disappeared when the daily maximum wind speed driven by tropical cyclone was more than 14 m s^{-1}, but the abundance of *C. polykrikoides* is lowered when the daily maximum wind speed was 5–14 m s^{-1}. In general, the strong wind speed driven by tropical cyclones generates turbulence in the water column and such turbulence causing physical damage on the organism may directly reduce the abundance of *C. polykrikodes*.

The cell abundance of *C. polykrikoides* in its red tide patches advected into aquaculture cages are one of the critical factors affecting survival of fish in cages; if the abundance of *C. polykrikoides* in the aquaculture cages is < 1,000 cells ml^{-1}, fish mortality and in tern economic loss is likely to be greatly reduced. Thus, strong winds generated by tropical cyclones may contribute in preventing fish in aquaculture cages from being killed due to *C. polykrikoides* red tide patches. Approximately 28 million fish from aquaculture in the South Sea of Korea were reported to be killed in the *Cochlodinium* red tide period in 2013 when only two tropical cyclones passed the aquaculture areas, causing a loss of USD $ 24 billion, while only 5 million fish from aquaculture in Korea were killed in 2012 when five tropical cyclones passed the aquaculture areas (NFRDI, 2014; Park et al., 2013a), causing a loss of USD $ 4

billion. The results of the study on tropical cyclones effects could be applied to *Cochlodinium* red tides in the coastal waters of the other countries such as Japan, China, Philippines, Taiwan, the Middle East, the west coasts of North and Mid America, the eastern coast of the USA, and the western coasts of India and Australia, which experience both *Cochlodinium* red tides and tropical cyclones (equivalent to typhoons, hurricanes, and willy-willies) (Fig. 6.2). In these areas, *Cochlodinium* red tide has caused massive fish death and economic loss (Fudge, 1977; Hallegraeff, 1992; Whyte et al., 2001; Fukuyo et al., 2002; Yan et al., 2002; Gárate-Lizárraga et al., 2004; Lara et al., 2004; Vershinin et al., 2005; Imai et al., 2006; Vargas-Montero et al., 2006; Anton et al., 2008; Azanza et al., 2008; Curtiss et al., 2008; Gómez-Villarreal et al., 2008; Tomas and Smayda, 2008; Verity, 2010; Philps et al., 2011; D'Silva et al., 2012; Ke et al., 2012; Kudela and Goble, 2012; Munir et al., 2012; Hamzehei et al., 2013; Park et al., 2013a; Maciel-Baltazar et al., 2013). Therefore, there is a high possibility that tropical cyclones in these waters (called as typhoons, hurricanes, tropical cyclones, or willy-willies) affect the outbreak, persistence, and decline of *Cochlodinium* red tides and thus it is worthwhile to explore this topics in these waters.

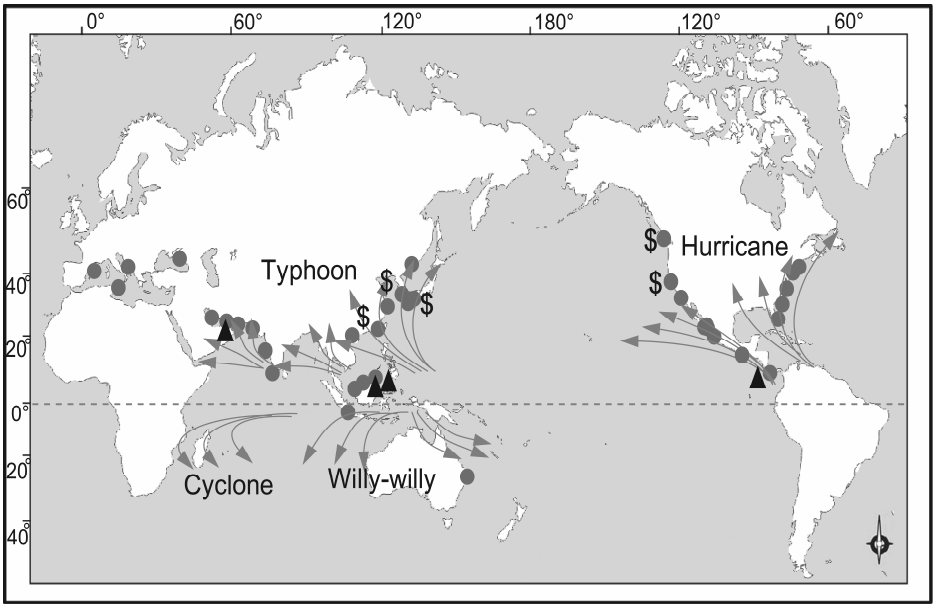

Fig. 6.2. Global distribution map of *Cochlodinium* red tides. Arrows indicate the general paths of tropical cyclones. Circles indicate the occurrence of *Cochlodinium* red tides. Dollar marks indicate the regions where economic loss occurred and solid triangles indicate massive fish death caused by the red tides.

The results of this study clearly show that fast-growing diatoms cause negative effects on *C. polykrikoides* with both physical contact and chemical stress; high abundance of *Skeletonema costatum*, *Chaetoceros danicus*, and *Thalassiosira decipiens* can reduce swimming speed of *C. polykrikoides*, which may inhibit vertical migration of *C. polykrikoides.* If *C. polykrikoides* does not reach nutrient-rich deep waters, it may not grow well. Moreover, *S. costatum* and *C. danicus* cause negative growth rates of *C. polykrikoides,* and thus they may directly lower the abundance of *C. polykrikoides* in the water column. Thus, if diatoms is abundant due to some reasons in the Korean coastal waters, the outbreak of

Cochlodinium red tides could be delayed or prevented by reducing swimming speed and the growth rate of *C. polykrikoides*. Diatoms usually grow faster than the other phytoplankton groups when the conditions favorable for photosynthesis are given. Nutrient concentrations in coastal waters are usually elevated after heavy rains. This condition may cause high abundances of diatoms and in turn low abundances of *C. polykrikoides*.

I established the 34th *Alexandrium* species, *Alexandrium pohangense* n. sp. Scientists and people in aquaculture industry are interested in *Alexandrium* species because several *Alexandrium* species are toxic and known to be responsible for paralytic shellfish poisoning (PSP). The productions of Pacific cupped oyster and Japanese carpet shell are approximately 4.27 million tons and 3.09 million tons, respectively, in 2007 in the world (KMI, 2009). The production of shellfish in aquaculture industry has gradually increased. The morphological characteristics in the genus *Alexandrium* are very complicated, and thus it is difficult to identify *Alexandrium* cells in the species level. In this study, I suggeste new useful criteria for identifying a species in the *Alexandrium* genus such as the angles between the cingulum and the bottom margin side of 1′ plate (α) and antero-posterioral axis of the cell and the point of the margin of apical pore plate (β).

I found that *Alexandrium pohangense* n. sp. is a mixotrophic dinoflagellate. Interestingly, this dinoflagellate is a specialist feeding on fast swimming *C. polykrikoides* cells. Furthermore, based on calculated grazing coefficients, it is suggested that *A. pohangense* sometimes has considerably grazing impacts on populations of *C.*

polykrikoides. Prior to this study, there have been no mixotrophic predator which is able to feed on *C. polykrikoides*. An *A. pohangense* cell is able to ingest maximum 7 *C. polykrikoides* cells a day and divide twice in three days (i.e., mixotrophic maximum growth rate = 0.5 d^{-1}). Moreover, *A. pohangense* lysed all cryptophyte species which are the nutritious prey to *C. polykrikoides*. Thus, *A. pohangense* may affect *C. polykrikoides* populations by feeding *C. polykrikodes* and lysing cryptophytes which are nutritional prey for *C. polykrikoides*. Jeong et al. (2004b) suggested that the presence of co-occurring cryptophytes may be partially responsible for the outbreak of *C. polykrikoides* in the offshore waters because the maximum mixotrophic growth rate of *C. polykrikoides* with added crptophyte *Teleaulax* sp. (0.324 d^{-1}) is almost twice the rate without prey (0.166 d^{-1}). Therefore, by eliminating the potential prey of *C. polykrikoides*, *A. pohangense* may lower the growth of *C. polykrikoides* and in turn delay or prevent the outbreak of *C. polykrikoides* red tides. Thus, *A. pohangense* should be taken into consideration in models for dynamics of *C. polykrikoides* red tides.

This study tested 3 hypotheses that tropical cyclones, competing diatoms, and a new mixotrophic species *A. pohangense* affect dynamics of *C. polykrikoides* red tides. These newly identified factors clearly give critical effects on dynamics of *C. polykrikoides* red tides directly or indirectly (Fig. 6.3). Tropical cyclones generate turbulence and it could directly damage the *Cochlodinium* cells or make the environment favorable for diatoms and small flagellates. Diatoms usually grow faster than dinoflagellates when surface nutrient concentrations are high and turbulence intensity is high (Banse, 1982; Thomas and Gibson, 1990a). Under these circumstances,

dense diatoms may reduce the *Cochlodinium* population by inhibition of swimming speed and growth rate of *Cochlodinium*. Moreover, the new predator, *A. pohagense,* also may reduce the *Cochlodinium* population by removing the potential prey of *Cochlodinium* and by directly removing *Cochlodinium* cells by feeding. I hope that the results of this study contribute in understanding harmful *C. polykrikoides* red tides, establishing prediction models, and developing methods of controlling the red tides.

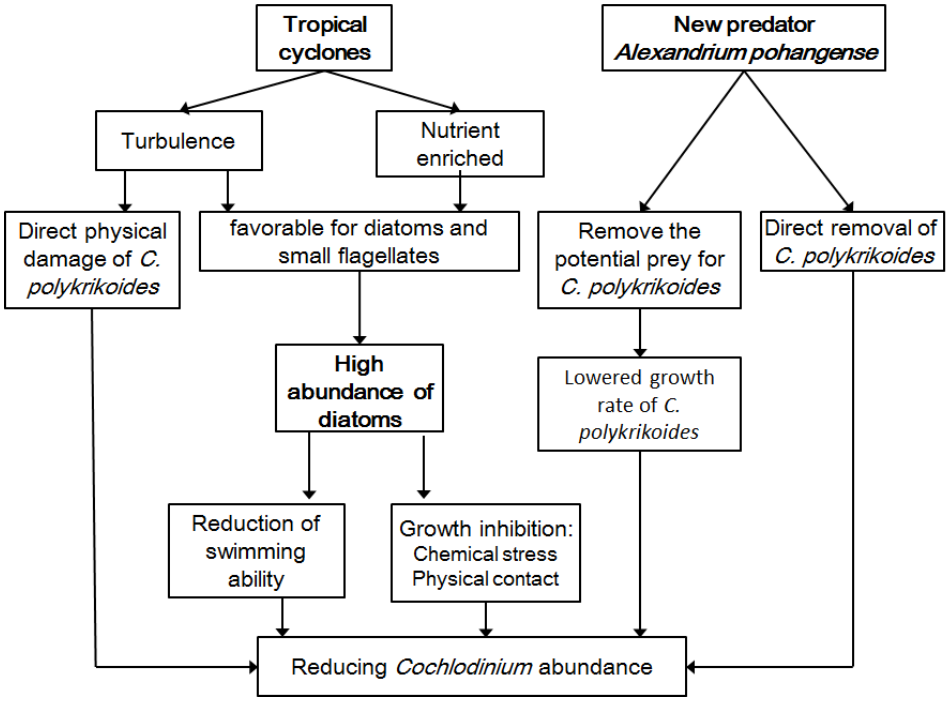

Fig. 6.3. Schematic diagram showing factors reducing the abundance of *Cochlodinium*.

Reference

Adolf, J.E., Bachvaroff, T.R., Krupatkina, D.N., Nonogaki, H., Brown, P.J.P., Lewitus, A.J., Harvey, H.R., Place, A.R., 2006. Species specificity and potential roles of *Karlodinium micrum* toxin, African J. Mar. Sci. 28, 415-419.

Allen, W.E., 1949. Data files, 1917-1949. Accession No. 81-19. Scripps Institution of Oceanography Archives, University of California, San Diego.

Anderson, D.M., 1997. Turning back the harmful red tide. Nature 388, 513-514.

Anderson, D.M., Alpermann, T.J., Cembella, A.D., Collos, Y., Masseret, E., Montresor, M., 2012. The globally distributed genus *Alexandrium*: multifaced roles in marine ecosystems and impacts on human health. Harmful Algae 14, 10-35.

Anton, A., Teoh, P.L., Mohd-Shaleh, S.R., Mohammad-Noor, N., 2008. First occurrence of *Cochlodinium* blooms in Sabah, Malaysia. Harmful Algae 7, 331-336.

Azanza, R.V., David, L.T., Borja, R.T., Baula, I.U., Fukuyo, Y., 2008. An extensive *Cochlodinium* bloom along the western coast of Palawan, Philippines. Harmful Algae 7, 324-330.

Balech, E., 1994. Three new species of the genus *Alexandrium* (dinoflagellate). Trans. Am. Microsc. Soc. 113, 216-220.

Balech, E., 1995. The genus *Alexandrium* Halim (Dinoflagellata). Sherkin Island Marine Station Publication, Sherkin Island, Co. Cork, Ireland.

Banse, K., 1982. Cell volumes, maximal growth rates of unicellular algae and ciliates and the role of ciliates in the marine pelagial.

Limnol. Oceanogr. 27, 1057-1071.

Berge, T., Hansen, P.J., Moestrup, Ø., 2008. Prey size spectrum and bioenergetics of the mixotrophic dinoflagellate *Karlodinium armiger*. Aquat. Microb. Ecol. 50, 289-299.

Blossom, H.E., Daugbjerg, N., Hansen, P.J., 2012. Toxic mucus traps: A novel mechanisms that mediates prey uptake in the mixotrophic dinoflagellate *Alexandrium pseudogonyaulax*. Harmful Algae 17, 40-53.

Bockstahler, K.R., Coats, D.W., 1993. Spatial and temporal aspects of mixotrophy in Chesapeake Bay dinoflagellates. J. Eukaryot. Microbiol. 40, 49-60.

Burkholder, J.M., Glibert, P.M., Skelton, H.M., 2008. Mixotrophy, a major mode of nutrition for harmful algal species in eutrophic waters. Harmful Algae 8, 77-93.

Cembella, A.D., Quilliam, M.A., Lewis, N.I., Bauder, A.G., Dell'Aversano, C., Thomas, K., Jellett, J., Cusack, R.R., 2002. The toxigenic marine dinoflagellate *Alexandrium tamarense* as the probable cause of mortality of caged salmon in Nova Scotia. Harmful Algae 1, 313-325.

Chan, A.T., 1978. Comparative physiological study of marine diatoms and dinoflagellates in relation to irradiance and cell size. I. Growth under continuous light. J. Phycol. 14, 396-402.

Chen, Y.L., Chen, H., Jan, S., Tuo, S., 2009. Phytoplankton productivity enhancement and assemblage change in the upstream Kuroshio after typhoons. Mar. Ecol. Prog. Ser. 385, 111-126.

Cho, E. 2006. Report on *Protoperidinium* sp. fed on *Cochlodinium*

polykrikodies (Gymnodiniales, Dinophyceae). Kor. J. Environ. Sci. 15, 385-386.

Cho, E., 2010. A comparative study on outbreak and non-outbreak of *Cochlodinium polykrikoides* Margalef in South Sea of Korea in 2007-2009. J. Kor. Soc. Mar. Environ. Safety 16, 31-41. (in Korean)

Chung, C., Gong, G., Hung, C., 2012. Effect of typhoon Morakot on microphytoplankton population dynamics in the subtropical Northwest Pacific. Mar. Ecol. Prog. Ser. 448, 39-49.

Curtiss, C.C., Langlois, G.W., Busse, L.B., Mazzillo, F., Silver, M. W., 2008. The emergence of *Cochlodinium* along the California Coast (USA). Harmful Algae 7, 337-346.

Daugbjerg, N., Hansen, G., Larsen, J., Moestrup, Ø., 2000. Phylogeny of some of the major genera of dinoflagellates based on ultrastructure and partial LSU rDNA sequence data, including the erection of three new genera of unarmoured dinoflagellates. Phycologia 39, 302-317.

D'Silva, M.S., Anil, A.C., Naik, R.K., D'Costa P.M., 2012. Algal blooms: a perspective from the coasts of India. Nat. Hazards 63, 1225-1253.

Elbrächter, M., 1977. On population dynamics in multi-species cultures of diatoms and dinoflagellates. Helgoländer wiss. Meeresunters 30, 192-200.

Emanuel, K., 2003. Tropical cyclones. Annu. Rev. Earth Planet. Sci. 31, 75-104.

Fistarol, G.O., Legrand, C., Selander, E., Hummert, C., Stolte, W., Granéli, E., 2004. Allelopathy in *Alexandrium* spp.: effect on a natural plankton community and on algal monocultures. Aquat. Microb. Ecol. 35, 45-56.

Fogel, M.L., Aguilar, C., Cuhel, R., Hollander, D.J., Willey, J.D., Paerl, H.W., 1999. Biological and isotopic changes in coastal waters induced by Hurricane Gordon. Limnol. Oceanogr. 44, 1359-1369.

Franks, P.J.S, Anderson, D.M., 1992. Alongshore transport of a toxic phytoplankton bloom in buoyancy current: *Alexandrium tamarense* in the Gulf of Maine. Mar. Bol. 112, 153-164.

Frost, B.W., 1972. Effects of size and concentration of food particles on the feeding behavior of the marine planktonic copepod *Calanus pacificus*. Limnol. Oceanogr. 17, 805-815.

Fudge, H., 1977. The "Red Tides" of Malta. Mar. Biol. 39, 381-386.

Fukuyo, Y., Imai, I., Kodama, M., Tamai, K., 2002. Red tide and other harmful algal blooms in Japan. In: Tayler, F.R.J., Trainer, V.L. (Eds.), Harmful algal blooms in the PICES region of the North Pacific. PICES Sci. Rep. No. 23, pp. 152.

Gárate-Lizárraga, I., López-Cortes, D.J., Bustillo-Guzmán, J.J., Hemández-Sandoval, F., 2004. Blooms of *Cochlodinium polykrikoides* (Gymnodiniaceae) in the Gulf of California, Mexico. Rev. Biol. Trop. 52(S1), 51-58.

Geraci, J.R., Anderson, D.M., Timperi, R.J., St. Aubin D.J., Early, G.A., Prescott, J.H., Mayo, C.A., 1989. Humpback whales (*Megaptera novaeangliae*) fatally poisoned by dinoflagellate toxin. Can. J. Fish. Aquat. Sci. 46, 1895-1898.

Giacobbe, M.G., Yang, X., 1999. The life history of *Alexandrium taylori* (Dinophyceae). J. Phycol. 35, 331-338.

Giovannoni, S.J., DeLong, E.F., Olsen, G.J., Pace, N.R., 1988. Phylogenetic group-specific oligodeoxynucleotide probes for identification of single microbial cells. J. Bacteriol. 170, 720-726.

Glibert, P.M., Burkholder, J.M., Kana, T.M., Alexander, J., Skelton,

H., Shilling, C., 2009. Grazing by *Karenia brevis* on *Synechococcus* enhances its growth rate and may help to sustain blooms. Aquat. Microb. Ecol. 55, 17-30.

Gobler, C.J., Berry, D.L., Anderson, O.R., Burson, A., Koch, F., Rodger, B.S., Moore, L.K., Goleski, J.A., Allam, B., Bowser, P., Tang, Y., Nuzzi, R., 2008. Characterization, dynamics, and ecological impacts of harmful *Cochlodinium polykrikoides* blooms on eastern Long Island, NY, USA. Harmful Algae 7, 293-307.

Gobler, C.J., Burson, A., Koch, F., Tang, Y., Mulholland, M.R., 2012. The role of nitrogenous nutrients in the occurrence of harmful algal blooms caused by *Cochlodinium polykrikoides* in New York estuaries (USA). Harmful Algae 17, 64-74.

Godhe, A., Asplund, M.E., Härnström, K., Saravanan, V., Tyagi, A., Karunasagar, I., 2008. Quantification of diatom and dinoflagellte biomasses in coastal marine seawater samples by Real-time PCR. Appl. Environ. Microbiol. 74, 7174-7182.

Gómez-Villarreal, M.C., Martínez-Gaxiola, M.D., Peña-Manjarrez, J.L., 2008. Algal blooms at Banderas Bay, Mexico (2000-2001), from SeaWiFS-sensor-data. Rev. Biol. Trop. 56, 1653-1664.

Gribble, K.E., Keafer, B.A., Quilliam, M.A., Cembella, A.D., Kulis, D.M., Manahan, A., Anderson, D.M., 2005. Distribution and toxicity of *Alexandrium ostenfeldii* (Dinophyceae) in the Gulf of Maine, USA. Deep-Sea Res. 52, 2745-2763.

Gu, H., Zeng, N., Liu, T., Yang, W., Müller, A., Krock, B., 2013. Morphology, toxicity, and phylogeny of *Alexandrium* (Dinophyceae) species along the coast of China. Harmful Algae 27, 68-81.

Guillard, R.R.L., Ryther, J.H., 1962. Studies of marine planktonic diatoms. I. *Cyclotella nana* Hustedt and *Detonula confervacea* (Cleve) Grun. Can. J. Microbiol. 8, 229-239.

Halim, Y., 1960. *Alexandrium minutum* n. gen. s. sp., dinoflagellate provocant "des eaus rouges". Vie. et Milieu 11, 102-105.

Hallegraeff, G.M., 1992. Harmful algal blooms in the Australian region. Mar. Pollut. Bull. 25, 185-190.

Hallegraeff, G.M., 1993. A review of harmful algal blooms and their apparent global increase. Phycologia 32, 79-99.

Hamzehei, S., Bidokhi, A.A., Mortazavi, M.S., Gheiby, A., 2013. Red tide monitoring in the Persian Gulf and Gulf of Oman using MODIS sensor data. Tech. J. Engin. App. Sci. 3, 1100-1107.

Hansen, P. J., 2011. The role of photosynthesis and food uptake for the growth of marine mixotrophic dinoflagellates. J. Eukaryot. Microbiol. 58, 203-214.

Hansen, P.J., Bjornsen, P.K., Hansen, B.W., 1997. Zooplankton grazing and growth: scaling within the 2-2,000 μm body size range. Limnol. Oceanogr. 42, 687-704.

Hansen, P.J., Nielsen, T.G., 1997. Mixotrophic feeding of *Fragilidium subglobosum* (Dinophyceae) on three species of *Ceratium*: effects of prey concentration, prey species and light intensity. Mar. Ecol. Prog. Ser. 147, 187-196.

Hansen, P.J., Calado, A. J., 1999. Phagotrophic mechanisms and prey selection in free-living dinoflagellates. J. Eukaryot. Microbiol. 46, 382-389.

Heinbokel, J.F., 1978. Studies on the functional role of tintinnids in the Southern California Bight. I. Grazing and growth rates in

laboratory cultures. Mar. Biol. 47, 177-189.

Huelsenbeck, J.P., Ronquist, F., 2001. MrBayes: Bayesian inference of phylogeny. Bioinformatics 17, 754-755.

Imai, I., Yamaguchi, M., Hori, Y., 2006. Eutrophication and occurrences of harmful algal blooms in the Seto Inland Sea, Japan. Plankton Benthos Res. 1, 71-84.

Jacobson, D.M., Anderson, D.M., 1996. Widespread phagocytosis of ciliates and other protists by marine mixotrphic and heterotrophic thecate dinoflagellates. J. Phycol. 32, 279-285.

Jeong, H.J., Shim, J.H., Kim, J.S., Park, J.Y., Lee, C.W., Lee, Y., 1999a. The feeding by the thecate mixotrophic dinoflagellate *Fragilidium* cf. *mexicanum* on red tide and toxic dinoflagellate. Mar. Ecol. Prog. Ser. 176, 263-277.

Jeong, H.J., Shim, J.H., Lee, C.W., Kim, J.S., Koh, S.M., 1999b. Growth and grazing rates of the marine planktonic ciliate *Strombidinopsis* sp. on red-tide and toxic dinoflagellates. J. Eukaryot. Microbiol.46, 69-76.

Jeong, H.J., Park, J.K., Choi, H.Y., Yang, J.S., Shim, J.H., Shin, Y.K., Yih, W.H., Kim, H.S., Cho, K.J., 2000. The outbreak of red tides in the coastal waters off Kohung, Chonnam, Korea. 2. The temporal and spatial waters variations in the phytoplanktonic community in 1997. J. Kor. Soc. Oceanogr. 5, 27-36. (written in Korean with English abstract)

Jeong, H.J., Yoo, Y.D., Kim, S.T., Kang, N.S., 2004a. Feeding by the heterotrophic dinoflagellate *Protoperidinium bipes* on the diatom *Skeletonema costatum*. Aquatic. Microb. Ecol. 36, 171-179.

Jeong, H.J., Yoo, Y.D., Kim, J.S., Kim, T.H., Kim, J.H., Kang, N.S., Yih, W., 2004b. Mixotrophy in the phototrophic harmful alga *Cochlodinium polykrikoides* (Dinophycean): prey species, the effects of prey concentration, and grazing impact. J. Eukaryot. Microbiol. 51, 563-569.

Jeong, H.J., Yoo, Y.D., Park, J.Y., Song, J.Y., Kim, S.T., Lee, S.H., Kim, K.Y., Yih, W.H., 2005a. Feeding by the phototrophic red-tide dinoflagellates: five species newly revealed and six species previously known to be mixotrophic. Aquat. Microb. Ecol. 40, 133-155.

Jeong, H.J., Park, J.Y., Nho, J.H., Park, M.O., Ha, J.H., Seong, K.A., Jeng, C., Seong, C.N., Lee, K.Y., Yih, W.H., 2005b. Feeding by red-tide dinoflagellates on the cyanobacterium *Synechococcus*. Aquat. Microb. Ecol. 41, 131-143.

Jeong, H.J., Yoo, Y.D., Seong, K.A., Kim, J.H., Park, J.Y., Kim, S.H., Lee, S.H., Ha, J.H., Yih, W.H., 2005c. Feeding by the mixotrophic dinoflagellate *Gonyaulax polygramma*: mechanisms, prey species, the effects of prey concentration, and grazing impact. Aquat. Microb. Ecol. 38, 249-257.

Jeong, H.J., Kim, J.S., Kim, J.H., Kim, S.T., Seong, K.A., Kim, T.H., Song, J.Y., Kim, S.K., 2005d. Feeding and grazing impact of the newly described heterotrophic dinoflagellate *Stoeckeria algicida* on the harmful alga *Heterosigma akashiwo*. Mar. Ecol. Prog. Ser. 295, 69-75.

Jeong, H.J., Ha, J.H., Park, J.Y., Kim, J.H., Kang, N.S., Kim, S., Kim, J.S., Yoo, Y.D., Yih, W., 2006. Distribution of the heterotrophic dinoflagellate *Pfiesteria piscicida* in Korean waters and its

consumption of mixotrophic dinoflagellates, raphidophytes and fish blood cells. Aquat. Microb. Ecol. 44, 263-278.

Jeong, H.J., Ha, J.H., Yoo, Y.D., Park, J.Y., Kim, J.H., Kang, N.S., Kim, T.H., Kim, H.S., Yih, W.H., 2007. Feeding by the *Pfiesteria*-like heterotrophic dinoflagellate *Luciella masanensis*. J. Eukaryot. Microbiol. 54, 231-241.

Jeong, H.J., Kim, J.S., Yoo, Y.D., Kim, S.T., Song, J.Y., Kim, T.H., Seong, K.A., Kang, N.S., Kim, M.S., Kim, J.H., Kim, S., Ryu, J., Lee, H.M., Yih, W.H., 2008. Control of the harmful alga *Cochlodinium polykrikoides* by the naked ciliate *Strombidinopsis jeokjo* in mesocosm enclosures. Harmful Algae 7, 368-377.

Jeong, H.J., Yoo, Y.D., Kim, J.S., Seong, K.A., Kang, N.S., Kim, T.H., 2010a. Growth, feeding and ecological roles of the mixotrophic and heterotrophic dinoflagellates in marine planktonic food webs. Ocean Sci. J. 45, 65-91.

Jeong, H.J., Yoo, Y.D., Kang, N.S., Rho, J.R., Seong, K.A., Park, J.W., Nam, G.S., Yih, W.H., 2010b. Ecology of *Gymnodinium aureolum*. I. Feeding in western Korean waters. Aquat. Microbial Ecol. 59, 239-255.

Jeong, H.J., Yoo, Y.D., Kang, N.S., Lim, A.S., Seong, K.A., Lee, S.Y., Lee, M.J., Lee, K.H., Kim, H.S., Shin, W., Nam, S.W., Yih, W., Lee, K., 2012. Heterotrophic feeding as a newly identified survival strategy of the dinoflagellate *Symbiodinium*. Proc. Nat. Acad. Sci. USA 109, 12604-12609.

Jeong, H.J., Yoo, Y.D., Lee, K.H., Kim, T.H., Seong, K.A., Kang, N.S., Lee, S.Y., Kim, J.S., Kim, S., Yih, W.H., 2013. Red tides

in Masan Bay, Korea in 2004-2005: I. Daily variations in the abundance of red tide organisms and environmental factors. Harmful Algae 30S, S75-S88.

John, U., Fensome, R.A., Medlin, L.K., 2003. The application of a molecular clock based on molecular sequences and the fossil record to explain biogeographic distributions within the *Alexandrium tamarense* "species complex" (Dinophyceae). Mol. Biol. Evol. 20, 1015-1027.

John, U., Litaker, R.W., Montresor, M., Murray, S., Brosnahan, M.L., Anderson, D.M., 2014. Formal revision of the *Alexandrium tamarense* species complex (Dinophyceae) taxonomy: The introduction of five species with emphasis on molecular-based (rDNA) classification. Protist 165, 779-804.

Kang, Y.S., Park, Y.T., Lim, W.A., Cho, E.S., Lee, C.K., Kang, Y.S., 2009. A comparative study on outbreak scale of *Cochlodinium polykrikoides* blooms. J. Kor. Soc. Oceanogr. 14, 229-239.

Kang, N.S., Jeong, H.J., Moestrup, Ø., Shin, W.G., Nam, S.W., Park, J.Y., de Salas, M.F., Kim, K.W., Noh, J.H., 2010. Description of a new planktonic mixotrophic dinoflagellate *Paragymnodinium shiwhaense* n. gen., n. sp. from the coastal waters off western Korea: morphology, pigments, and ribosomal DNA gene sequence. J. Eukaryot. Microbiol. 57, 121-144.

Ke, Z., Huang, L., Tan, Y., Song, X., 2012. A dinoflagellate *Cochlodinium geminatum* bloom in the Zhujiang (Pearl) River estuary in autumn 2009. Chin. J. Oceanol. Limn. 30, 371-378.

Kim, H., Lee, C., Lee, S., Kim, H., Park, C., 2001. Physico-chemical factors on the growth of *Cochlodinium polykrikoides* and nutrient utilization. J. Korean Fish. Soc. 34, 445-456.

Kim, D., Matsuyama, Y., Nagasoe, S., Yamaguchi, M., Yoon, Y., Oshima, Y., Imada, N., Honjo, T., 2004. Effects of temperature, salinity and irradiance on the growth of the harmful red tide dinoflagellate *Cochlodinium polykrikoides* Margalef (Dinophyceae). J. Plankton Res. 26, 61-66.

Kim, Y.S., Jeong, C.S., Seong, G.T., Han, I.S., Lee, Y.S., 2010. Diurnal vertical migration of *Cochlodinium polykrikoides* during the red tide in Korean coastal sea waters. J. Environ. Biol. 31, 687-693.

Kim, T.W., Lee, K., Lee, C.K., Jeong, H.D., Suh, Y.S., Lim, W.A., Kim, K.Y., Jeong, H.J., 2013. Interannual nutrient dynamics in Korean coastal waters. Harmful Algae 30S, S15-S27.

Kita, T., Fukuyo, Y., 1988. Description of the Gonyaulacoid dinoflagellate *Alexandrium hiranoi* sp. nov. inhabiting tidepools on Japanese Pacific coast. Bull. Plank. Soc. Japan 35, 1-7.

Kondo, K., Seike, Y., Date, Y., 1990. Red tides in the brackish lake Nakanoumi (II). Relationships between the occurrence of *Prorocentrum minimum* red tide and environmental conditions. Bull. Plankton Soc. Jpn, 37, 19-34.

Korea Maritime Institute (KMI). 2009. A basic study to advance Korea's fisheries industry. pp. 394.

Kremp, A., Tamminen, T., Spilling, K., 2008. Dinoflagellate bloom formation in natural assemblage with diatoms: nutrient competition and growth strategies in Baltic spring phytoplankton. Aquat. Microb. Ecol. 50, 181-196.

Kremp, A., Tahvanainen, P., Litaker, W., Krock, B., Suikkanen, S., Leaw, C.P., Tomas, C., 2014. Phylogenetic relationships, morphological variation, and toxin patterns in the *Alexandrium*

ostenfeldii (Dinophyceae) complex: implications for species boundaries and identities. J. Phycol. 50, 81-100.

Kudela, R.M., Gobler, C.J., 2012. Harmful dinoflagellate blooms caused by *Cochlodinium* sp.: global expansion and ecological strategies facilitating bloom formation. Harmful Algae 14, 71-86.

Landsberg, J.H., Flewelling, L.J., Naar, J., 2009. *Karenia brevis* red tides, brevetoxins in the food web, and impacts on natural resources: decadal advancements. Harmful Algae 8, 598-607.

Lara, M.D.C.C., Altamirano, R.C., Sierra-Beltrán, A.P., 2004. Presence of *Cochlodinium catenatum* (Gymnodiniales: Gymnodiniaceae) in red tides of Bahía de Banderas, Mexican Pacific. Rev. Biol. Trop. 52, 35-49.

Leaw, C.P., Lim, P.T., Ng, B.K., Cheah, M.Y., Ahmad, A., Usup, G., 2005. Phylogenetic analysis of *Alexandrium* species and *Pyrodinium bahamense* (Dinophyceae) based on theca morphology and nuclear ribosome gene sequence. J. Phycol. 44, 550-565.

Lee, D., 2008. *Cochlodinium polykrikoides* blooms and eco-physical conditions in the South Sea of Korea. Harmful Algae 7, 315-323.

Lee, Y.S., Park, Y.T., Kim, Y.S., Kim, K.Y., Park, J.S., Go, W.J., Jo, Y.J., Park, S.Y., 2001. Countermeasure and outbreak mechanism of *Cochlodinium polykrikoides* red tide. 1. Environmental characteristics on outbreak and disappearance of *Cochlodinium polykrikoides* bloom. The Sea 6, 259-264. (in Korean with English abstract)

Lee, C., Park, T., Park, Y., Lim, W., 2013. Monitoring and trends in harmful algal blooms and red tides in Korean coastal waters, with emphasis on *Cochlodinium polykrikoides*. Harmful Algae

30S, S3-S14.

Lee, K.H., Jeong, J.H., Jang, T.Y., Lim, A.S., Kang, N.S., Kim, J., Kim, K.W., Park, K., Lee, K., 2014a. Feeding by the newly described mixotrophic dinoflagellate *Gymnodinium smaydae*: Feeding mechanism, prey species, and effect of prey concentration. J. Exp. Mar. Biol. Ecol. 459, 114-125.

Lee, S.K., Jeong, H.J., Jang, S.H., Lee, K.H., Kang, N.S., Lee, M.J., Potvin, É., 2014b. Mixotrophy in the newly described dinoflagellate *Ansanella granifera*: feeding mechanism, prey species, and effect of prey concentration. Algae 29, 137-152.

Leflaive, J. and Ten-Hage, L., 2009. Chemical interactions in diatoms: role of polyunsaturated aldehydes and precursor. New Phytologist 184, 794-805.

Li, A., Stoecker, D.K., Coats, D.W., 2000. Mixotrophy in *Gyrodinium galatheanum* (dinophyceae): grazing responses to light intensity and inorganic nutrients. J. Phycol. 36, 33-45.

Lilly, E.L., Halanych, K.M., Anderson, D.M., 2007. Species boundaries and global biogeography of the *Alexandrium tamarense* complex (Dinophyceae). J. Phycol. 43, 1329-1338.

Lim, W.A., Jung, C.S., Lee, C.K., Cho, Y.C., Lee, S.G., Kim, H.G., Chung, I.K., 2002. The outbreak, maintenance and decline of the red tide dominated by *Cochlodinium polykrikoides* in the coastal waters off southern Korea from August to October, 2000. The Sea 7, 68-77. (in Korean with English abstract).

Lim, W.A., Lee, Y.S, Lee, S.G., Lee, J.Y., 2007. Distribution and community structure of phytoplankton in the southeast coastal waters during Summer 2006. J. Kor. Soc. Oceanogr. 12,

370-379. (written in Korean with English abstract)

Lim, W.A., Lee, Y.S., Lee, S.G., 2008. Characteristics of environmental factors related to outbreak and decline of *Cochlodinium polykrikoides* bloom in the southeast coastal waters of Korea, 2007. J. Kor. Soc. Oceanogr. 13, 325-332. (written in Korean with English abstract)

Lim, W.A., Lee, Y.S., Park, J.G., 2009. Characteristics of *Cochlodinium polykrikoides* bloom in southeast coastal waters of Korea, 2008. J. Kor. Soc. Oceanogr. 14, 155-162. (written in Korean with English abstract)

Lim, A.S., Jeong, H.J., Jang, T.Y., Jang, S.H., Franks, P.J.S., 2014a. Inhibition of growth rate and swimming speed of the harmful dinoflagellate *Cochlodinium polykrikoides* by diatoms: Implications for red tide formation. Harmful Algae 37, 53-61.

Lim, A.S., Jeong, H.J., Jang, T.Y., Yoo, Y.D., Kang, N.S., Yoon, E.Y., Kim, G.H., 2014b. Feeding by the newly described heterotrophic dinoflagellate *Stoeckeria changwonensis*: A comparison with other species in the family Pfiesteriaceae. Harmful Algae 34, 11-21.

Lim, A.S., Jeong, H.J., Kim, J.H., Lee, S.Y., 2015a. Description of the new phototrophic dinoflagellate *Alexandrium pohangense* sp. nov. from Korean coastal waters. Harmful Algae 46, 49-61.

Lim, A.S., Jeong, H.J., Jang, T.Y., Kang, N.S., Jang, S.H., Lee, M.J., 2015b. Differential effects of typhoons on ichthytoxic *Cochlodinium polykrikoides* red tides in the South sea of Korea during 2012-204. Harmful Algae 45, 26-32.

Lin, I., Liu, W.T., Wu, C., Wong, G.T.F., Hu, C., Chen, Z., Liang, W.,

Yang, Y., Liu, K., 2003. New evidence for enhanced ocean primary production triggered by tropical cyclone. Geophys. Res. Lett. 30, 1718, doi:10.1029/2003GL017141.

Litaker, R.W., Vandersea, M.W., Kibler, S.R., Reece, K.S., Stokes, N.A., Steidinger, K.A., Millie, D.F., Bendis, B.J., Pigg, R.J., Tester, P.A., 2003. Identification of *Pfiesteria piscicida* (Dinophyceae) and *Pfiesteria*-like organisms using internal transcribed spacer-specific PCR assays. J. Phycol. 39, 754-761.

Ma, H., Krock, B., Tillmann, U., Bickmeyer, U., Graeve, M., Cembella, A., 2011. Mode of action of membrane-disruptive lytic compounds from the marine dinoflagellate *Alexandrium tamarense*. Toxicon 58, 247-258.

Maciel-Baltazar, E., Hernández-Becerril, D.U., 2013. Species of athecate dinoflagellates (Dinophyta) from coasts of Chiapas, southern Mexican Pacific. Rev. Biol. Mar. oceanogr. 48, 245-259.

MacKenzie, L., Todd, K., 2002. *Alexandrium camutascutulum* sp. nov. (Dinophyceae): a new dinoflagellate species from New Zealand. Harmful Algae 1, 295-300.

MacKenzie, L., de Salas, M., Adamson, J., Beuzenberg, V., 2004. The dinoflagellate genus *Alexandrium* (Halim) in New Zealand coastal waters: comparative morphology, toxicity and molecular genetics. Harmful Algae 3, 71-92.

Margalef, R., 1961. Hidrografía y fitoplancton de un área marina de la costa meridional de Puerto Rico. Invest. Pesq. 18, 33-96.

Matsubara, T., Nagaseo, S., Yamasaki, Y., Shikata, T., Shimasaki, Y., Oshima, Y., Honjo, T., 2007. Effects of water temperature, salinity and irradiance on the growth of the dinoflagellate

Akashiwo sanguinea. J. Exp. Mar. Biol. Ecol. 342, 226-230.

Medlin, L., Elwood, H.J., Stickel, S., Sogin, M.L., 1988. The characterization of enzymatically amplified eukaryokic 16S-like rRNA-coding regions. Gene 71,491-499.

Ministry for Food, Agriculture, Forestry and Fisheries (MIFAFF), 2008. The Technique of Wintering Culture of the Sea Bream in Net-cage Culture System in the Southern Sea, Korea. Report of MIFAFF, Busan, Korea. pp. 262.

Mulhollannd, M., Morse, R.E., Boneillo, G.E., Bernhardt, P.W., Filippino, K.C., Procise, L.A., Blanco-Garcia, J.L., Marshall, H.G., Egerton, T.A., Hunley, W.S., Moore, K.A., Berry, D.L., Gobler, C.J., 2009. Understanding causes and impacts of the dinoflagellate, *Cochlodinium polykrikoides*, blooms in the Chesapeake Bay. Estuaries and Coasts 32, 734-747.

Munir, S., Naz, T., Burhan, Z., Siddiqui, P.J.A., Morton S.L., 2012. First report of the athecate, chain forming dinoflagellate *Cochlodinium fulvescens* (Gymnodiniales) from Pakistan. Pak. J. Bot. 44, 2129-2134.

Murray, S., Hoppenrath, M., Orr, R.J.S., Bolch, C., John, U., Diwan, R., Yauwenas, R., Harwood, T., de Salas, M., Neilan, B., Hallegraeff, G., 2014. *Alexandrium diversaporum* sp. nov., a new non-saxitoxin producing species: Phylogeny, morphology and *sxtA* genes. Harmful Algae 31, 54-65.

Nagasoe, S., Toda, S., Shimasaki, Y., Oshima, Y., Uchida, T., Honjo, T., 2006a. Growth inhibition of *Gyrodinium instriatum* (Dianophyceae) by *Skeletonema costatum* (Bacillariophyceae). African J. Marine Sci. 28, 325-329.

Nagasoe, S., Kim, D., Shimasaki, Y., Oshima, Y., Tamaguchi, M.,

Honjo, T., 2006b. Effects of water temperature, salinity and irradiance on the growth of the red tide dinoflagellate *Gyrodinium instriatum* Freudenthal et Lee. Harmful Algae 5, 20-25.

National Fisheries Research & Development Institute (NFRDI), 2014. Monitoring, management and mitigation of red tide. Annual report of NFRDI on red tide of Korea, Busan, Korea (written in Korean).

Nygaard, K., Tobiesen, A., 1993. Bacterivory in algae: A survival strategy during nutrient limitation. Limnol. Oceanogr. 38, 273-379.

Oh, S.J., Yoon, Y.H., Kim, D.-I., Shimasaki, Y., Oshima, Y., Honjo, T., 2006. Effects of light quantity and quality on he growth of the harmful dinoflagellate *Cochlodinium polykrikoides* Margalef (Dinophyceae). Algae 21, 311-316.

Orr, R.J.S., Stüken, A., Rundberget, T., Eikrem, W., Jakobson, K.S., 2011. Improved phylogenetic resolution of toxic and non-toxic *Alexandrium* strains using a concatenated rDNA approach. Harmful Algae 10, 676-688.

Oviatt, C., Lane, P., French III.F., Donaghay, P., 1989. Phytoplankton species and abundance in response to eutrophication in coastal marine mesocosms. J. Plankton Res. 11, 1223-1244.

Paasche, E. 1973. Silicon and the ecology ofmarine plankton diatoms. 1. *Thalassiosira pseuclonana* (Cyclotella nana) grown in a chemost at with silicate as limiting nutrient.Mar. Biol. 19, 117-126.

Park, J.G., Jeong, M.K., Lee, J.A., Cho, K., Kwon, O., 2001. Diurnal vertical migration of a harmful dinoflagellate, *Cochlodinium*

polykrikoides (Dinophyceae), during a red tide in coastal waters of Namhae Island, Korea. Phycologia 40, 292-297.

Park, M.G., Kim, S.J., Kim, H.S., Myung, G.O., Kang, Y.G., Yih, W.H., 2006. First successful culture of the marine dinoflagellate *Dinophysis acuminata*. Aquat. Microb. Ecol. 45, 101-106.

Park, T.G., Lim, W.A., Park, Y.T., Lee, C.K, Jeong, H.J., 2013a. Economic impact, management and mitigation of red tides in Korea. Harmful Algae 30S, S131-S143.

Park, J. Jeong, H.J., Yoo, Y.D., Yoon, E.Y., 2013b. Mixotrophic dinoflagellate red tides in Koean waters: distribution and ecophysiology. Harmful Algae 30S, S28-S40.

Park, M.G., Kim, M., Kang, M., 2013c. A dinoflagellate *Amylax triacantha* with plastids of the Cryptophyte origin: phylogeny, feeding mechanism, and growth and grazing responses. J. Eukaryot. Microbiol. 60, 363-376.

Philps, E.J., Badylak, S., Christman, M., Wolny, J., Brame, J., Garland, J., Hall, J., Hart, J., Landsberg, J., Lasi, L., Lockwood, J., Paperno, R., Scheidt, D., Staples, A., Steidinger, K., 2011. Scales of temporal and spatial variability in the distribution of harmful algae species in the Indian River Lagoon, Florida, USA. Harmful Algae 10, 277-290.

Pierce, R.H., Henry, M.S., Blum, P.C., Lyons, J., Cheng, Y.S., Yazzie, D., Zhou, Y., 2003. Brevetoxin concentrations in marine aerosol: human exposure levels during a *Karenia brevis* harmful algal bloom. Bull. Environ. Contam. Toxicol. 70, 161-165.

Prince, J.F., 1981. Upper ocean response to a hurricane. J. Phys. Oceanogr. 11, 153-175.

Roberts, E.C., Wootton, E.C., Davidson, K., Jeong, H.J., Lowe, C.D., Montagnes, D.J.S., 2011. Feeding in the dinoflagellate *Oxyrrhis marina*: linking behavior with mechanisms. J. Plankton Res. 33, 603-614.

Ronquist, F., Huelsenbeck, J.P., 2003. MRBAYES 3: Bayesian phylogenetic inference under mixed models. Bioinformatics 19, 1572-1574.

Ross, O.N., Sharples, J., 2007. Phytoplankton motility and the competition for nutrients in the thermocline. Mar. Ecol. Prog. Ser. 347, 21-38.

Rountos, K.J., Tang, Y., Cerrato, R.M., Gobler, C.J., Pikitch, E.K., 2014. Toxicity of the harmful dinoflagellate *Cochlodinium polykrikoides* to early life stages of three estuarine forage fish. Mar. Ecol. Prog. Ser. 505, 81-84.

Sanders, R.W., 2011. Alternative nutritional strategies in protists: symposium introduction and a review of freshwater protists that combine photosynthesis and heterotrophy. J. Eukaryot. Microbiol. 58, 181-184.

Scholin, C.A., Herzog, M., Sogin, M., Anderson, D.M., 1994. Identification of group and strain specific genetic makers for globally distributed *Alexandrium* (Dinophyceae) Ⅱ. Sequence analysis of a fragment of the LSU rRNA gene. J. Phycol. 30, 999-1011.

Selina, M.S., Morozova, T.V., 2005. First records of dinoflagellates *Alexandrium margalefi* Balech, 1994 and *A. tamutum* Montresor, Beran et John, 2004 in the seas of the Russian far east. Russ. J. Mar. Biol. 31, 187-191.

Seong, K.A., Jeong, H.J., 2011. Interactions between the pathogenic

bacterium *Vibrio parahaemolyticus* and red-tide dinoflagellates. Ocean Sci. J. 46, 105-115.

Sieg, R.D., Poulson-Ellestad, K.L., Kubanek, J., 2011. Chemical ecology of the marine plankton. Nat. Prod. Rep. 28, 388-399.

Skovgaard, A., Hansen, P.J., Stoecker, D.K., 2000. Physiology of the mixotrophic dinoflagellate *Fragilidium subglobosum*. 1. Effects of phagotrophy and irradiance on photosynthesis and carbon content. Mar. Ecol. Prog. Ser. 201, 129-136.

Smayda, T.J., 1997. Harmful algal blooms: their ecophysiology and general relevance to phytoplankton blooms in the sea. Limnol. Oceanogr. 42, 1137-1153.

Stamatakis, A., 2006. RaxML-VI-HPC: maximum likelihood-based phylogenetic analyses with thousands of taxa and mixed models. Bioinformatics 22, 2688-2690.

Stoecker, D.K., 1999. Mixotrophy among dinoflagellates. J. Eukaryot. Microbiol. 46, 397-401.

Strathmann, R.R., 1967. Estimating the organic carbon content of phytoplankton from cell volume or plasma volume. Limnol. Oceanogr. 12, 411-418.

Tamura, K., Dudley, J., Nei, M., Kumar, S., 2007. MEGA4: molecular evolutionary genetics analysis (MEGA) software v. 4.0. Mol. Biol. Evol. 24, 1596-1599.

Tang, Y., Gobler, C.J., 2009. Characterization of the toxicity of *Cochlodinium polykrikoides* isolates from Northeast US estuaries to finfish and shellfish. Harmful Algae 8, 454-462.

Tang, Y.Z., Gobler, C.J., 2010. Allelopathic effects of *Cochlodinium*

polykrikoides isolates and blooms from the estuaries of Long Island, New York, on co-occurring phytoplankton. Mar. Ecol. Prog. Ser. 406, 19-31.

Thomas, W.H., Gibson, C.H., 1990a. Effects of small-scale turbulence on microalgae. J. Applied Phycol. 2, 71-77.

Thomas, W.H., Gibson, C.H., 1990b. Quantified small-scale turbulence inhibits a red tide dinoflagellate, *Gonyaulax polyedra* Stein. Deep-Sea Res. 37, 1583-1593.

Thomas, W.H., Vernet, M., Gibson, C.H., 1995. Effects of small-scale turbulence on photosynthesis, pigmentation, cell division, and cell size in the marine dinoflagellate *Gonyaulax polyedra* (Dinophyceae). J. Phycol. 31, 50-59.

Tillmann, U., John, U., 2002. Toxic effects of *Alexandrium* spp. on heterotrophic dinoflagellates: an allelochemical defense mechanism independent of PSP-toxin content. Mar. Ecol. Prog. Ser. 230, 47-58.

Tomas, C.R., 1978. *Olisthodiscus luteus* (Chrysophyceae). I. Effects of salinity and temperature on growth, mortality and survival. J. Phycol. 14, 309-313.

Tomas, C.R., Smayda, T.J., 2008. Red tide blooms of *Cochlodinium polykrikoides* in a coastal cove. Harmful Algae 7, 308-317.

Van Dolah, F.M., 2000. Marine algal toxins: origins, health effects, and their increased occurrence. Environ. Health Perspect. 108(S1), 133-141.

Vargas-Montero, M., Freer, E., Jiménez-Montealegre, R., Guzmán, J.C., 2006. Occurrence and predominance of the fish killer *Cochlodinium polykrikoides* on the Pacific coast of Costa Rica. African J. Mar. Sci. 28, 215-217.

Verity, P.G., 2010. Expansion of potentially harmful algal taxa in a Georgia Estuary (USA). Harmful Algae 9, 144-152.

Vershinin, A.O., Moruchkov, A.A., Leighfield, T., Sukhanova, I.N., Pan'kov, S.L., Morton, S.L., Ramsdell, J.S., 2005. Potentially toxic algae in the coastal phytoplankton of the Northeast Black Sea in 2001-2002. Oceanology 45, 224-232.

Wang, J., Zhang, Y., Li, H., Cao, J., 2013. Competitive interaction between diatom *Skeletonema costatum* and dinoflagellate *Prorocentrum donghaiense* in laboratory culture. J. Plankton Res. 35, 367-378.

White, A.W., 1976. Growth inhibition caused by turbulence in the toxic marine dinoflagellate *Gonyaulax excavata*. J. Fish. Res. Bd. Can. 33, 2598-2602.

Whyte, J.N.C., Haigh, N., Ginther, N.G., Keddy, L.J., 2001. First record of blooms of *Cochlodinium* sp. (Gymnodiniales, Dinophyceae) causing mortality to aquacultured salmon on the west coast of Canada. Phycologia 40, 298-304.

Wichard, T., Poulet S.A., Halsband-lenk, C., Albaina, A., Harris, R., Lie, D., Pohnert, G., 2005. Survey of the chemical defeence potential of diatoms: screening of fifty one species for α, β, ɣ, δ-unsaturated aldehydes. J. Chem. Ecol. 31, 949-958.

Wootton, E.C., Zubkov, M.V., Jones, D.H., Jones, R.H., Martel, C.M., Thornton, C.A., Roberts, E.C., 2007. Biochemical prey recognition by planktonic protozoa. Envion. Microbiol. 9, 216-222.

Yamasaki, Y., Nagaseo, S., Matsubara, T., Shikata. T., Shimasaki, Y., Oshima Y., Honjo, T., 2007. Growth inhibition and formation of morphologically abnormal cells of *Akashiwo sanguinea*

(Hirasaka) G. Hansen et Moestrup by cell contact with *Cochlodinium polykrikoides* Margalef. Mar. Biol. 152, 157-163.

Yamasaki, Y., Ohmichi, Y., Shikata, T., Hirose, M., Shimasaki, Y., Oshima Y., Honjo, T., 2010. Species-specific alleopathic effects of the diatom *Skeletonema costatum*. An Int. J. Mar. Sci., Thalassas 27, 21-32.

Yamatogi, T., Sakaguchi, M., Takagi, N., Iwataki, M., Matsuoka, K., 2005. Effects of temperature, salinity and light intensity on the growth of a harmful dinoflagellate *Cochlodinium polykrikoides* Margalef occurring in coastal waters of west Kyushu, Japan. Bull. Plankton Soc. Jp 52, 4-10.

Yan, T., Zhou, M., Zou, J., 2002. A national report on harmful algal blooms in China. In: Tayler, F.R.J., Trainer, V.L. (Eds.) Harmful algal blooms in the PICES region of the North Pacific. PICES Sci. Rep. No. 23, pp. 152.

Yoo, Y.D., Jeong, H.J., Kim, M.S., Kang, N.S., Song, J.Y., Shin, W., Kim, K.Y., Lee, K., 2009. Feeding by phototrophic red-tide dinoflagellates on the ubiquitous marine diatom *Skeletonema costatum*. J. Eukaryot. Microbiol. 56, 413-420.

Yoo, Y.D., Yoon, E.Y., Jeong, H.J., Lee. K.H., Hwang, Y.J., Seong, K.A., Kim, J.S., Park, J.Y., 2013. The newly described heterotrophic dinoflagellate *Gyrodinium moestrupii*, an effective protistan grazer of toxic dinoflagellates. J. Eukaryot. Microbiol. 60, 13-24.

Zar, J.H., 1984. Biostatistical analysis. Prentice Hall, Englewood Cliffs, New Jersey. pp. 97-235.

Zheng, M.G., Tang, D., 2007. Offshore and nearshore chlorophyll

increases induced by typhoon winds and subsequent terrestrial rainwater runoff. Mar. Ecol. Prog. Ser. 333, 61-74.

국문초록

적조란 미세조류의 대번성에 의해 해수 표면의 색이 변화하는 것을 말한다. 혼합영양성인 *Cochlodinium polykrikoides*는 종종 많은 나라의 연안에서 적조 패치를 형성하고 때때로 그로 인해 자연환경과 양식장 내에서 물고기 대량 폐사를 야기하기도 한다. 이 종에 의해 우리나라의 양식업에서는 매년 1-60만 달러에 해당하는 피해를 입고 있다. 이 종에 대한 생리학적 연구 즉, 성장에 있어서의 온도, 빛, 염분, 그리고 영양염류에 의한 성장 반응 연구는 많이 이루어졌음에도 불구하고, *Cochlodinium* 적조의 발생과 지속 그리고 감소의 메커니즘은 아직 완전히 이해되지 않은 상태이다.

Cochlodinium polykrikoides 적조 변동의 더 나은 이해를 위하여, 태풍, 경쟁적인 규조류, 그리고 새로운 혼합영양성 천적과 같은 지금까지 밝혀진 바 없는 물리학적, 생물학적 요인들에 의한 영향을 살펴보았다.

우리나라는 매년 *Cochlodinium* 적조 기간 동안 수개의 태풍을 경험한다. 태풍은 일반적으로 강한 바람과 많은 비를 동반하며, 이는 적조에 영향을 주는 중요한 환경적 생물학적 요인들을 변화시킨다. 강한 바람은 적조생물의 성장에 영향을 줄 수 있는 다양한 와류를 형성 시키고 식물플랑크톤 군집의 변화를 야기한다. 몇몇의 연구에 의하면 태풍이 지난 후 수층의 우점종이 편모류에서 규조류로 변화한 것으로 나타났다. 또한 *Cochlodinium*의 분포는 규조류의 분포와 서로 상반된 경향을 보인다. 그러나 *Cochlodinium* 적조에 대한 태풍의 영향에 대해서는 아직 잘 연구된 바가 없다. 태풍이 *Cochlodinium* 적조의 발생과 지속 그리고 쇠퇴에 미치는 영향을 알아보기 위해 2012년부터 2014년까지 우리나라 남해안에 영향을 주었던 14개의 태풍, 일일최대풍속과 일일 최대

Cochlodinium 밀도를 분석하였다. 그 결과 일일최대풍속이 14 m s^{-1} 이상의 바람이 불었을 때 *Cochlodinium* 적조발생이 억제되었으나, 5m s^{-1} 이하의 풍속은 큰 영향을 미치지 않는 것으로 나타났다. 따라서 태풍은 일일최대 풍속에 따라 *Cochlodinium*움 적조의 발생과 지속에 다른 영향을 주는 것으로 나타났다.

경쟁적인 규조류가 *Cochlodinium* 적조에 미치는 영향을 연구한 결과, 경쟁적인 규조류가 일정 밀도 이상을 초과하였을 때 물리적 접촉과 화학적 스트레스를 통해 *Cochlodinium*의 성장률과 수영속도를 낮추는 것으로 나타났다. 따라서 규조류의 밀도가 높을 때 *Cochlodinium* 적조의 발생이 예방되거나 지연될 수 있음을 알 수 있다.

현재까지 *Cochlodinium*에 대한 몇몇 섬모충과 종속영양성 원생생물 천적은 발견된 바 있으나, 효과적인 혼합영양성 와편모조류 천척은 발견되지 않았다. 2014년 코클로디니움 적조 기간 동안 우리나라 동해안의 연안에서 *Alexandrium* 속의 종을 발견하여 단종배양체를 확립하였다. 이 *Alexandrium* 종은 혼합영양성 종으로 코클로디니움 만을 선택적으로 섭식하는 것을 밝혔다. 또한 이 종의 형태학적 분자생물학적 특성을 분석하여 그 결과를 바탕으로 신종이라는 것을 밝혔으며, *Alexandrium pohangense*로 명명하였다.

해양생태계에서의 *Alexandrium pohangense*의 역할을 알아보기 위해, 실내실험을 통해 코클로디니움의 밀도에 따른 *A. pohangense*의 성장률과 섭식률을 측정하였다. 그 결과 *C. polykoides*에 대한 *A. pohangense*의 최대섭식률은 7 cells $predator^{-1}$ d^{-1}이였으며, 자가영양성 최대 성장률이 0.1 d^{-1}인데 비해 혼합영양성 최대 성장률은 0.5 d^{-1}에 달하였다. 또한 실내실험의 결과와 현장의 밀도 데이터를 혼합하여 자연상태에서의 *A. pohagense*의 코클로디니움 군집에 대한 포식압을 구하였다. *A. pohangense*와 동시에 출현하는 *C. polykrikoides*에 대한 포식압

은 1.57 d^{-1}에 달하였으며 이는 하루 동안 *A. pohangense* 군집에 의해 *C. polykrikoides* 군집이 최대 79 %까지 제거가 될 수 있음을 의미한다.

결과적으로 현장 관찰, 다양한 형태의 데이터의 분석, 실내에서의 다양한 섭식 실험과 형태학적 분자생물학적 분석을 통해 태풍, 경쟁적인 규조류, 그리고 새로운 혼합영양성 와편모류인 *A. pohangense*가 *Cochlodinium* 밀도에 큰 영향을 줄 수 있음을 밝혔으며, 이로 인해 *C. polykrikoides* 적조에 영향을 줄 수 있을 것으로 판단된다. 코클로디니움 적조의 발생과 지속, 소멸에 대한 예측 및 제어에 태풍과 경쟁적인 생물 종들의 상호작용이 고려되어야 할 것으로 판단된다.

주 요 어: 알렉산드리움, 코클로디니움, 태풍, 생태학, 포식, 분류학, 유해조류 번성
학 번: 2011-30921